

**Proceedings for the Workshop of IMPRS for Astronomy and Astrophysics
Braunfels, Hesse, September 14-17, 2009**

Workshop of IMPRS for Astronomy and Astrophysics took place at r at [Fuerstenhoff hotel](#) in [Braunfels, Hesse](#). A very specific scientific program which was meant to strengthen the team work has been followed. In Particular, teams of 2 to 3 students invented a topic from three broad fields:

1. Stellar Astrophysics (code: SA)
2. Galactic Astrophysics (code: GA)
3. Extragalactic Astrophysics and Cosmology (code: EG)

Each such team then presented the selected topic by splitting the work over the team members. Each member approached the common topic by contributing, either of:

1. Review-Introduction
2. Milestone Discoveries
3. Black-board problem solution

Each talk will have available 30-40 minutes hence each team will have 1.5 hours. Each Session was chaired by the last speaker of the previous session.

Day 1:
September 14, 2009

Session 1: Stellar Astrophysics

Chair: E. Angelakis

Rainer Rolffs	Energy Production in Stars and Elsewhere
Alex Kreplin	Circumstellar disks around young stellar objects
Marion Wienen	Overview of star formation

Session 2: Extragalactic Astrophysics and Cosmology

Chair: W. Wienen

Filomena Volino	Introduction to General Relativity
Er Xinzhong	Cosmology without General Relativity
Sibylle Anderl	Space and time in the philosophy of Kant

Day 2:
September 15, 2009

Session 3: Extragalactic Astrophysics and Cosmology
Chair: S. Anderl

Chin-Shin Chang	Active Galaxies
Rusen Lu	Active Galaxies
Marios Karouzos	Active Galaxies

Session 4: Extragalactic Astrophysics and Cosmology
Chair: M. Karouzos

Jiannis Nestoras	Gamma-Ray Bursts
Frank Schinzel	Gamma-Ray Bursts

Day 3:
September 16, 2009

Session 5: Galactic Astrophysics
Chair: J. Nestoras

Xuyang Gao	Galactic Plane Surveys
Fangchun Liu	Chemistry in Star Forming Regions
Fujun Du	Chemistry in Star Forming Regions

Session 6: Extragalactic Astrophysics and Cosmology
Chair: F. Liu

Brenda Miranda Ocejo	Sunyaev Zel'dovich effect
Xun Shi	Sunyaev Zel'dovich effect
Felipe Navarrete	Sunyaev Zel'dovich effect



Energy Production in Stars and Elsewhere

Rainer Rolffs

IMPRS retreat, 14 September 2009

International Max Planck Research School (IMPRS) for Astronomy and Astrophysics at
the Max Planck Institute for Radio Astronomy in Bonn and the Universities of Bonn
and Cologne

Energy Production in Stars and Elsewhere

Feel free to interrupt for discussions and questions!

Rainer Rolffs

IMPRS retreat, 14 September 2009

International Max Planck Research School (IMPRS) for Astronomy and Astrophysics at the Max Planck Institute for Radio Astronomy in Bonn and the Universities of Bonn and Cologne

No Outline...

... to keep the story suspenseful and enthralling

... ok, a glance:

there will be huge adventures of our tiny hero, who will travel from cold, lonely outer space to the fervent heat of inner stars.... will he be able to escape from that hell?

Maybe he will even visit us here in Braunfels.

And there will be exciting calculations and enormous numbers (hey, we're scientists!)

Once Upon A Time...

Once Upon A Time...

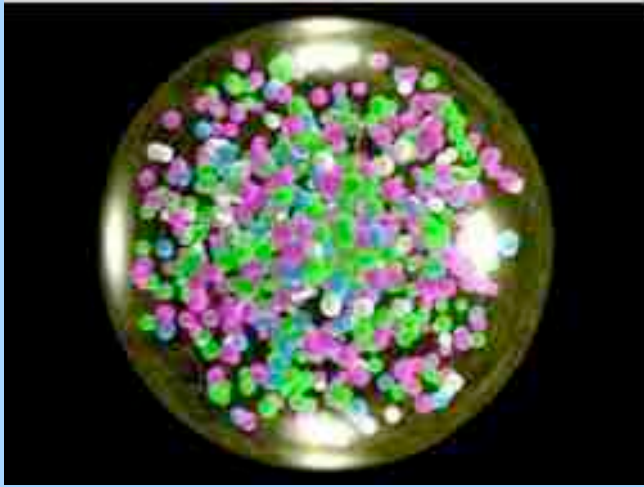


- ♦ beginning of space and time?
- ♦ energy conserved?
- ♦ what is powering inflation and expansion?

Energy is *produced* in the Big Bang and stored in matter, light, expansion field. After that, it is only *transformed*.

The Second Law of Thermodynamics leads to a dispersal of energy.

The Birth of Proty

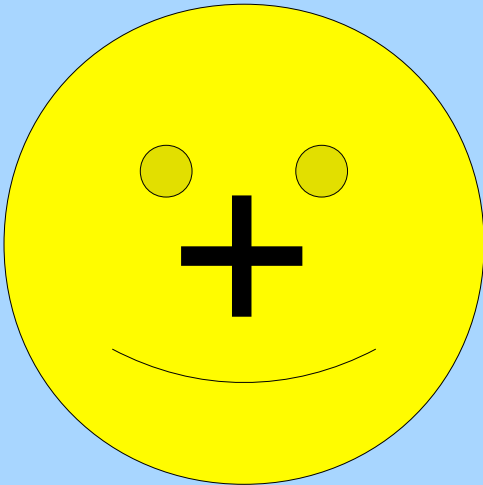


A millisecond after the BB, Proty condenses out of the quark-gluon plasma, switching between neutron and proton.

After 1 second, he decides to be a proton.

His rest mass is $m_p = 1.67262158 \times 10^{-27}$ kg, his size about (-15) m.

His kinetic energy is around $(-3) m_p$, but with time he loses it to these nasty photons which stretch out.

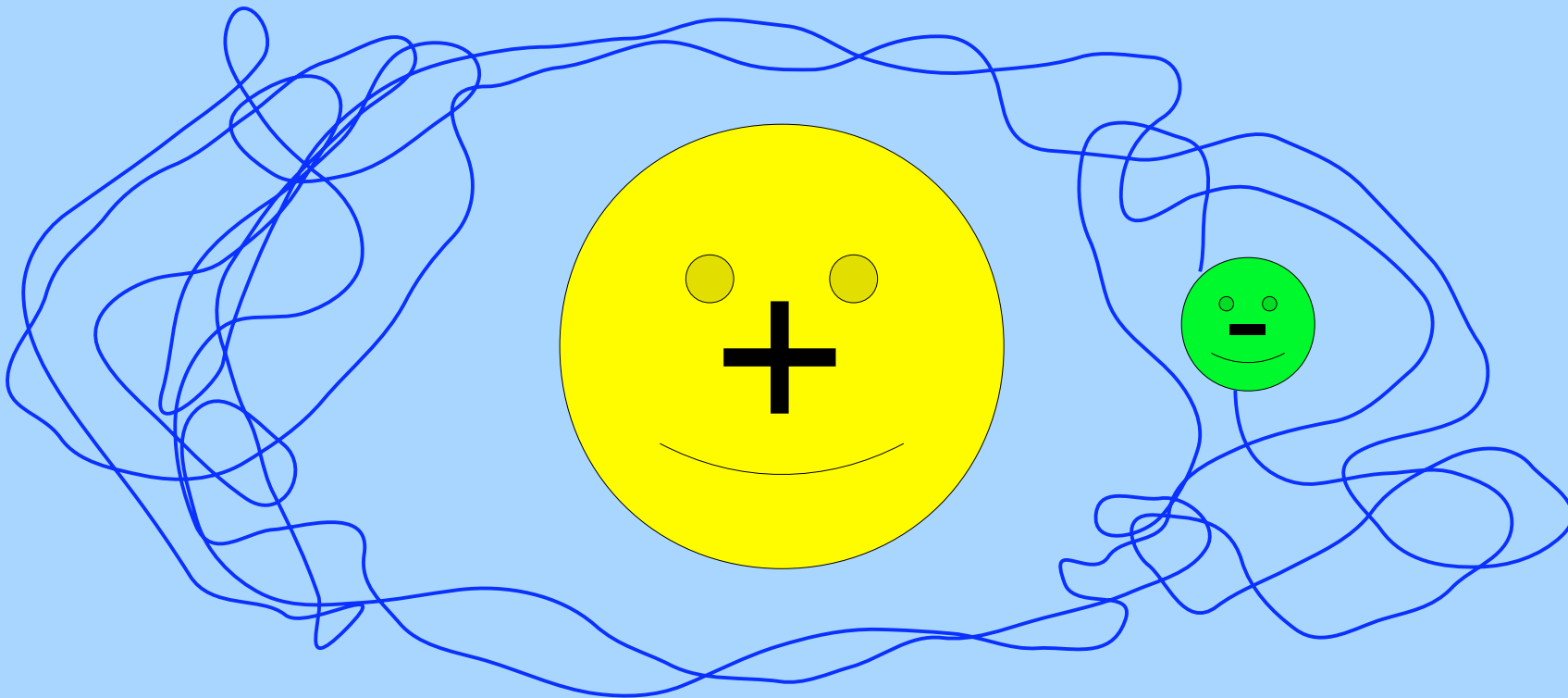


Finding Elly

He is attracting electrons, but these nasty photons don't let them stay together.

After some (5) years and a kinetic energy of only $3(-10) m_p$ (3000 K), the photons have lost enough energy that he finally finds Elly.

He doesn't care that she is exactly like all other electrons.



Density Rises Again

More and more other atoms collide with them, even two at almost the same time – now Proty is part of molecular hydrogen!

Density Rises Again

More and more other atoms collide with them, even two at almost the same time – now Proty is part of molecular hydrogen!

It gains kinetic energy. The collisions become so hard that it's ionized again.

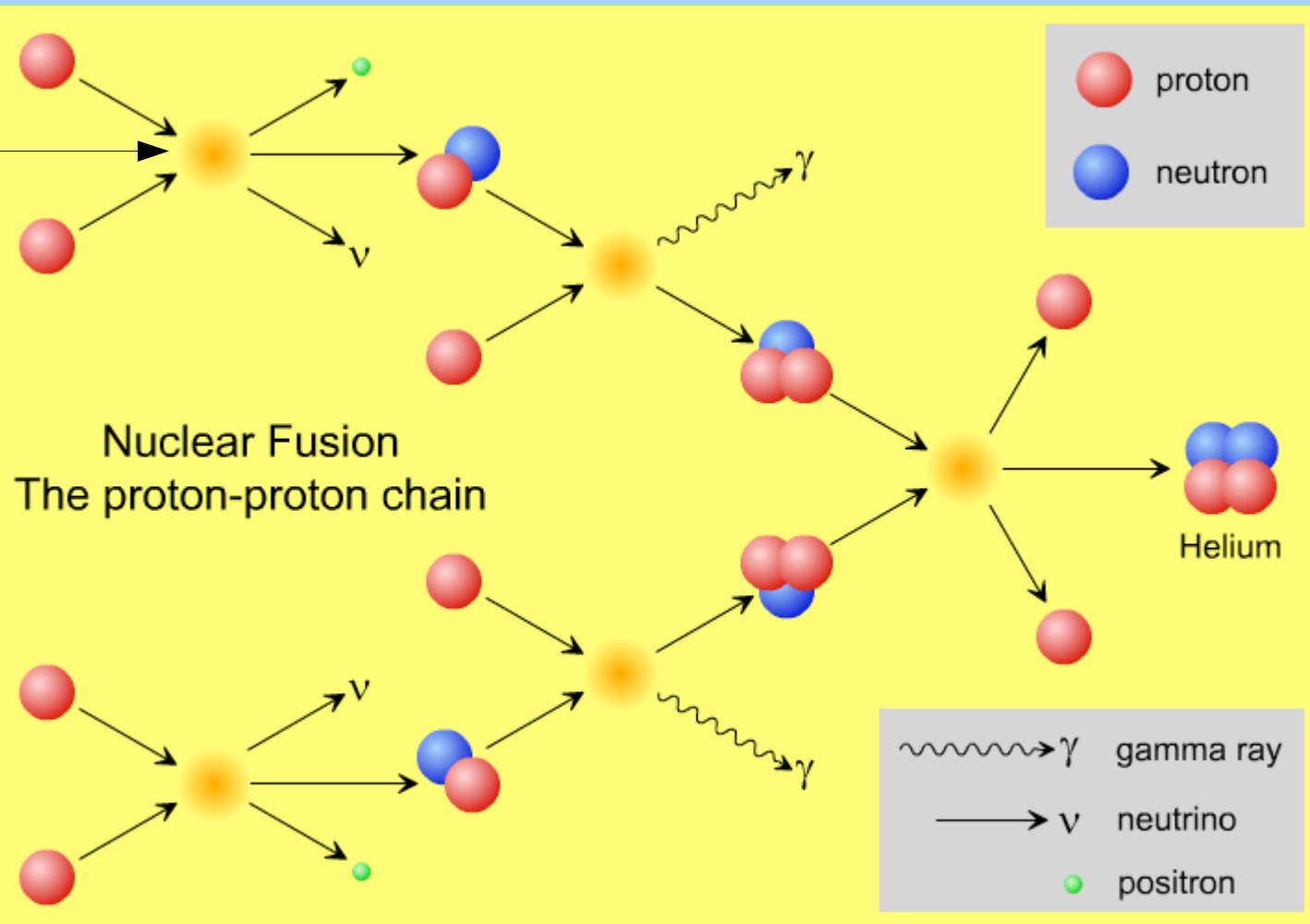
Where is that energy coming from?

It's Getting Crowded

Proton does not want the other protons to get so close – but what can he do except for the electric repulsion?

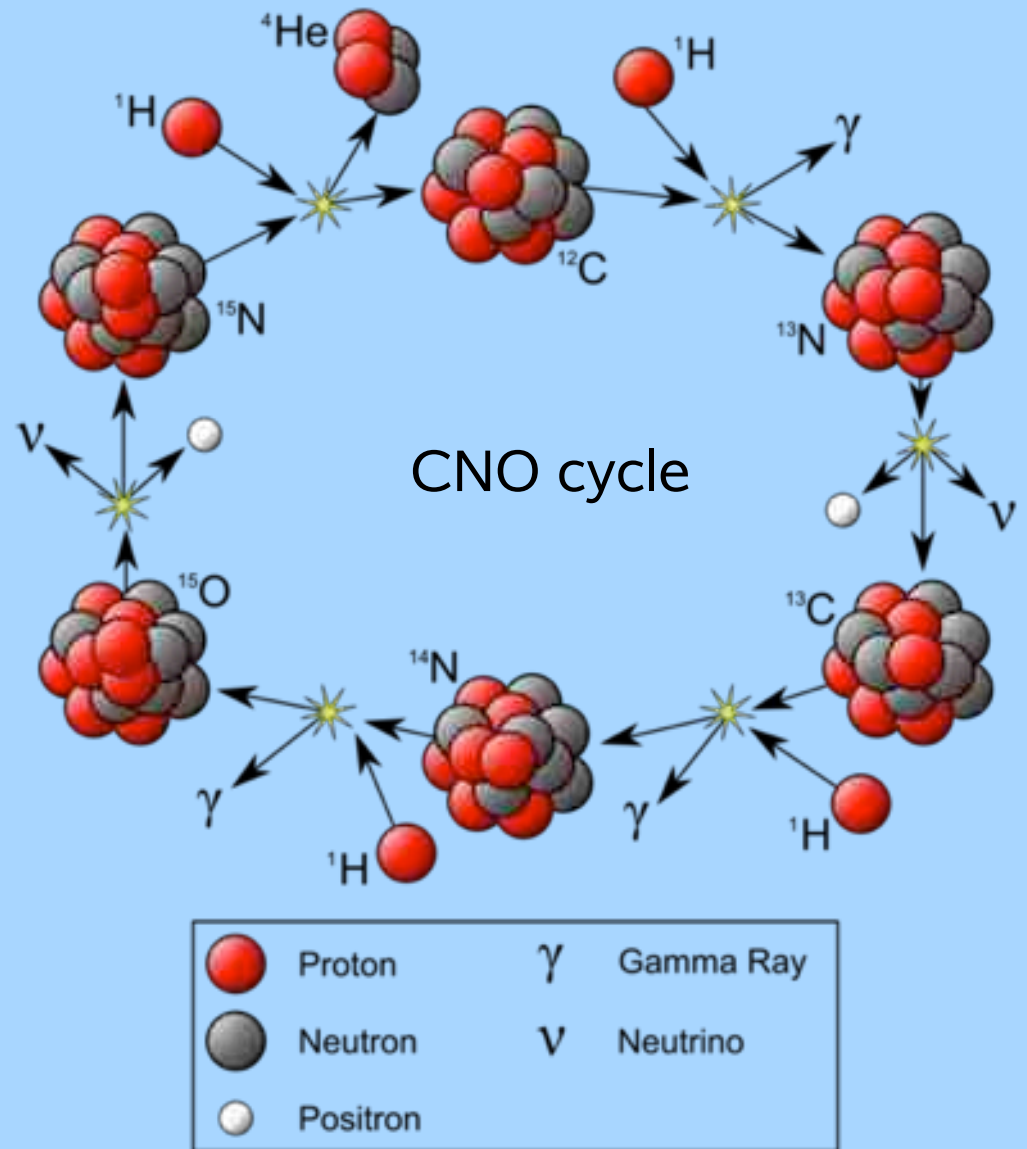
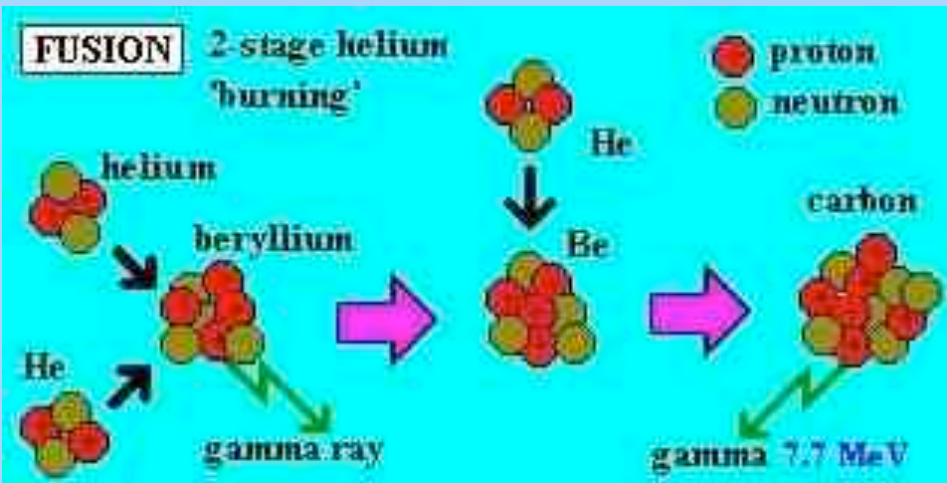
His kinetic energy reaches $(-6) m_p$ – puh, all those collisions...

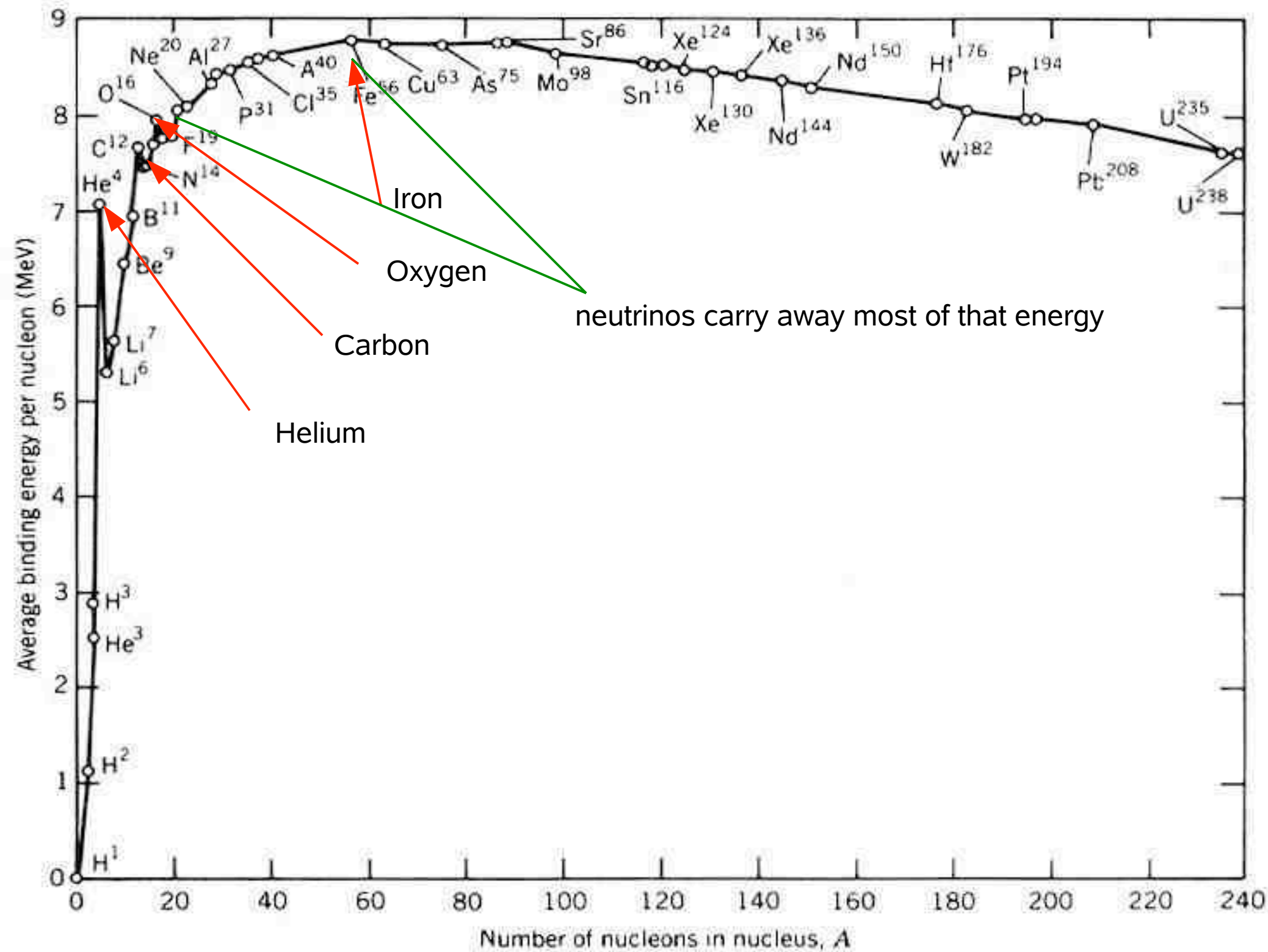
very unlikely!



New Neighbors

Proton is not used to such close vicinity – but at least he's still a proton!
Now even more neighbors are arriving.





Escape From Hell

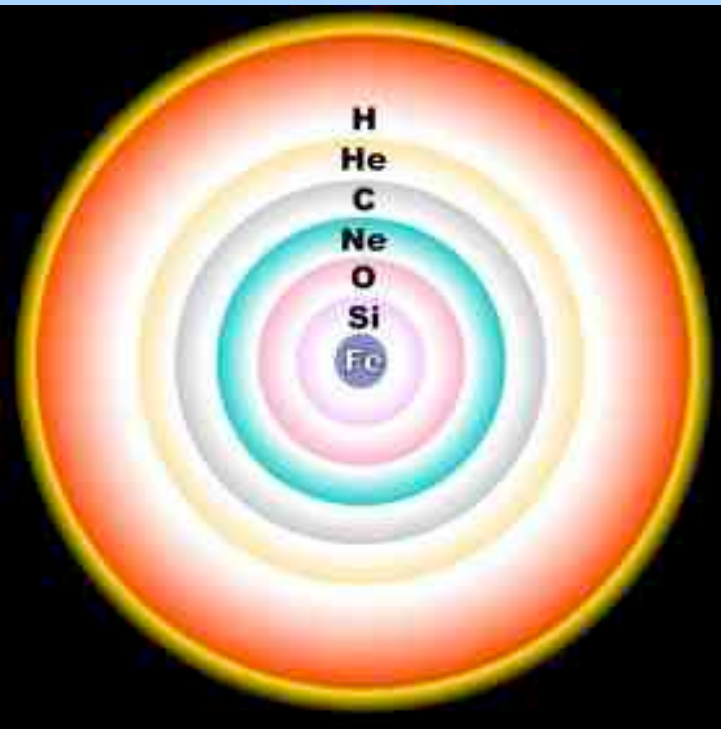
Trapped in such a strong gravitational potential, how would he ever get out of hell?

Escape From Hell

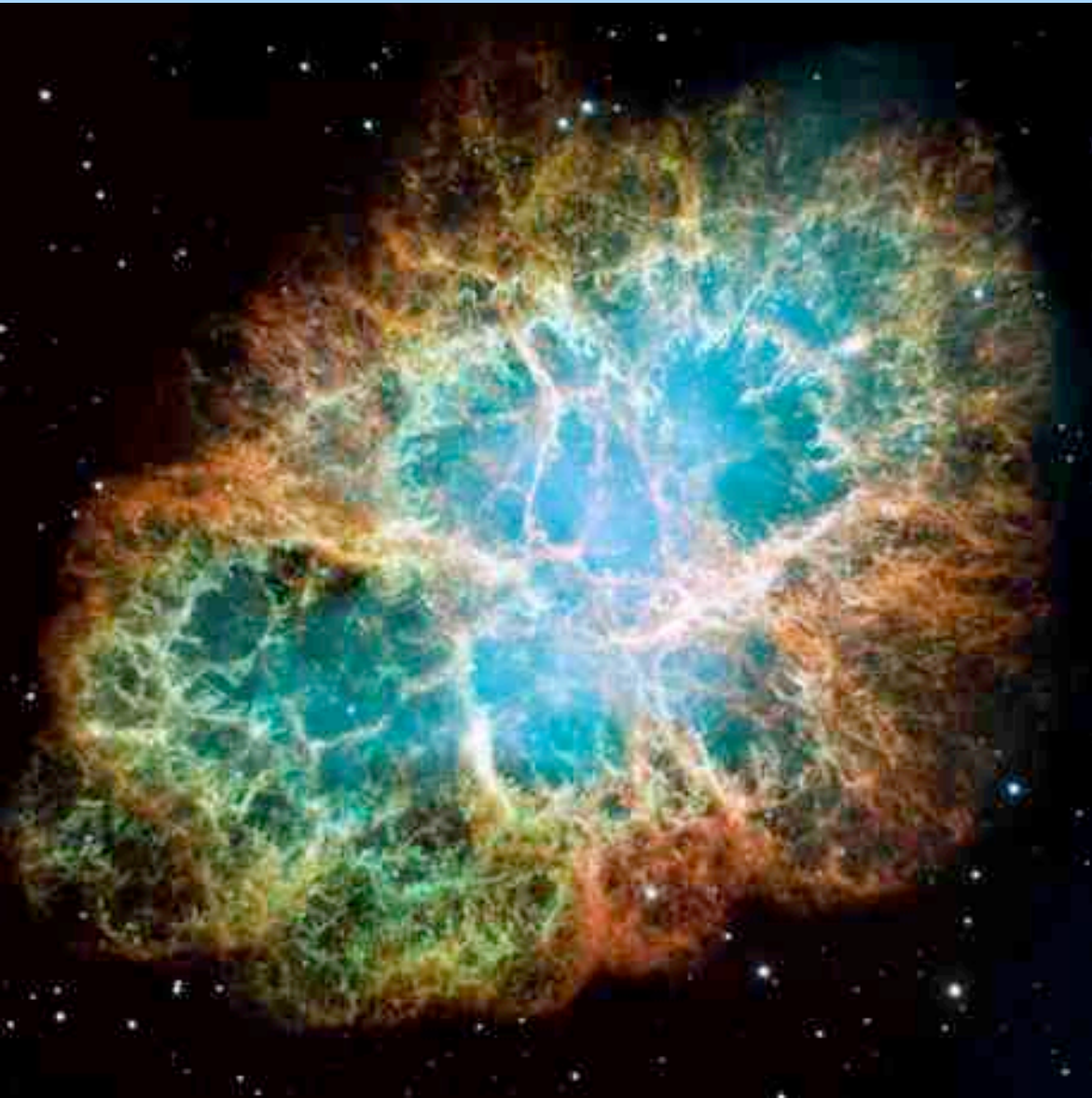
Trapped in such a strong gravitational potential, how would he ever get out of hell?

Ironically, the answer is again... gravity!

The iron core collapses when it's too heavy, a small fraction of the energy released disrupts the rest of the star - **SUPERNOVA !!!**



From Uranium to Helium

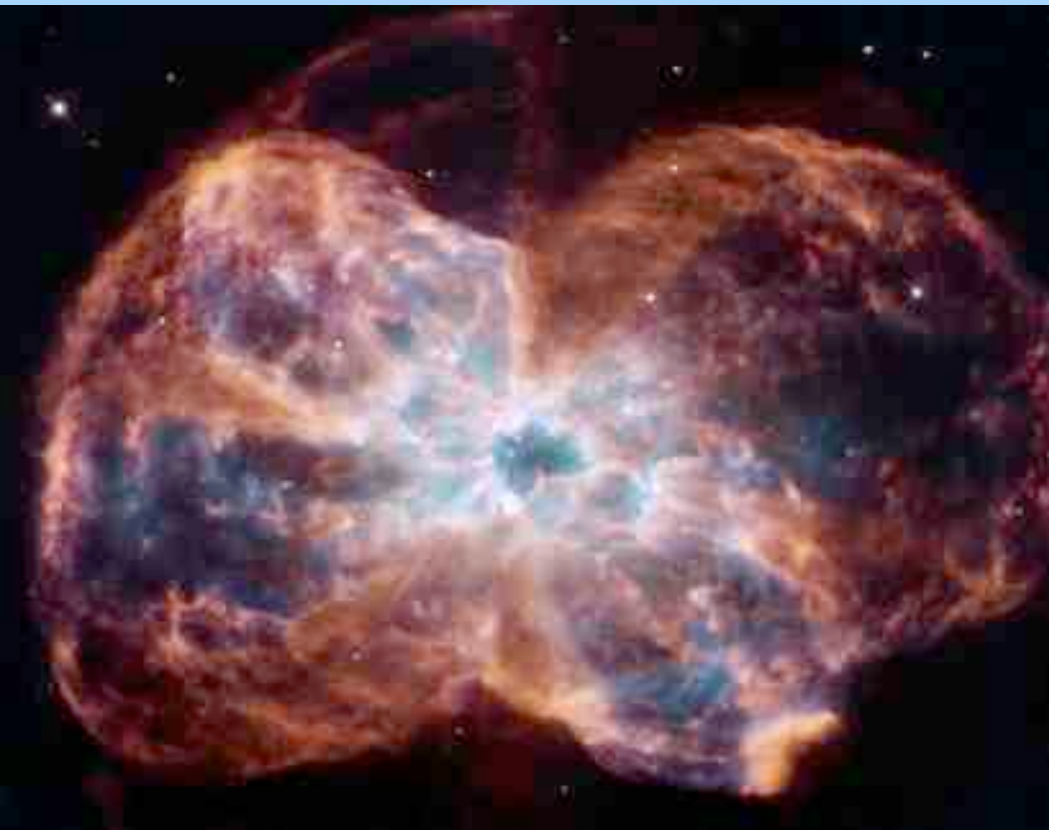


After that really explosive event, Protos finds himself in Uranium. As he doesn't feel comfortable with so many others (232), he leaves the nucleus with his nearest neighbors: α -decay

They calm down and find electrons, and help to cool their surroundings by collisional excitation and radiative de-excitation.

From SNR to PN

It's getting denser and cooler... now again hotter, he's ionized and ...right back in hell!



Well, it's not too bad in a carbon nucleus, especially now in the star's envelope. The shell burning expands it and... Proty's carbon is illuminated by a White Dwarf.

Again? - No, Earth!!!

This time he has enough angular momentum to prevent the hell, instead he's going to paradise – with a bit of patience though



Proty is incorporated by a plant using photosynthesis. It stores around 5(-3) of the incoming radiation as biomass.

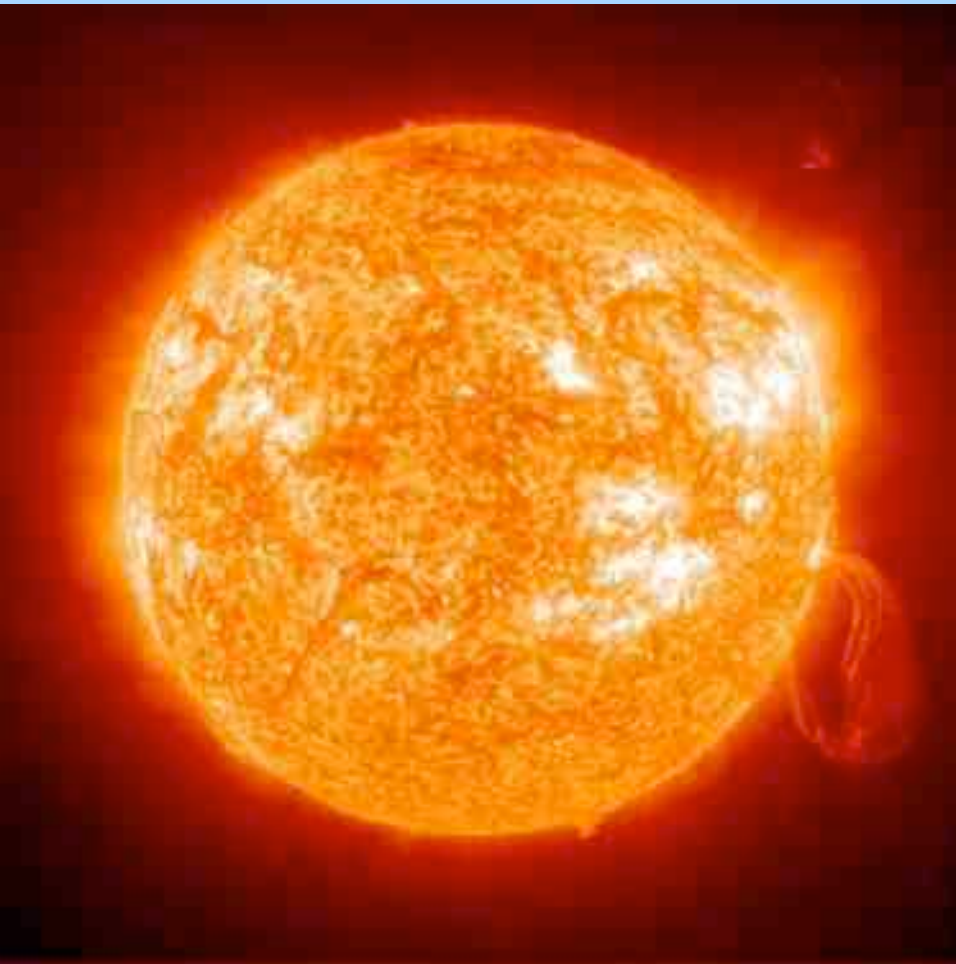
But then a volcano erupts – he is buried for a long time.



Why Does the Sun Shine?

In the meantime, a certain species of animals develop.
They start to talk and discuss this question.

The solar luminosity is $3.846(26) \text{ W}$



<i>Reason</i>	<i>Time Scale [years]</i>
God makes it shine	As long as He wants
Burning Coal	2(3)
Heat from formation	3(7)
Contracting	Radius prop. $1/\text{Time}$
Radioactivity	1(10)
Hydrogen Fusion	1(11)

Since 1919, fusion idea developed by Perrin, Eddington, Bethe and many more

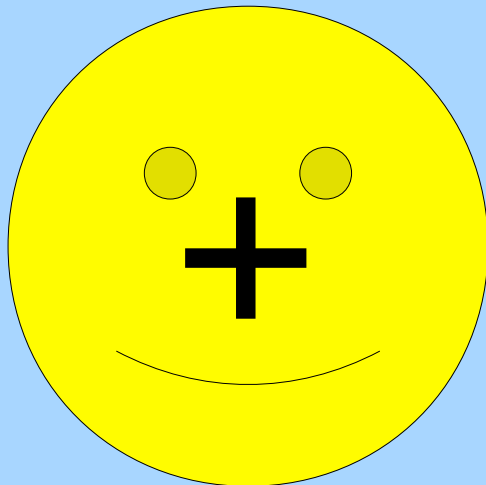
Where Is Proty Now?

They also grub out Proty's ancient plant and bring him into the atmosphere again. In fact, 80 % of mankind's energy use relies on fossil fuels, causing an energy and climate crisis.

Where Is Proty Now?

They also grub out Proty's ancient plant and bring him into the atmosphere again. In fact, 80 % of mankind's energy use relies on fossil fuels, causing an energy and climate crisis.

Proty is respired by a tomatoe plant; maybe one of us ate him a few weeks ago and he is now dust in this room.



What will be Proty's future?

More adventures to come until his death in a Black Hole !

Circumstellar disks around young stellar objects

IMPRS retreat
Braunfels, 14.09.09

Alexander Kreplin



- Overview: circumstellar disks
- Disk models
- The inner rim
- Observational techniques: V921 Sco
- Future Instruments
- Summary



- Overview: circumstellar disks
- Disk models
- The inner rim
- Observational techniques: V921 Sco
- Future Instruments
- Summary

Circumstellar disks



Evolution of young stellar objects

- Classification scheme of YSO's (Lada 1987)

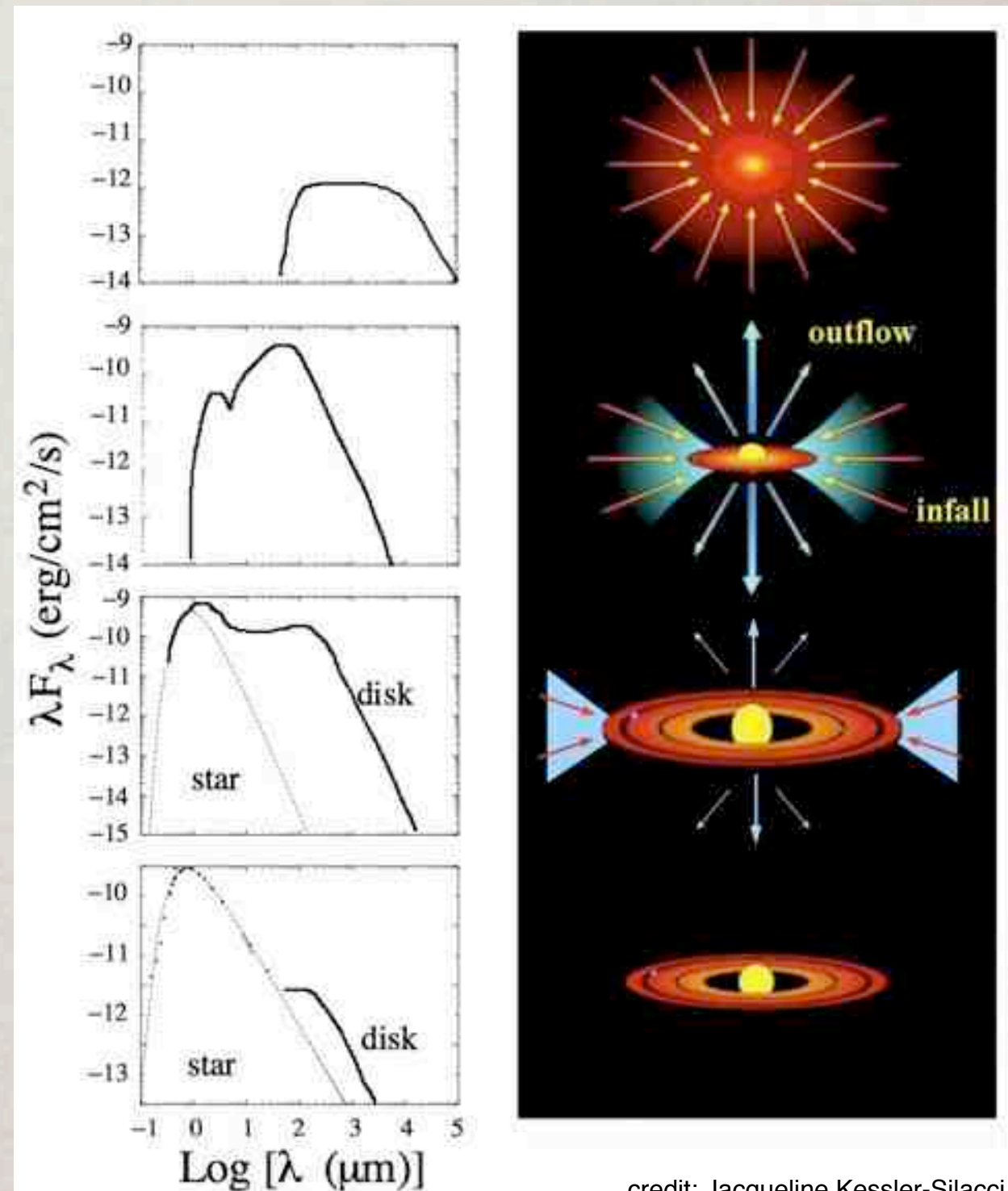
- ➡ Class 0: only submm-emission which indicates a deep embedded object
- ➡ Class I: steep positive spectral slope due to the presence of large amounts of circumstellar dust
- ➡ Class II: negative spectral slope indicates less dust than class I sources
- ➡ Class III: the weak mid- and near-infrared excess emission indicates little or no circumstellar dust

Class 0

Class I

Class II

Class III



credit: Jacqueline Kessler-Silacci

Circumstellar disks

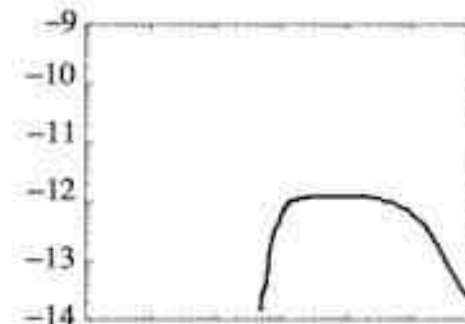


Evolution of young stellar objects

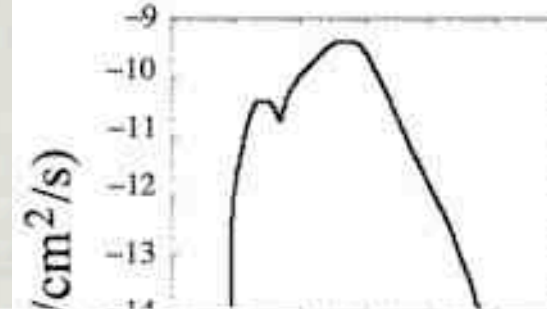
- Classification scheme of YSO's (Lada 1987)

- ➡ Class 0: only submm-emission which indicates a deep embedded object
- ➡ Class I: steep positive spectral slope due to the presence of large amounts of circumstellar dust
- ➡ Class II: negative spectral slope indicates less dust than class I sources
- ➡ Class III: the weak mid- and near-infrared excess emission indicates little or no circumstellar dust

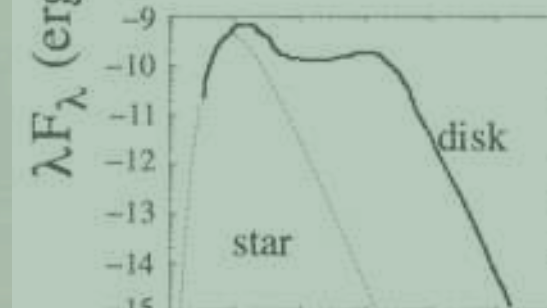
Class 0



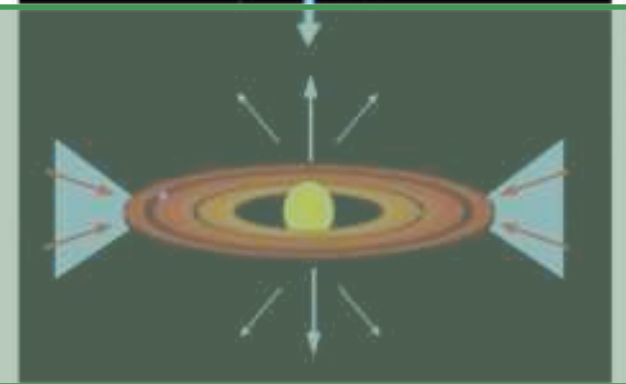
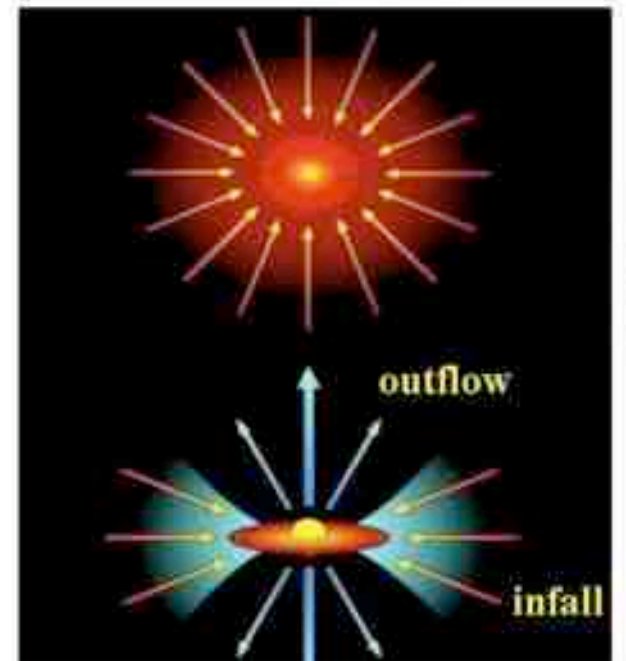
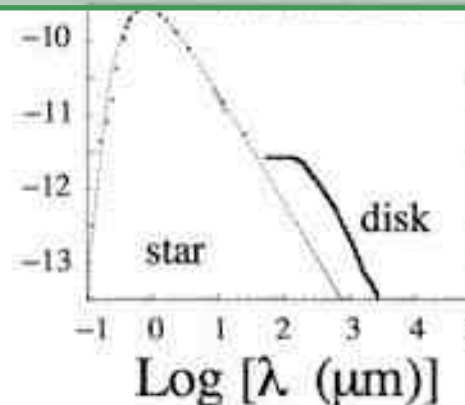
Class I



Class II



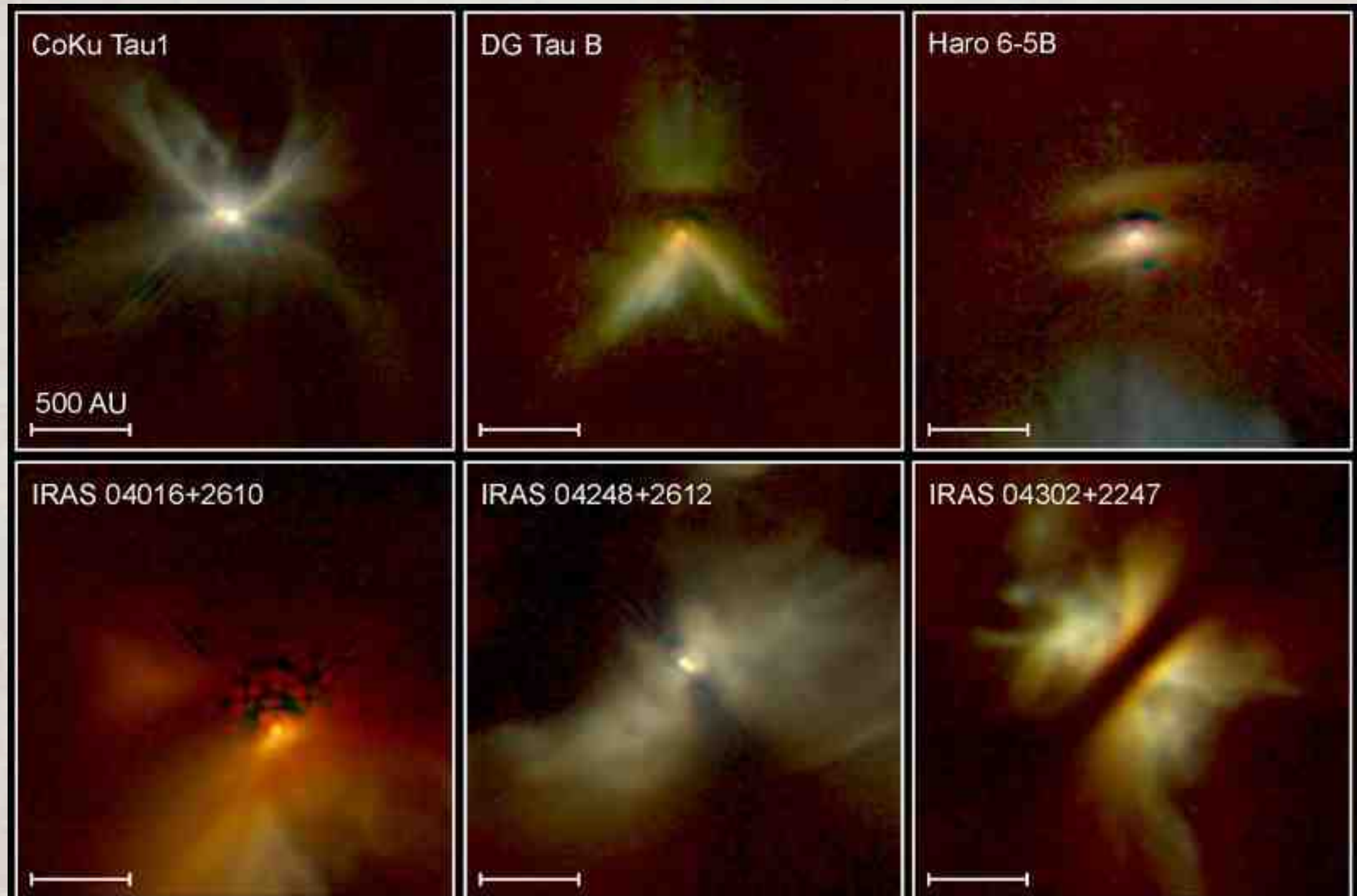
Class III



credit: Jacqueline Kessler-Silacci

Circumstellar disks

Circumstellar disks are visually detected



Young Stellar Disks in Infrared

HST • NICMOS

PRC99-05a • STScI OPO

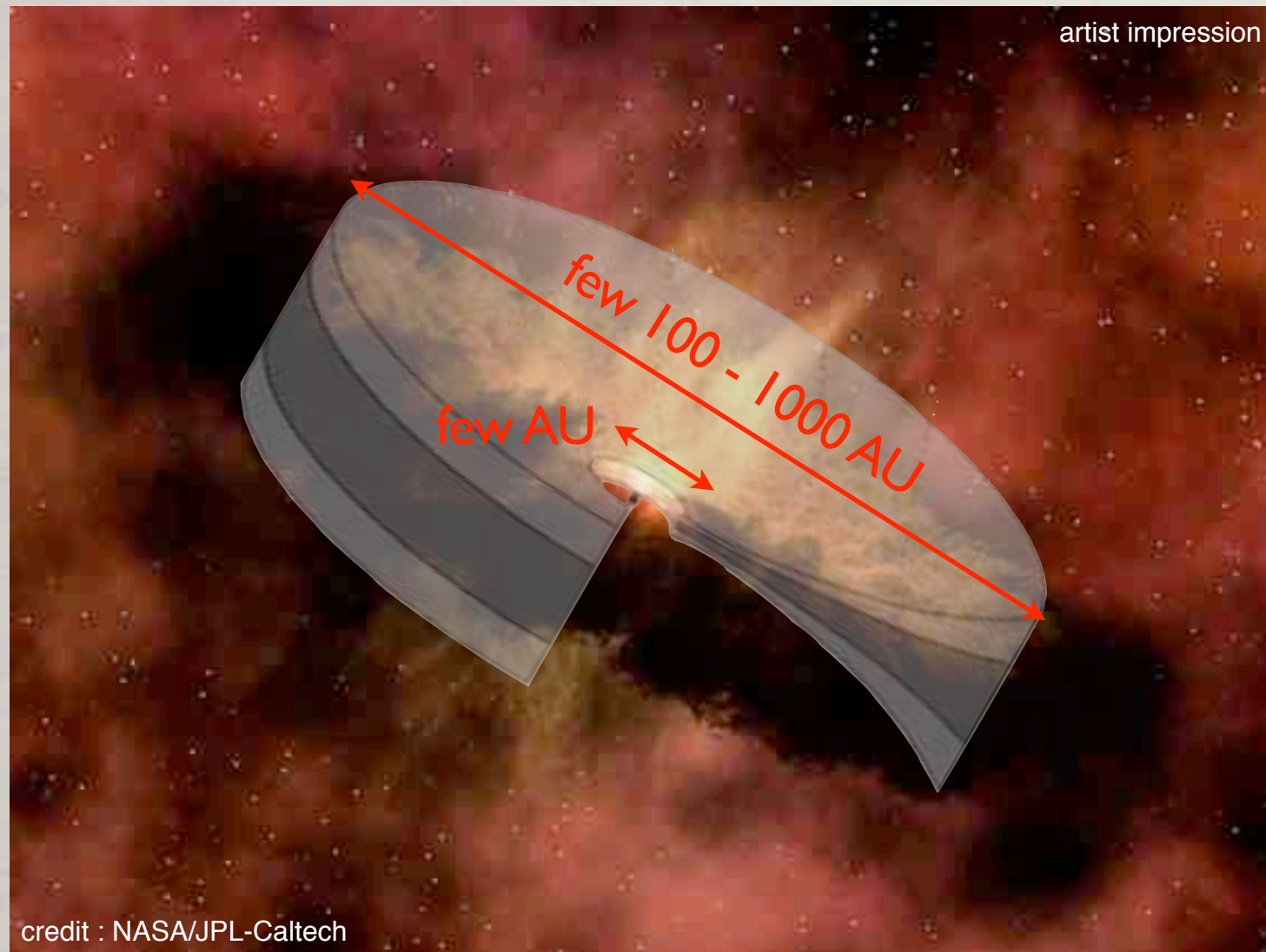
D. Padgett (IPAC/Caltech), W. Brandner (IPAC), K. Stapelfeldt (JPL) and NASA

Circumstellar disks



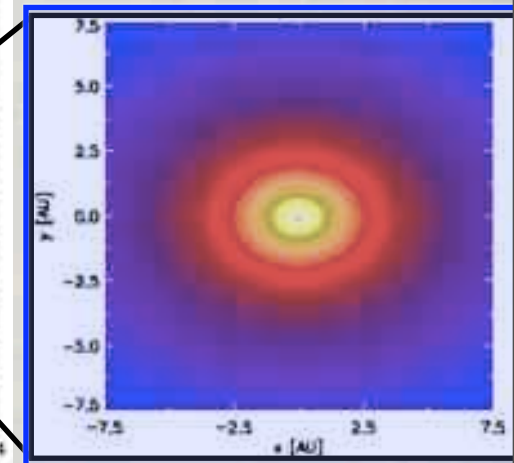
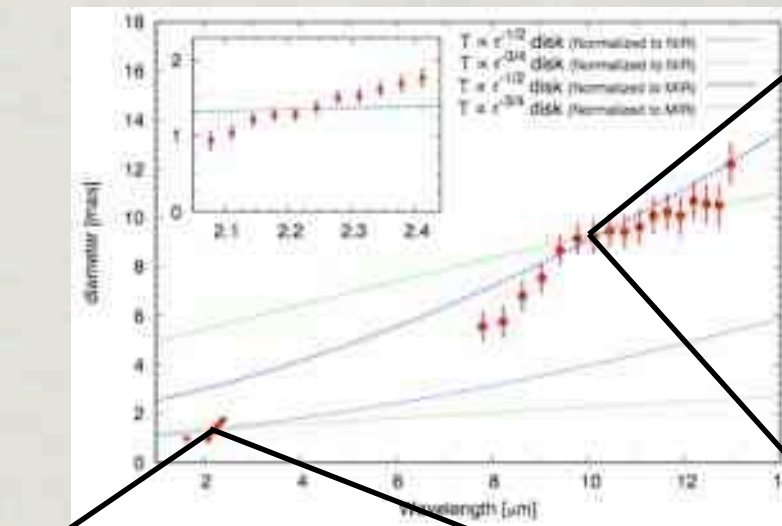
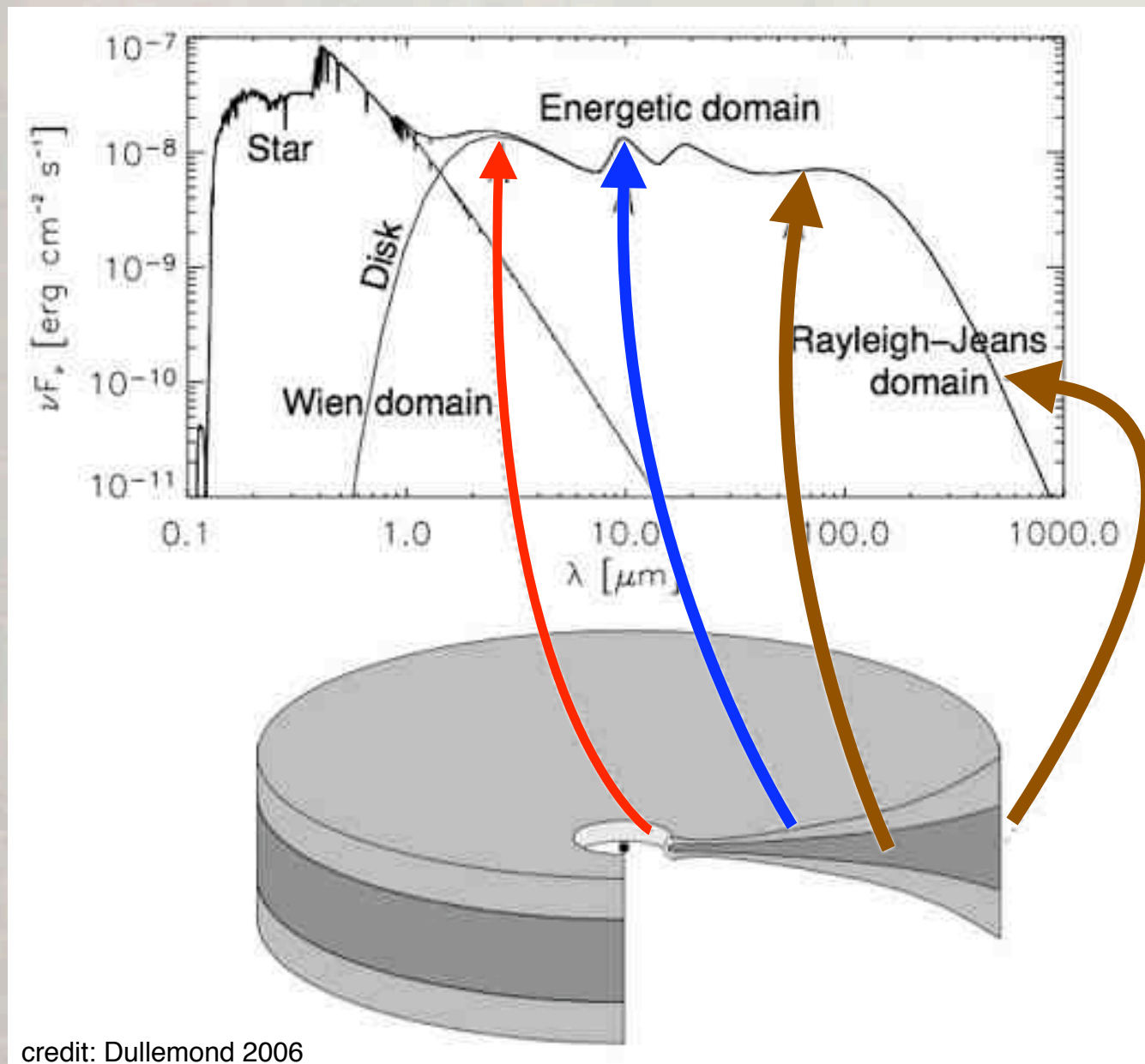
- Protostar is surrounded by a circumstellar dust and gas disk
 - ➡ disks also detected in the case of intermediate-mass stars (Millan-Gabet 2000)
- Since the nearest star forming regions are about 140 pc away, high angular resolution is required ($1 \text{ AU} \approx 7 \text{ mas}$)
 - ➡ Interferometry
(e.g. with a 200 m baseline at $\lambda = 2.2 \mu\text{m}$ one gets an angular resolution of $\alpha = 2.7 \text{ mas}$)
- Observations at different wavelengths provide information about different regions of the disk !
 - ➡ Multiwavelength analysis required to study the whole disk

Circumstellar disks



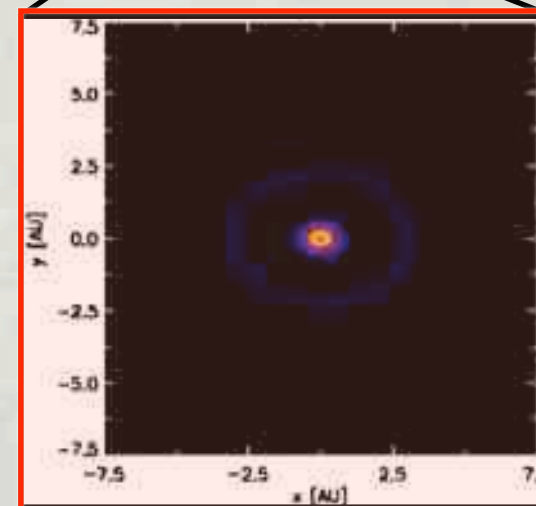
- Protostar is surrounded by a circumstellar dust and gas disk
 - ➡ disks also detected in the case of intermediate-mass stars (Millan-Gabet 2000)
 - Since the nearest star forming regions are about 140 pc away, high angular resolution is required ($1 \text{ AU} \approx 7 \text{ mas}$)
 - ➡ Interferometry
(e.g. with a 200 m baseline at $\lambda = 2.2 \mu\text{m}$ one gets an angular resolution of $\alpha = 2.7 \text{ mas}$)
- Observations at different wavelengths provide information about different regions of the disk !
 - ➡ Multiwavelength analysis required to study the whole disk

Circumstellar disks

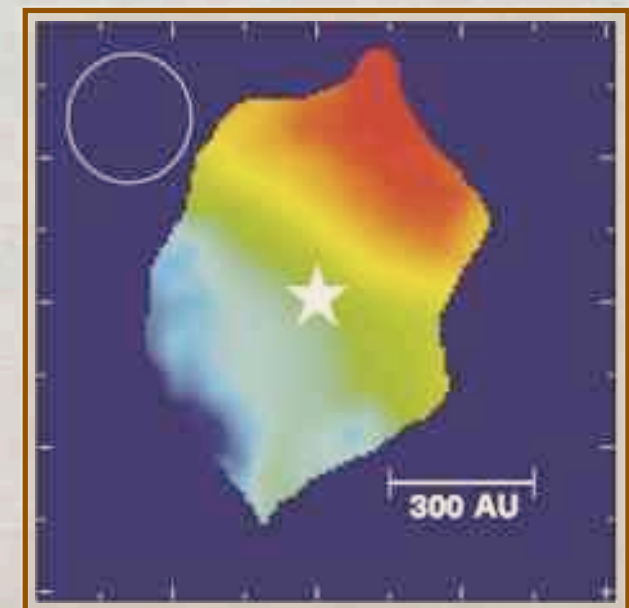


MWC 147

Kraus et al. 2007, A&A



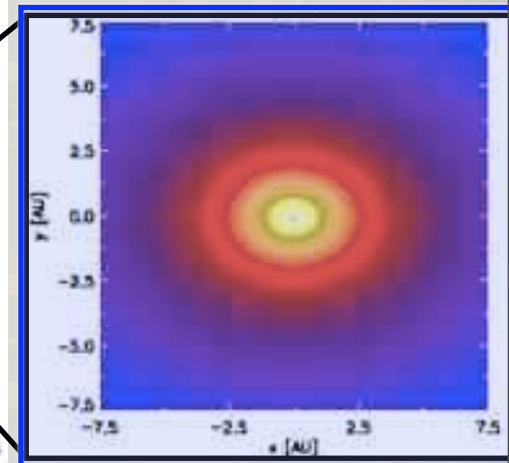
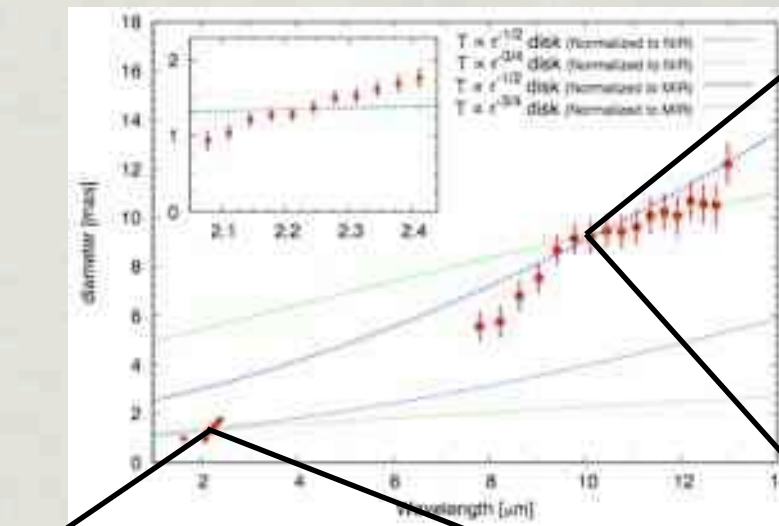
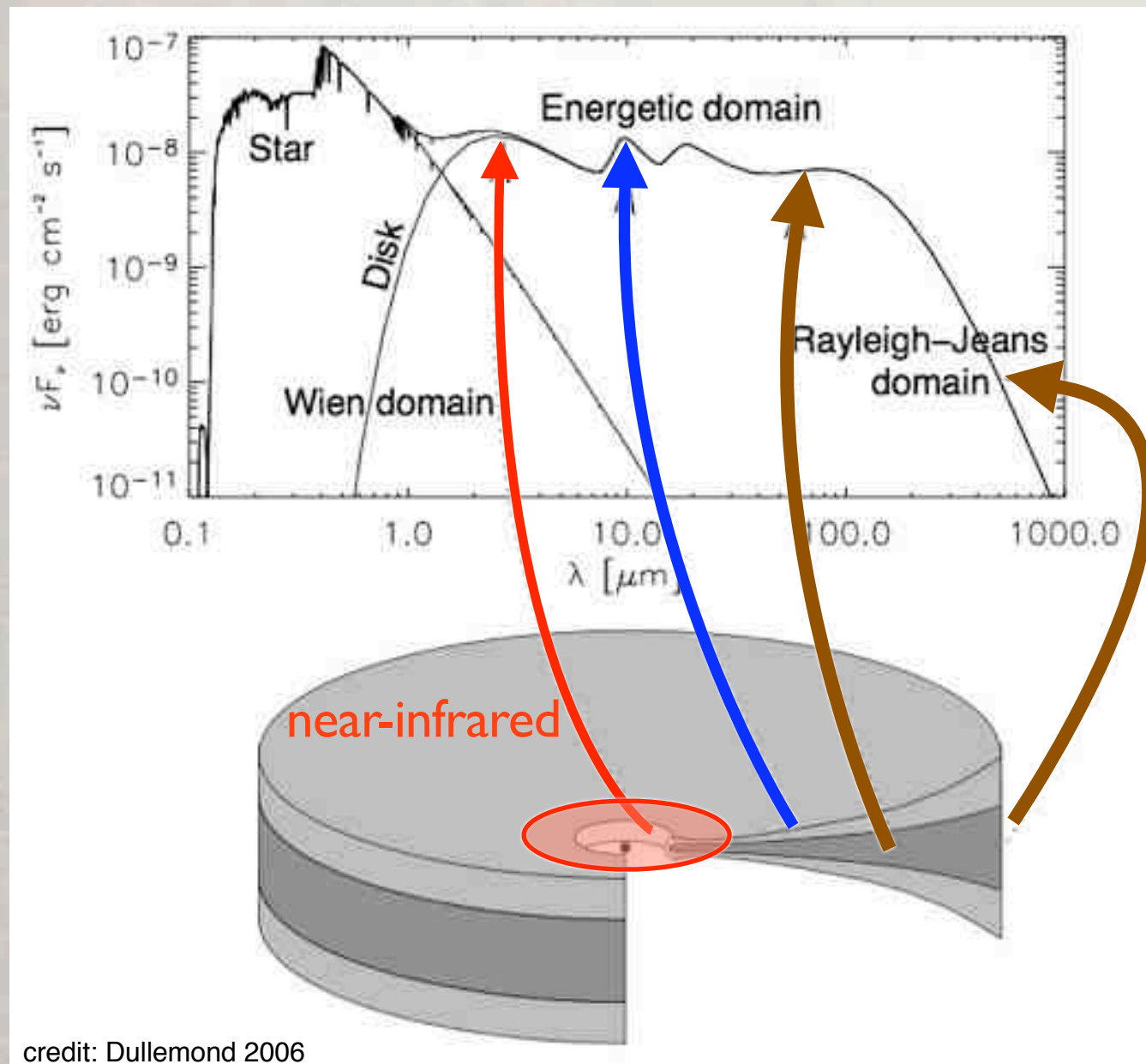
MWC 480



Mannings 1997, Nature

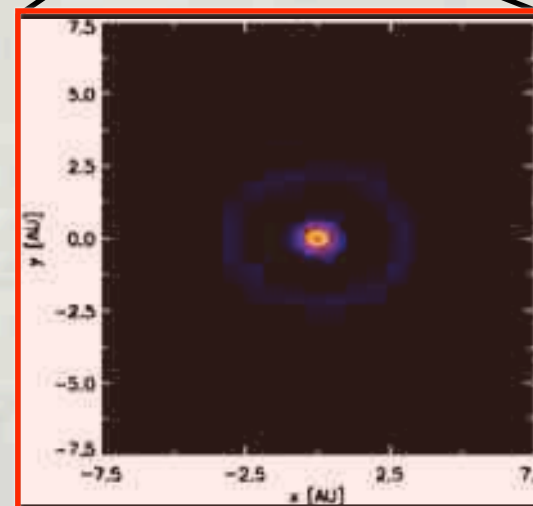
- Open Questions:
- ➡ What is the shape of the inner rim ?
 - puffed-up rim (Dullemond et al. 2001)
 - curved rim (Isella et al. 2002)
 - ➡ Flaring behaviour of the disk ?
 - self-shadowed disk

Circumstellar disks

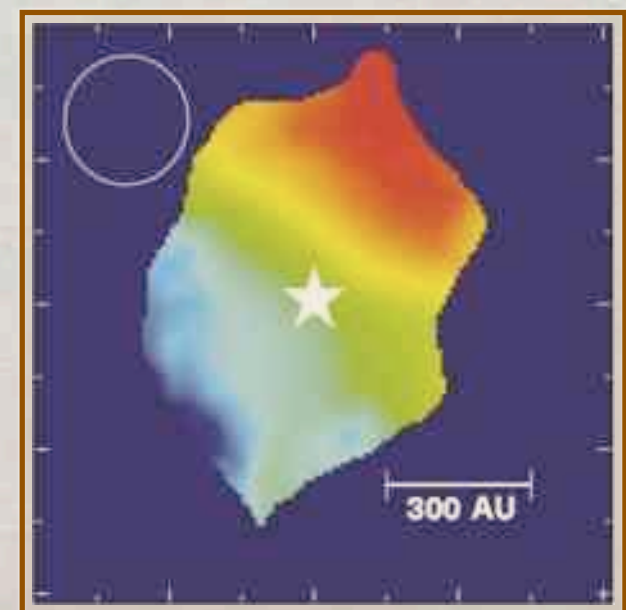


MWC 147

Kraus et al. 2007, A&A



MWC 480



Mannings 1997, Nature

- Open Questions:
- ➡ What is the shape of the inner rim ?
 - puffed-up rim (Dullemond et al. 2001)
 - curved rim (Isella et al. 2002)
 - ➡ Flaring behaviour of the disk ?
 - self-shadowed disk

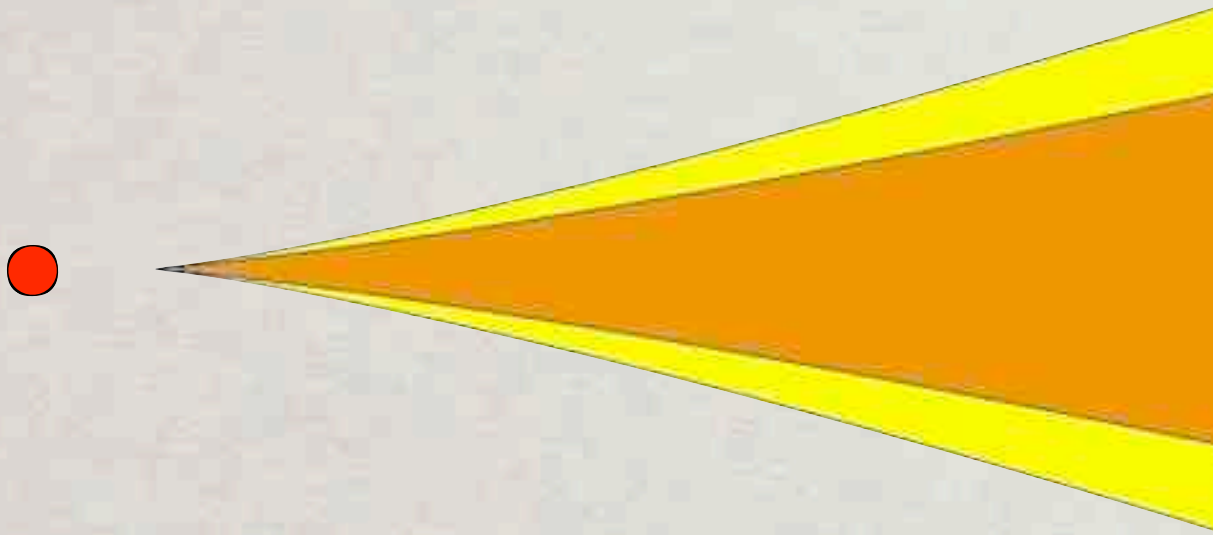
Outline



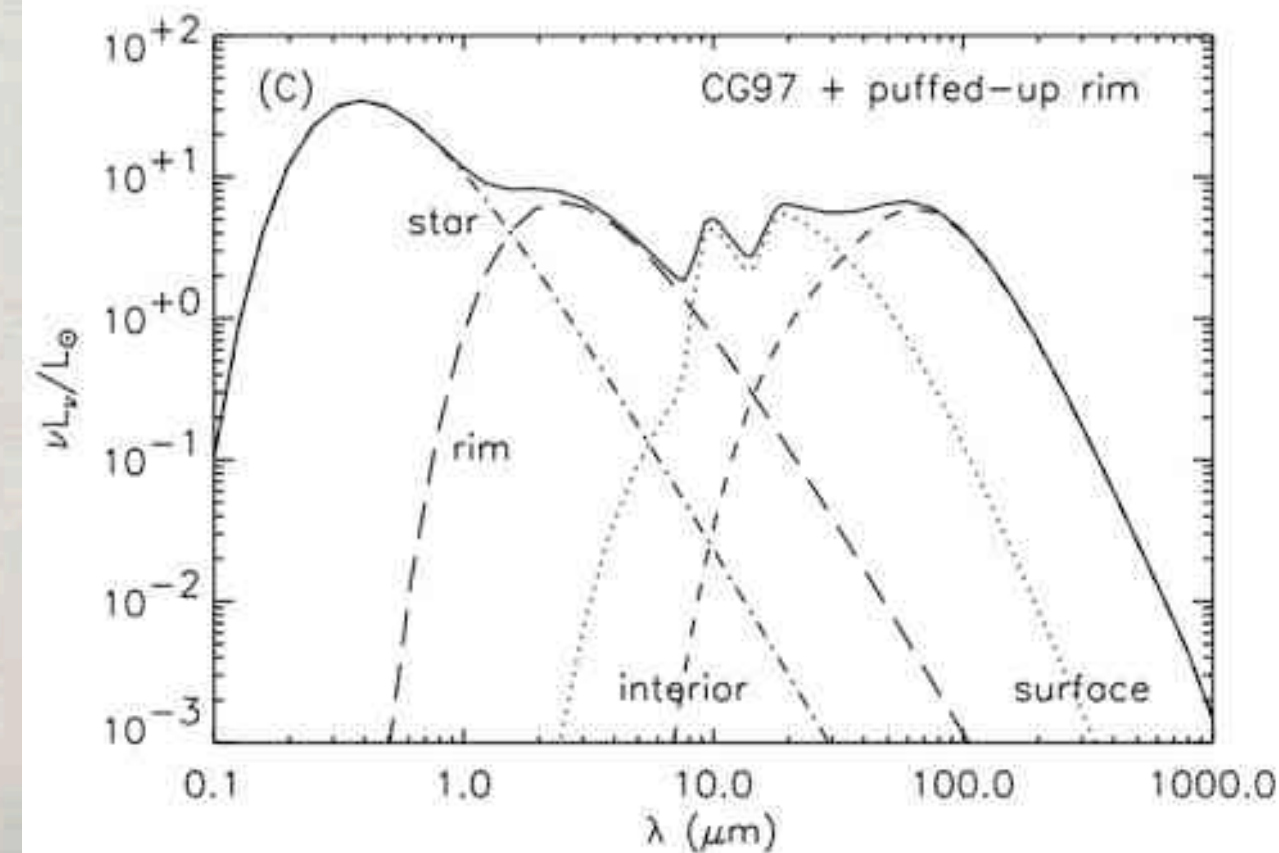
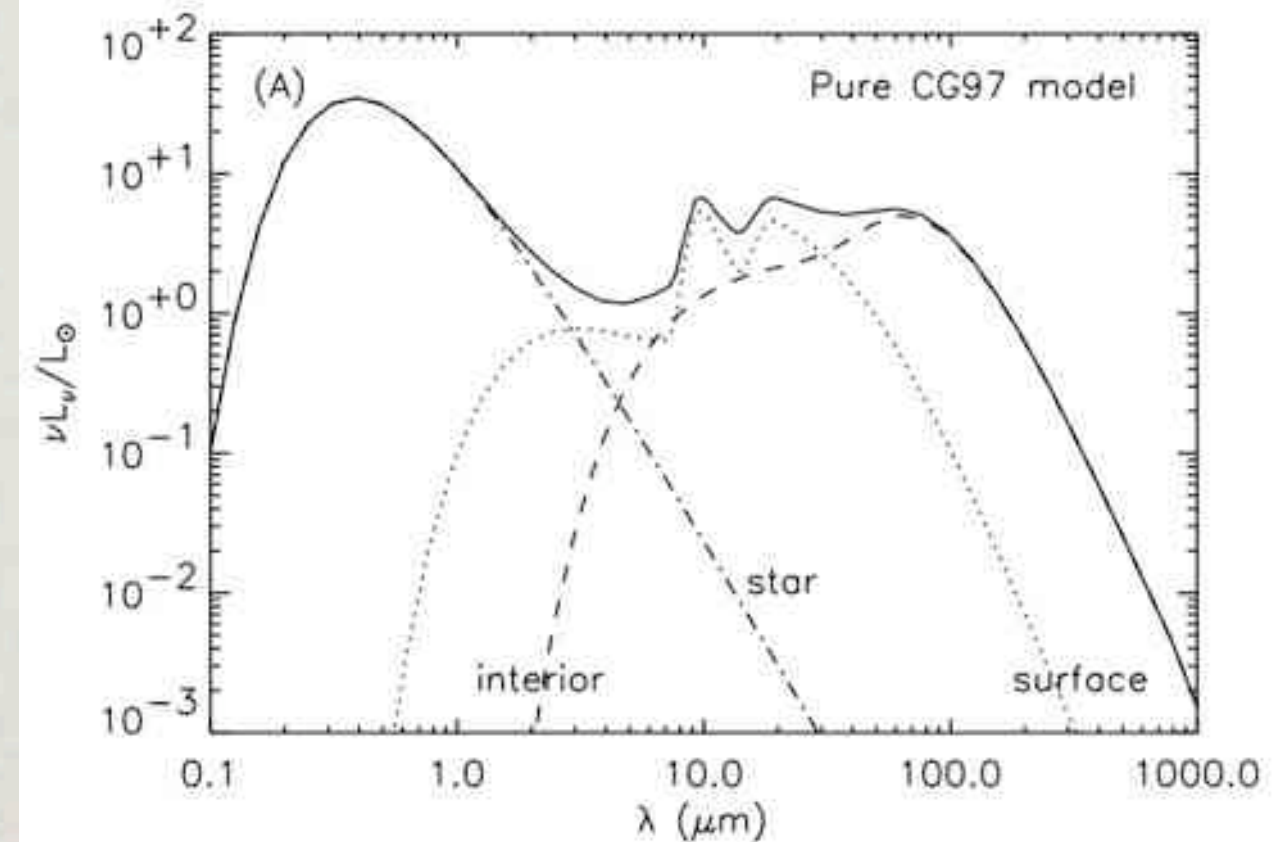
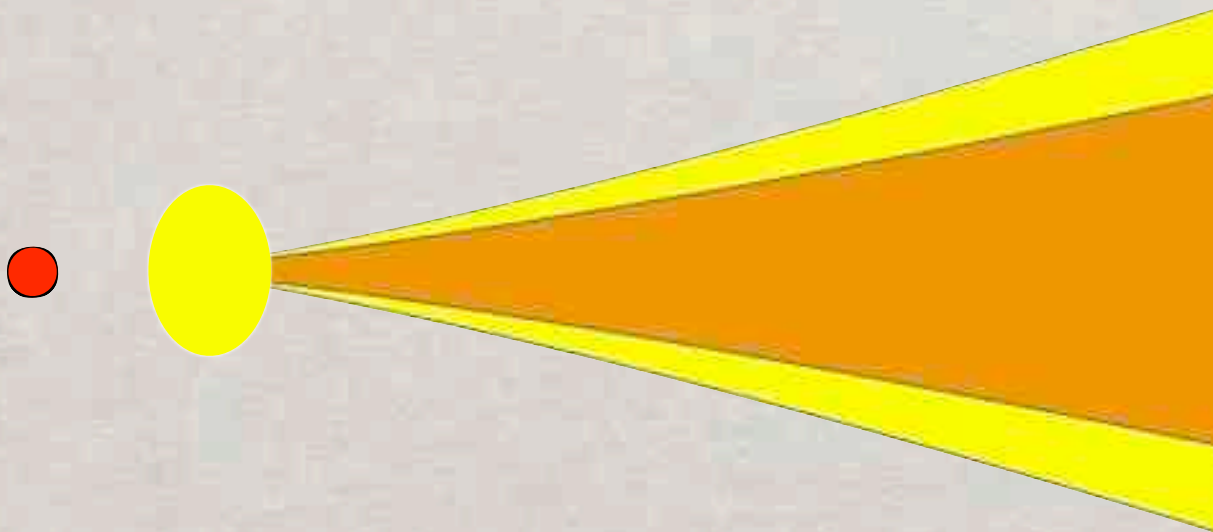
- Overview: circumstellar disks
- **Disk models**
- The inner rim
- Observational techniques: V921 Sco
- Future Instruments
- Summary

Disk models

- Chiang-Goldreich model (C & G 1997)



- Puffed-up inner model (Dullemond et al. 2001)



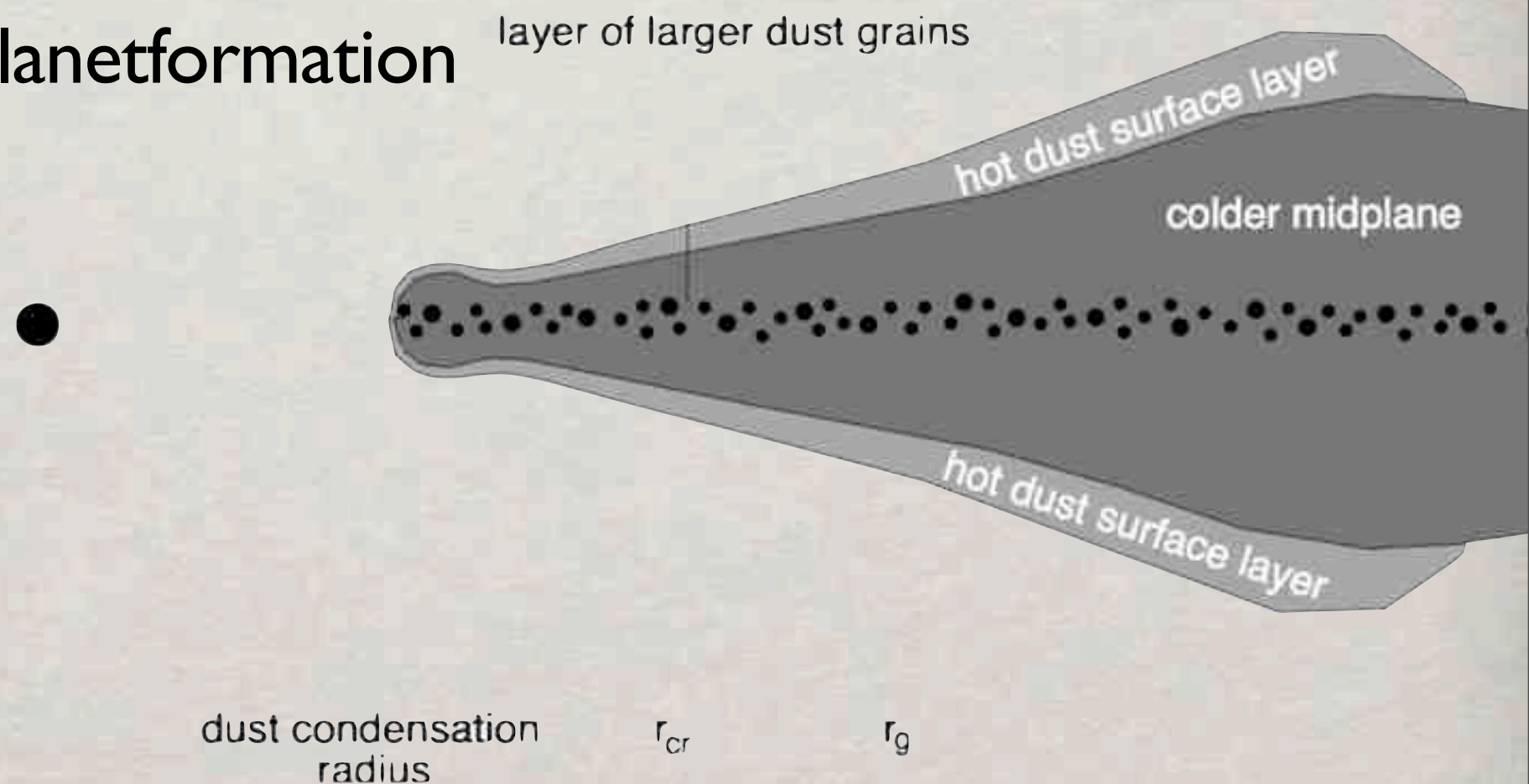
Dust disk



- Dust settling in the cooler mid-plane
 - grain growth
- Photoevaporation removes gas from disk
 - influences planetformation

- dust particles follow the gas flow

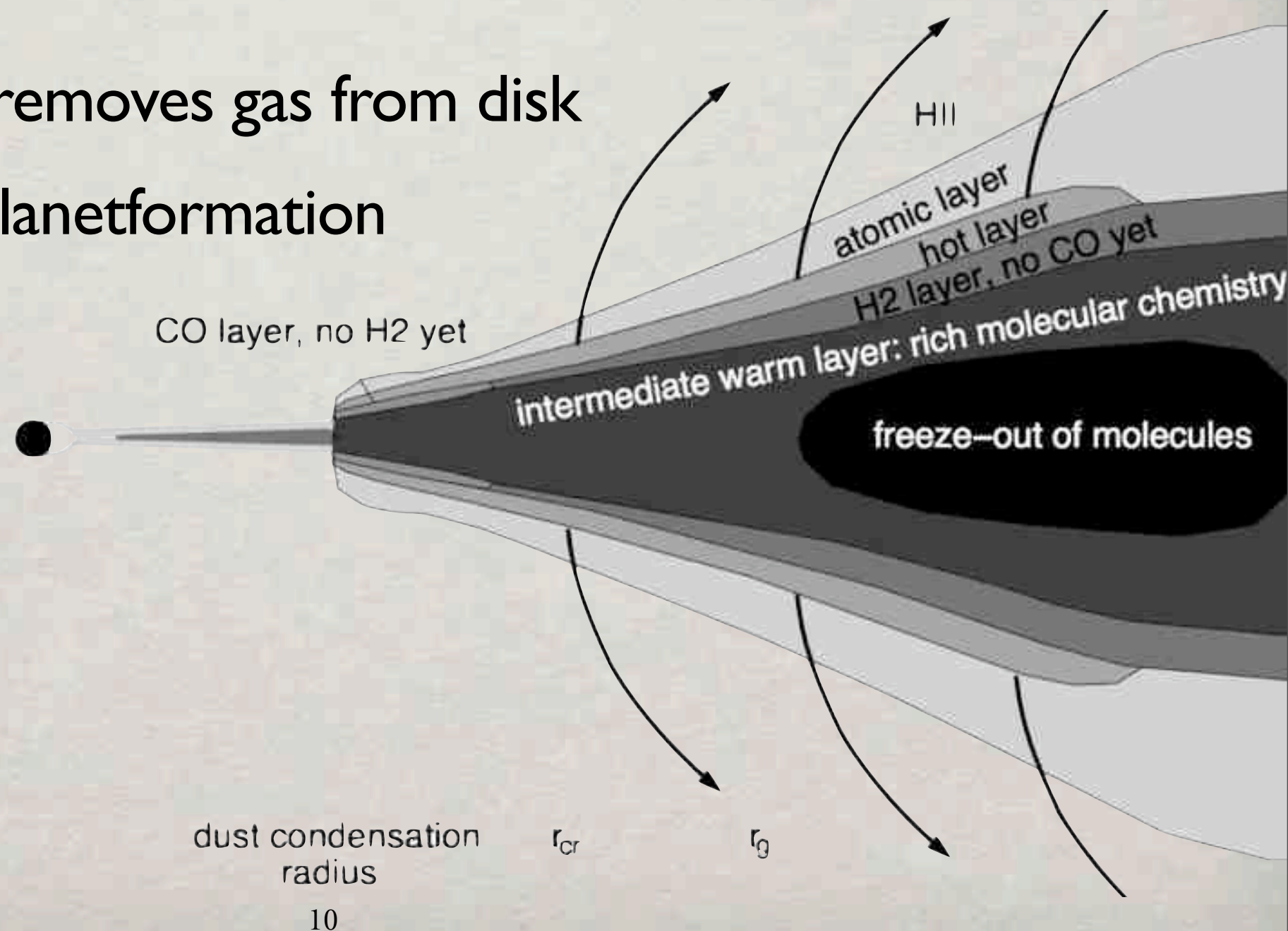
- formation of gas planets is suppressed



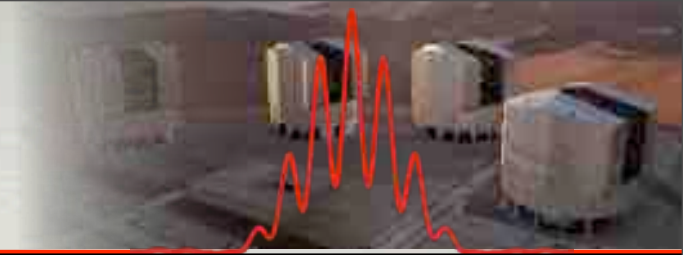
Gas disk



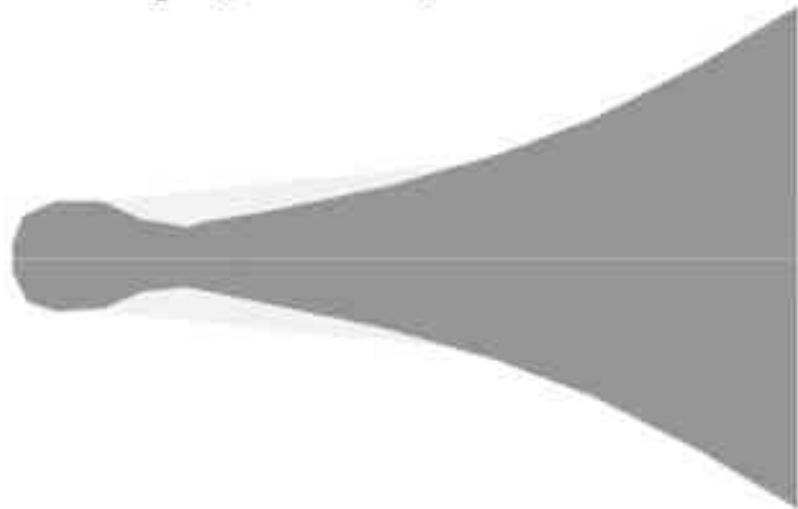
- Dust settling in the cooler mid-plane
 - grain growth
- Photoevaporation removes gas from disk
 - influences planetformation
- dust particles follow the gas flow
- formation of gas planets is suppressed



Shadowing or planetary gap ?



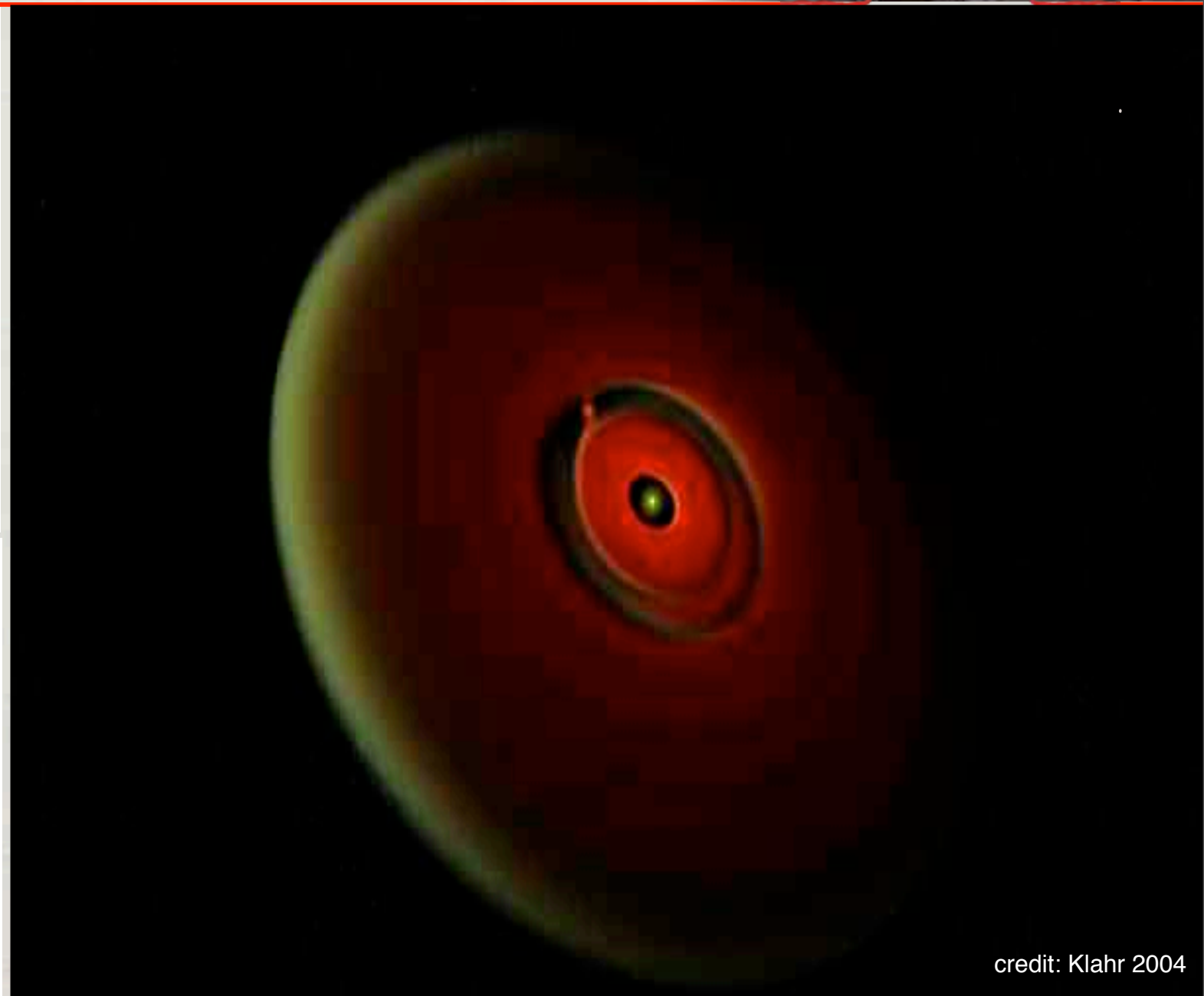
Group I (flared disk)



Group II (self-shadowed disk)



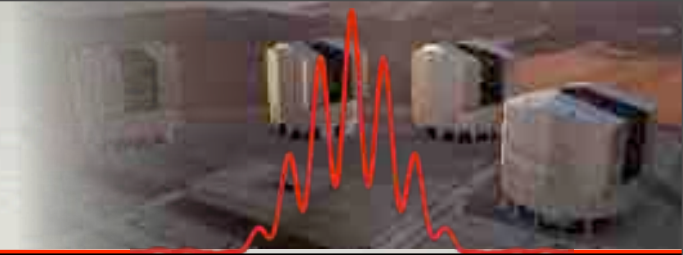
credit: Dullemond 2004



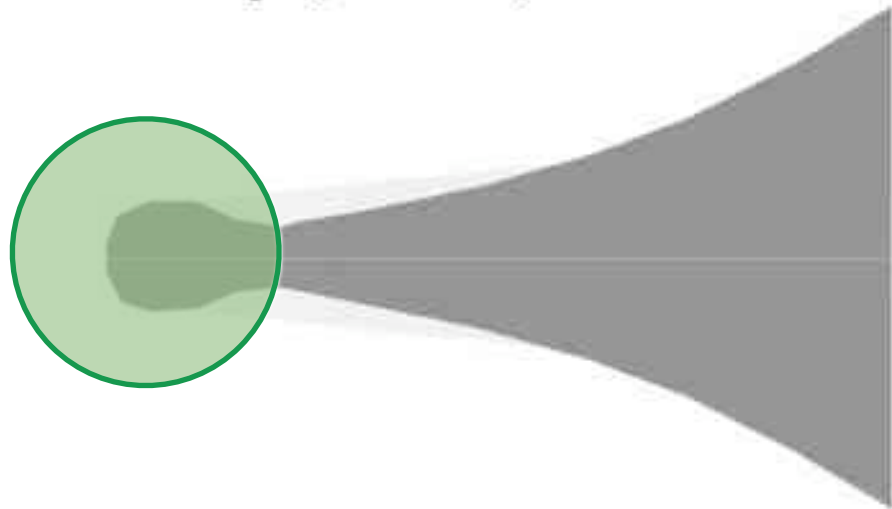
credit: Klahr 2004

- Puffed-up inner rim leads to shadowing of parts of the disk
→ detectable, but still confusion with planetary gaps

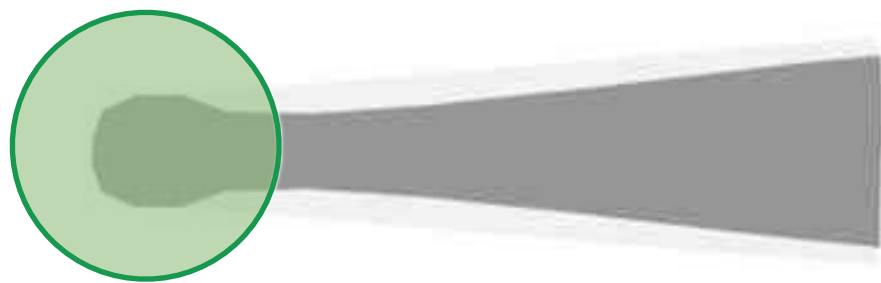
Shadowing or planetary gap ?



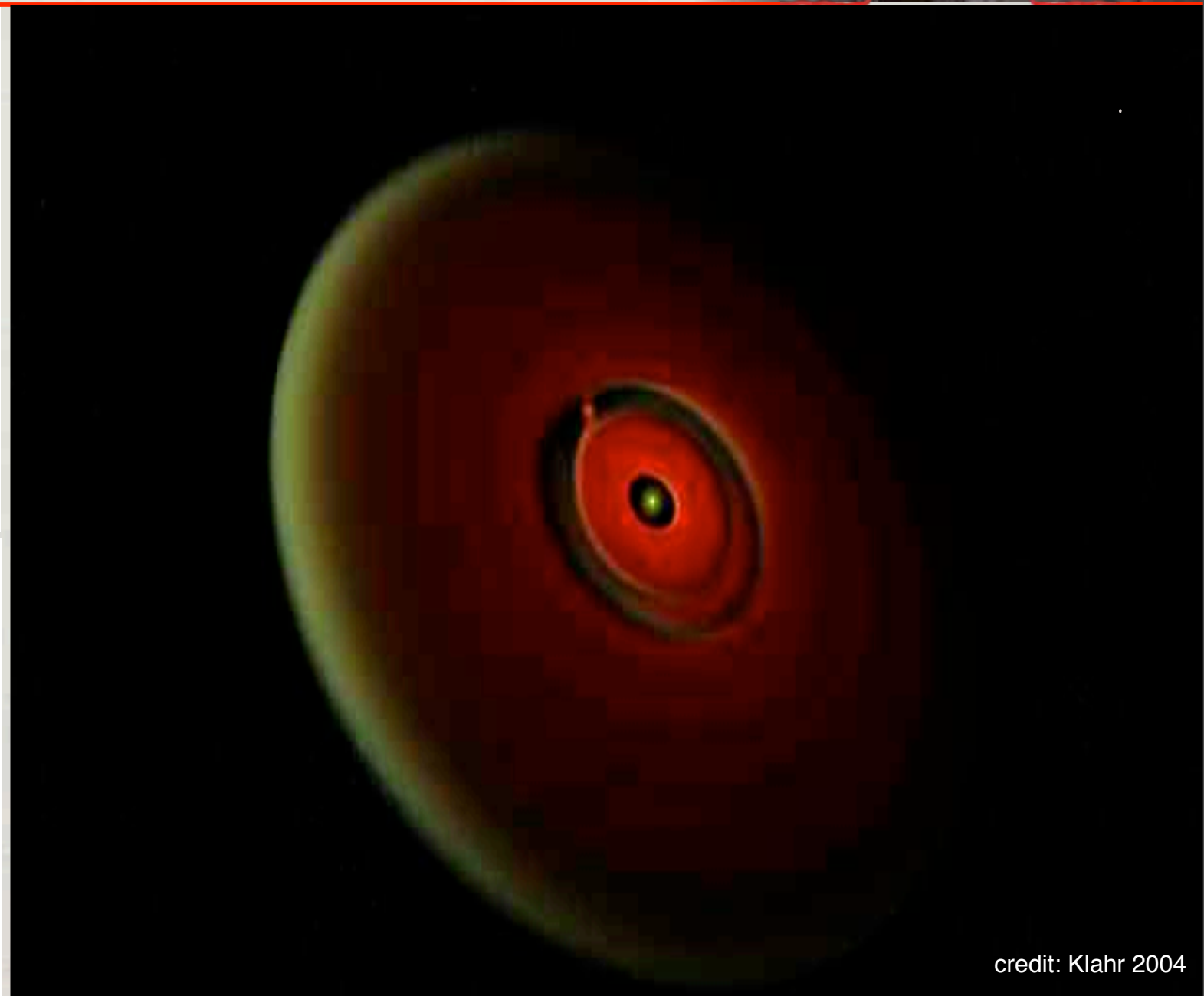
Group I (flared disk)



Group II (self-shadowed disk)



credit: Dullemond 2004



credit: Klahr 2004

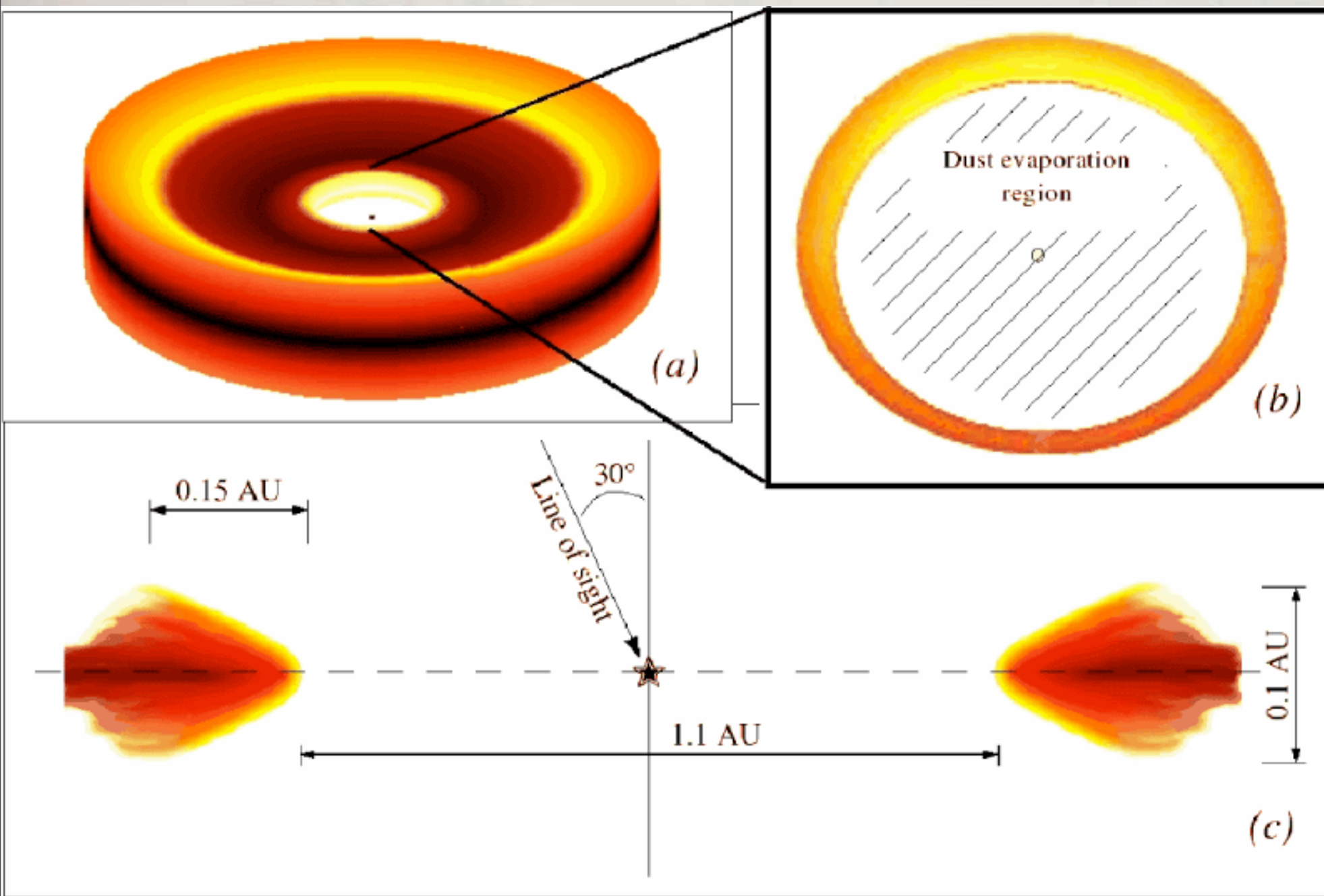
- Puffed-up inner rim leads to shadowing of parts of the disk
→ detectable, but still confusion with planetary gaps



- Overview: circumstellar disks
- Disk models
- **The inner rim**
- Observational techniques: V921 Sco
- Future Instruments
- Summary

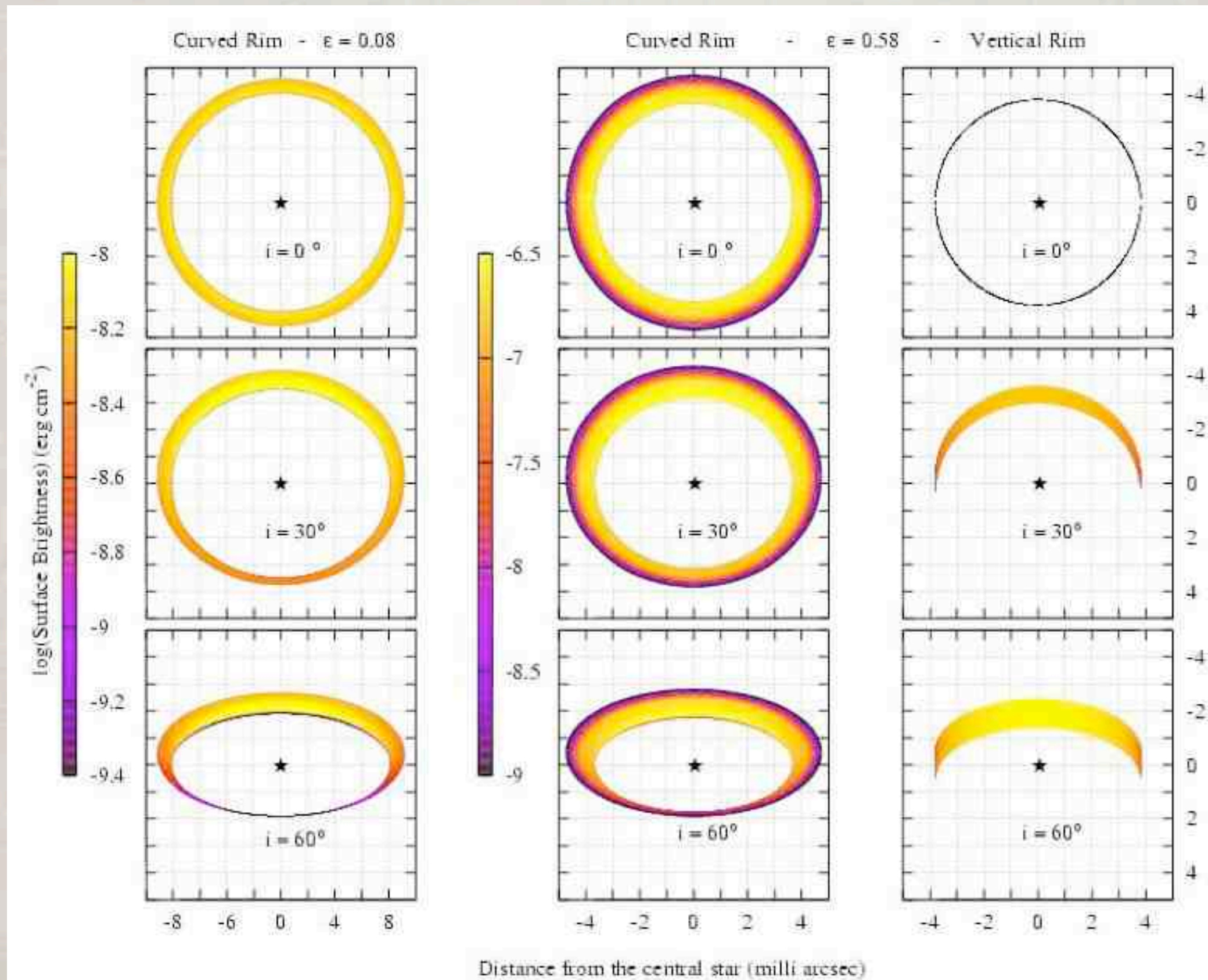
The inner rim

- The inner rim should be curved and NOT be vertical



Isella et al. 2007

The inner rim

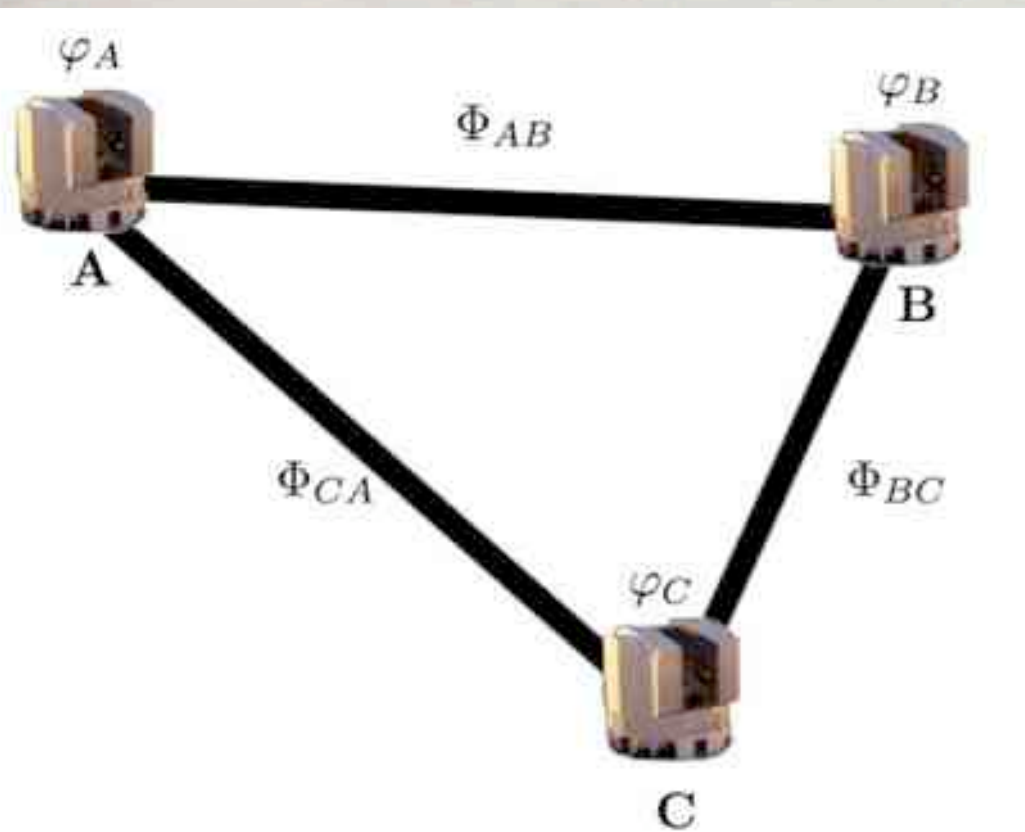


Isella et al. 2005

The inner rim

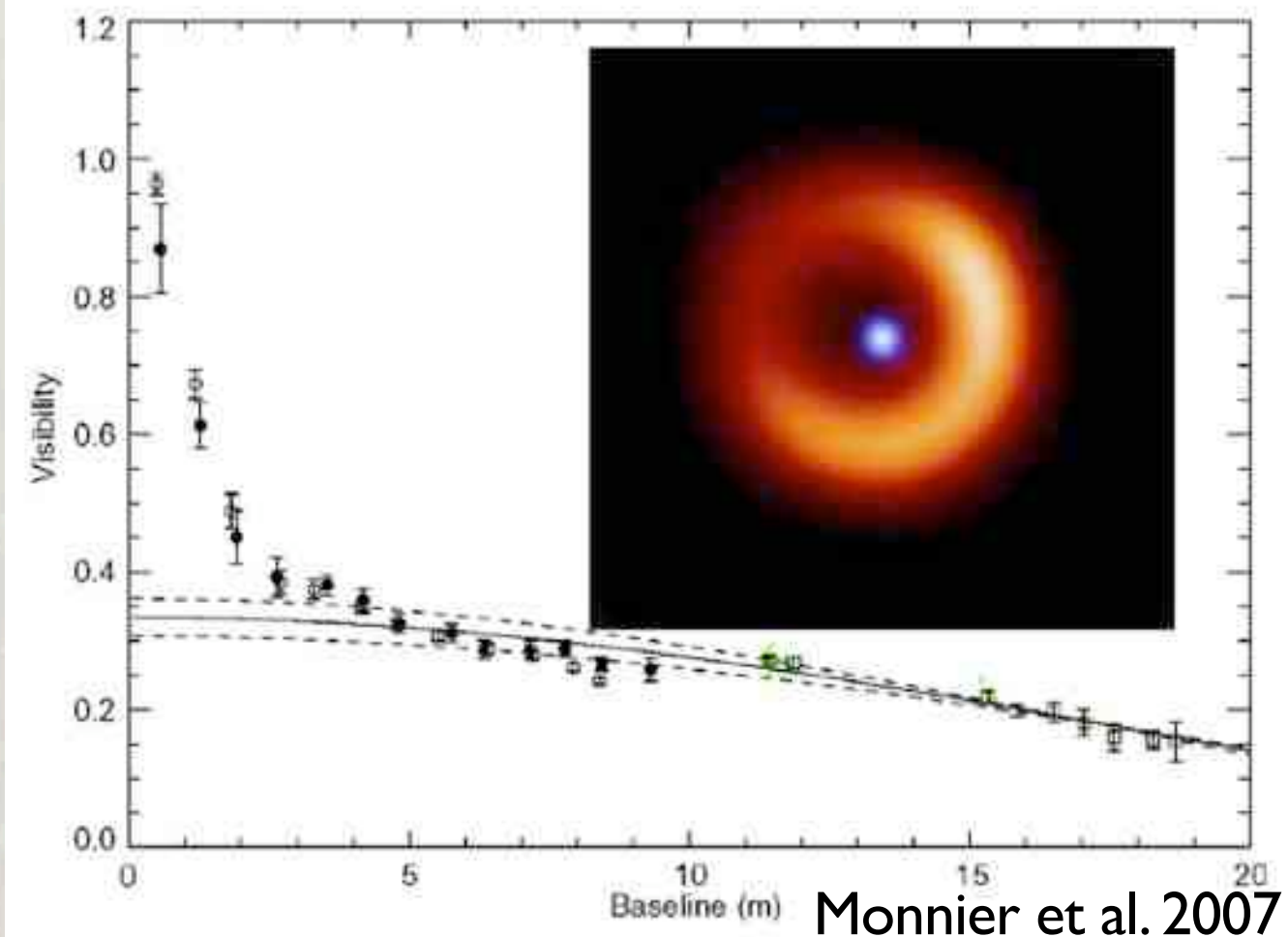
- Closure phases contain information about the inner rim

→ CP measures the degree of asymmetry of the brightness distribution on the sky



$$\begin{aligned}\tilde{\Phi}_{AB} &:= \Phi_{AB} + \varphi_B - \varphi_A \\ \tilde{\Phi}_{BC} &:= \Phi_{BC} + \varphi_C - \varphi_B \\ \tilde{\Phi}_{CA} &:= \Phi_{CA} + \varphi_A - \varphi_C\end{aligned}$$

$$\begin{aligned}\Phi_{CP} &:= \tilde{\Phi}_{AB} + \tilde{\Phi}_{BC} + \tilde{\Phi}_{CA} \\ &= \Phi_{AB} + \varphi_B - \varphi_A + \Phi_{BC} + \varphi_C - \varphi_B + \Phi_{CA} + \varphi_A - \varphi_C \\ &= \Phi_{AB} + \Phi_{BC} + \Phi_{CA}\end{aligned}$$



Monnier et al. 2007



- Overview: circumstellar disks
- Disk models
- The inner rim
- **Observational techniques: V921 Sco**
- Future Instruments
- Summary

Observational techniques

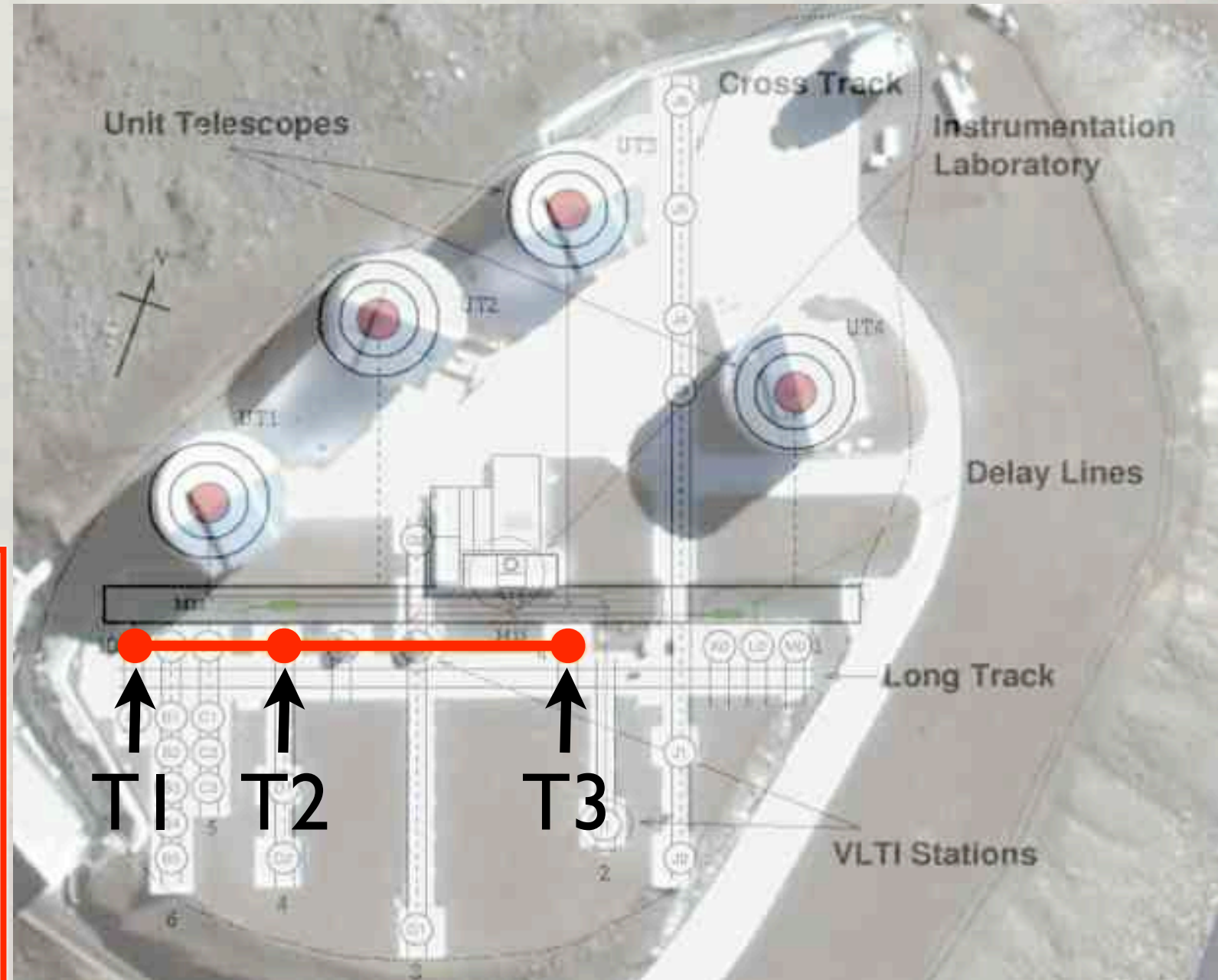
Very Large Telescope Interferometer (VLTI)

Dates: 2007-05-13
2007-05-14

Telescopes: 3 AT's in a linear
configuration

Aperture: 1.8 m

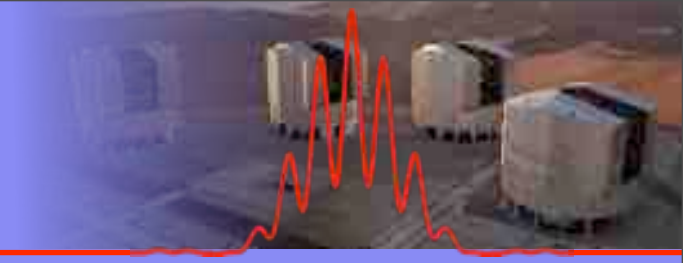
Baselines: 32 m, 64m, 96 m



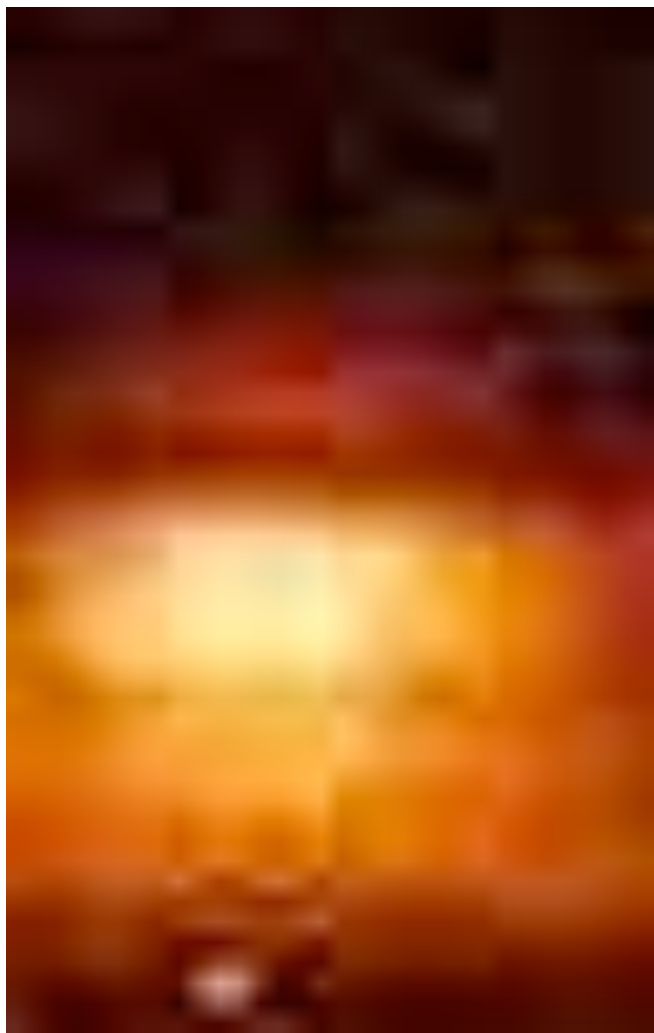
credit: Google Earth



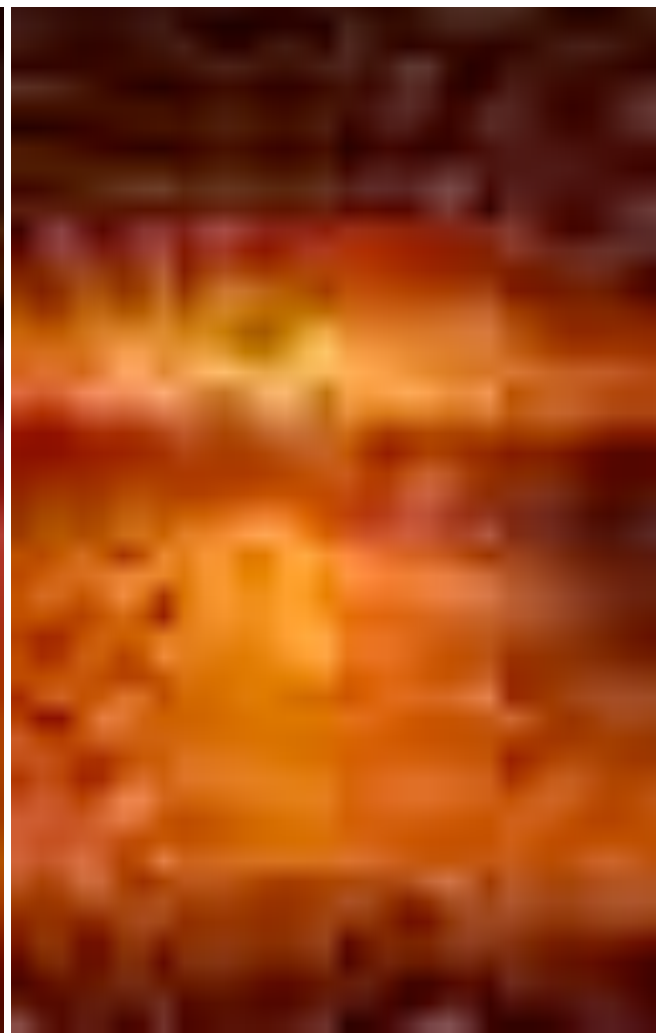
AMBER instrument



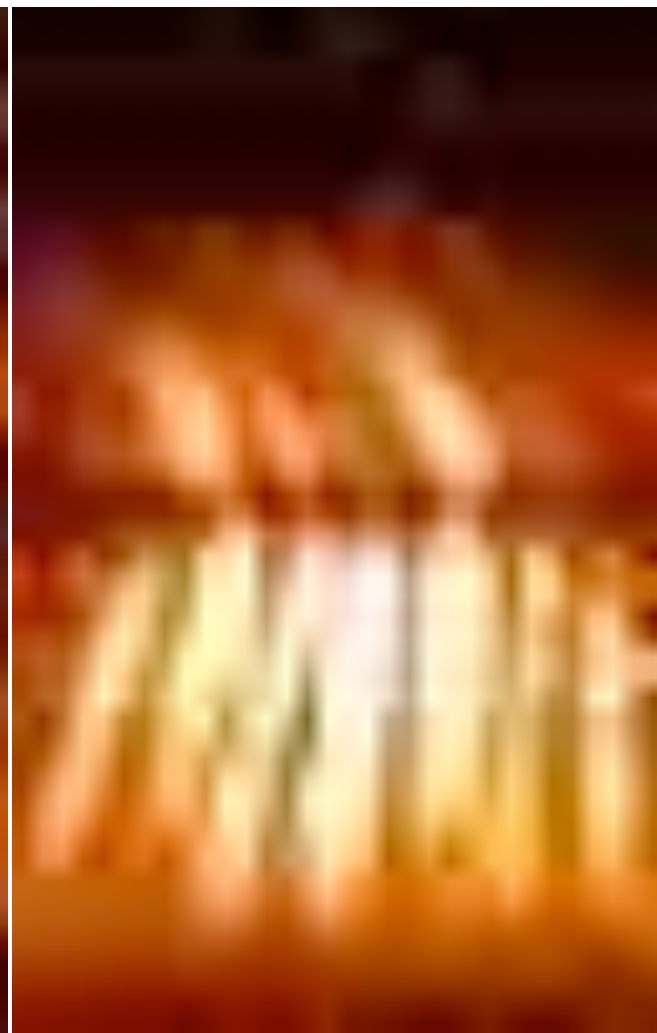
AMBER produces spectrally dispersed Michelson Interferograms



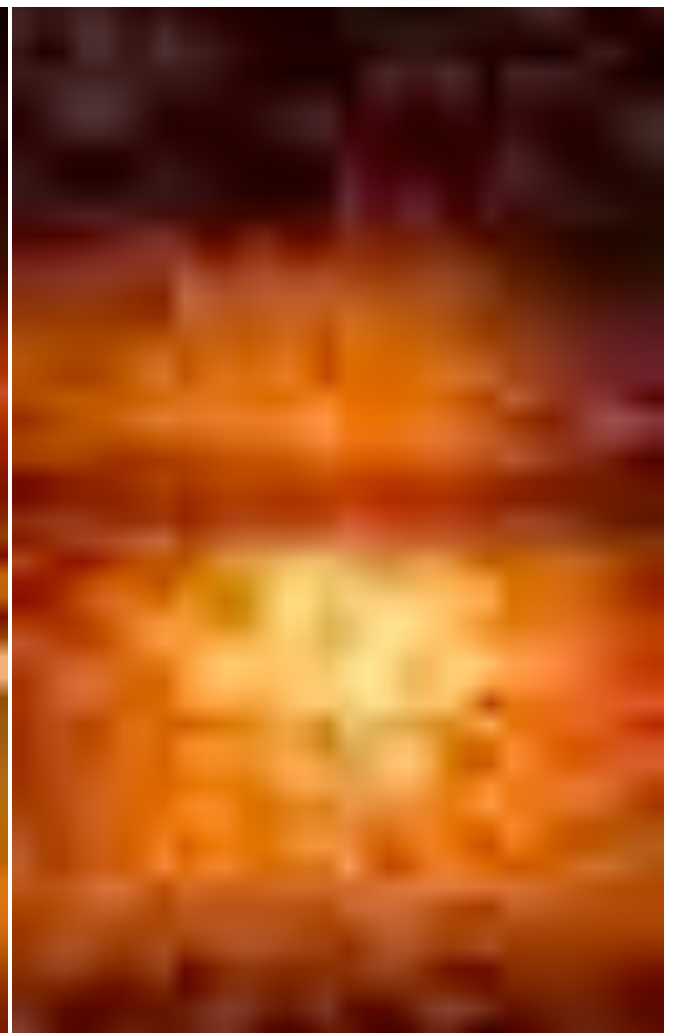
photometric
beam 1



photometric
beam 2



interferometric
beam



photometric
beam 3

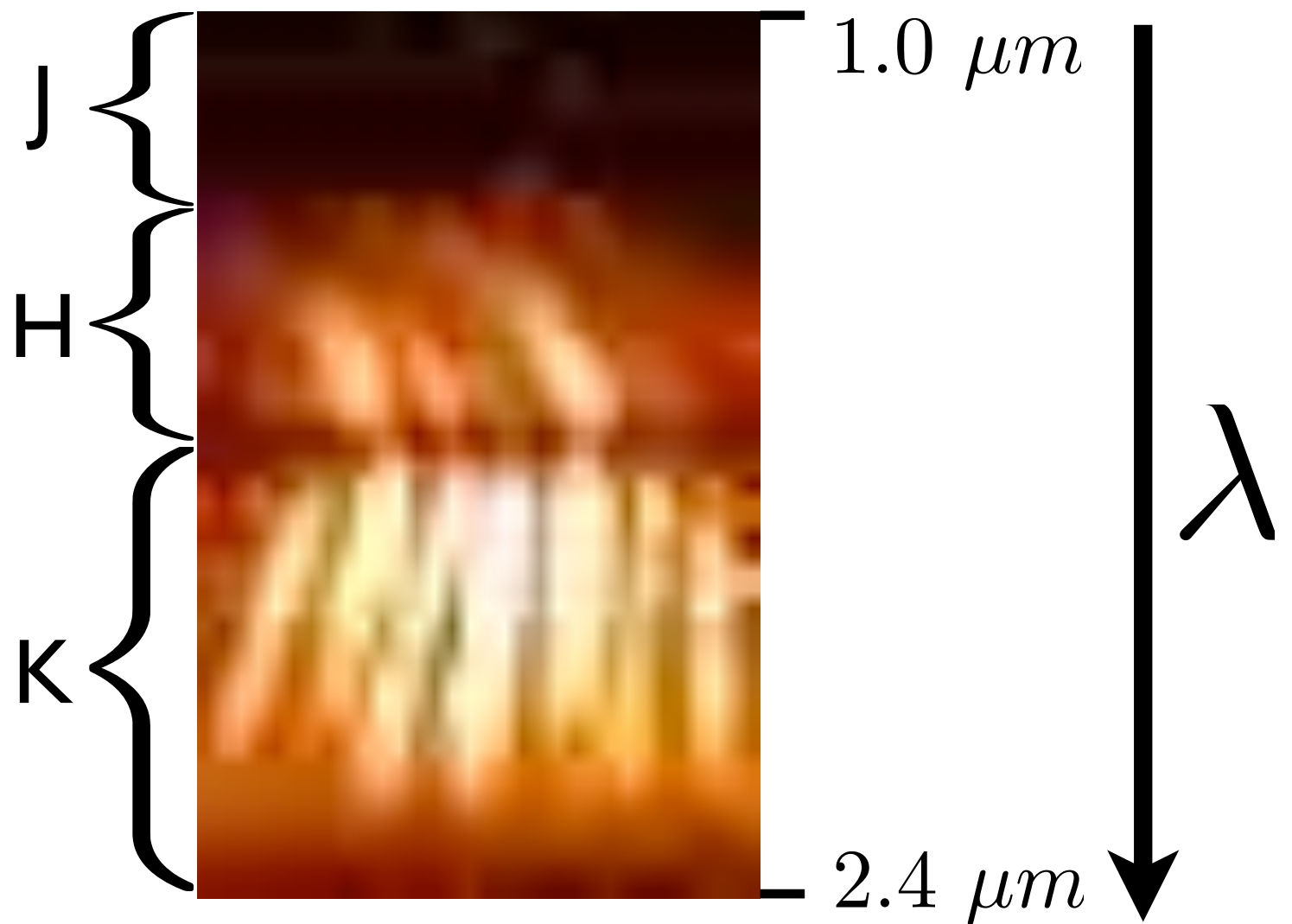


AMBER provides different spectral resolution modes

HIGH ($R = 12000$)

MEDIUM ($R = 1500$)

LOW ($R = 30$)

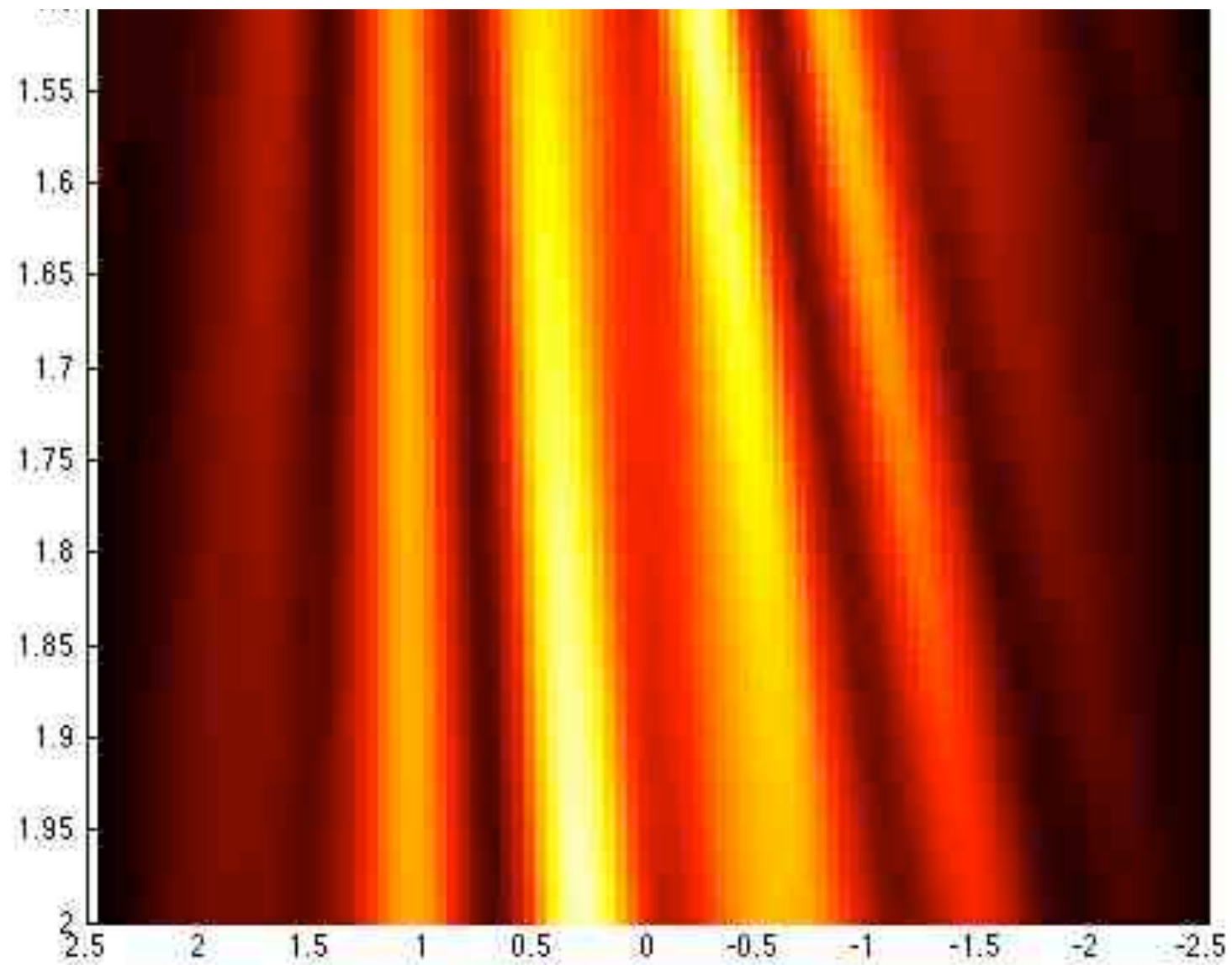
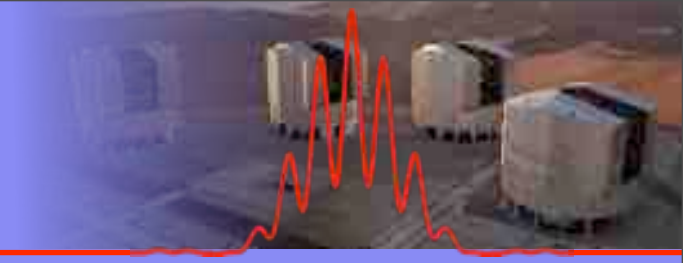


➡ observation carried out in LOW resolution

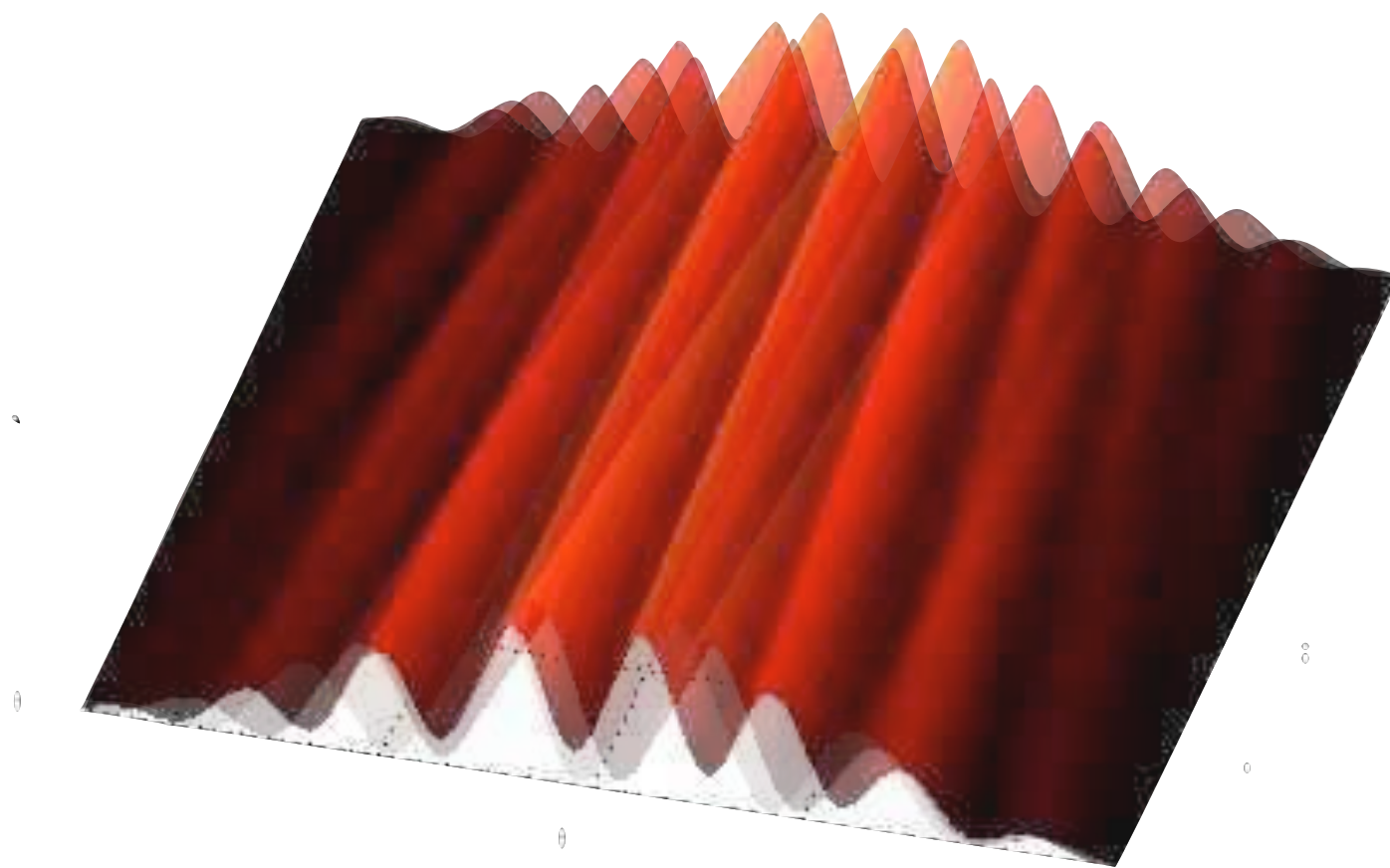
Observational techniques



Observational techniques



Interferometric Observations with AMBER/VLTI



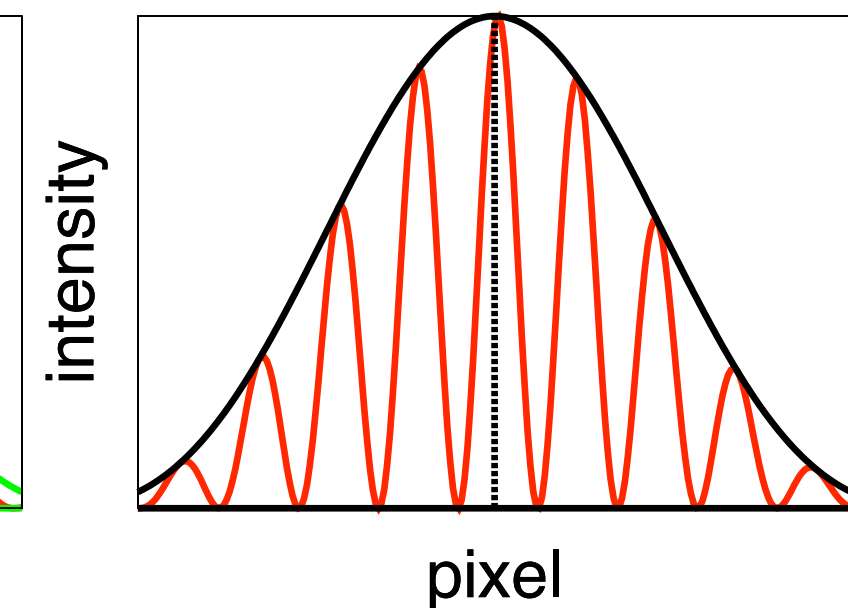
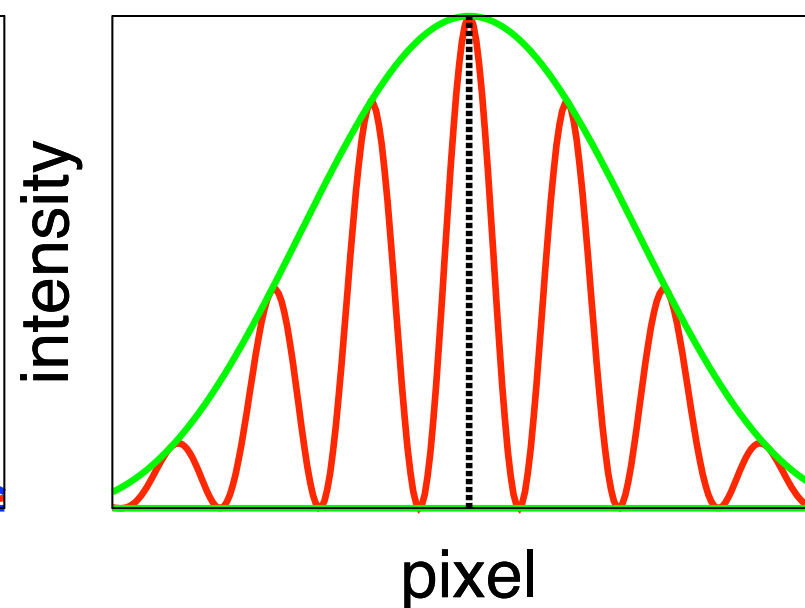
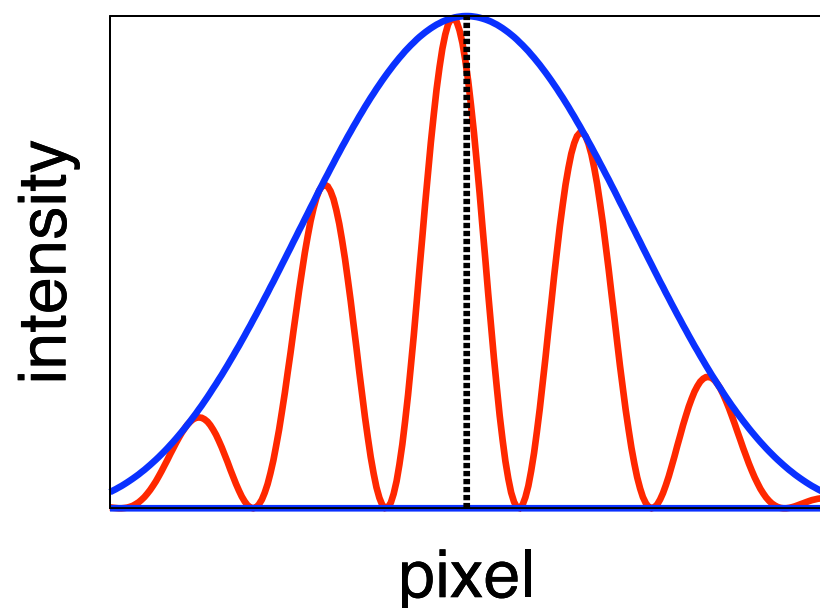
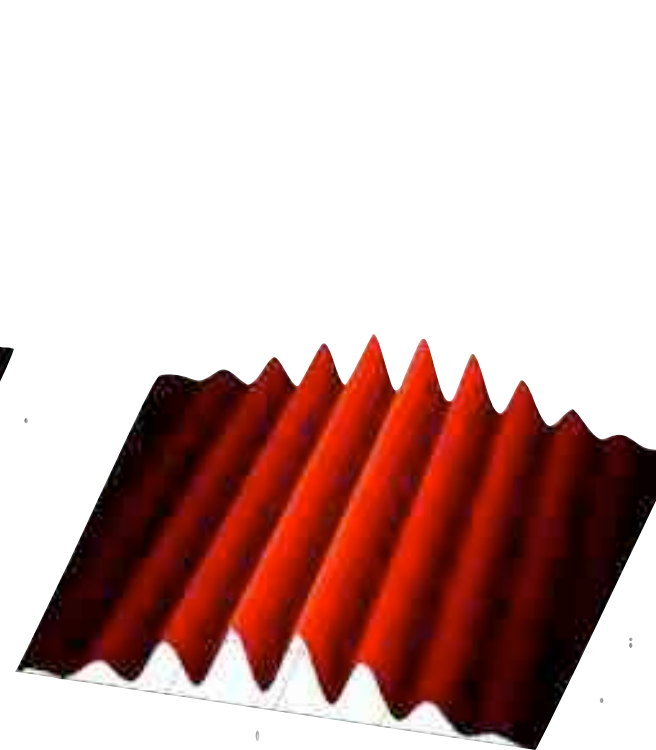
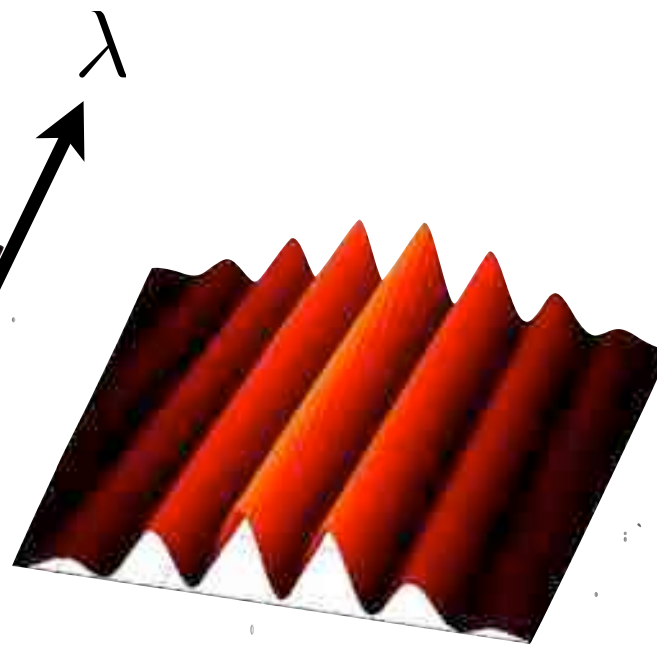
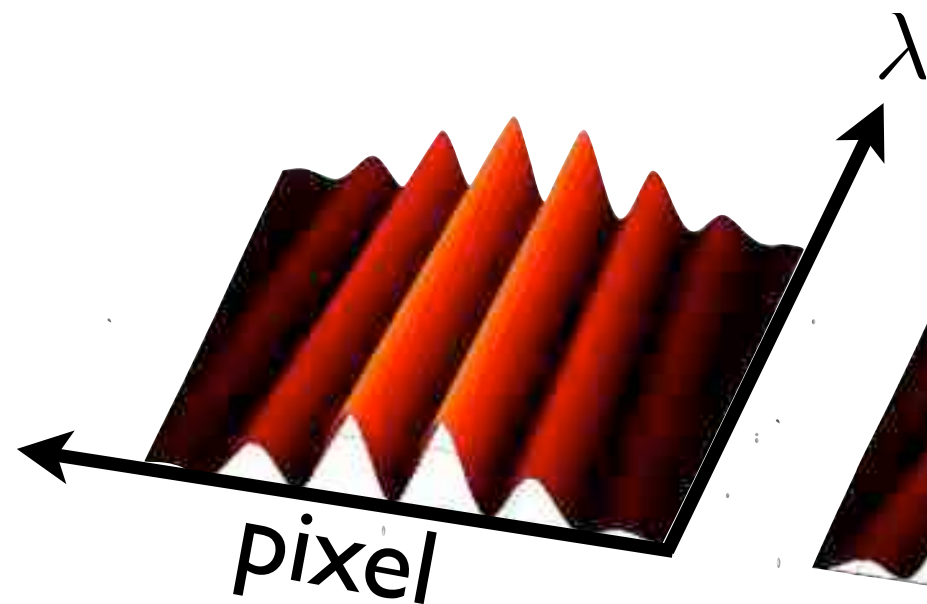
Interferometric Observations with AMBER/VLTI



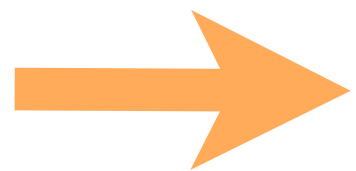
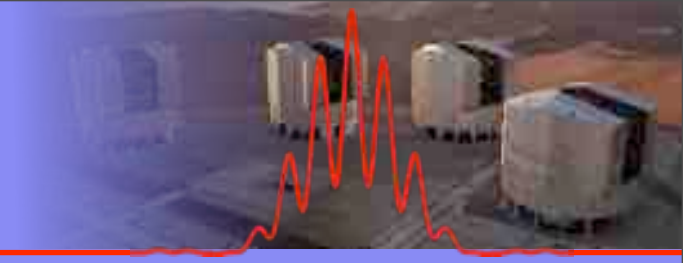
Baseline 1

Baseline 2

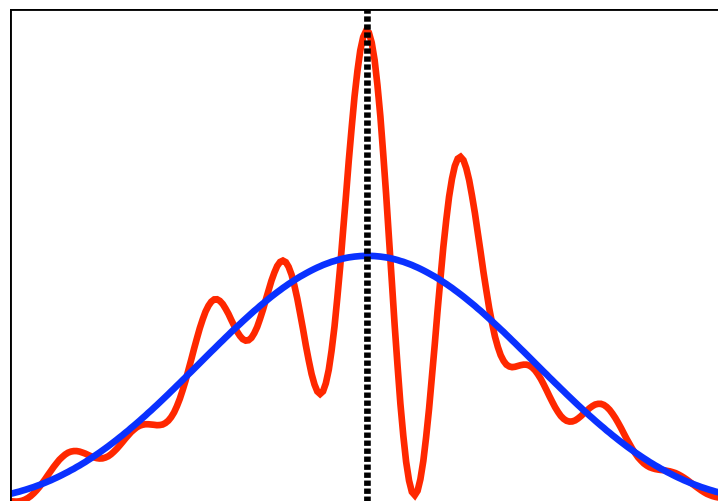
Baseline 3



Interferometric Observations with AMBER/VLTI

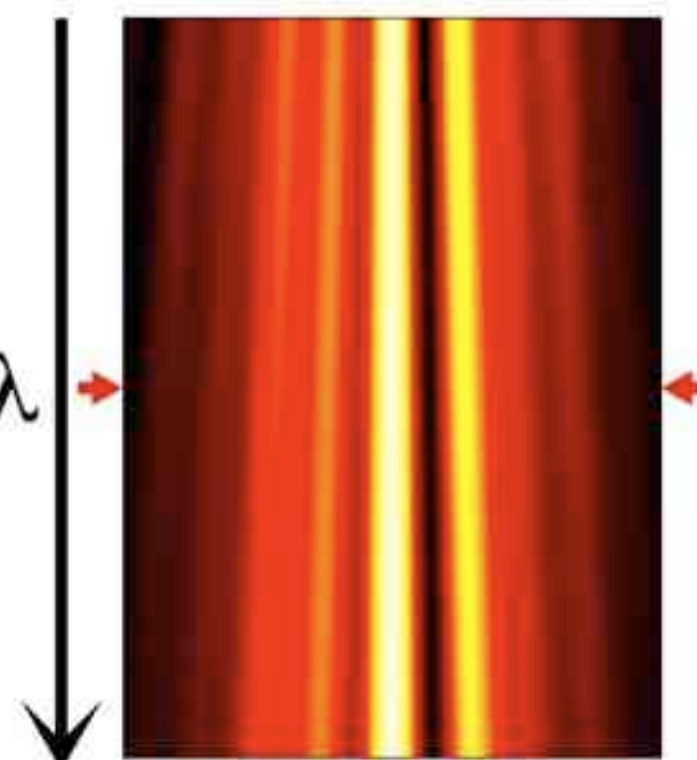


intensity



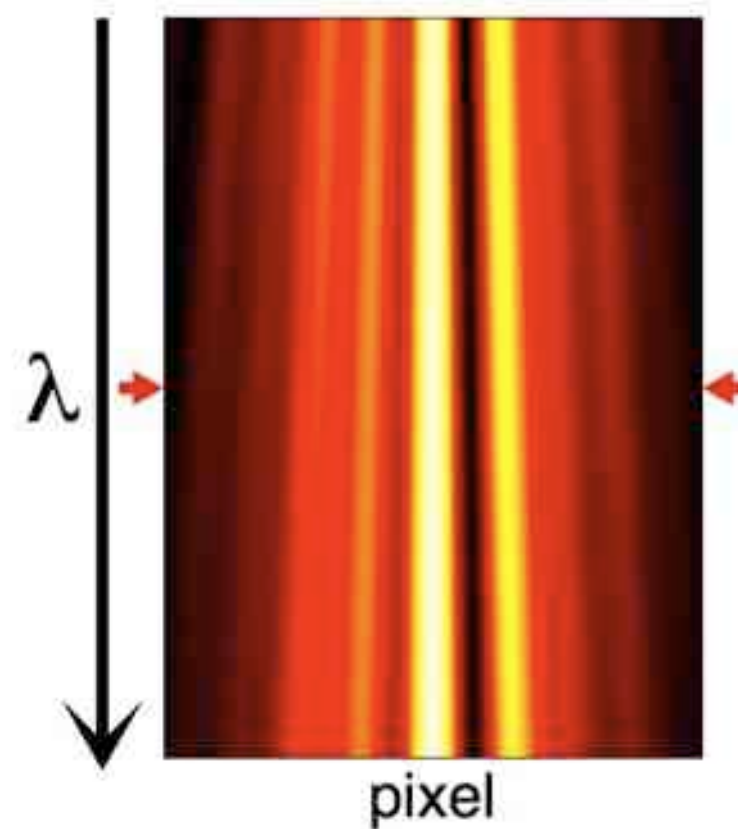
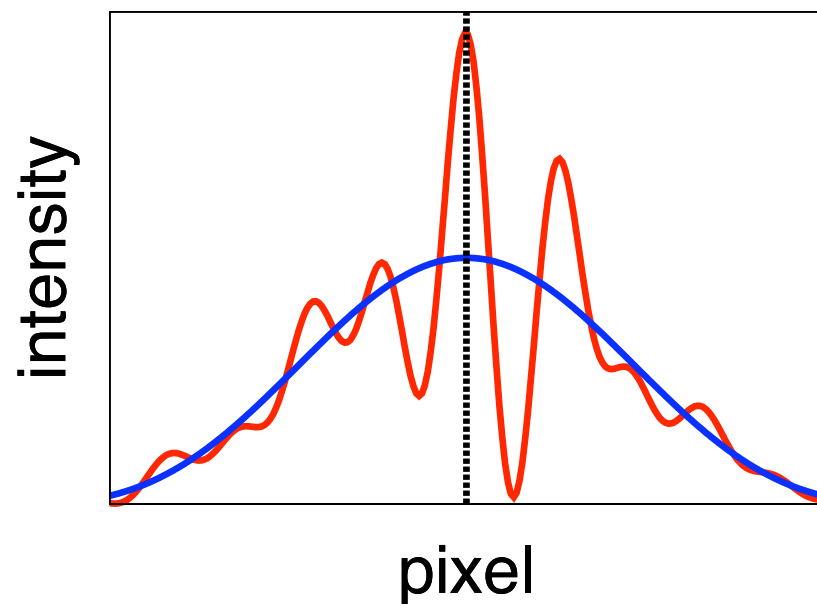
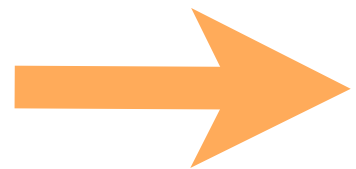
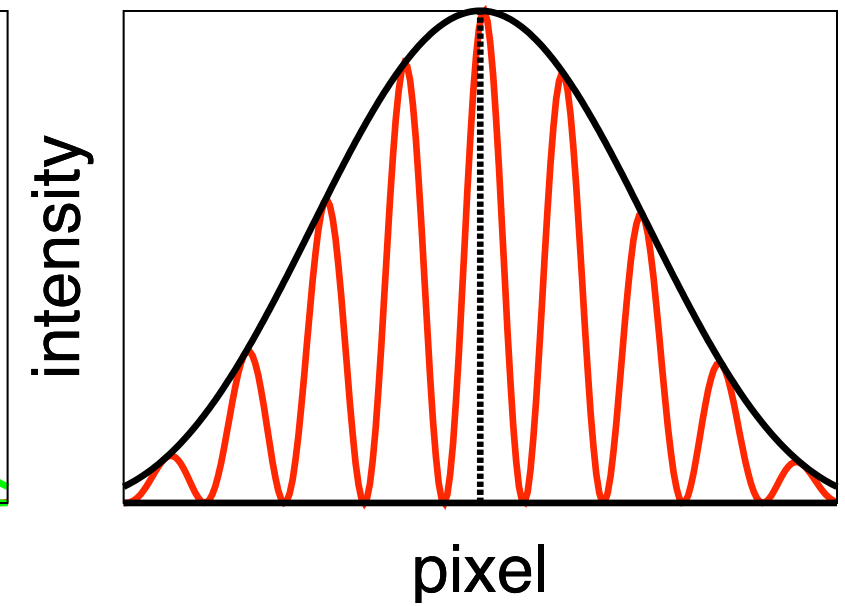
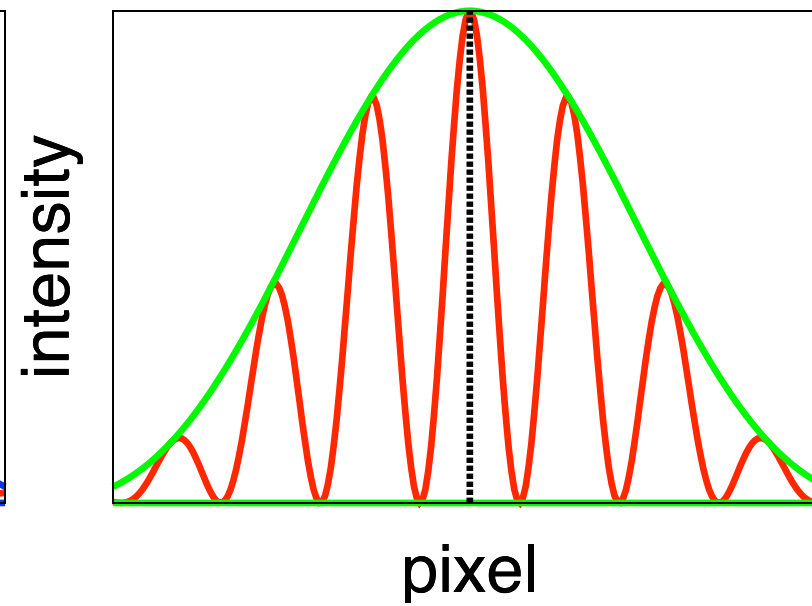
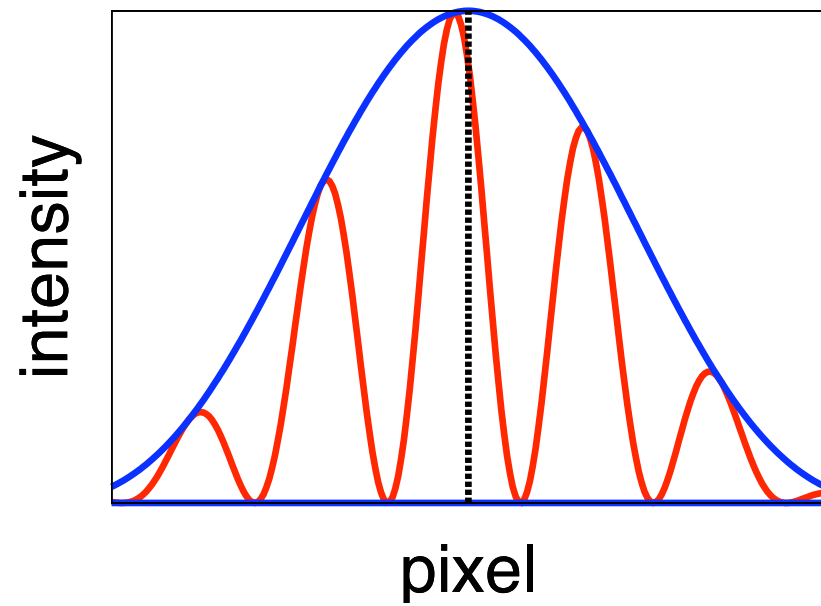
pixel

λ

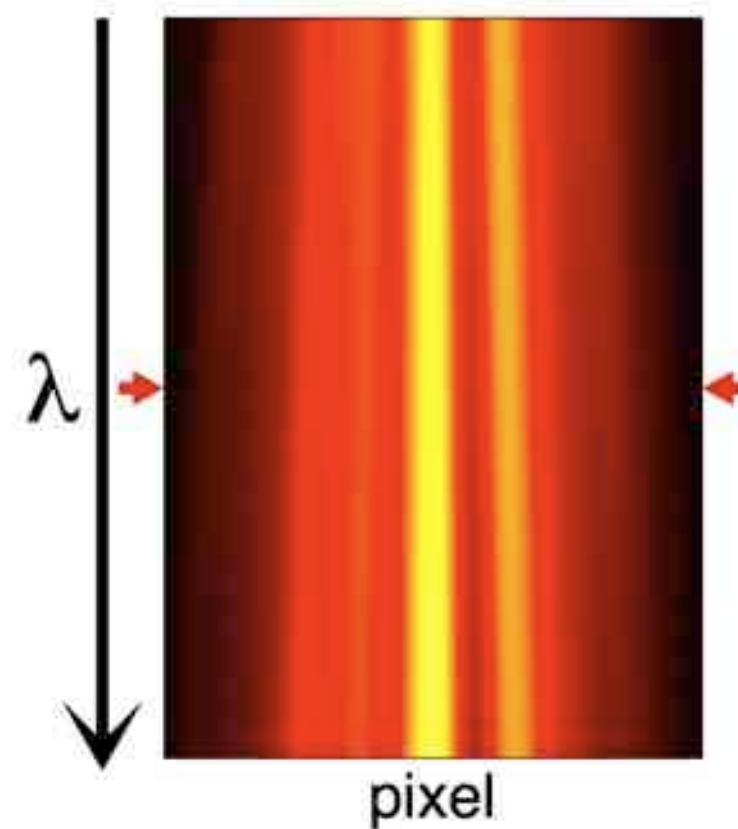
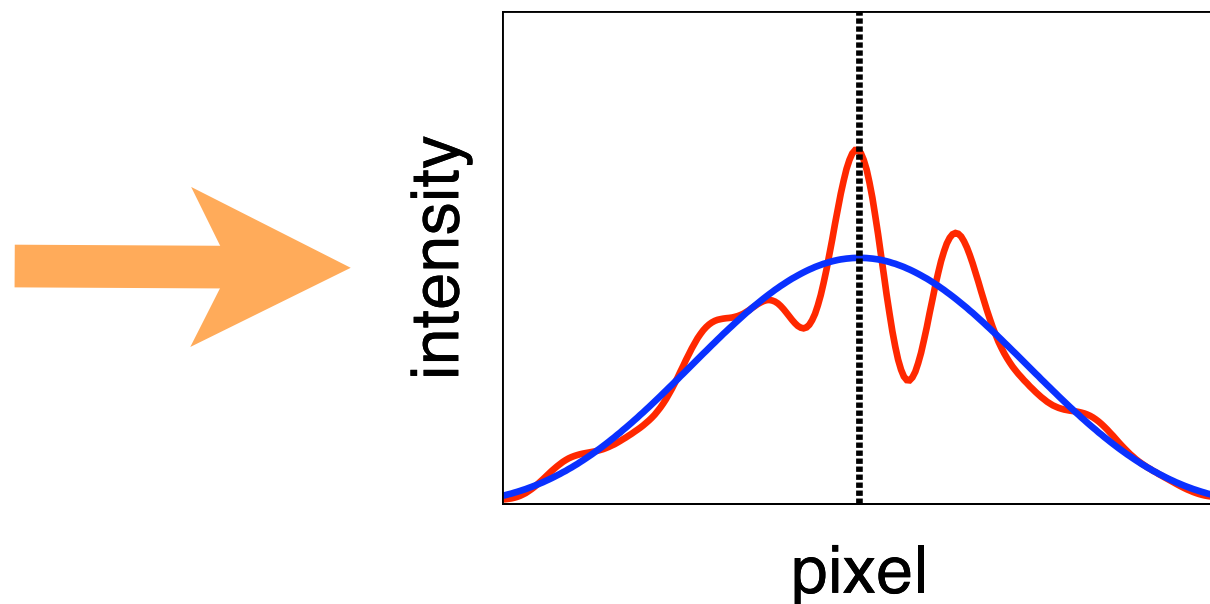
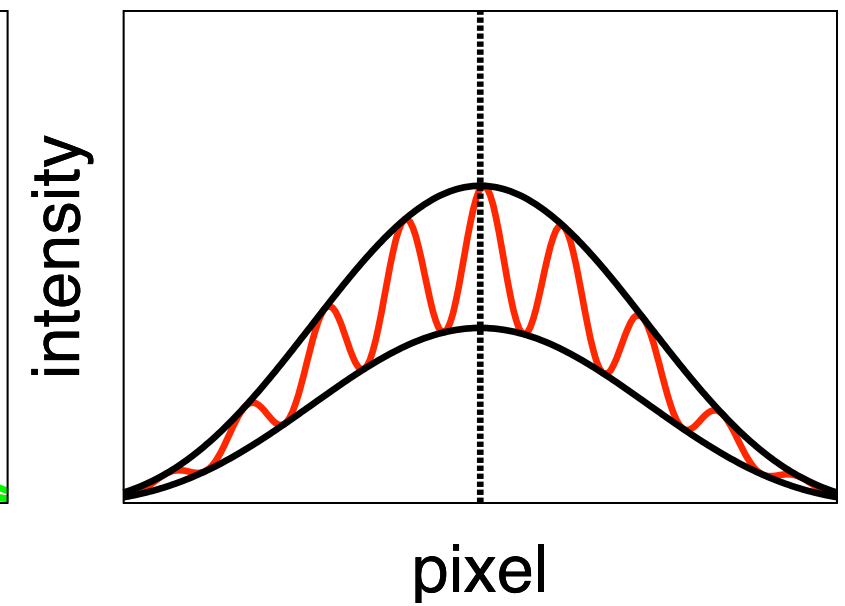
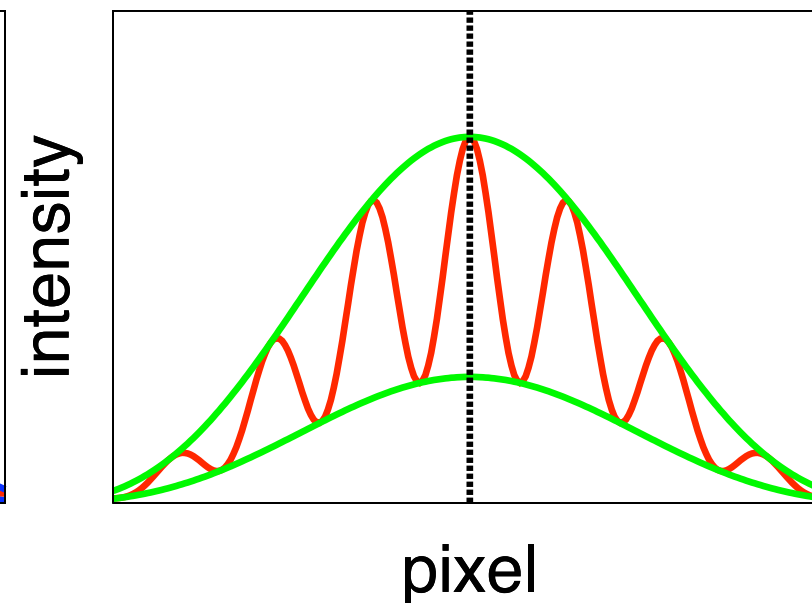
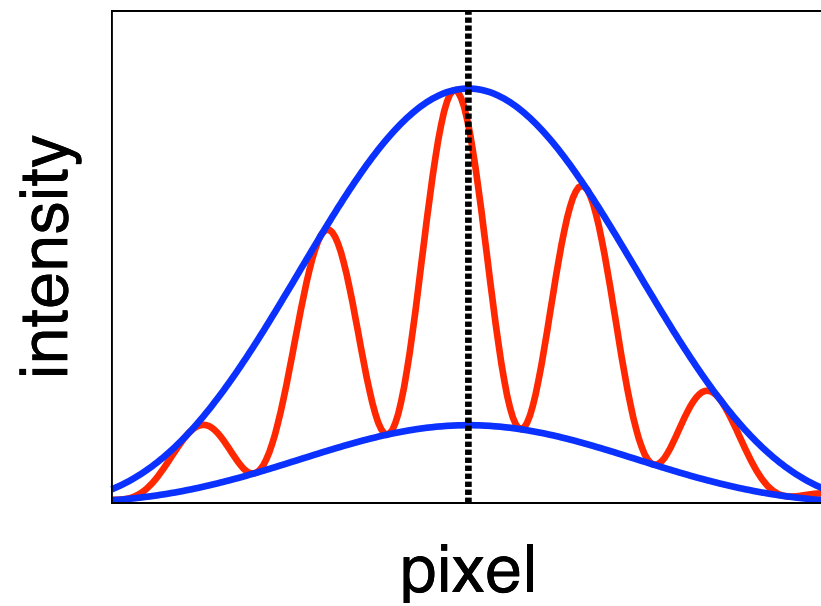


pixel

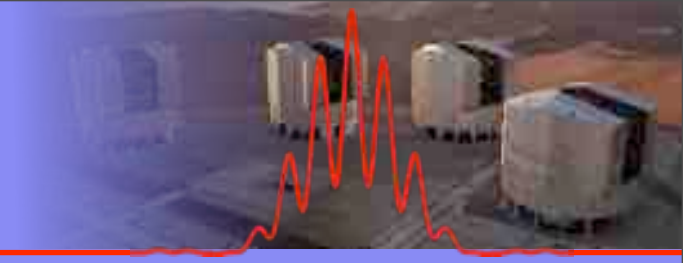
Interferometric Observations with AMBER/VLTI



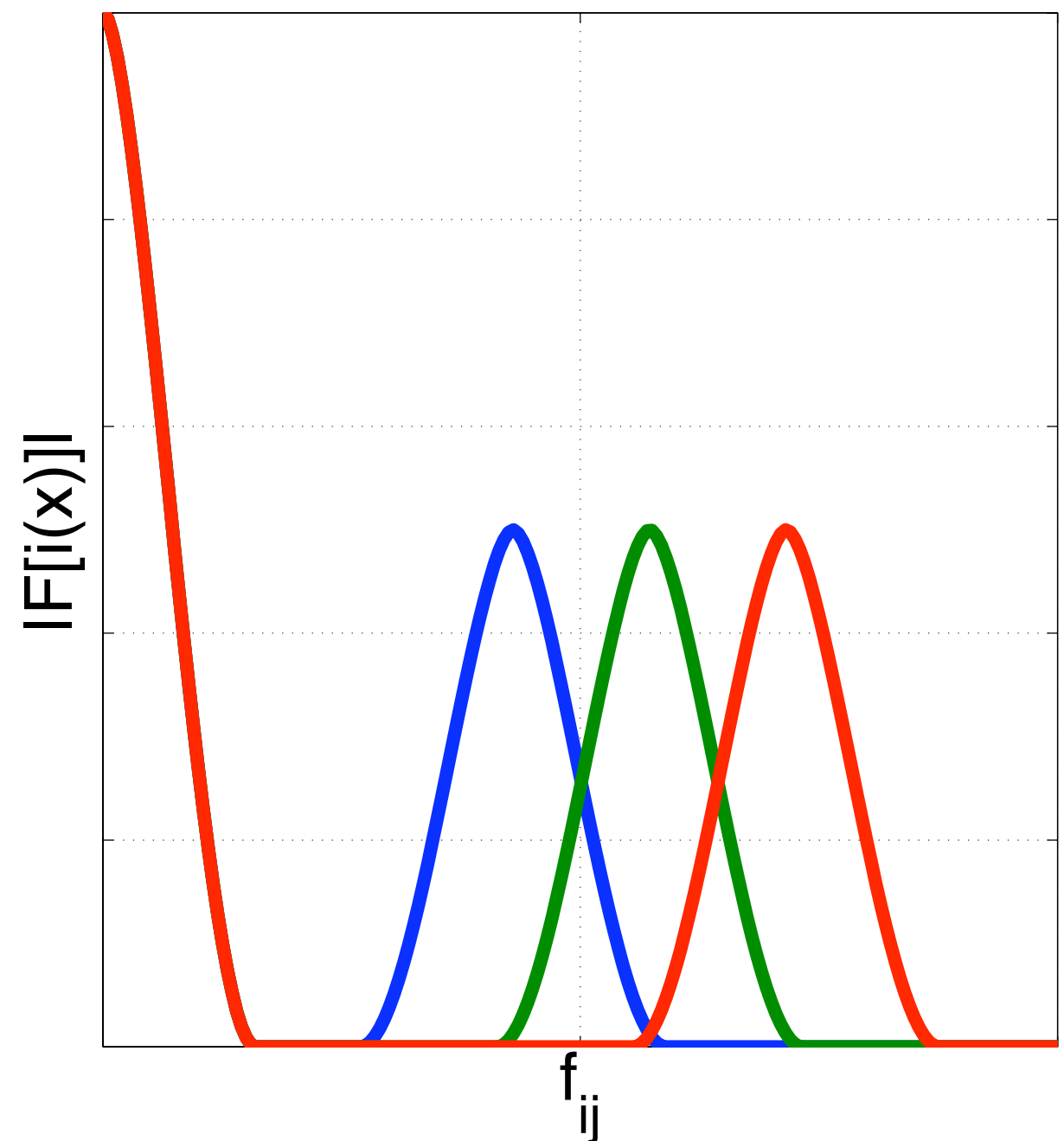
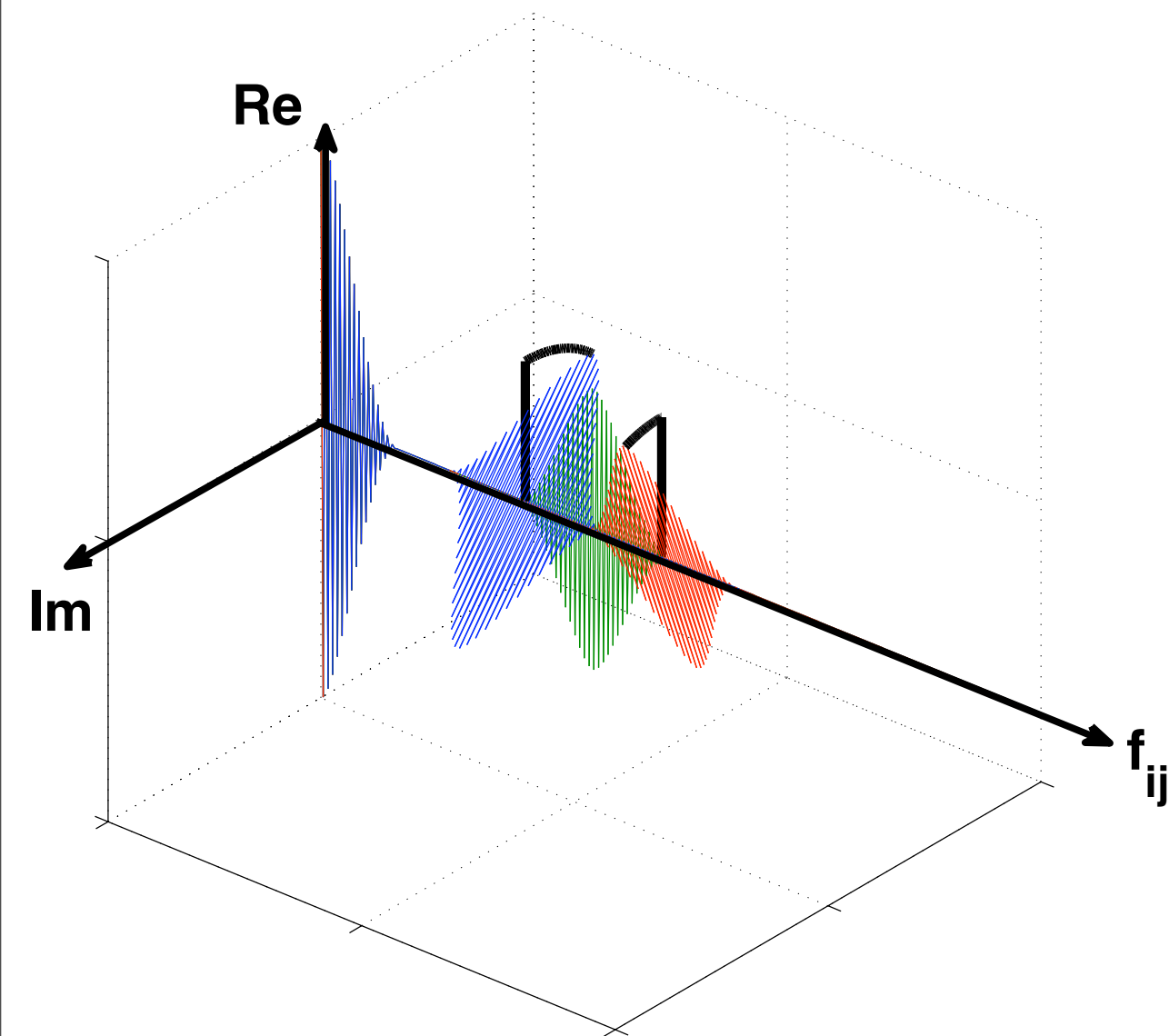
Interferometric Observations with AMBER/VLTI



Interferometric Observations with AMBER/VLTI



- Fourieranalysis is difficult because of fringepeak overlap



The Object: V92 | Sco



The equation of the AMBER interferogram

$$I_k = \sum_i^{N_{\text{tel}}} a_k^i F^i + \sum_{i < j}^{N_{\text{tel}}} \sqrt{a_k^i a_k^j} C_B^{ij} \text{Re}[F_c^{ij} \cdot e^{i(2\pi\alpha_k f^{ij} + \phi_s^{ij} + \phi_B^{ij})}]$$

with the coherent flux:

$$F_c^{ij} = 2N \sqrt{t^i t^j} V^{ij} e^{i(\phi^{ij} + \phi_p^{ij})}$$

can be rewritten in terms of so called “carrier waves”

$$I_k = \sum_i^{N_{\text{tel}}} a_k^i F^i + \underbrace{\sum_{i < j}^{N_{\text{tel}}} [c_k^{ij} R^{ij} + d_k^{ij} I^{ij}]}_{m_k}$$

$$c_k^{ij} = C_B^{ij} \frac{\sqrt{a_k^i a_k^j}}{\sqrt{\sum_k a_k^i a_k^j}} \cos(2\pi\alpha_k f^{ij} + \phi_s^{ij} + \phi_B^{ij})$$

$$d_k^{ij} = C_B^{ij} \frac{\sqrt{a_k^i a_k^j}}{\sqrt{\sum_k a_k^i a_k^j}} \sin(2\pi\alpha_k f^{ij} + \phi_s^{ij} + \phi_B^{ij})$$

in matrix form:

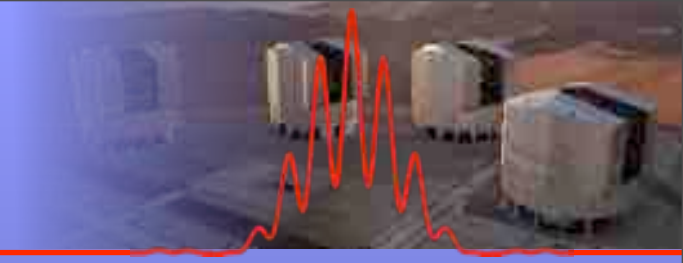
$$\begin{pmatrix} m_1 \\ \vdots \\ m_k \end{pmatrix} = V2PM \cdot \begin{pmatrix} \vdots \\ R^{ij} \\ \vdots \\ I^{ij} \\ \vdots \end{pmatrix}$$

$$R^{ij} = \sqrt{\sum_k a_k^i a_k^j} \text{Re}[F_c^{ij}]$$

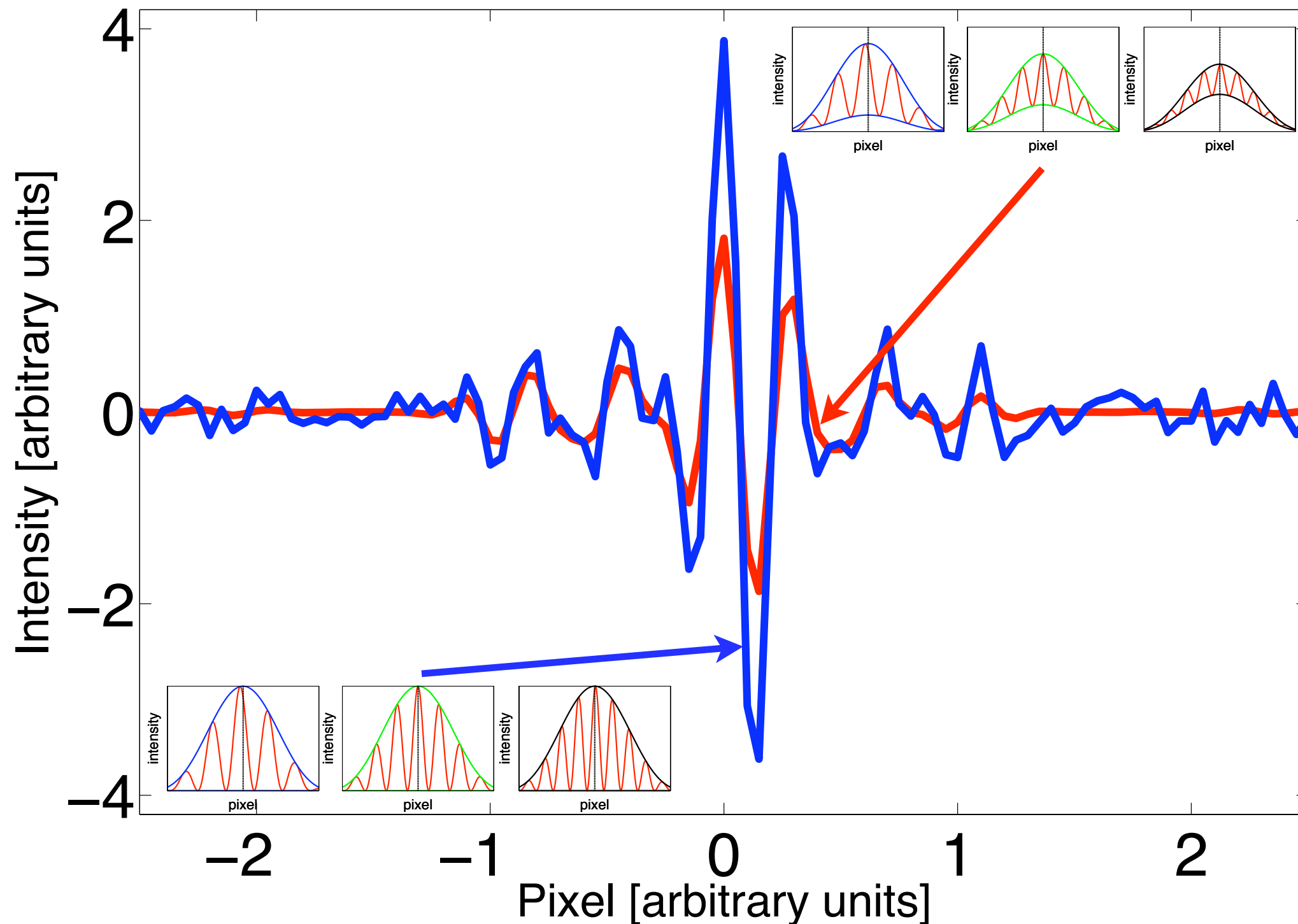
$$I^{ij} = \sqrt{\sum_k a_k^i a_k^j} \text{Im}[F_c^{ij}]$$

with the “Visibility to Pixel Matrix”, containing the carrier waves c_k and d_k

Interferometric Observations with AMBER/VLTI

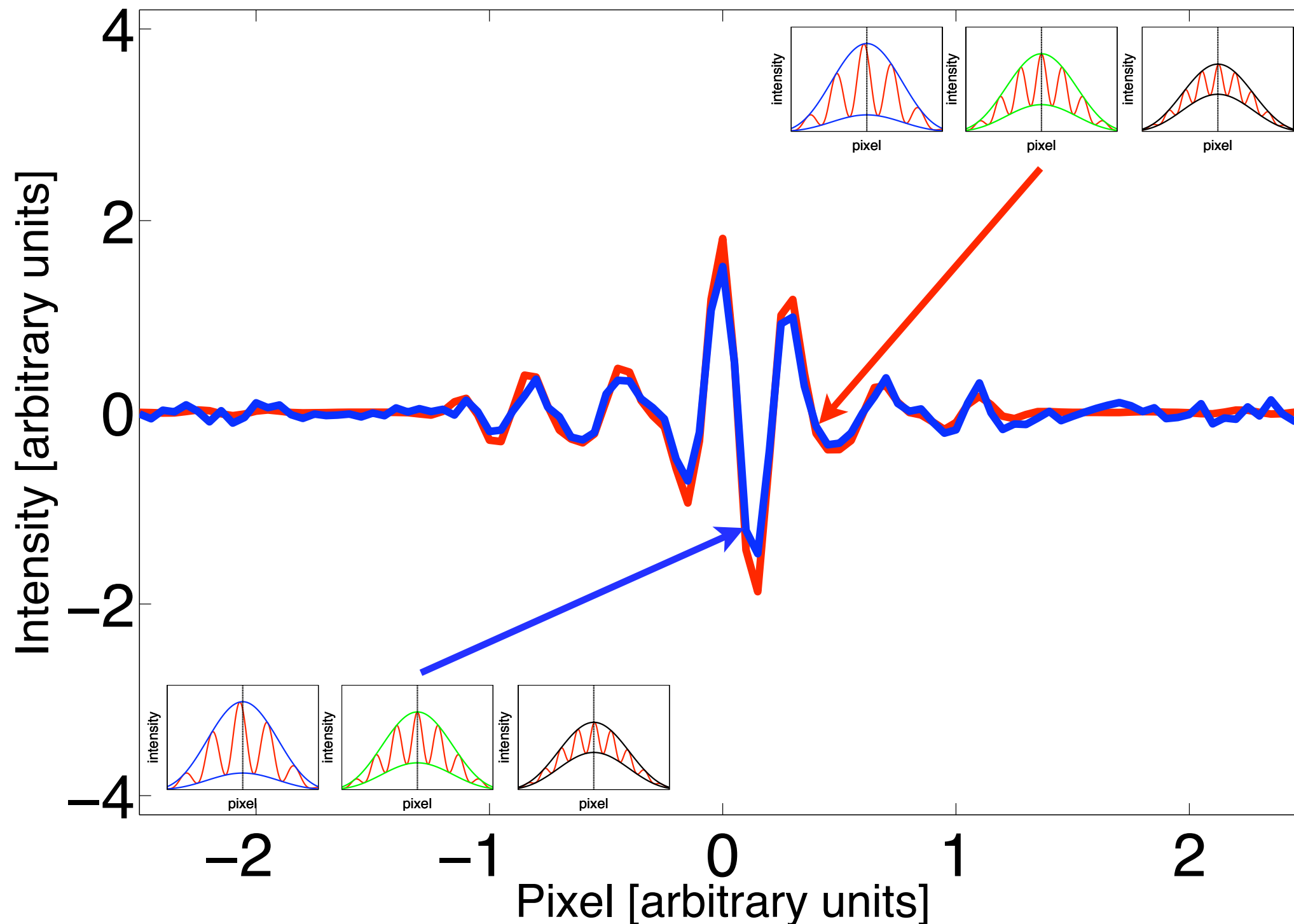


- alternative algorithm has to be used



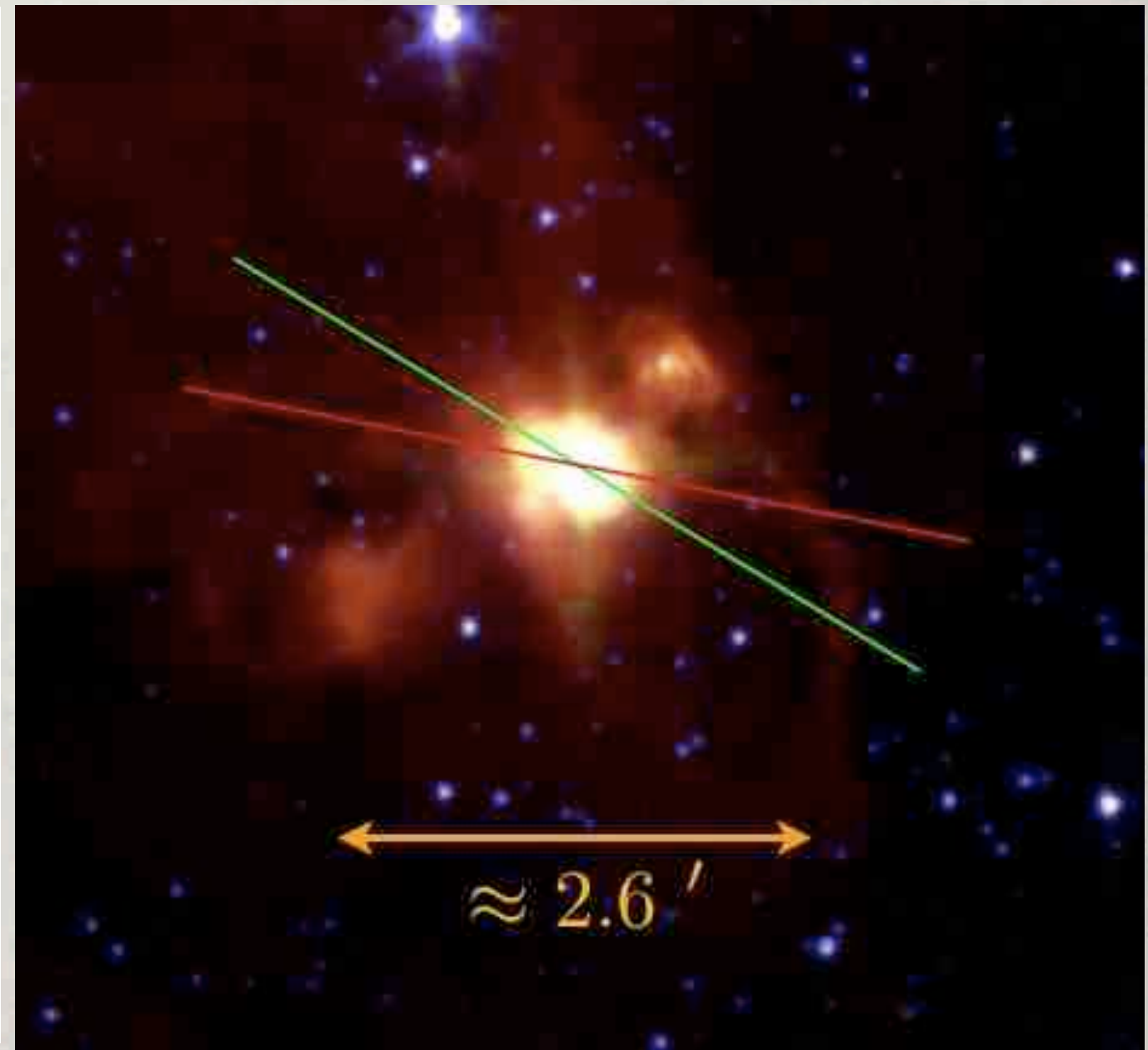
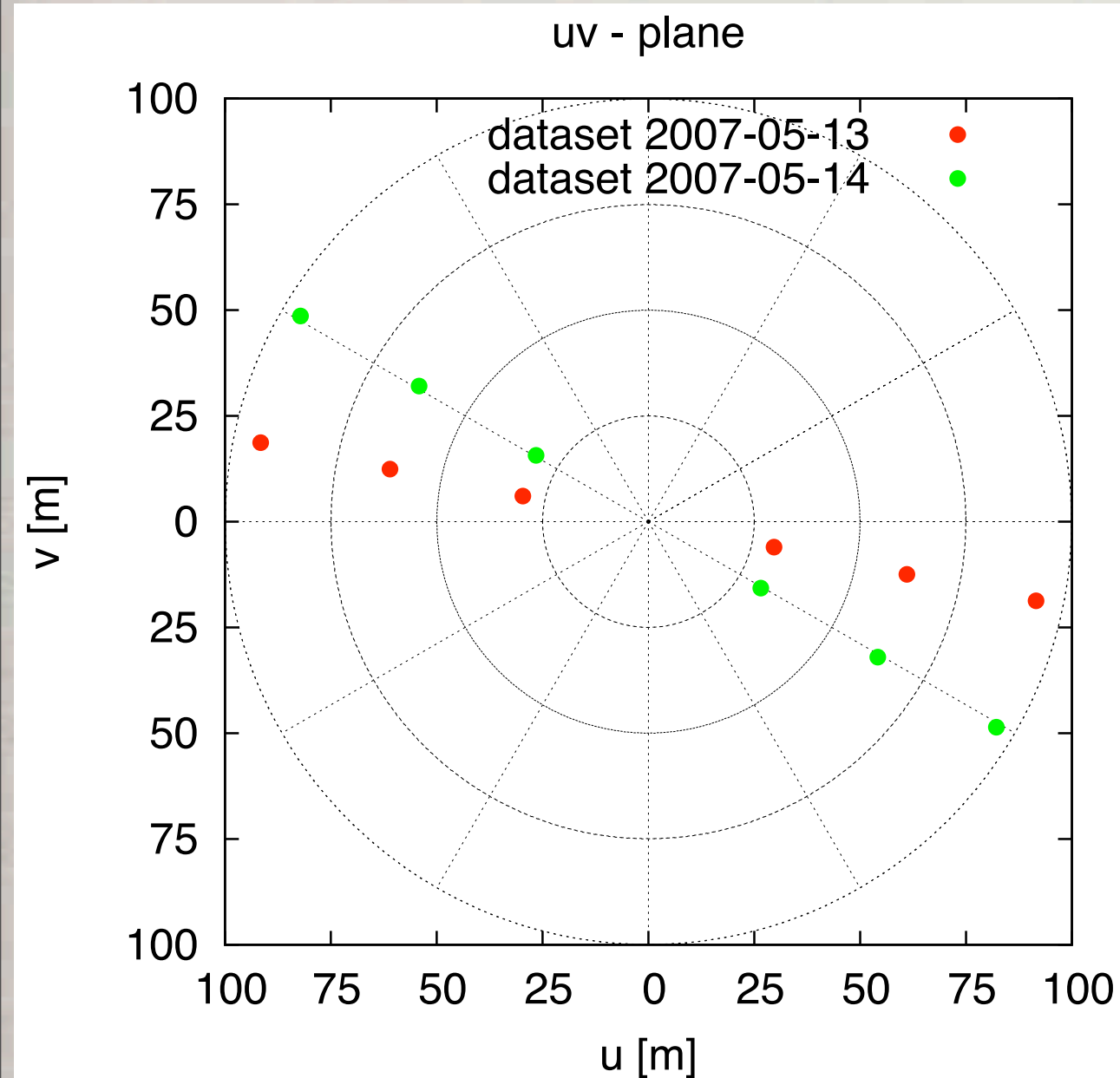
Interferometric Observations with AMBER/VLTI

- This is in principle a fringe fitting process called **P2VM - Algorithm** (Tatulli 2007)



The Object: V92 I Sco

uv - plane coverage



B1 = 31 m
B2 = 62 m
B3 = 93 m

2007.05.13 : $\Theta_{\text{pos}} = 79^\circ$

2007.05.14 : $\Theta_{\text{pos}} = 59^\circ$

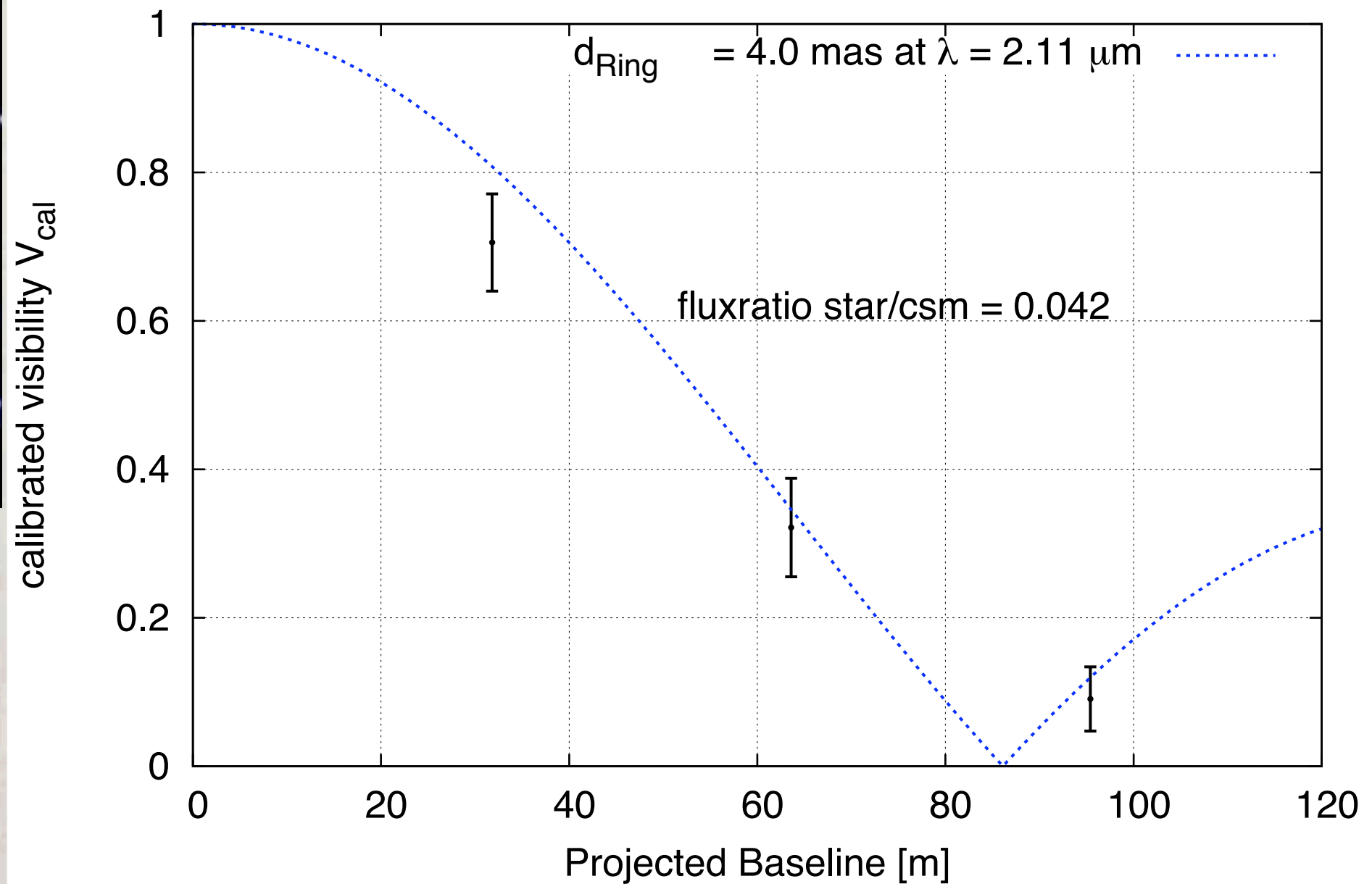
- The coverage in position angle of $\sim 20^\circ$ could not be used to analyse possible asymmetries in the source structure

The Object: V921 Sco



$$\Theta_{\text{pos}} = 59^\circ$$

2007-05-14 -- exp.time: 100 ms -- $\Delta\text{PA} = 58.7 - 60.1^\circ$ -- $\text{PA}_{\text{avg}} = 59.40^\circ$



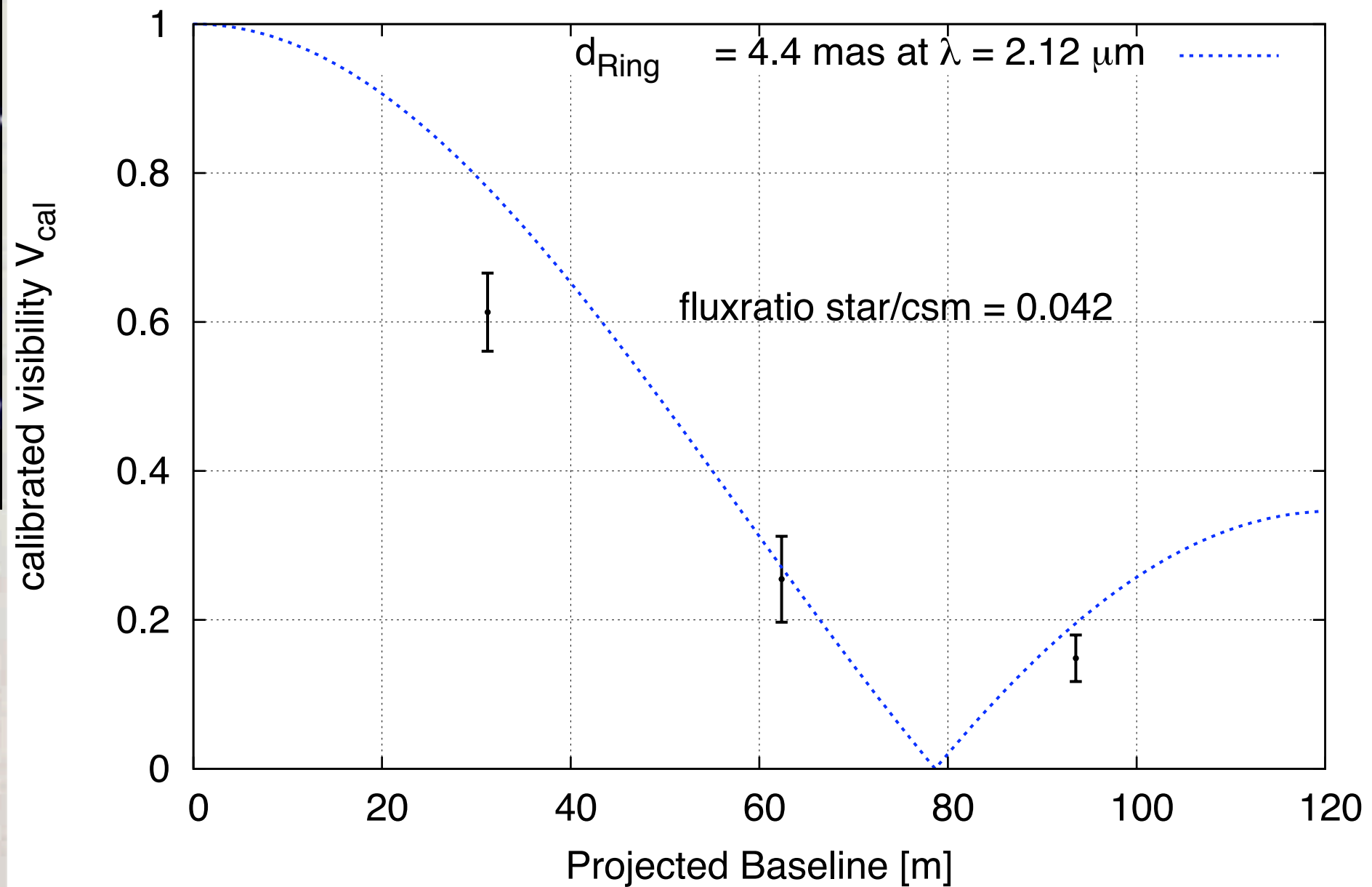
$$d_{\text{ring}} = 4.0 \pm 0.2 \text{ mas}$$

The Object: V921 Sco



$$\Theta_{\text{pos}} = 79^\circ$$

2007-05-13 -- exp.time: 100 ms -- $\Delta\text{PA} = 77.9 - 79.2^\circ$ -- $\text{PA}_{\text{avg}} = 78.46^\circ$



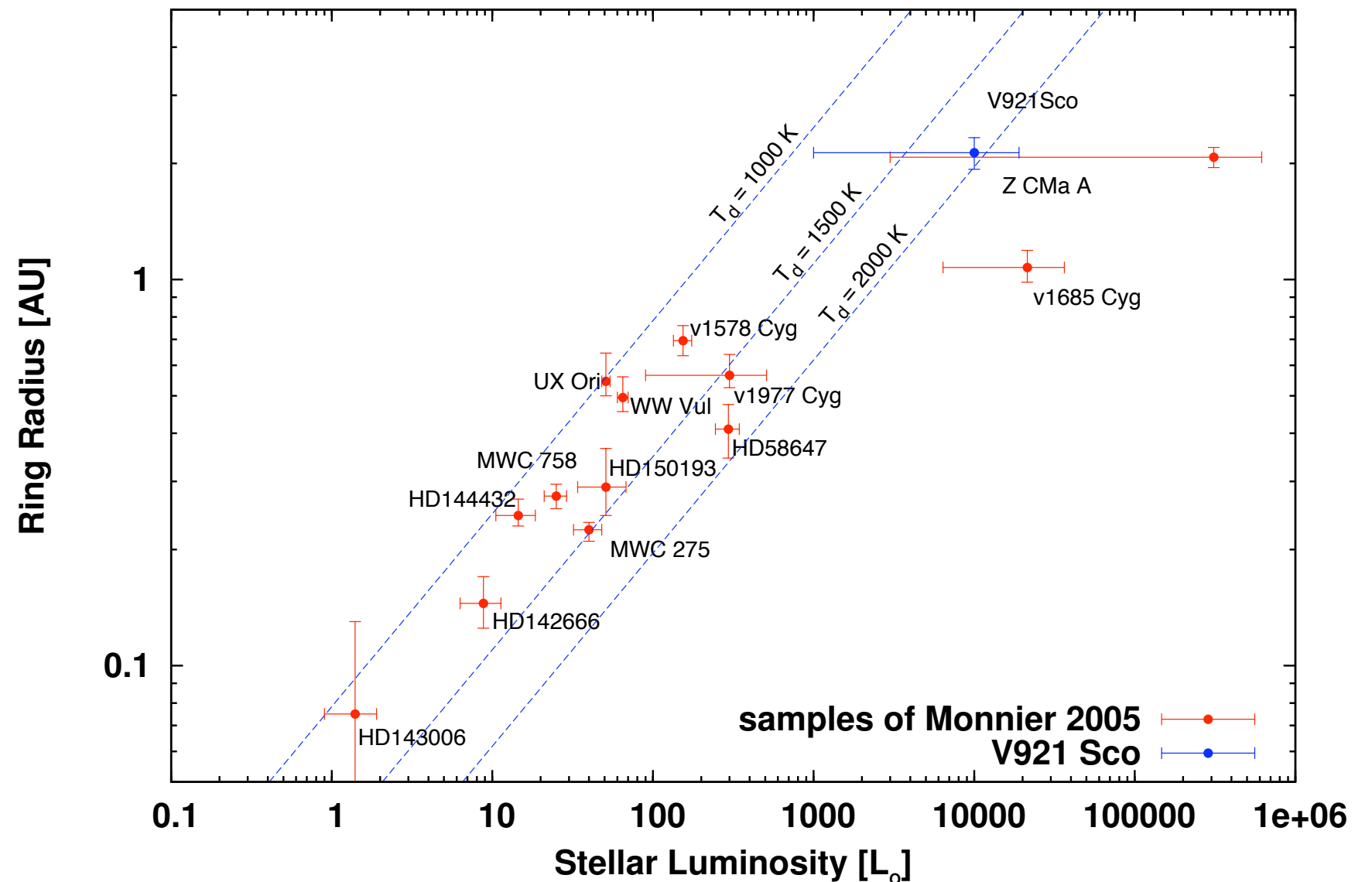
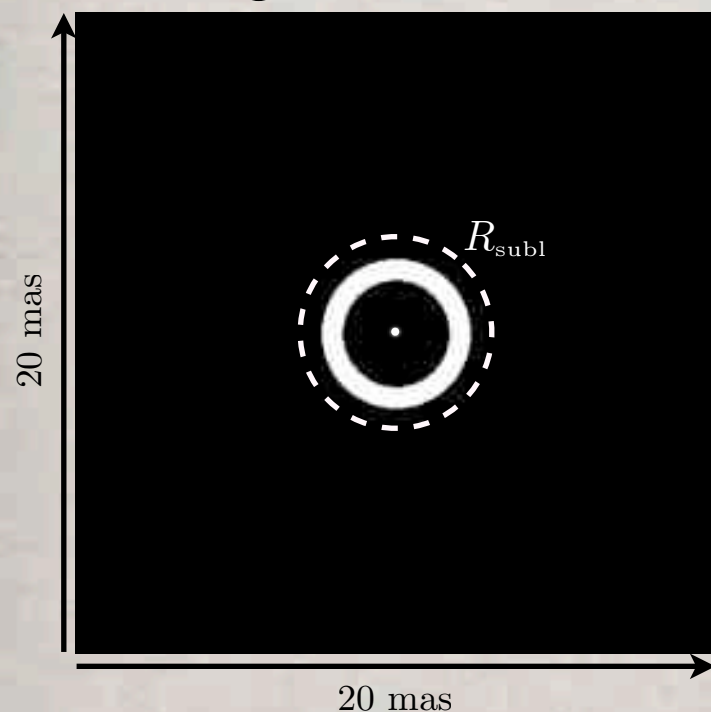
$$d_{\text{ring}} = 4.4 \pm 0.4 \text{ mas}$$

The Object: V921 Sco

Size-Luminosity relation

(Monnier & Millan-Gabet 2002)

- To interpret the nature of the near-infrared emitting region, the fitted ring-radius is compared to the expected dust sublimation radius
ring model + star



Dust sublimation radius: $R_s = 1.1 \sqrt{\epsilon} \left(\frac{L_\star}{1000 L_\odot} \right)^{\frac{1}{2}} \left(\frac{T_s}{1500 \text{ K}} \right)^{-2}$

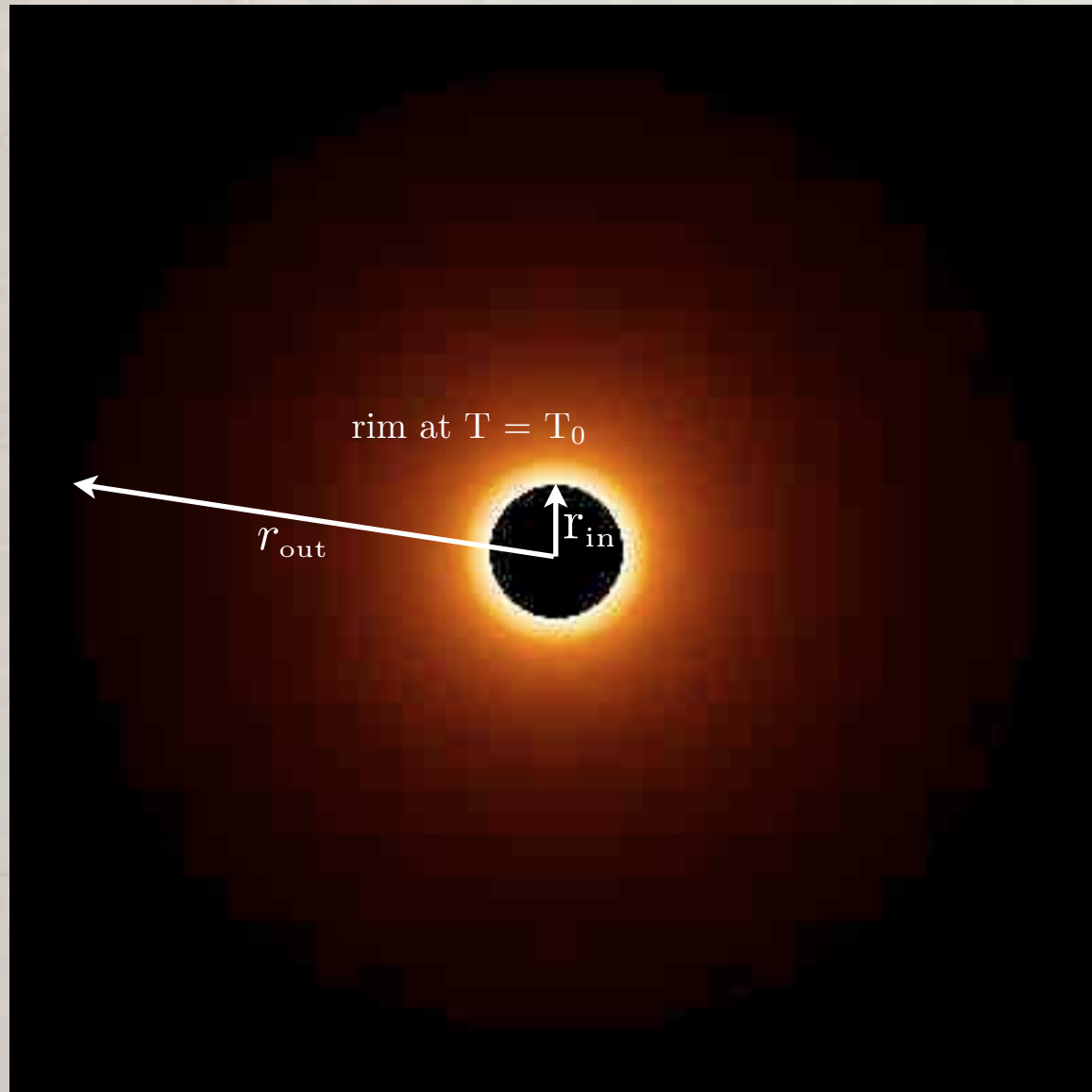
with the ratio of the dust absorption efficiencies:

$$\epsilon = \frac{Q_{\text{abs}}(T_\star)}{Q_{\text{abs}}(T_{\text{subl}})}$$

The Object: V92 I Sco



Temperature-gradient model



- To get a first more physical approach a temperature-gradient model was used to reconstruct the visibility which was already successfully applied to YSO's (e.g. Bertout et al. 1988, Malbet et al. 1995)

Temperature profile:

$$T(r) = T_0 \cdot \left(\frac{r}{r_{\text{in}}} \right)^{-q}$$

r_{in} : inner disk radius

q : exponent

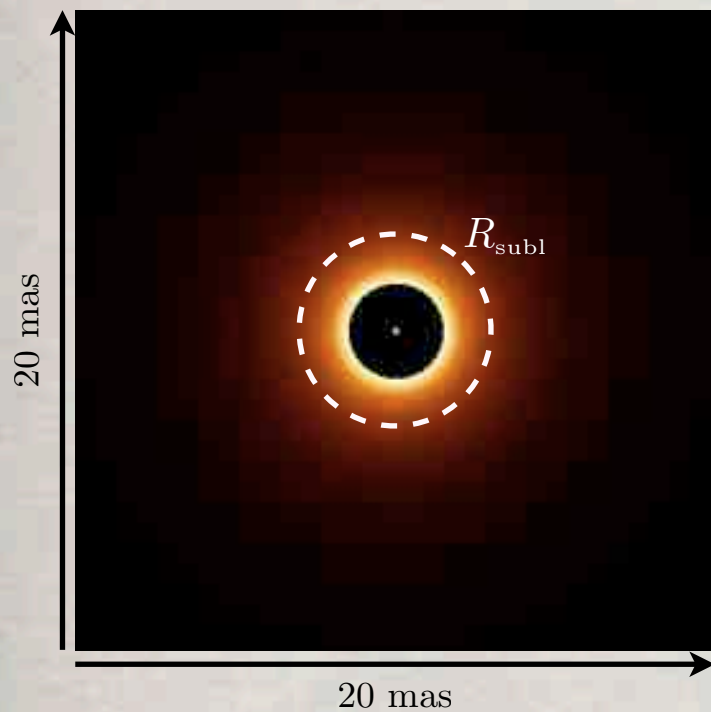
T_0 : Temperature at $r = r_{\text{in}}$

$$F_{\lambda} = \frac{2\pi}{d^2} \cdot \cos(\phi) \cdot \int_{r_{\text{in}}}^{r_{\text{out}}} B_{\lambda}(T(r)) r dr$$

The Object: V921 Sco



2-component temperature-gradient model (disk+star):



$$\begin{aligned} q &= 0.55 \\ d &= 1.15 \text{ kpc} \\ r_{\text{in}} &= 1.7 \text{ AU} \\ r_{\text{out}} &= 13.2 \text{ AU} \\ T_0 &= 1500 \text{ K} \end{aligned}$$

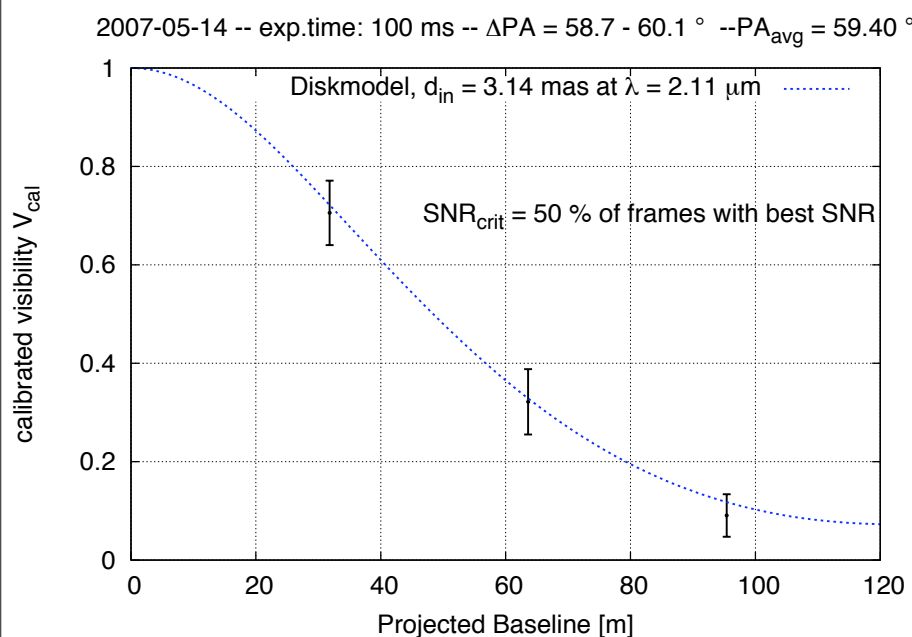
$$\begin{aligned} R_{\star} &= 17.3 R_{\odot} \\ T_{\star} &= 13225 \text{ K} \end{aligned}$$

This model is able to reproduce both the observed SED and observed multiwavelength visibilities

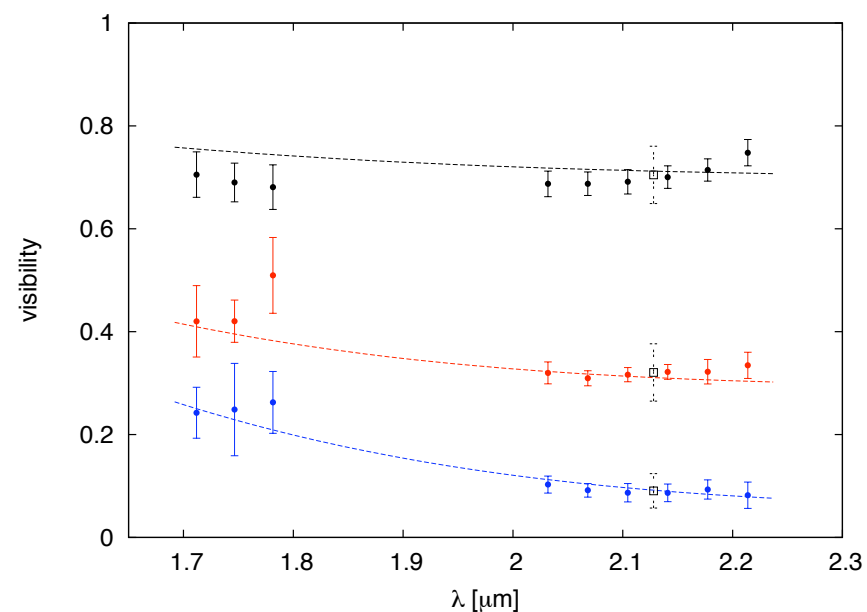
Problem:

The inner dust-disk radius is smaller than the dust sublimation radius

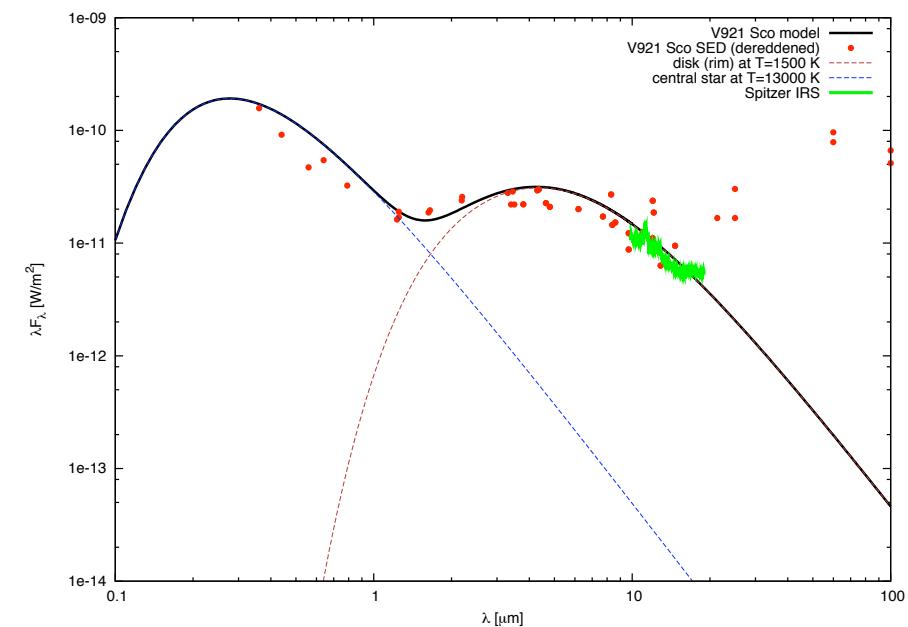
visibility modelling at 2.1 μm



multiwavelength visibility modelling



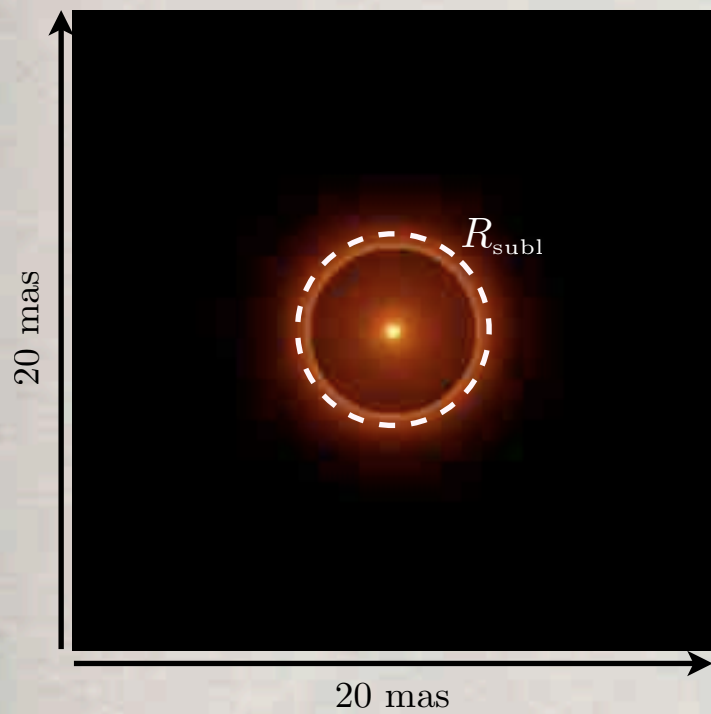
SED modelling



Modelling



3-component temperature-gradient model (gas disk + dust disk + star):



$$q = 1.3$$

$$d = 1.15 \text{ kpc}$$

$$r_{\text{in}} = 2.9 \text{ AU}$$

$$r_{\text{out}} = 14.5 \text{ AU}$$

$$T_0 = 1500 \text{ K}$$

$$q = 0.2$$

$$d = 1.15 \text{ kpc}$$

$$r_{\text{in}} = 0.12 \text{ AU}$$

$$r_{\text{out}} = 2.9 \text{ AU}$$

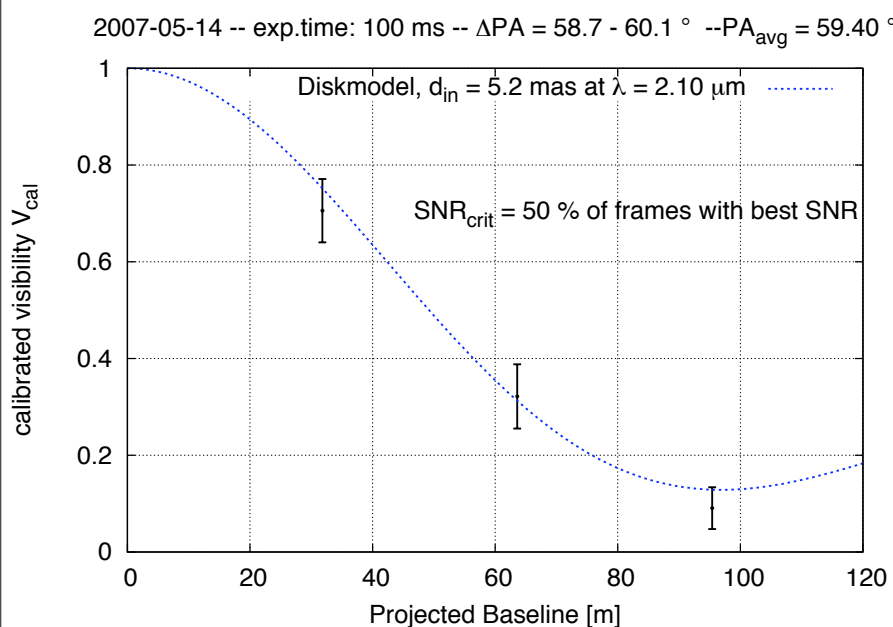
$$T_0 = 2000 \text{ K}$$

$$R_{\star} = 17.3 R_{\odot}$$

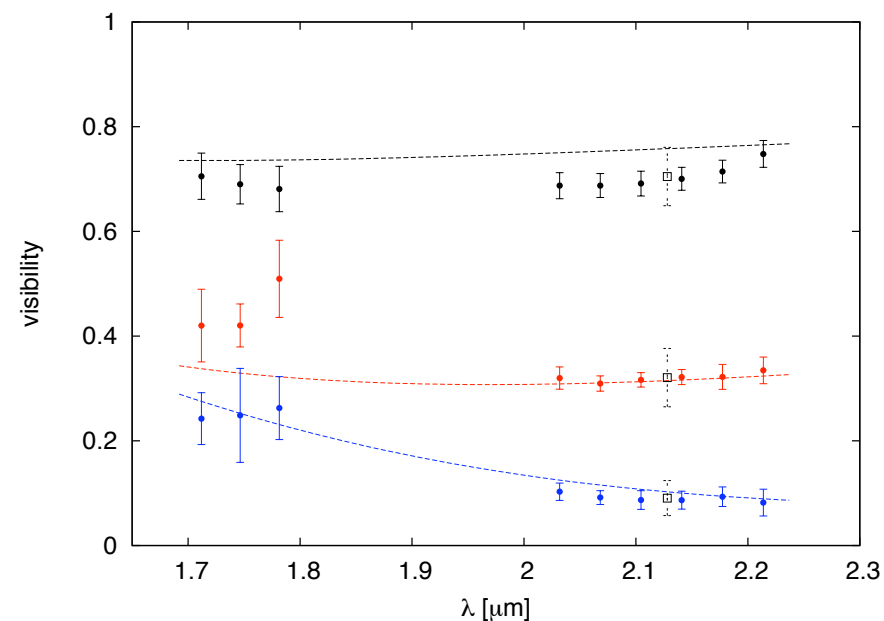
$$T_{\star} = 13225 \text{ K}$$

This model is able to reproduce both the observed SED and observed multiwavelength visibilities

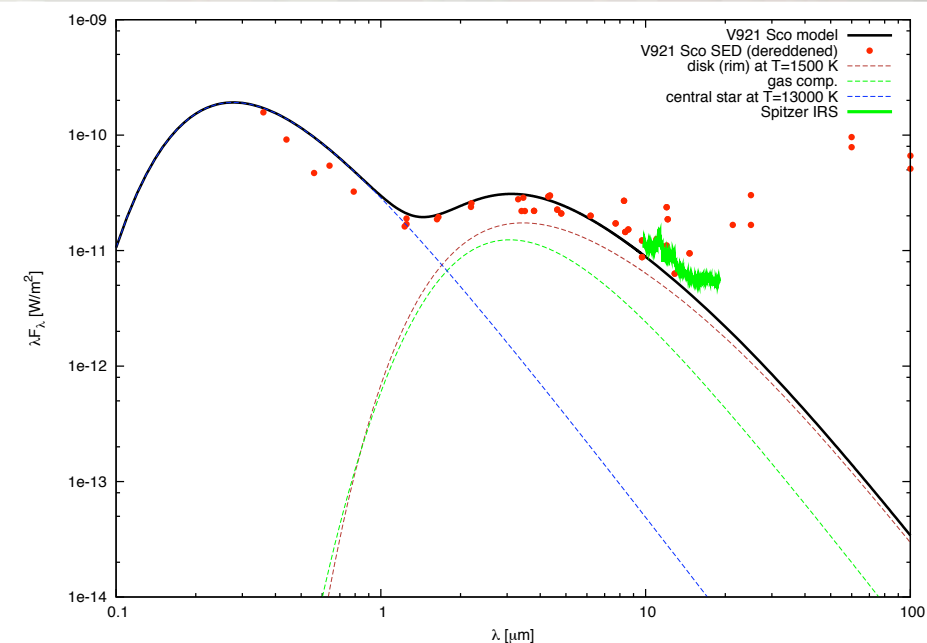
visibility modelling at $2.1 \mu\text{m}$



multiwavelength visibility modelling



SED modelling



Modelling

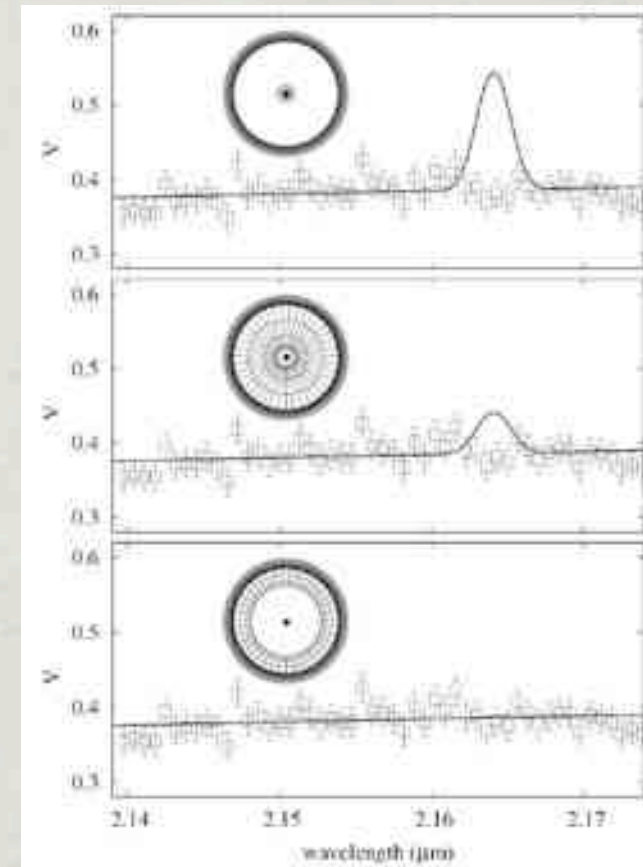
- For the given stellar parameters the measured ring radius is more compact than expected

- One reason might be that the stellar luminosity could be overestimated

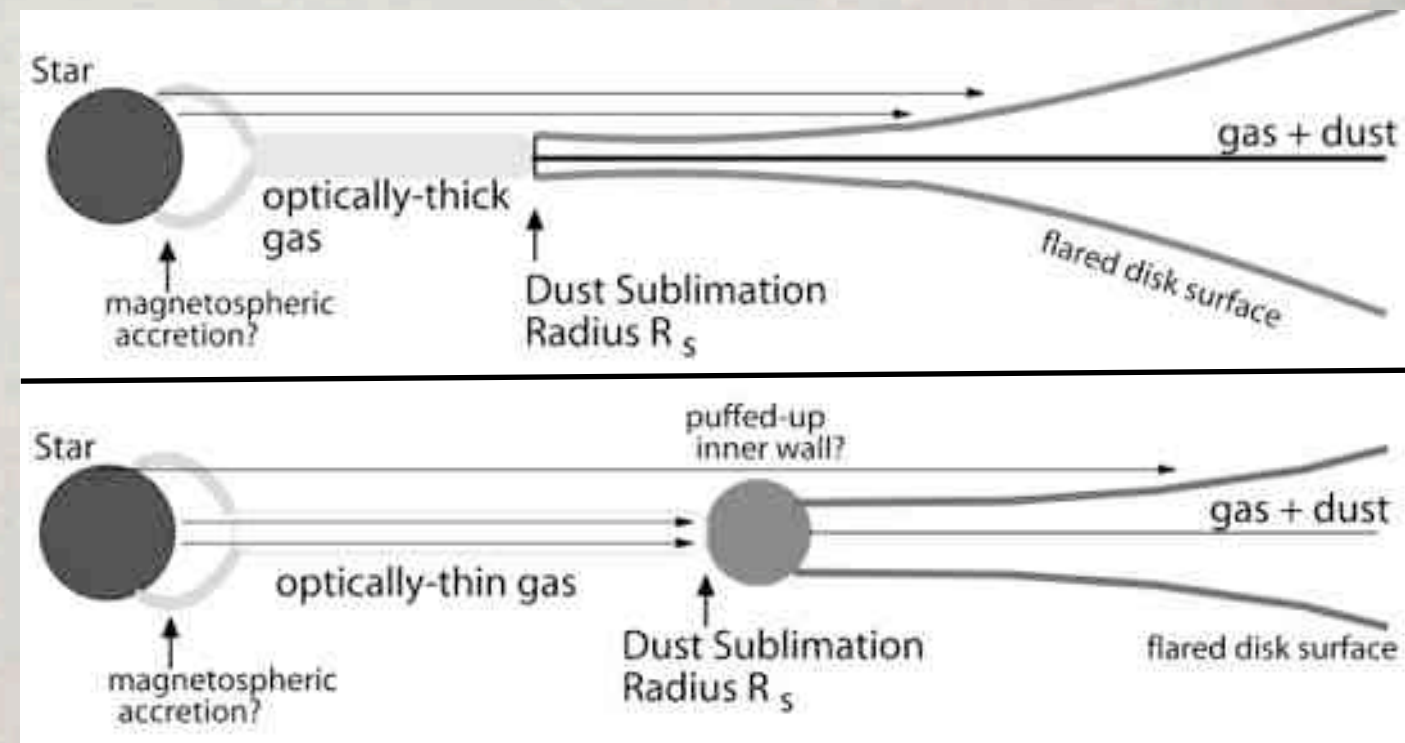
➡ The dust sublimation radius is not compact in contrast to the expected one

- An optically-thin inner gas disk could contribute to the total near-infrared emission

➡ Such inner gaseous disks were already successfully observed in YSO's
e.g. MWC 147 (Kraus et al. 2007)
MWC 748 (Isella et al. 2008)



Tatulli 2007 et al.



Monnier et al. 2005



- For the given stellar parameters the measured ring radius is more compact than expected

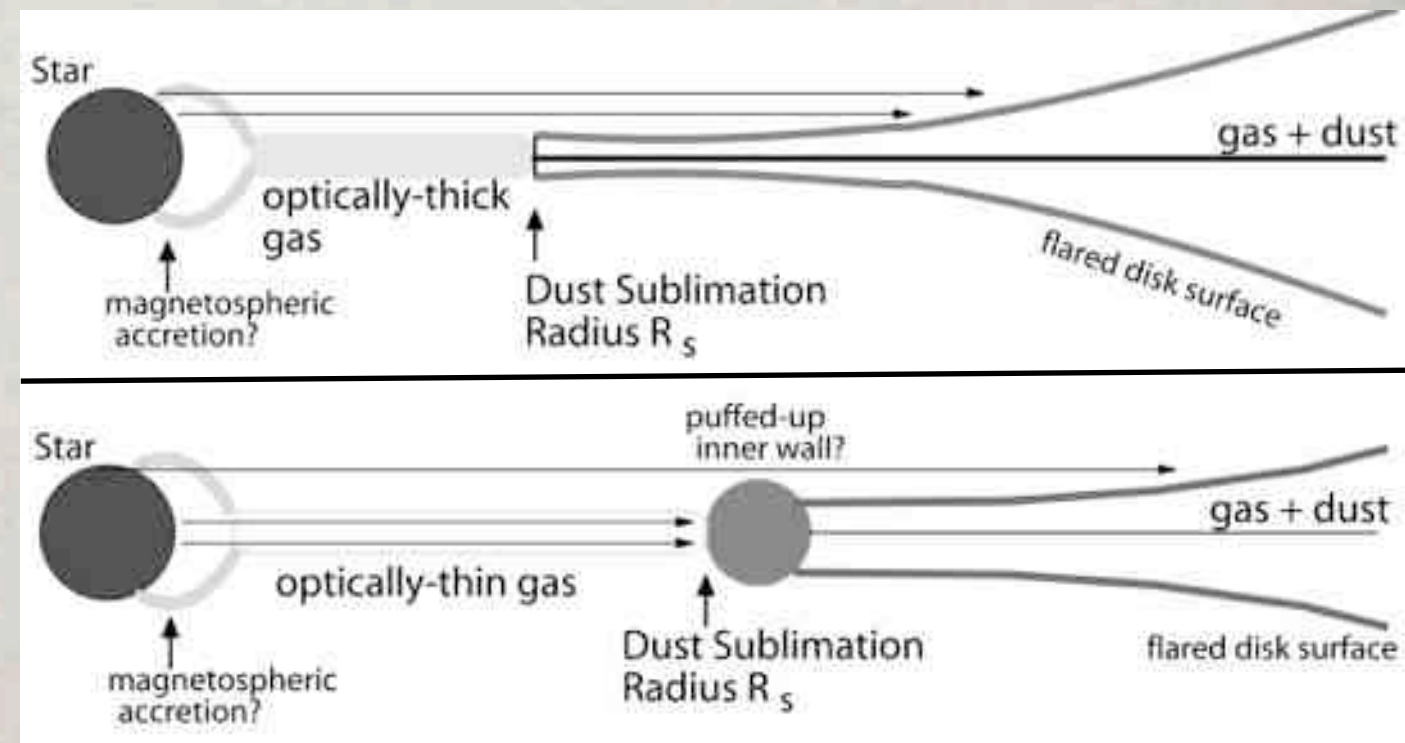
- One reason might be that the stellar luminosity could be overestimated

Tatulli 2007 et al.

- ➡ The dust sublimation radius is not compact in contrast to the expected one

- An optically-thin inner gas disk could contribute to the total near-infrared emission

- ➡ Such inner gaseous disks were already successfully observed in YSO's
e.g. MWC 147 (Kraus et al. 2007)
MWC 748 (Isella et al. 2008)



Monnier et al. 2005

Modelling

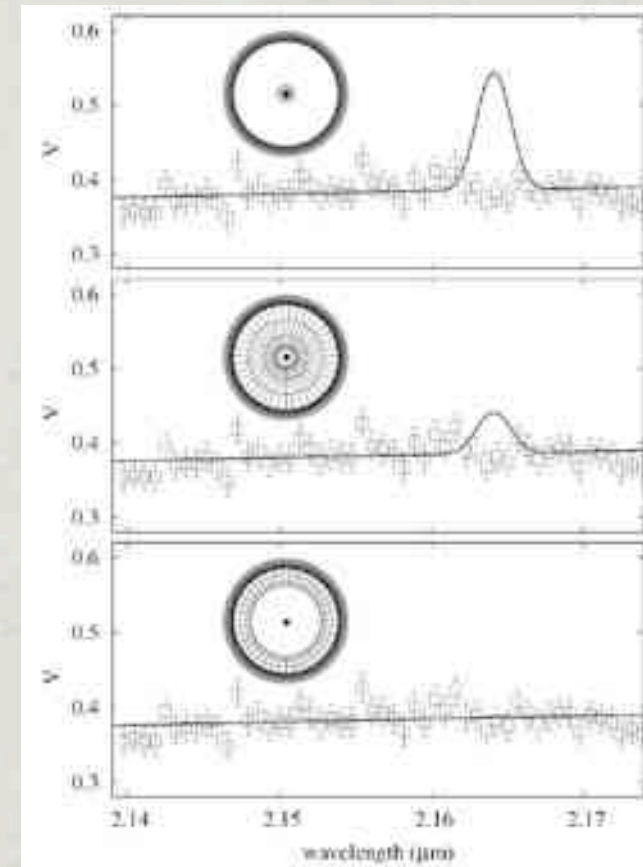
- For the given stellar parameters the measured ring radius is more compact than expected

- One reason might be that the stellar luminosity could be overestimated

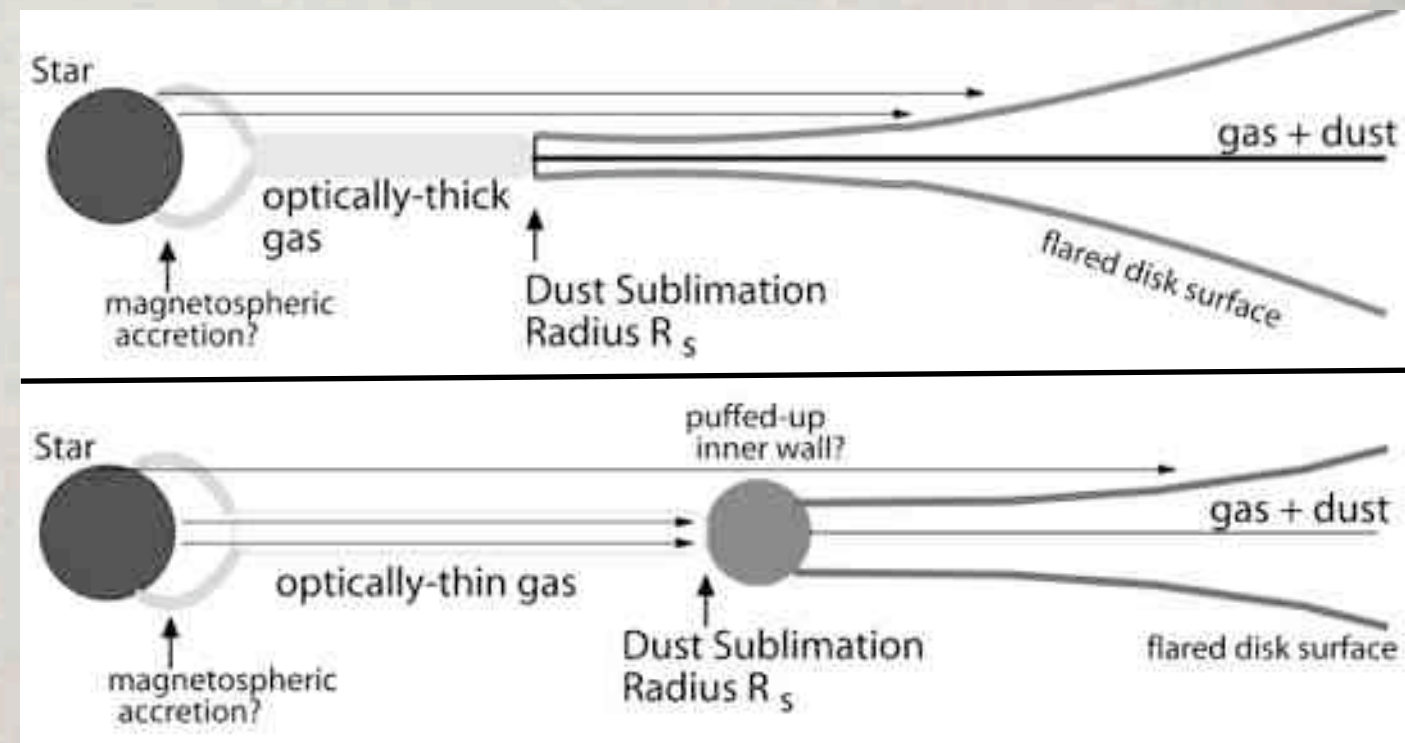
➡ The dust sublimation radius is not compact in contrast to the expected one

- An optically-thin inner gas disk could contribute to the total near-infrared emission

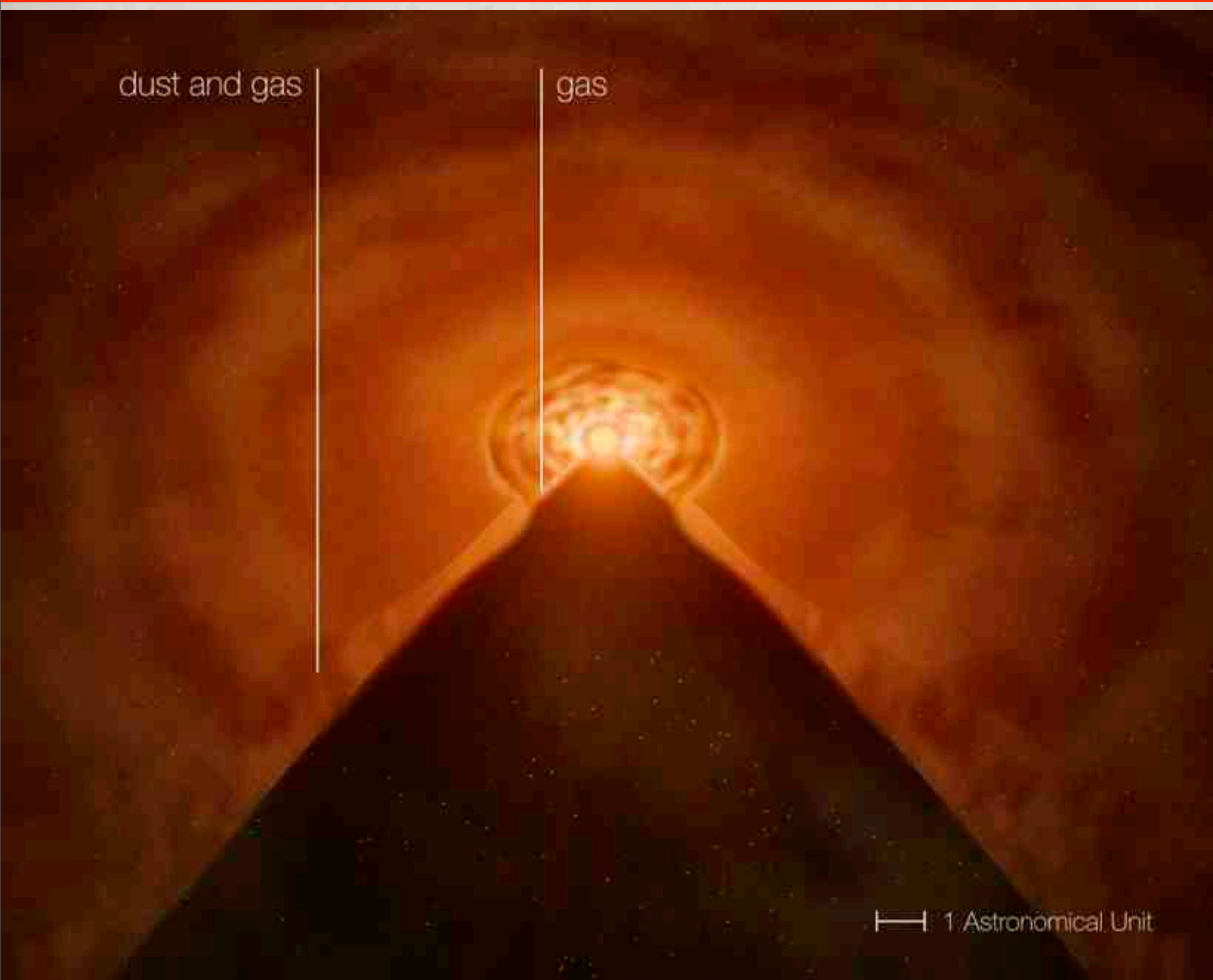
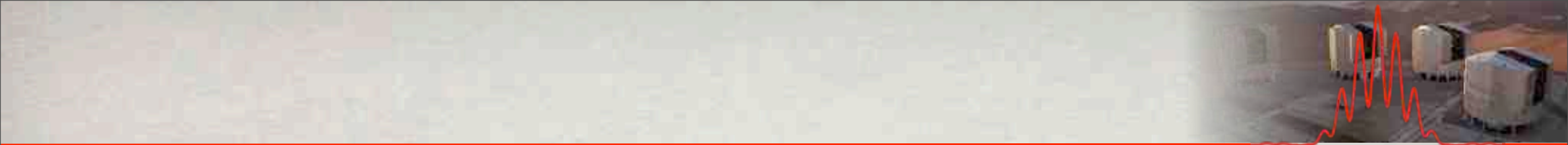
➡ Such inner gaseous disks were already successfully observed in YSO's
e.g. MWC 147 (Kraus et al. 2007)
MWC 748 (Isella et al. 2008)

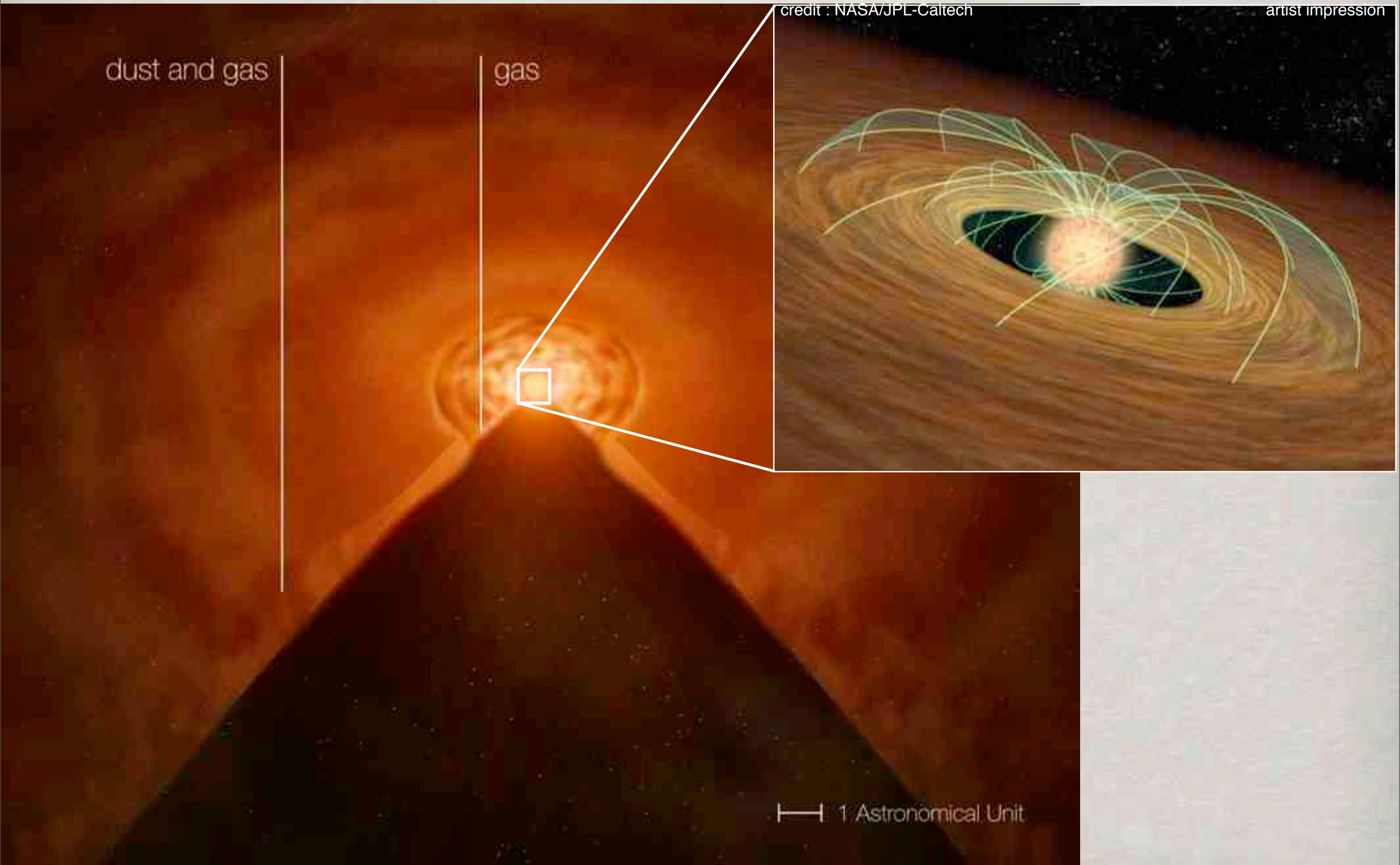
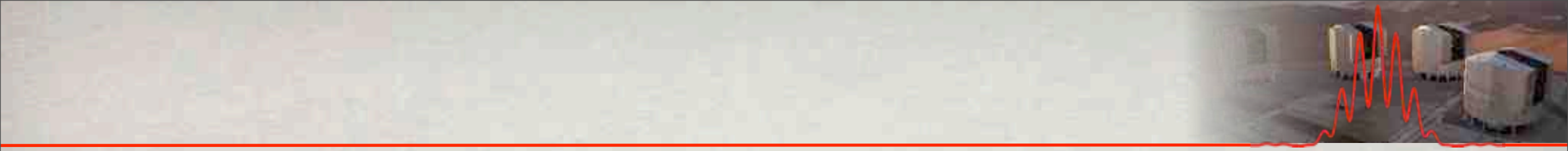


Tatulli 2007 et al.



Monnier et al. 2005



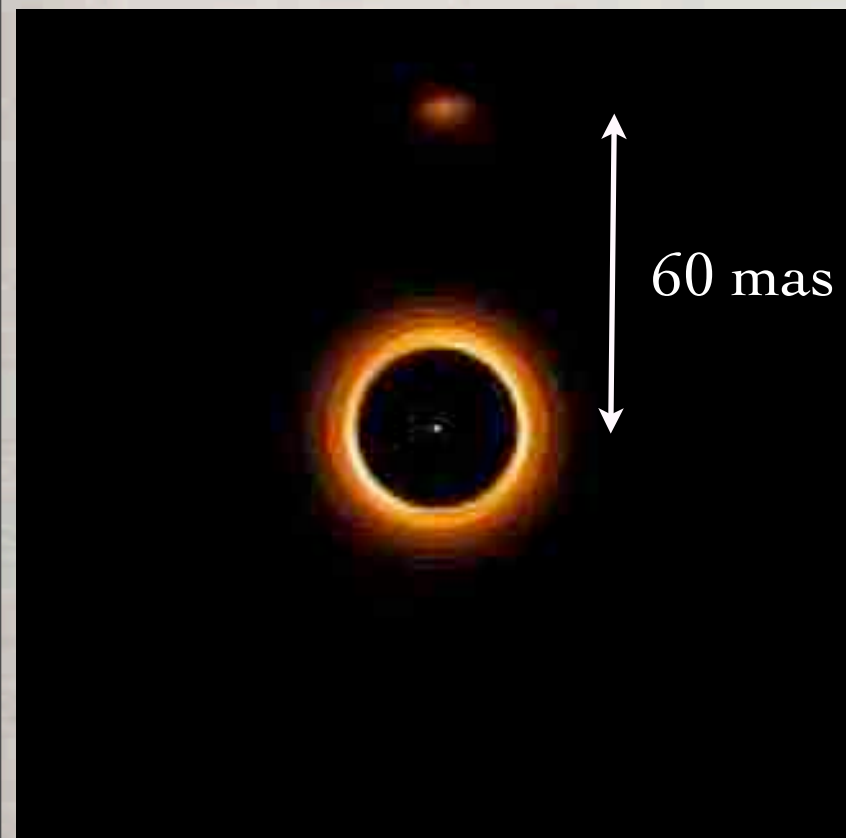




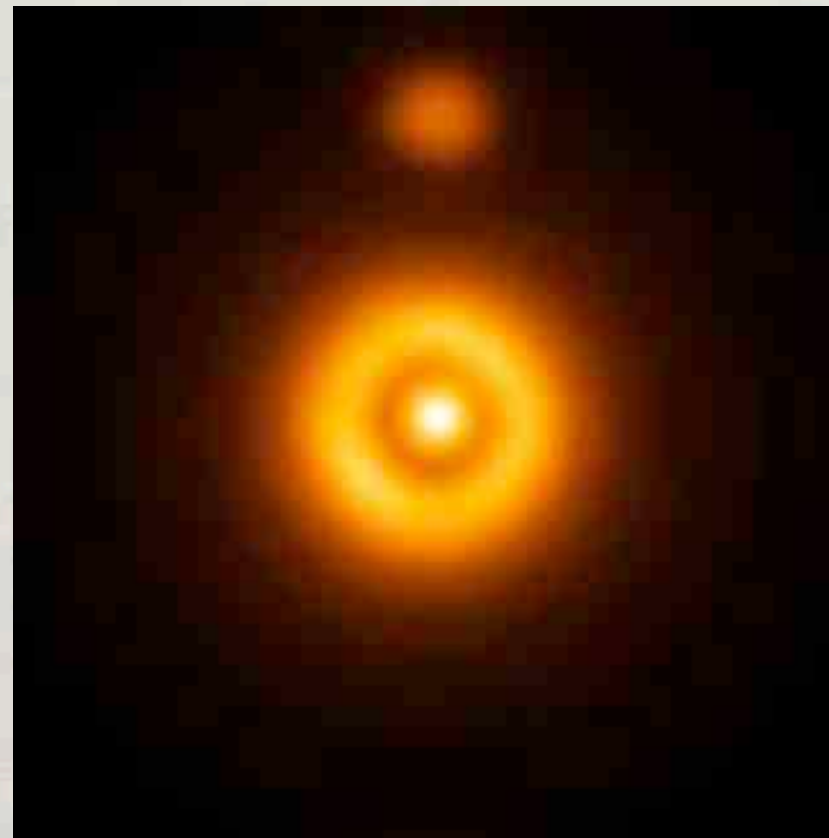
- Overview: circumstellar disks
- Disk models
- The inner rim
- Observational techniques: V921 Sco
- **Future Instruments**
- Summary



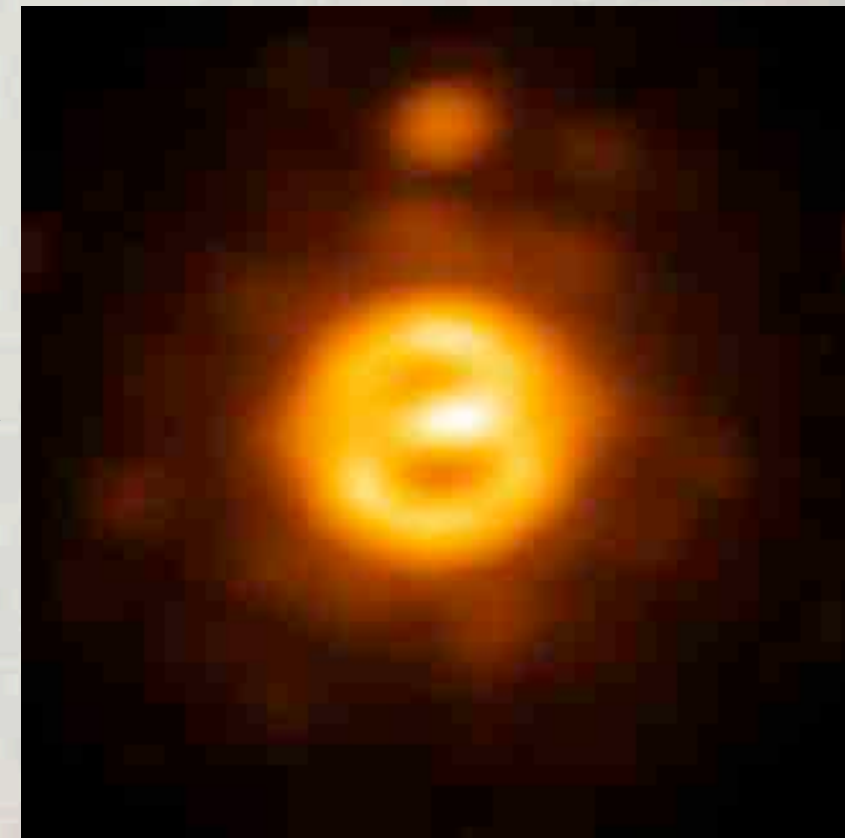
MATISSE (Multi AperTure mid-Infrared SpectroScopic Experiment)



model image



folded image

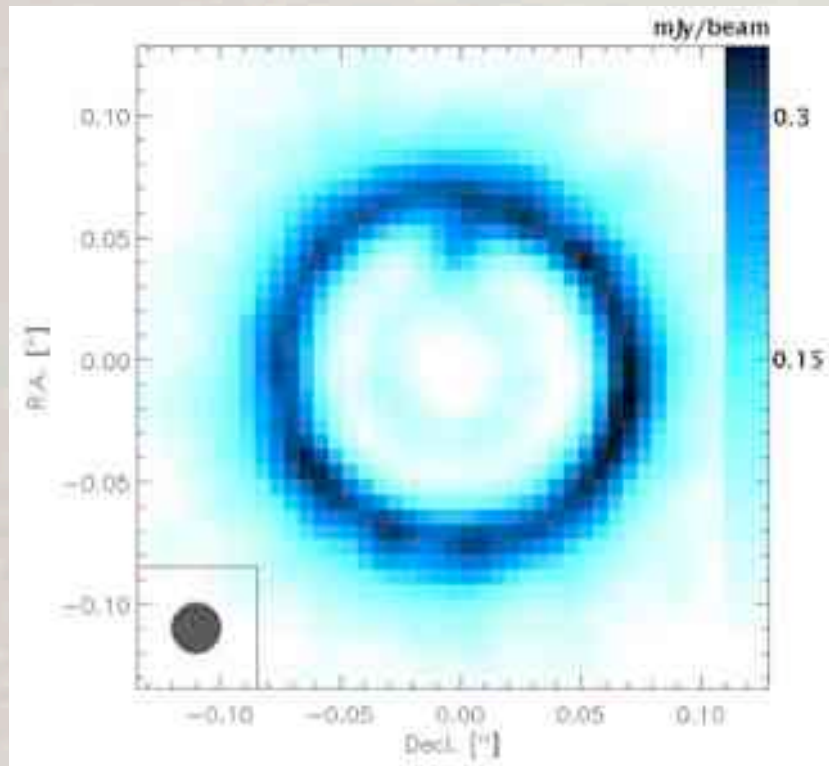


reconstructed image

- planet 200 times fainter than central star

Future Instruments

ALMA (Atacama Large Millimeter/submillimeter Array)



Extract of ALMA Science Objectives:

“Image the gas kinematics in protoplanetary disks around young sun-like stars with a resolution of a few astronomical units out to a distance of 150 pc (roughly the distance to the star forming clouds in Ophiuchus or Corona Australis), enabling the study of their physical, chemical and magnetic field structures and detection of the tidal gaps created by planets undergoing formation in the disks.”

Outline

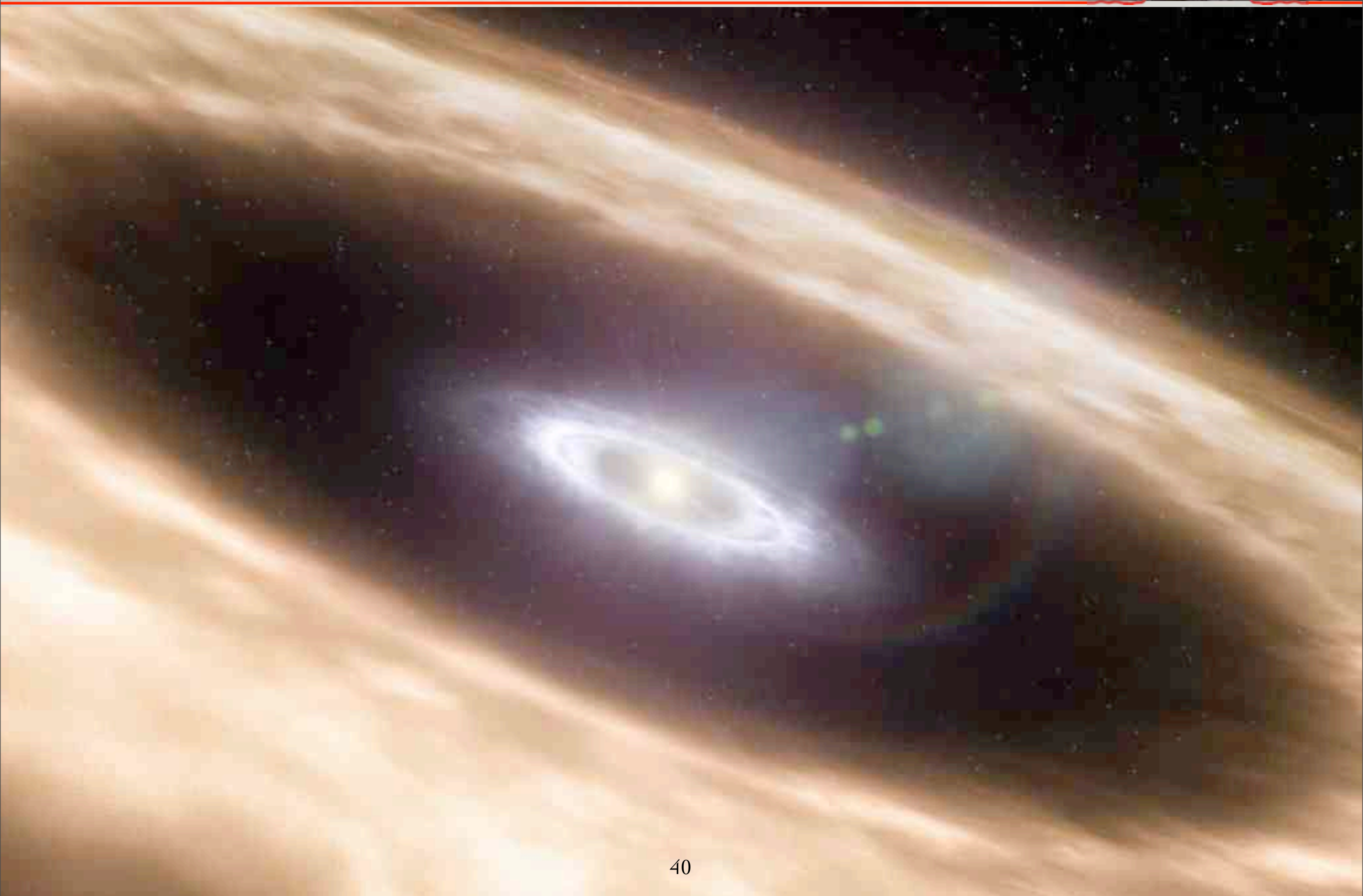


- Overview: circumstellar disks
- Disk models
- The inner rim
- Observational techniques: V921 Sco
- Future Instruments
- **Summary**



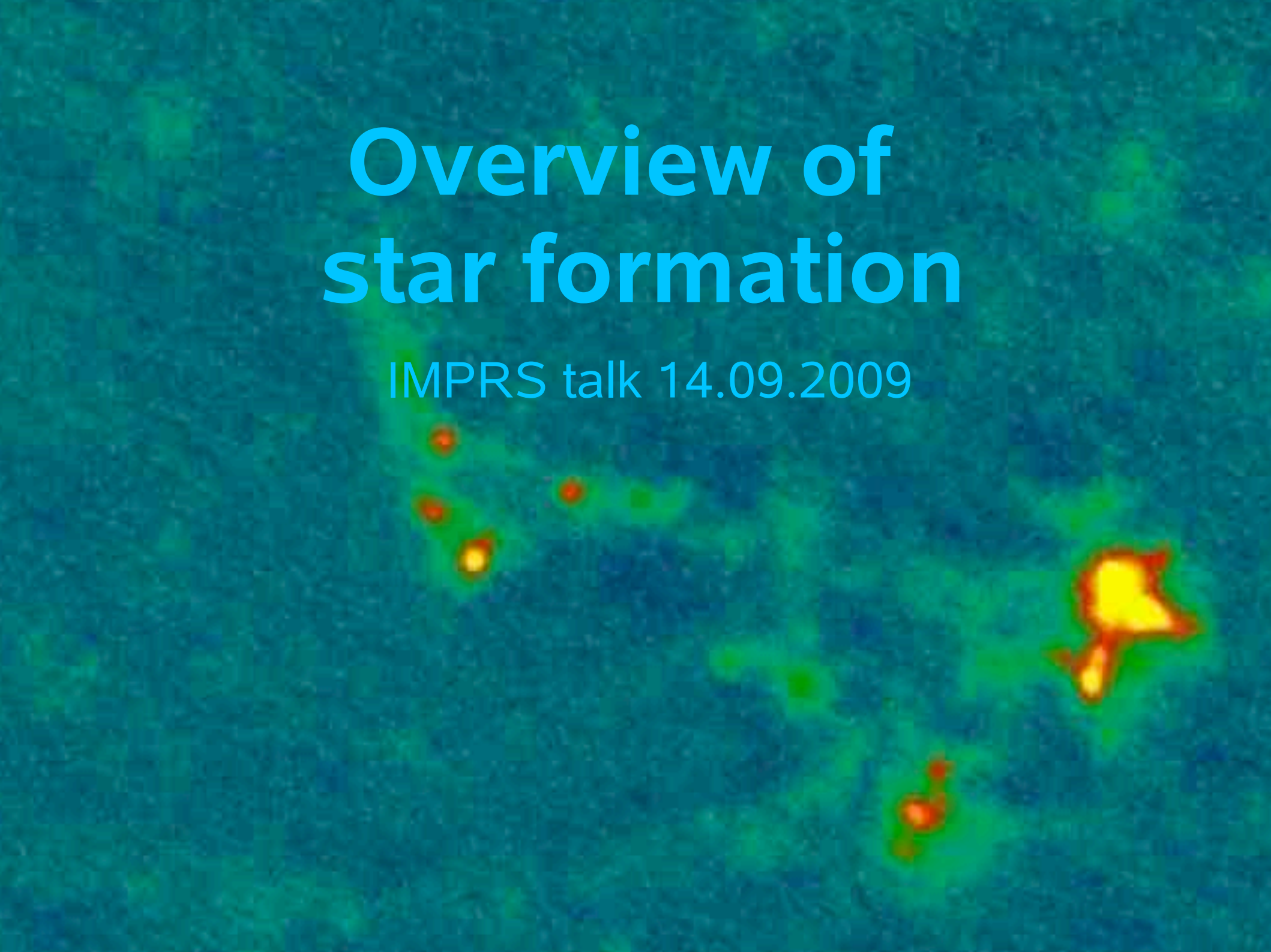
- The investigation of circumstellar disks, especially around intermediate mass stars, are important to understand the formation of high mass stars. → stars with $M_{\star} > 10M_{\odot}$ are embedded during their whole pre-main sequence life.
- and since we are combining at least three telescopes at the same time, we get closure phase information which reveal information about the rim structure
- with future instruments like ALMA and MATISSE we will be able to investigate circumstellar disks in more detail
 - constraints on disk mass, dust and gas composition etc.
 - detect finally planetary gaps / self shadowed disks directly

Thanks for your attention



Overview of star formation

IMPRS talk 14.09.2009



Outline

- The Interstellar medium: composition and different phases
- Initial conditions and stages of star formation
- Interstellar molecules
- Conditions of molecular clouds:
 - equilibrium and stability
 - instabilities
- Cloud collapse
- Models of star formation

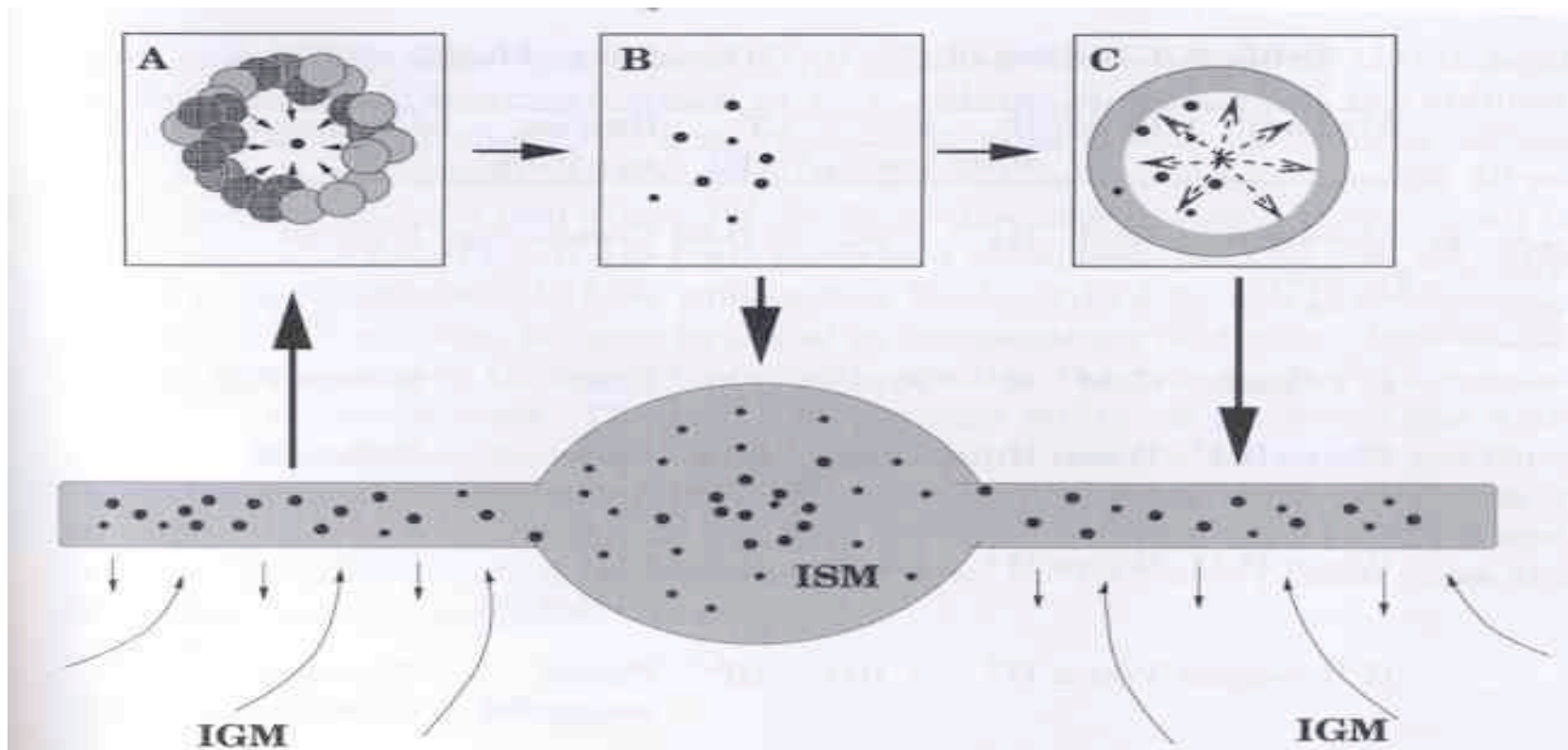
The Interstellar Medium

- first observational evidence by the discovery of Ca II lines in spectra of the binary star δ Orionis by J.Hartmann in 1904
- investigation by E. Hubble in 1922: scattering of light of nearby cool stars by dust clouds (reflection nebulae) and excitation of the gas by hot stars (emission nebulae)
- The ISM is an extremely tenuous gas consisting of :
 - Hydrogen (H_2 , H I, HII, e^-) (90%)
 - Helium (He I, He II)
 - other elements (e.g. C, O, Ne, Mg, Fe)
 - Molecules (e.g. CO, CS)
 - Dust
 - Cosmic ray particles
 - Magnetic fields
 - radiation fields

Interactions within the ISM

- formation of stars or whole stellar associations by collapse of cloud cores

- deposition of matter back into the ISM e.g. through winds from massive stars or mass ejections



Energy transfer in the ISM

Heating mechanisms :

- Photoionization of neutral particles
- Cosmic ray ionization of H_2
- Photoeffect on dust particles
- Photodissociation of molecules
- Excitation of H_2 by UV radiation and collisional deexcitation
- Chemical heating
- Dissipation of turbulence and shocks
- Potential energy released by the gravitational collapse of a molecular cloud

Energy transfer in the ISM

Cooling mechanisms :

- Free-free emission of electrons in HII regions
- Recombination of ionized particles
- Collisional excitation with emission of radiation
- Collisions of gas particles with dust

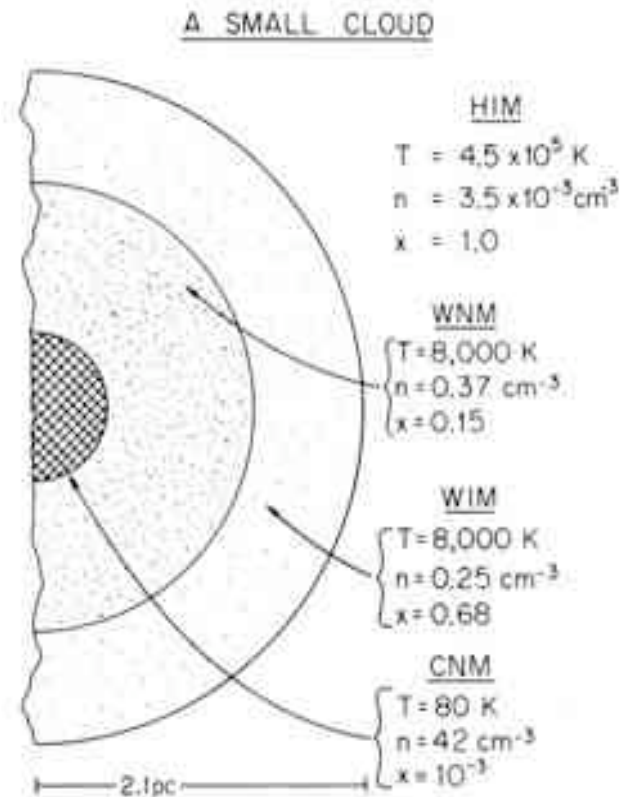
Different phases of the ISM

- The balance of heating and cooling processes determine the **temperature** and thus the **phase** of the ISM
- different phases coexist in pressure equilibrium

$$p = nkT$$

with the pressure p , the number density n , Boltzmann's constant k and temperature T

- **three phases:**
 - a hot phase (shocked gas from supernova explosions, coronal gas)
 - a warm phase (atomic hydrogen and ionized hydrogen gas)
 - a cold phase (molecular and atomic hydrogen gas and dust)



different phases of the ISM from
McKee & Ostriker 1977

Star formation

- Two categories:
 - low-mass ($M < 8 M_{\odot}$) star formation
 - high-mass star formation
- problems for the investigation of massive star forming regions:
 - larger distance and smaller number,
 - heavily extincted,
 - short evolution time scales,
 - dynamic and complex environments

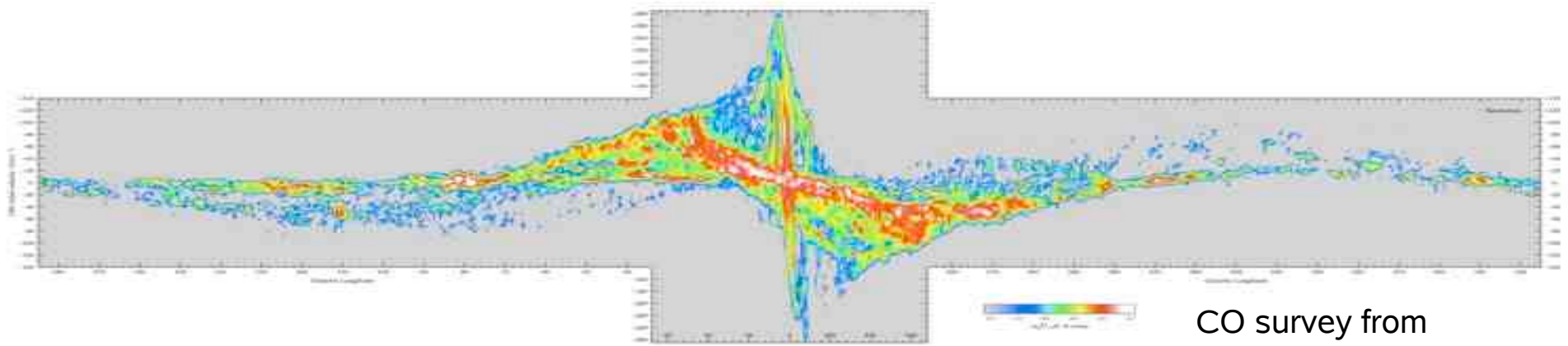
Initial conditions of star formation

Low-mass stars:

- fragmentation of clumps in dark clouds into **prestellar cores**, identified as **Bok Globules** in the optical (Bok & Reilly 1947)
- **diffuse, cold clouds** with low mass and column density (Lombardi & Alves 2001)
- formation of **protostars** by contraction of dense, compact cores with (Myers & Benson 1983)
 - temperatures of ~ 10 K
 - sizes of ~ 0.05 pc
 - masses of $0.5 - 5 M_{\odot}$
 - densities of $10^5 - 10^6 \text{ cm}^{-3}$

High-mass star formation

Giant molecular clouds (GMCs)



- large scale CO surveys ➡ formation of massive stars in GMCs
- diameters of 10-100 pc, masses of $10^{5-6.5} M_{\odot}$, mean densities of several 100 cm^{-3} (Stutzki & Guesten 1990)
- possess substructures:
 - clumps ➡ overdense structures, which could form whole clusters, radii about 3-5 pc and masses of $10^3-10^4 M_{\odot}$
 - cores could form individual stars or multiple systems


Initial stages of massive star formation

- early known stages:
 - **hot cores**: compact, infrared-bright regions with densities of $\sim 10^7 \text{ cm}^{-3}$, temperatures of $\geq 100 \text{ K}$, a diameter of $\sim 0.1 \text{ pc}$ and total mass of several hundred M_{\odot} .
 - **HII regions**: ionization of the remaining molecular cloud surrounding a massive protostar, diameters of $\geq 10^{18} \text{ cm}$ and densities of $\leq 10^4 \text{ cm}^{-3}$, associated with free-free continuum observed in cm surveys (Palla et al. 1991)
 - **young stellar objects** $< 10^5$ years can be traced by water and methanol maser surveys (Walsh et al. 1997, 1998, 2003)

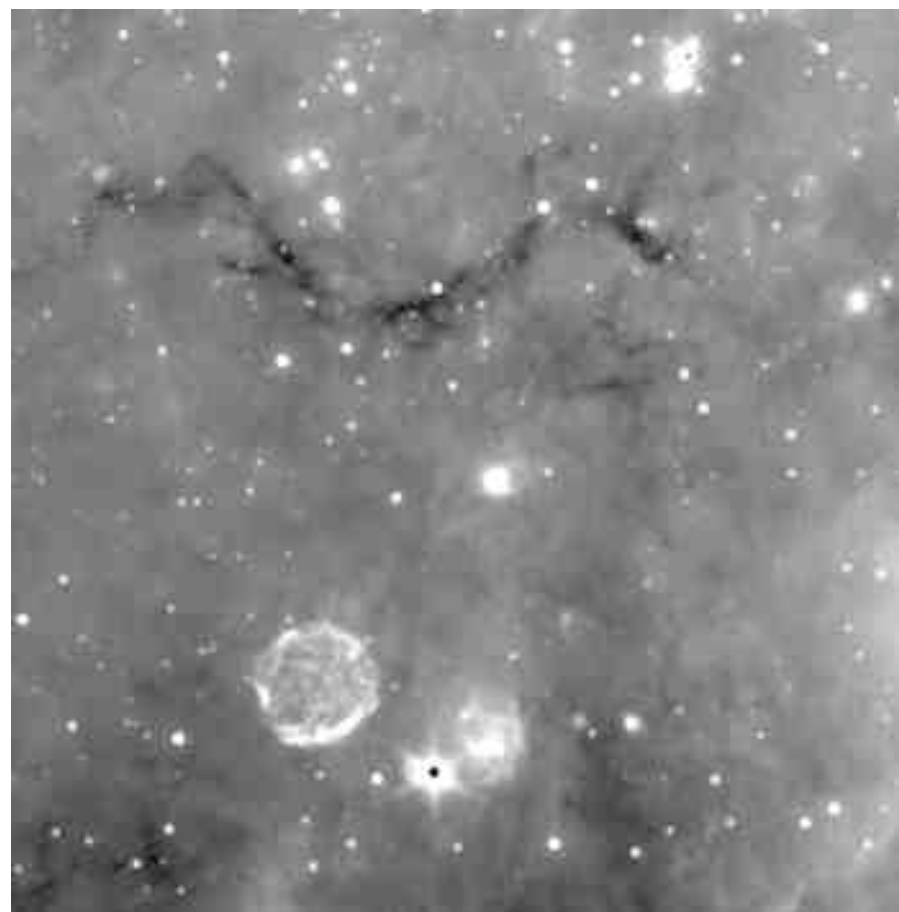
Initial stages of massive star formation

- still unknown: youngest massive protostars
 - (sub)mm dust continuum
 - high-density molecular tracer
- lack of temperature and velocity
 - ➡ spectral line emission is necessary
- obtaining: - linewidth,
 - velocity ➡ kinematic distances
 - ➡ mass & luminosity

Infrared Dark Clouds (IRDCs)

- earliest, cold phases are deeply embedded  not probed in the mid-infrared
- extinction features against mid-IR background
- first detection by ISO and MSX
(Perault et al. 1996, Egan et al. 1998)
- Largest 1.2 mm-dust continuum survey of IRDCs by Rathborne et al. (2006)

IRDC11-00



Interstellar molecules

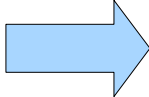
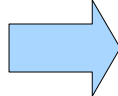
- beginning of molecular astrophysics in 1930s:
discovery of CH, CH⁺ and CN in diffuse clouds
- detection by absorption of optical light from background stars
- extension to more complex species, many found in dense cores, in shock-heated regions of Orion, Sagittarius B2 at the Galactic center and in envelopes of evolved, giant stars
- in 1960s: discovery of OH, NH₃, H₂CO and H₂O
- in 1970s: H₂ and CO were identified
- to date over 100 molecules have been found

Abundances and properties of some molecules

- H_2 : the major constituent of cold interstellar clouds as well as hotter environments, e.g. clouds irradiated by a luminous star or shocked by a stellar wind, abundance $X=1$
- CO : $X = 8 \cdot 10^{-5}$, best observed at 2.6mm, low density tracer ($n \sim 10^3 \text{ cm}^{-3}$)
- OH : $X = 3 \cdot 10^{-7}$, detected at 18 cm, magnetic field probe
- NH_3 : $X = 2 \cdot 10^{-8}$, inversion transitions at 1.3 cm, low temperature probe at high densities ($n \sim 10^5 \text{ cm}^{-3}$)
- H_2CO : $X = 2 \cdot 10^{-8}$, detected at 2.1 mm, high density probe ($n \sim 10^6 \text{ cm}^{-3}$)
- CS : $X = 1 \cdot 10^{-8}$, transition at 3.1 mm, high density probe ($n \sim 10^5 \text{ cm}^{-3}$)

Conditions of molecular clouds

Cloud equilibrium and stability

- Theoretical model for a molecular cloud:
 - uniform-temperature sphere supported by internal pressure against self-gravity with a maximum possible mass, the Jeans value
 - Clouds with masses exceeding this limit  gravitational collapse
- all observed clouds larger than dense cores  masses exceeding the Jeans limit, but not collapsing
- assuming all clouds are gravitationally unstable, one would expect a star forming rate of $\sim 25 M_{\odot} \text{ year}^{-1}$ in our Galaxy, but the observed rate is $\sim 5 M_{\odot} \text{ year}^{-1}$

 most clouds not unstable, a stabilizing support

Conditions of molecular clouds

Fragmentation of large- and small-scale structures

- spiral arms of the Galaxy of 10 kpc
 - giant molecular clouds of 1 kpc
 - molecular clouds of 10 pc
 - molecular cores of 0.1 pc
 - protostars of 100 AU
- large-scale structures: from spiral arms to molecular clouds, stabilized by thermal, rotational, turbulent and magnetic support
- small-scale structures: molecular cores and protostars, supported by thermal and magnetic pressure


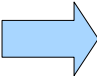
Cloud equilibrium and stability

- kinetic energy of each gas particle, $\frac{3}{2} k T$ with temperature T and Boltzmann constant k , produces a gas pressure which opposes gravitational contraction
- virial theorem for a gravitationally bound cloud:

$$2T + 2U + W + M = 0$$

with the total kinetic energy $T = \frac{1}{2} m v^2$,
the energy contained in random, thermal motion $U = \frac{3}{2} P V_{\text{cl}}$ with
cloud volume V_{cl} ,
the gravitational energy $W \sim \frac{-M^2}{R}$,
the magnetic energy $M \sim B^2 V_{\text{cl}}$

Cloud Support by Rotation

- angular momentum of molecular clouds originates from the ISM and the rotation of the Galaxy, coupling by magnetic fields and shocks
- some angular momentum is lost by magnetic braking:
 - the magnetic field in the Galaxy penetrates molecular clouds
 - it will be winded up by the rotation of a contracting cloud with increasing angular velocity stretched magnetic field lines produce opposite angular momentum and reduce the angular velocity of the cloud which remains nearly constant
- assumption of solid rotation of a very dense contracting cloud due to friction at high viscosity  constant angular velocity

$$F_z = m \omega^2 R \quad \text{and} \quad F_G = \frac{GmM}{R^2}$$

- the collapse cannot be prevented by rotation within the radius, where centrifugal force F_z equals gravitational force F_G
- outside this radius: collapse proceeds only partially  disk formation

Cloud Support by Turbulence

- the average thermal velocity of molecules is $1\text{-}10 \text{ km s}^{-1}$, while observed velocities of interstellar clouds are $10\text{-}100 \text{ km s}^{-1}$

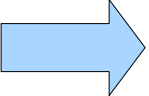

 the motion of interstellar gas is influenced by **turbulence and compression** in general

- the decay time of turbulence can be smaller than the free-fall time during stellar collapse

 **follow-up shocks will disperse the clump before it can form protostellar cores**

- Theoretically, turbulences should be dissipative. However, observations show well ordered magnetic fields over the dimensions of the clouds which prevents turbulence from dominating over magnetic fields.

Cloud Support by magnetic fields

- molecular clouds are partially ionized  the gas is a very good conductor, the magnetic field lines tethered to the gas
 - the contraction of the cloud brings together adjacent field lines and results in a larger field strength, as $B \sim R^{-2}$
 - the increase of B with density is called flux freezing
 - the field tension and the magnetic pressure gradient rise
-  these forces together with an increased gradient in the thermal pressure can oppose self-gravity

Instabilities in the interstellar gas

- non-equilibrium processes in the IS gas transform that gas from the low interstellar density ($\sim 10^{-23} \text{ g cm}^{-3}$) to high stellar density ($\sim 10^2 \text{ g cm}^{-3}$)

Gravitational instability (“Jeans instability”)

Two forces on a volume element of 1 cm^3 in a spherically symmetric mass distribution :

- The inwards directed gravitational force $F_g = G \rho M R^{-2}$ with the density ρ , the constant of gravitation G and the mass M within the distance R
- The outward directed force due to the pressure gradient $F_p = \frac{dP}{dr}$

with $P = \rho T \frac{R_g}{\mu}$ (μ mean molecular weight, R_g gas constant):

Gravitational instability (“Jeans instability”)

$$F_p = \frac{d}{dr} (T \rho R_g \mu^{-1}) = T R_g \mu^{-1} \frac{d\rho}{dr}$$

Then, the equation of motion is

$$\frac{d^2 r}{dt^2} = -\frac{GM}{R^2} - \frac{R_g T}{\mu} \frac{1}{\rho} \frac{d\rho}{dr}$$

The gas will start to **contract for negative acceleration**

$$\frac{GM}{R^2} > \frac{R_g T}{\mu} \frac{1}{\rho} \frac{d\rho}{dr}$$

using the approximation $\frac{d\rho}{dr} = \frac{\rho}{R}$ and $R = \left(\frac{3}{4\pi} \frac{M}{\rho}\right)^{\frac{1}{3}}$

$$M_{Jeans} = \left(\frac{3}{4\pi}\right)^{\frac{1}{2}} \left(\frac{R_g T}{\mu G}\right)^{\frac{3}{2}} \left(\frac{1}{\rho}\right)^{\frac{1}{2}}$$

is **the Jeans mass**, the critical mass of instability for contraction or the minimum mass of contraction for the ambient values of T, ρ and μ

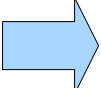
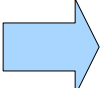
- for IS clouds with neutral hydrogen : $M_{Jeans} \sim 10^5 M_{\odot}$
- for dense molecular clouds: $M_{Jeans} \sim 25 M_{\odot}$

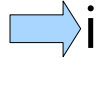
Thermal instabilities

Energy balance in the ISM is determined by

- processes of energy input and output
- processes of heating and cooling (radiation)

Increase of density ρ of a gas volume element by random or superimposed fluctuations to $\rho + d\rho$.

- effective cooling decreases the temperature T by an amount dT  the pressure will decrease with respect to the surroundings  compression of the volume element

- effective cooling: fast emission of energy gain from contraction  increase of density and formation of instability


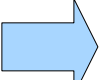

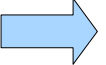

- thermal instability: cooling is more efficient than heating, when

$$t_c < t_h$$

with the cooling time t_c and heating time t_h .

- exponential increase of density fluctuations with the cooling time scale

Ambipolar diffusion

- magnetic pressure as a major support of molecular clouds, but much smaller magnetic energy per unit mass of a star than in the ISM
- **ambipolar diffusion**  explanation of reduced influence of the magnetic field
- co-existence of ions, electrons and neutral particles in a molecular cloud with ratio of charged to neutral particles $\sim 10^{-7}$
- **coupling of the magnetic field to the charged particles** by electromagnetic forces, **coupling of charged particles to the neutral component** by viscous forces
- movement of the molecular cloud relative to the magnetic field 
separation of charged particles and **decoupling of the magnetic field from the neutral gas** 
formation of a **cloud core consisting of neutral gas without magnetic forces**
- problems: - poorly known degree of ionization or dependence from density
- support of clouds by magnetic forces perpendicular to magnetic lines 
contraction of plasma along the magnetic lines and formation of a disk with efficient cooling  further contraction

Cloud collapse

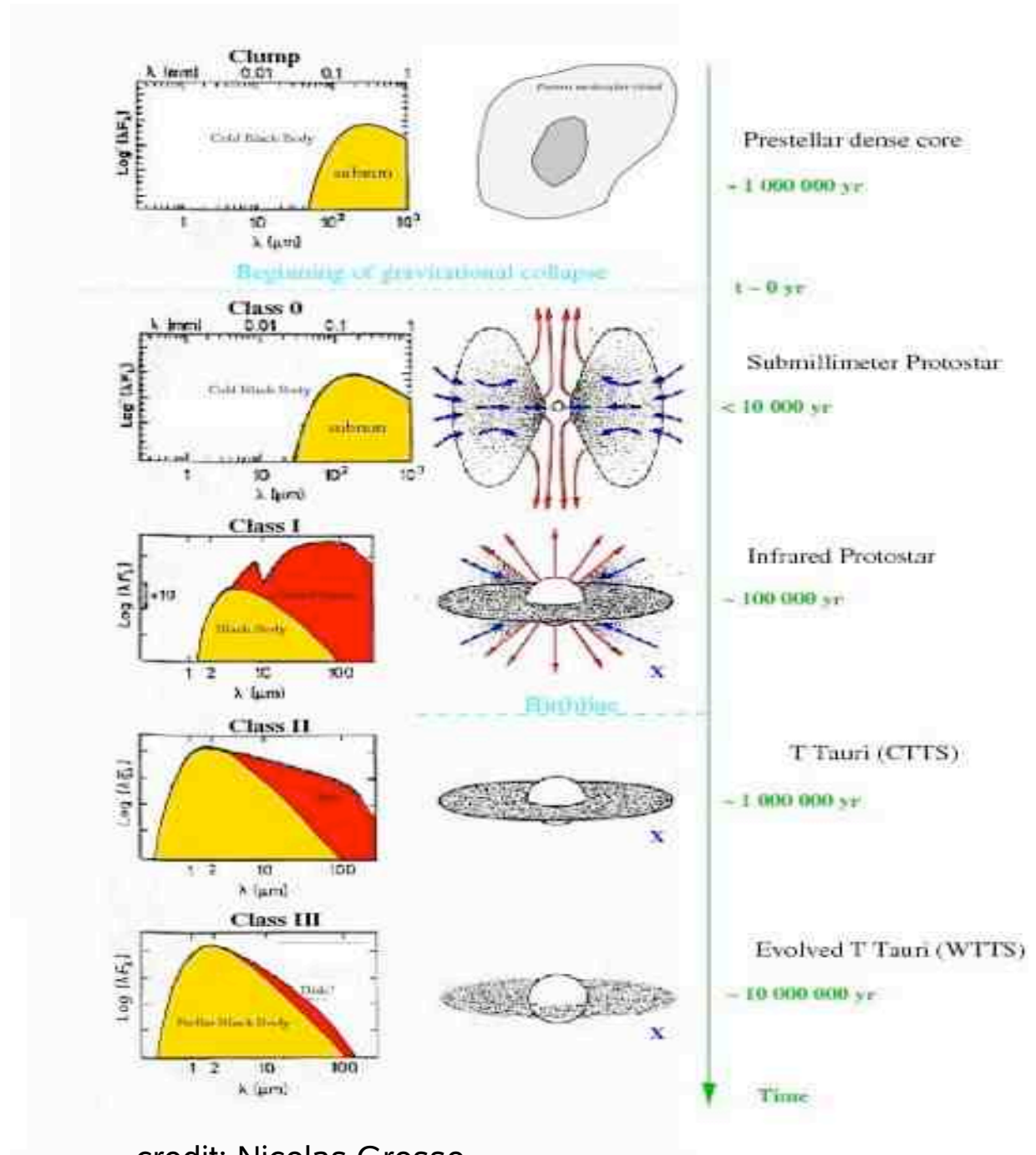
- star formation in the densest parts of molecular clouds →
high extinction by associated dust avoids observations →
process described only theoretically
- gravitational force dominates that of thermal and magnetic pressure
- beginning of contraction, increase of density towards the centre
- free-fall collapse time proportional to $(G\rho)^{-1/2}$ → smaller in the interior
→ inside-out-collapse: interior begins to collapse before the outer regions
- observations of dense cores in CO and at higher densities in NH_3
- end of collapse in a protostar, which pulls in cloud material by its gravitational attraction

Infrared/Submillimeter Young Stellar Object Classification

(Lada 1987 + André, Ward-Thompson, Barsony 1993)


Low-mass star formation

- compact cores in diffuse cold dark clouds
- deeply embedded protostars, strong accretion, collimated outflows
- emerging protostars (I.R.) accretion, increase of mass, heating, outflows
- young stellar objects, less embedded, thick disk
- pre-main sequence or young main sequence stars
- thin disk



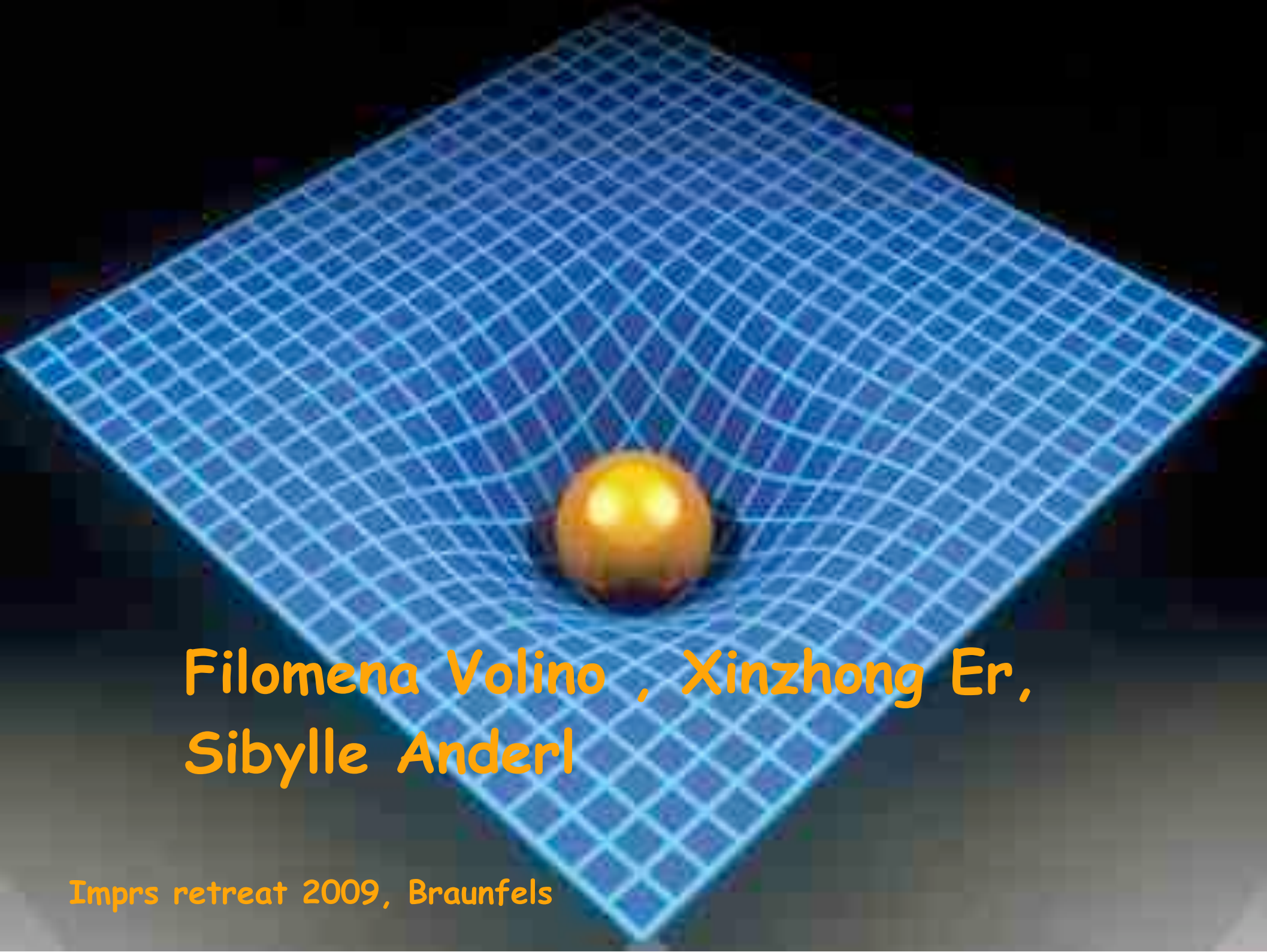
credit: Nicolas Grosso

High-mass star formation

- theoretical problems compared to low-mass s.f.:
radiation pressure halts infall 
- two different main models:
 - high accretion rates through disks (Padoan & Nordlund 2002)
 - merging to high-mass star in the centre of star clusters (Bonnell et al. 1998)
- observational evidence of
 - model I : strongly collimated molecular outflows indicating high accretion rates through disks (Beuther et al. 2002)
 - model II : concentration of most massive stars in regions of young stellar clusters (Zinnecker & Bate 2002)

Conclusion

- molecular clouds form out of the ISM and fragment into substructures such as clumps and cores
- some well known initial phases of star formation
- still unknown earliest phases of MSF
- most clouds in energetic equilibrium
- instabilities in the ISM can lead to cloud collapse
- better understanding of low-mass than high-mass star formation



Filomena Volino , Xinzhong Er,
Sibylle Anderl

Imprs retreat 2009, Braunfels

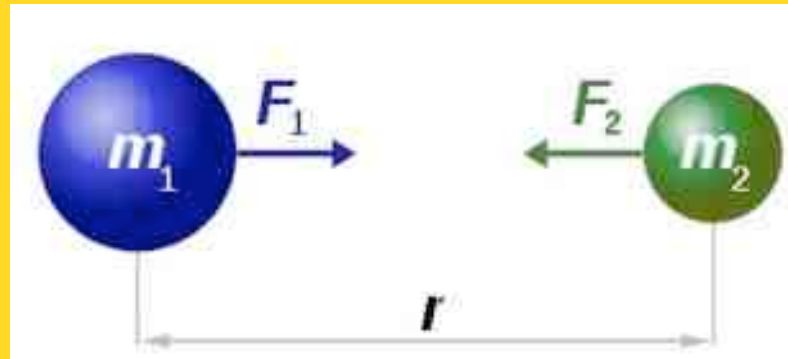
Outline

- Gravity, from Newton to Einstein
- Framework of GR
- Cosmological principle
- Relativistic cosmology

Newtonian gravity

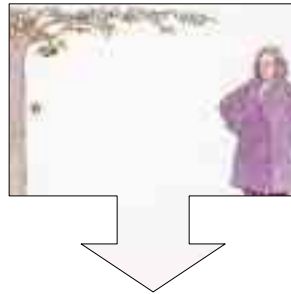
$$\mathbf{F}_1 = m_1 \ddot{\mathbf{x}}_1 = G \frac{m_1 m_2}{|\mathbf{x}_1 - \mathbf{x}_2|^2} \frac{\mathbf{x}_2 - \mathbf{x}_1}{|\mathbf{x}_1 - \mathbf{x}_2|}$$

$$\mathbf{F}_2 = m_2 \ddot{\mathbf{x}}_2 = G \frac{m_1 m_2}{|\mathbf{x}_1 - \mathbf{x}_2|^2} \frac{\mathbf{x}_1 - \mathbf{x}_2}{|\mathbf{x}_1 - \mathbf{x}_2|} = -\mathbf{F}_1$$



why do we need new theory of gravity? ?

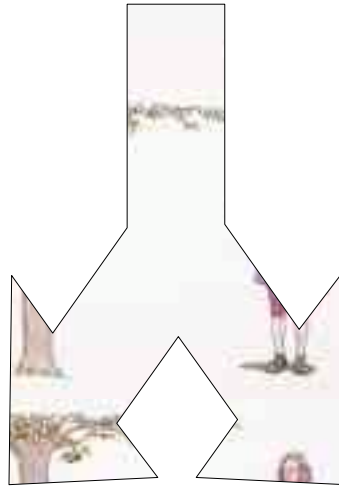
- 1865 J.C. Maxwell, electromagnetism
- search for 'ether', *luminis feris*
- contraction of length and slow down of a clock when moving through ether!!
(Lorentz, Fitzgerald, Poincare', 1895)



hypothesis not verifiable!!

why do we need new theory of gravity? ?

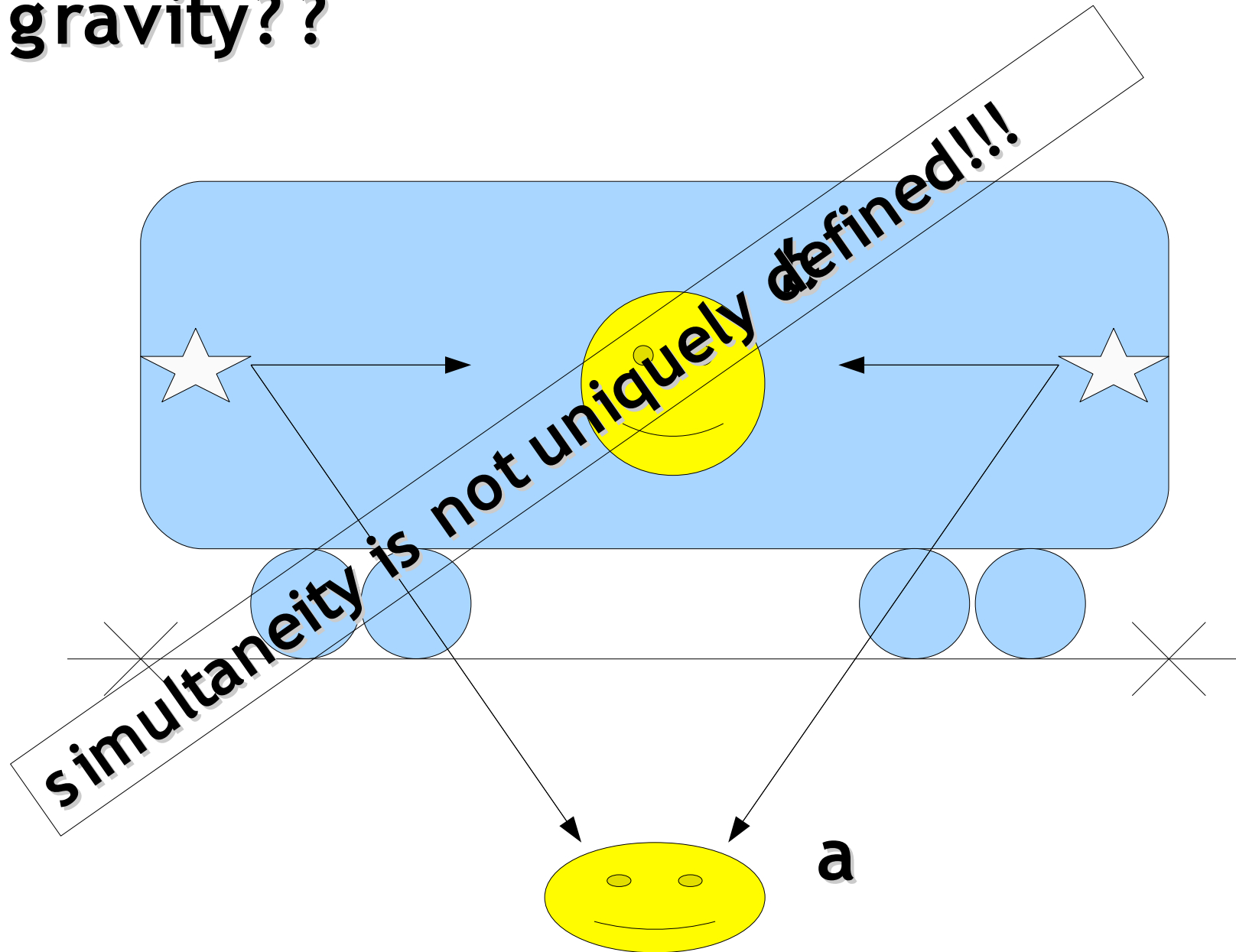
- special relativity (Einstein, 1905)



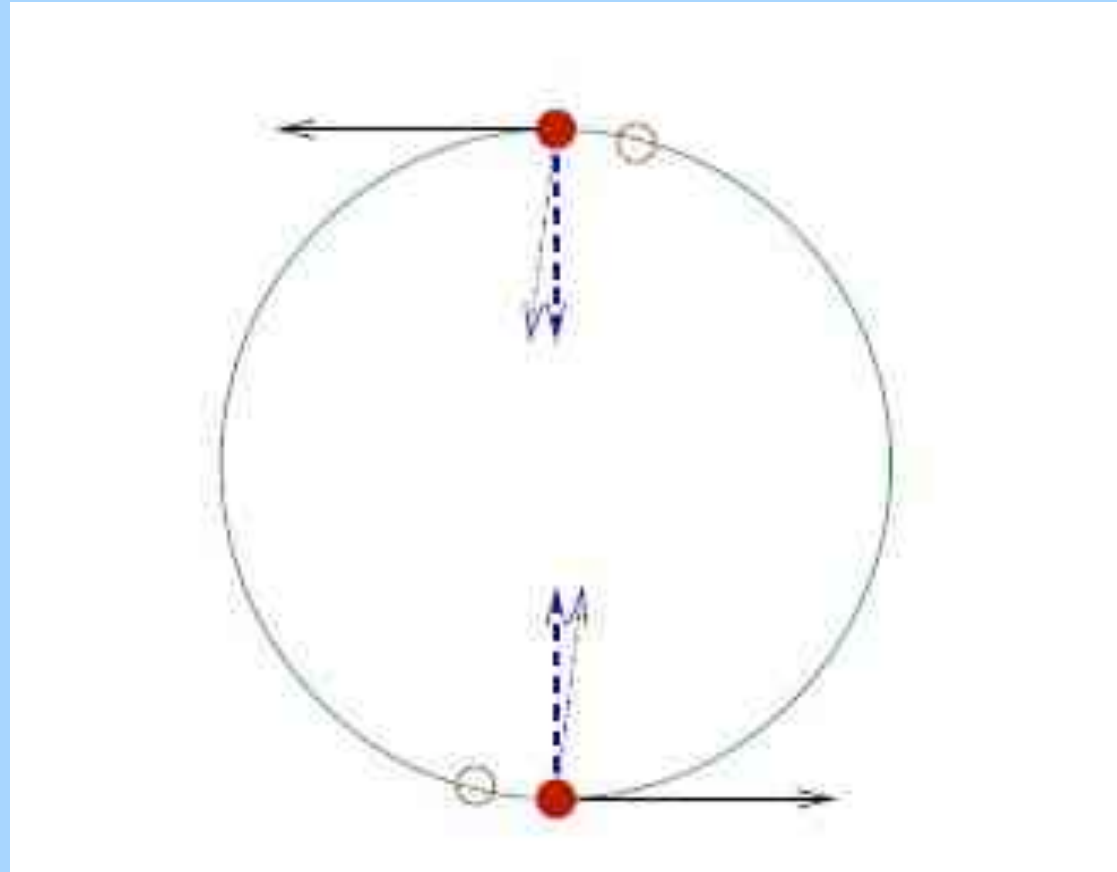
all observers are
equivalent as far
as dynamical
experiments

constancy of
velocity of light
(quite heuristic
statement for the
time!!)

- why do we need new theory of gravity? ?

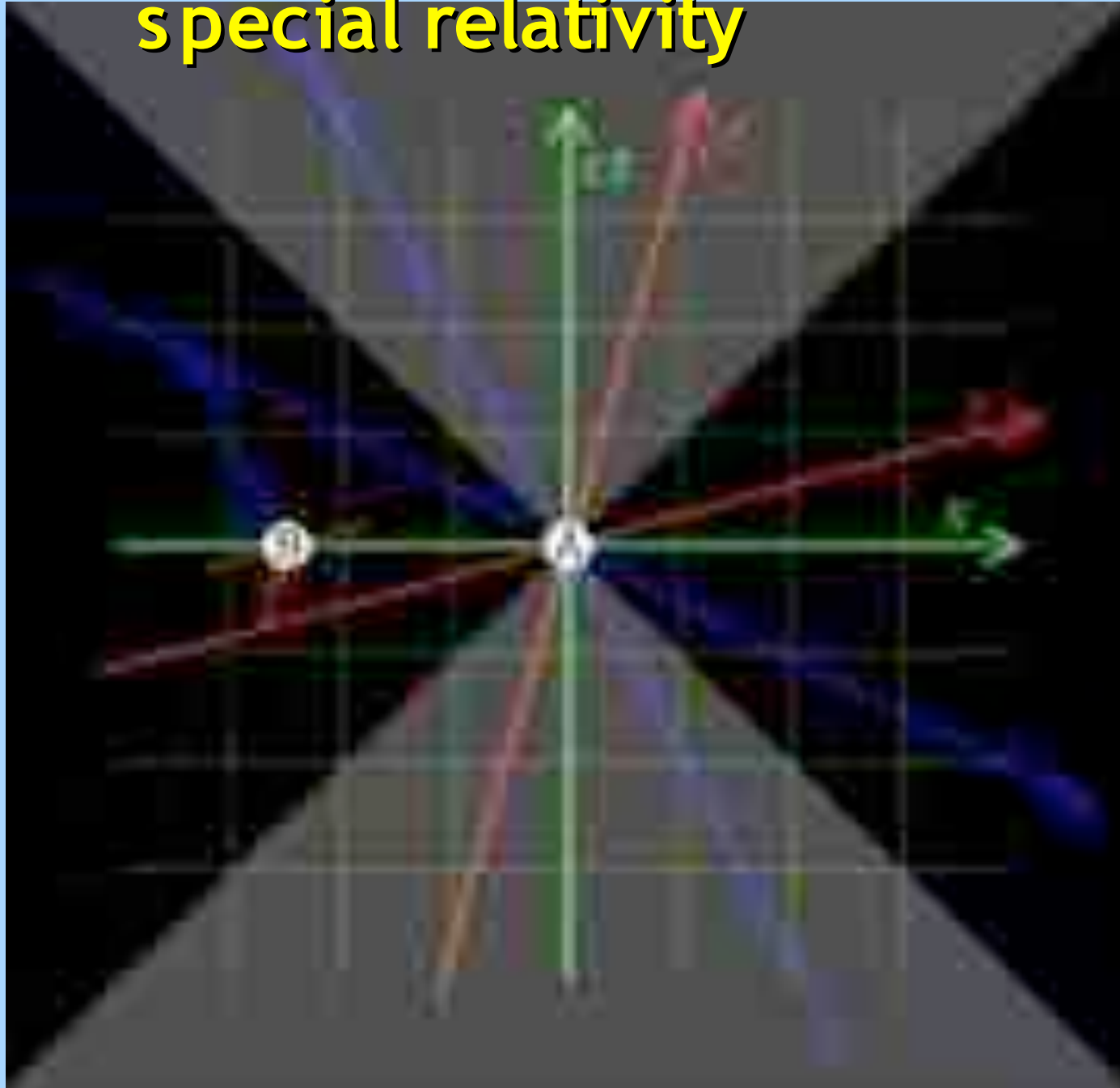


- why do we need new theory of gravity? ?



inconsistencies between
Newtonian gravity and S R

special relativity



- space and time merge together and form a four continuum space-time
- the interval between 2 events $P(t,x,y,z)$ and $P'(t+dt,x+dx,y+dy,z+dz)$ is

$$ds^2 = dt^2 - dx^2 - dy^2 - dz^2$$

- Minkowsky space-time

general relativity

(or, investigating Newton's second law in a non inertial frame)

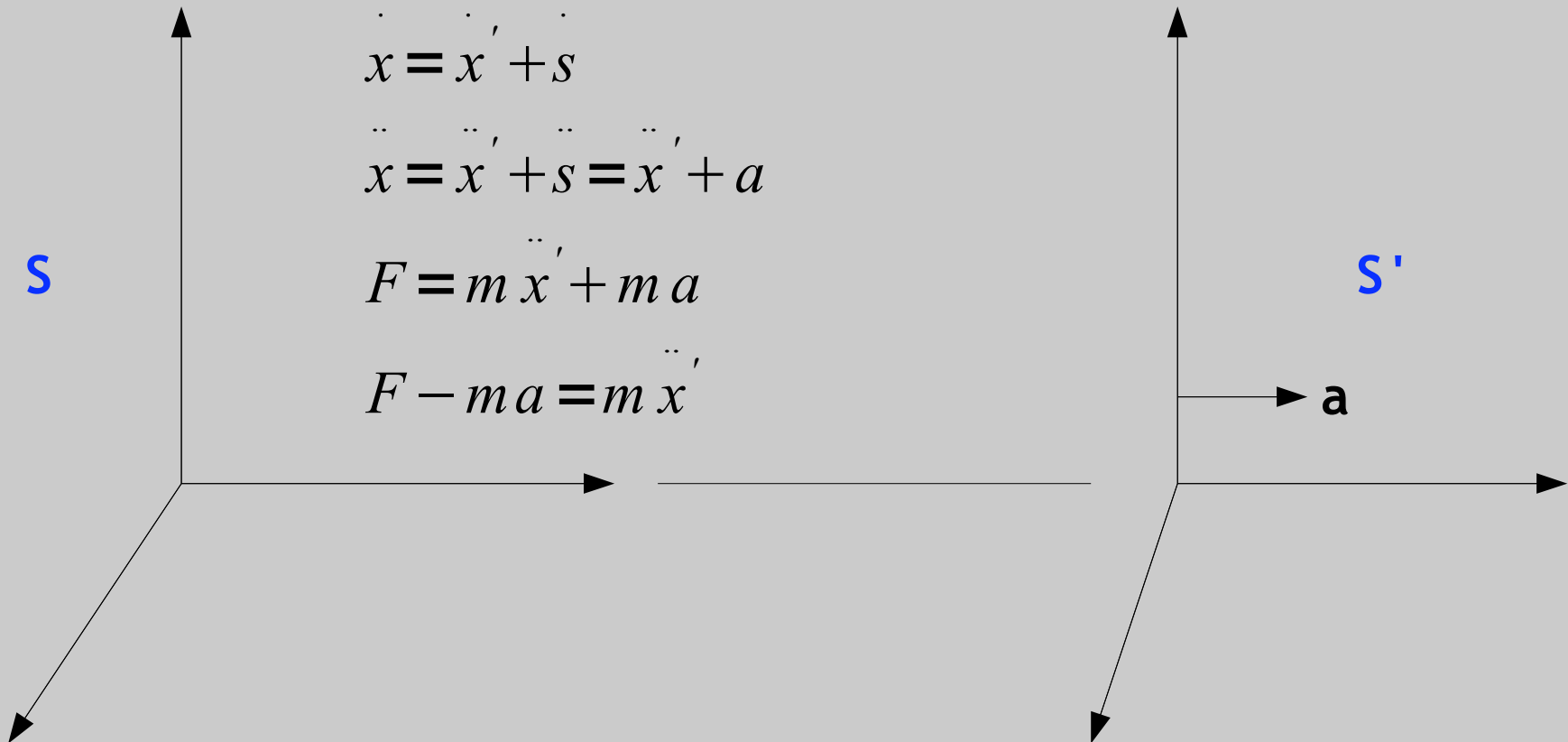
$$x = x' + s; y = y'; z = z'$$

$$\dot{x} = \dot{x}' + \dot{s}$$

$$\ddot{x} = \ddot{x}' + \ddot{s} = \ddot{x}' + a$$

$$F = m \ddot{x}' + m a$$

$$F - m a = m \ddot{x}'$$



in S' the body experiences the 'additional' inertial force

- How do we detect an inertial frame?
- Observer in absolute acceleration respect the absolute space
- No meaning to the notion of 'motion', only to the notion of 'relative motion'
- A body in an empty space cannot be said in motion

Mass to define an inertial frame!

general relativity

(or gravity as inertial effect!)

- All inertial forces in Newtonian theory are proportional to the mass of the body experiencing them
- If we drop 2 bodies in the Earth's gravitational field, then they experience $m_1 g$ and $m_2 g$.
- Gravity arises when using a non inertial frame



The principle of equivalence

A frame linearly accelerated relative to an inertial frame in special relativity is locally identical to a frame at rest in a gravitational field (*Gedankenexperiment*)

- The motion of a gravitational test particle in a gravitational field is independent of its mass and composition
- The gravitational field is coupled to everything

theory	position	velocity	Time	Acceleration
newtonian	relative	relative	absolute	absolute
SR	relative	relative	relative	absolute
GR	relative	relative	relative	relative

- All reference systems are equivalent!! (or all physical laws can be formulated in a way which is equivalent for all r.f. or coordinates)

1st summary

Special relativity vs GR

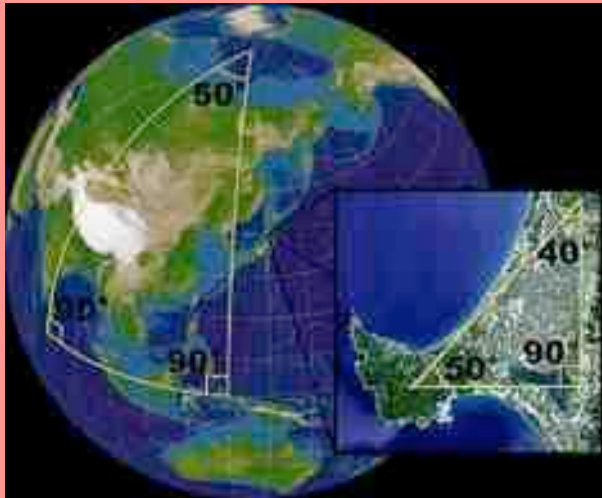
- All inertial reference frames are equivalent
- Mass energy equivalence
- Linearly accelerated field relative to an inertial frame is equivalent to a frame at rest in gravitational field
- Gravity and acceleration are locally equivalent

all observers are equivalent (all observers must be capable to discovery law of physics)

or

all physical law should have a tensorial form

Mathematical framework of GR



A sphere is a 2-dim manifold: it can be represented by collection of 2-dim maps

Space-time is 4-dim manifold

$$x^{\mu} = (x^0, x^1, x^2, x^3)$$

in Newtonian theory
it is used the
formalism of
vectors , in GR it is
used the formalism
of tensors

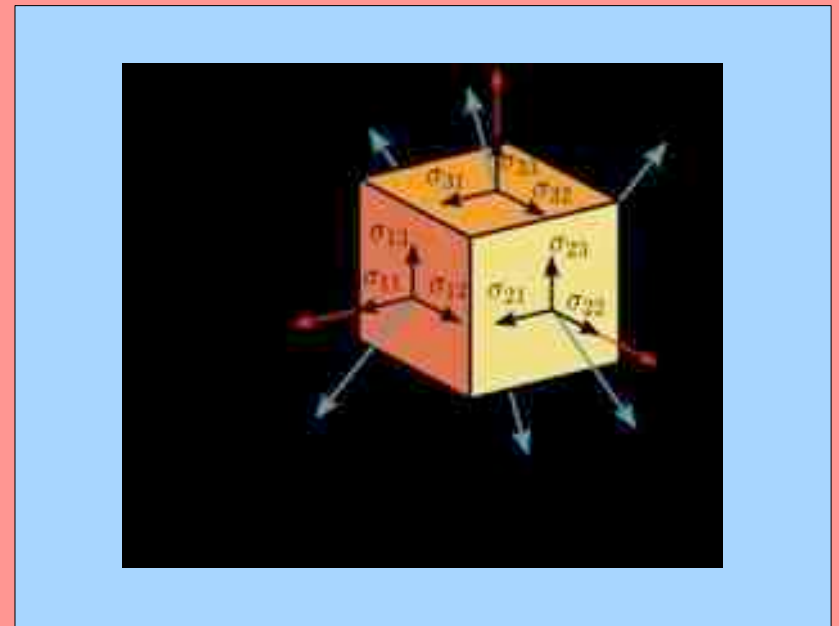
Mathematical framework of GR

Many physical quantities are regarded as correspondences between sets of vectors (input vector- tensor - output vector)

Tensors as expression of relationship between vectors:

Independent on the coordinate system!!

$$\sigma = \begin{pmatrix} \sigma_{11} & \sigma_{12} & \sigma_{13} \\ \sigma_{12} & \sigma_{22} & \sigma_{23} \\ \sigma_{13} & \sigma_{23} & \sigma_{33} \end{pmatrix}$$
$$\sigma = T^{(e_1)} \quad T^{(e_2)} \quad T^{(e_3)}$$



Tensor metric

$$a^2 := g_{\mu\nu} dx^\mu dx^\nu \longrightarrow \text{Length of a vector}$$

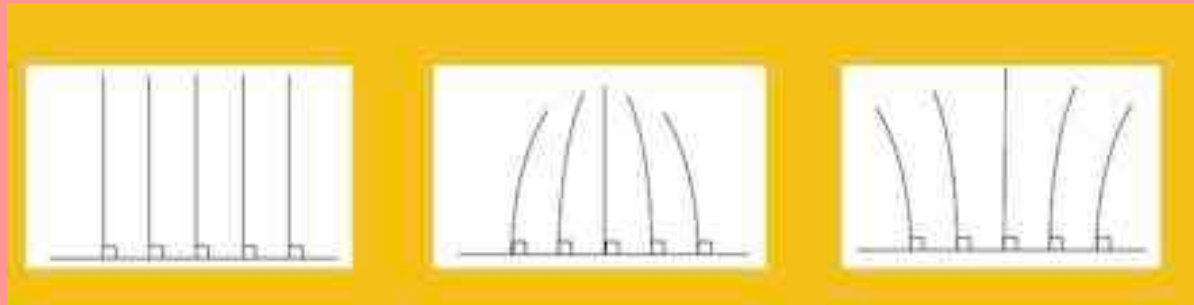
$$ds^2 = g_{\mu\nu} dx^\mu dx^\nu \longrightarrow \text{Interval between 2 neighbouring points}$$

For polar coordinates: $ds^2 = dr^2 + r^2 d\phi^2$ $g = \begin{pmatrix} 1 & 0 \\ 0 & r^2 \end{pmatrix}$

Minkowsky space: $ds^2 = dt^2 - dx^2 - dy^2 - dz^2$ $g = \begin{pmatrix} -1 & 0 & 0 & 0 \\ 0 & 1 & 0 & 0 \\ 0 & 0 & 1 & 0 \\ 0 & 0 & 0 & 1 \end{pmatrix}$

Geodesic equation

- Shortest curve connecting 2 fixed points (straight line as closely as possible in local inertial frame)
- Trajectory of freely falling particles



How does it change the distance between 2 neighbouring points??

Geodesic equation

In a curved space time, particles moving along geodesics will accelerate towards or away from each other



Curvature tensor describes gradient of gravitational accelerations, the so called 'tidal forces'

2nd summary

Geodesic equation

- In Newtonian theory gravitational field (gradient of potential) is source of acceleration
- In GR curvature is source of tidal effect, thus acceleration



Curvature (metric) as potential

What's the source of gravity? ?

- Equivalence mass-energy

$$T^{\mu\nu}(x^\alpha) = \rho_0(x^\alpha) \langle U^\mu U^\nu \rangle(x^\alpha)$$

(transport of μ momentum in the direction ν)

$T^{\mu\nu}$ as source of gravity!!

$$G^{\alpha\beta} = k T^{\alpha\beta}$$

Die größte Eselei

- empty Minkowsky space-time as the only possible solution for a static Universe

$$G^{\alpha\beta} + \Lambda g^{\alpha\beta} = k T^{\alpha\beta}$$

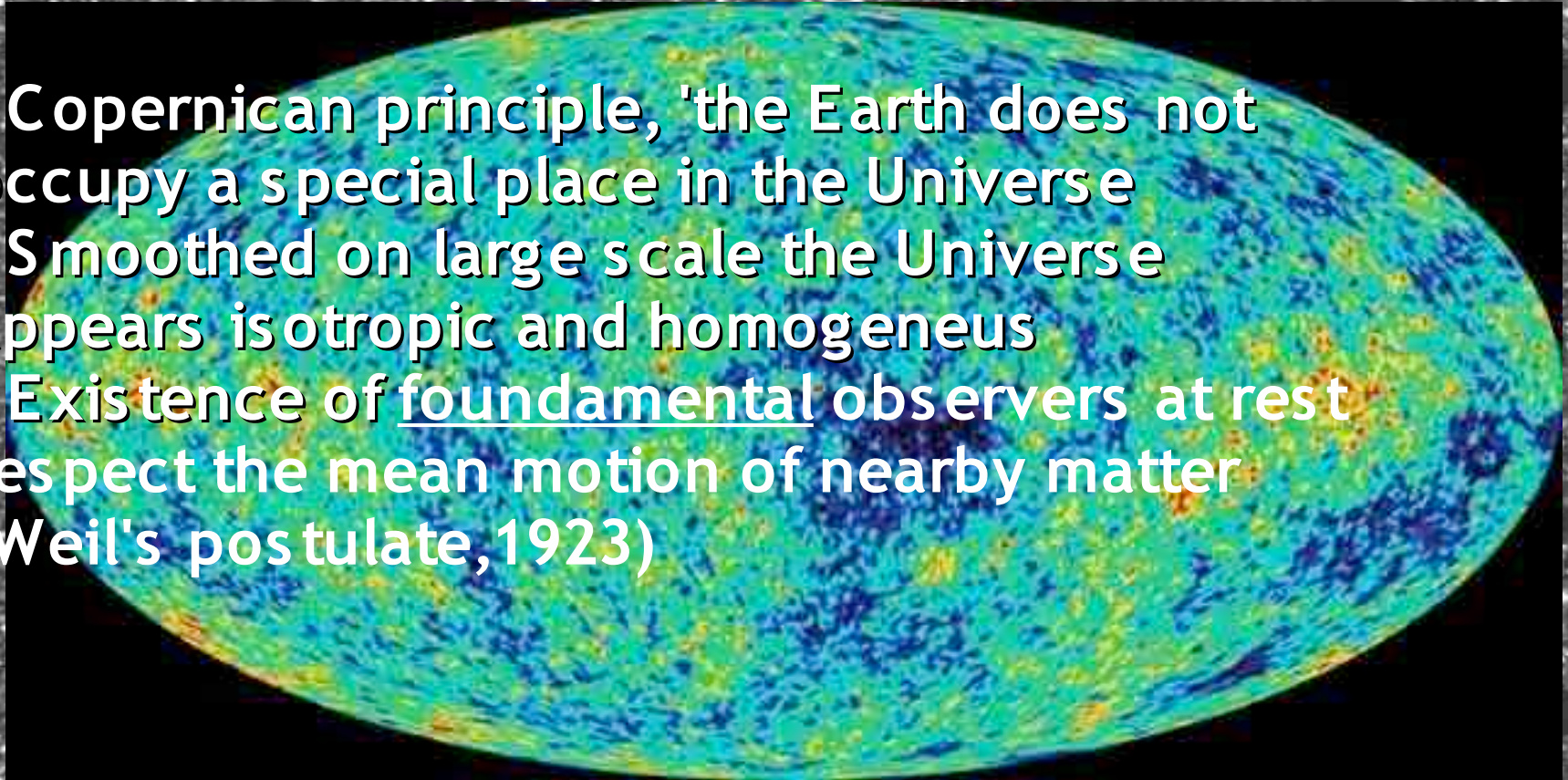
- expansion of the Universe

$$G_{\alpha\beta} = -\Lambda g_{\alpha\beta} + k T_{\alpha\beta}$$

- (dark energy)

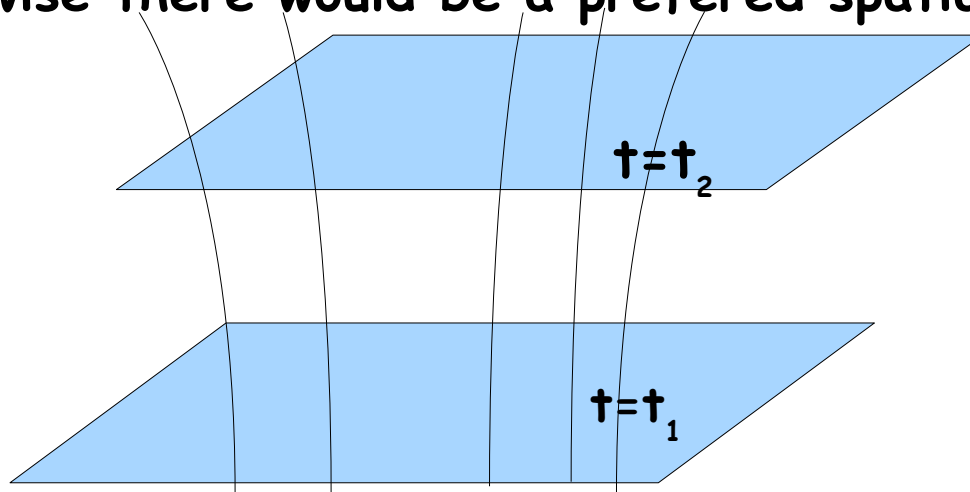
The cosmological principle

- Copernican principle, 'the Earth does not occupy a special place in the Universe'
- Smoothed on large scale the Universe appears isotropic and homogeneous
- Existence of fundamental observers at rest respect the mean motion of nearby matter (Weil's postulate, 1923)



cosmological principle, it leads to the RW metric by simple symmetry considerations:

1 set of observers on the first hypersurface; not to violate the assumption of homogeneity all the observers must reach the 2nd hypersurface in the same time; also their velocity must be orthogonal in order to keep the homogeneity at cosmic time t (otherwise there would be a preferred spatial direction).

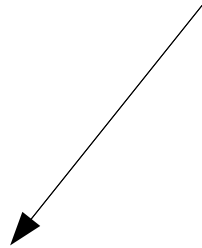


$$c^2 d\tau^2 = (cdt)^2 - d\Sigma^2(t)$$

$$c^2 d\tau^2 = (cdt)^2 - d\Sigma^2(t)$$

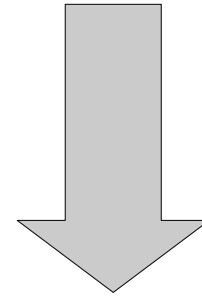
$$\Delta \Sigma^2 = \gamma_{ij}(x^k) \Delta x^i \Delta x^j$$

$$\gamma_{ij}(t, x^k) = a^2(t) \sigma_{ij}(x^k)$$



**Time independent spatial
geometry**

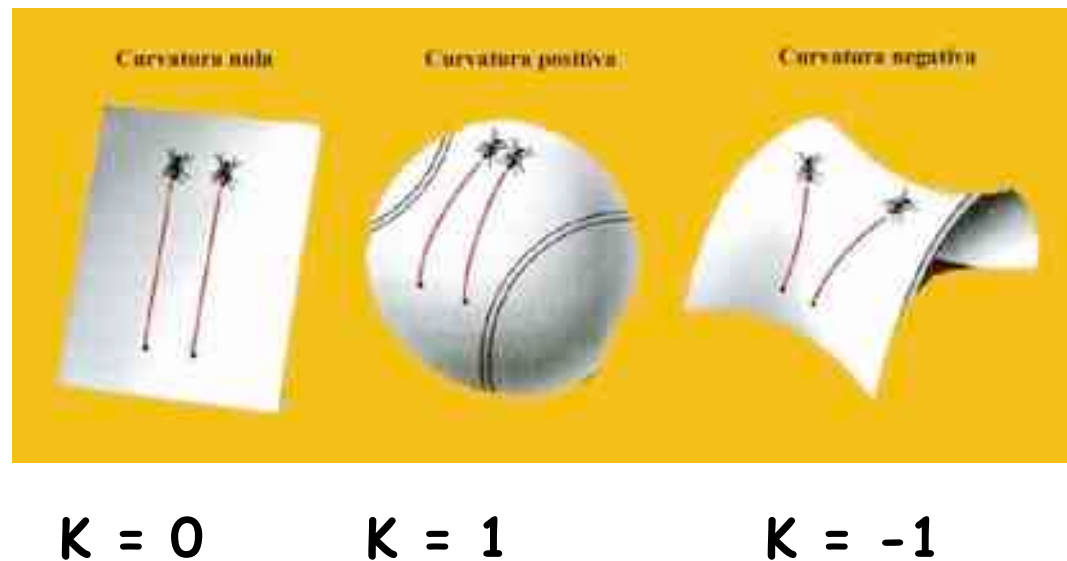
**The ratio of distances at later
time must be independent of x^k and
 Δx^k !! (not to violate homogeneity)**



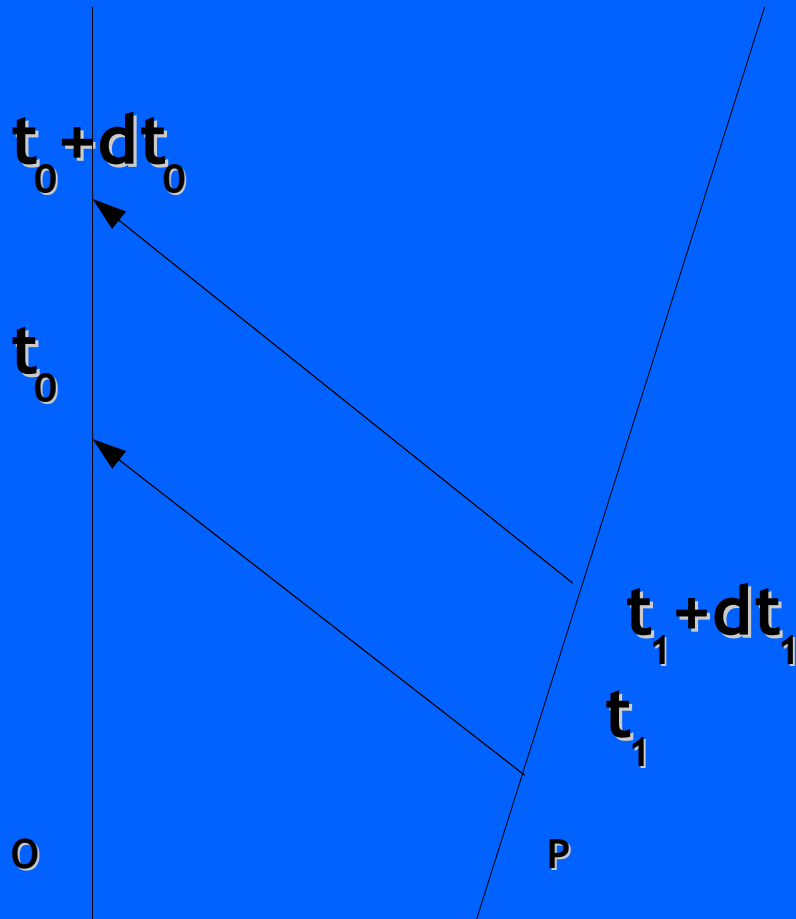
**The time evolution of three-
dimensional metric is uniform in
space**

$$c^2 d\tau^2 = (cdt)^2 - a^2(t) \sigma_{ij}(x^k) dx^i dx^j$$

$$d\sigma^2 = \frac{dr^2}{1 - k r^2 / R^2} + r^2 (d\theta^2 + \sin^2(\theta) d\phi^2) = \frac{dr^2}{1 - k r^2 / R^2} + r^2 d\Omega^2$$



Propagation of light



$$\int_{t_1 + dt_1}^{t_0 + dt_0} \frac{dt}{a(t)} = \int_{t_1}^{t_0} \frac{dt}{a(t)}$$

$$\int_{t_1 + dt_1}^{t_0 + dt_0} \frac{dt}{a(t)} - \int_{t_1}^{t_0} \frac{dt}{a(t)} = \int_{t_0}^{t_0 + dt_0} \frac{dt}{a(t)} - \int_{t_1}^{t_1 + dt_1} \frac{dt}{a(t)} = 0$$

$$\frac{dt_0}{a(t_0)} = \frac{dt_1}{a(t_1)}$$

$$t_0 > t_1 \rightarrow a(t_0) > a(t_1)$$

$$1 + z = \nu_1 / \nu_0 = a(t_0) / a(t_1)$$

Propagation of light

for small distances:

$$t_0 \approx t_1 + dt$$

$$1+z = \frac{a(t_0)}{a(t_0 - dt)} \simeq \frac{a(t_0)}{a(t_0) - \dot{a}(t_0)dt} \simeq 1 + \frac{\dot{a}(t_0)}{a(t_0)} dt$$

$$z \simeq \dot{a}(t) r$$

Interpreting z as velocity of recession 

redshift proportional to distance r !!

Relativistic cosmology

- cosmological principle =====>> Robertson-Walker metric (metric of space-time)
- Weyl's postulate (existence of perfect fluid)
- General relativity with cosmological term

$$\frac{-k + \dot{a}^2 + 2\ddot{a}a}{a^2} + \Lambda = 8\pi p; \quad 3\frac{k + \dot{a}^2}{a^2} - \Lambda = 8\pi \rho$$

By homogeneity, density and pressure can only be function of time!!

Relativistic cosmology

$$8\pi \frac{d(\rho a^3)}{dt} = -3a^2 \dot{a} 8\pi p \longrightarrow \text{Conservation of energy!!}$$

Friedmann's equations are consistent
with conservation of energy
(field equation were actually designed to
be consistent with this !!)

Relativistic cosmology

$$\frac{-k + \dot{a}^2 + 2\ddot{a}a}{a^2} + \Lambda = 8\pi p; \quad 3\frac{k + \dot{a}^2}{a^2} - \Lambda = 8\pi \rho$$

$$H^2 = \frac{\dot{a}^2}{a^2} = \frac{8\pi\rho}{3} + \frac{\Lambda}{3} - \frac{k}{a^2}$$

$$\rho_c = \frac{3}{8\pi} H^2$$

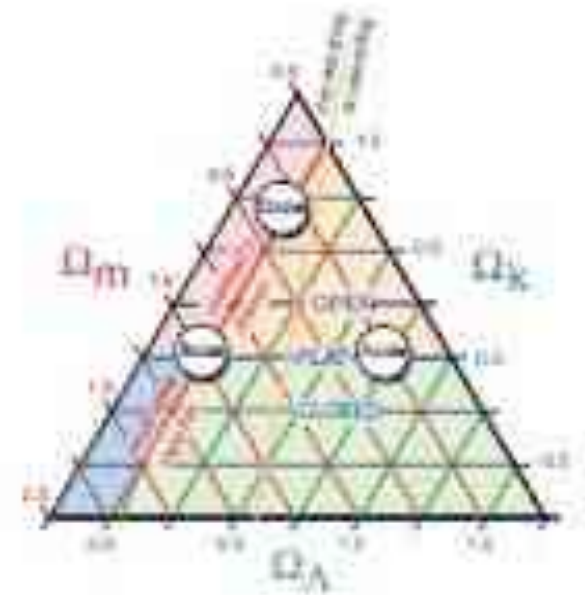
$$\Omega_M = \frac{\rho}{\rho_c}$$

$$\Omega_\Lambda = \frac{\Lambda}{3H^2} \quad \Omega_M + \Omega_\Lambda + \Omega_k = 1$$

$$\Omega_M + \Omega_\Lambda < 1 \leftarrow k = -1$$

$$\Omega_M + \Omega_\Lambda = 1 \leftarrow k = 0$$

$$\Omega_M + \Omega_\Lambda > 1 \leftarrow k = 1$$



3rd summary

Relativistic cosmology

RW metric describes pattern of galaxies
(fundamental particles) redshift, Hubble's
law

RW metric in Einstein's field equations :
Friedman's equations, different cosmological
models

Bibliography

- Introducing Einstein's relativity,
R. D'Inverno
- Chandra, Nasa

Olber's paradox (1826)

Why is the sky dark?

assuming:

- the space is Euclidean and infinite
- the average number of stars per unit of volume and the average luminosity of each star is constant throughout space and time (provided that these averages are taken over sufficiently large area)
- the Universe has been existing for an infinite time and it is static on large scale

The total luminosity would be infinite!!!

$$\frac{(4\pi r^2 dr) l}{4\pi r^2} = l dr$$

- Too young Universe or expanding Universe

Immanuel Kant, born in 22 April 1724, Koenigsberg, Prussia. Kant was the last influential philosopher of modern philosophy in the classic sequence of the theory of knowledge during the Enlightenment beginning with thinkers John Locke, George Berkeley and David Hume.



Immanuel Kant, wikipedia

(following relates to the point 1 and 2 of the other one)

One of Kant's most prominent works is the **Critique of Pure Reason**, an investigation into the limitations and structure of reason itself. He suggested that by understanding the sources and limits of human knowledge we can ask fruitful metaphysical questions. He asked if an object can be known to have certain properties prior to the experience of sensation of that object. He concluded that all objects about which the mind can think must conform to its manner of thought. For example, if you always wore blue spectacles, you could be sure of seeing everything blue. However, it is possible that there are objects not blue, or with such nature which the mind cannot know, so the principle in the "blue world" cannot be applied outside of experience.

Empiricists and Rationalists The empiricists believed that knowledge is acquired through experience alone, but the rationalists maintained that such knowledge is open to Cartesian doubt and that reason alone provides us with knowledge. Kant argues, however, that using reason without applying it to experience will lead to illusions, while experience will be purely subjective without first being subsumed under pure reason.

'a priori' and empirical An 'empirical' proposition is one which we cannot know except by the help of sense-perception, either our own or that of someone else whose testimony we accept. An 'a priori' proposition is one which though it may be elicited by experience, is seen, when known, to have a basis other than experience.

Space and time (point 4) According to Kant, the outer world causes only the matter of sensation, but our own mental apparatus orders this matter in space and time, so that anything would be impossible if space and time were not kinds of pure 'a priori' intuitions.(think about the geometry and mathematics)

After applying the space and time to things that are not experienced, Kant maintains, we find ourselves troubled by 'antinomies' –that is to say, by mutually contradictory propositions each of which can apparently be proved.

Antinomies (point 5 and 6)

- is it infinite of both space and time?
- every composite substance both is, and is not, made up of simple parts?
- two kinds of causality, one according to the laws of nature, the other that of freedom?
- there is, and is not, an absolutely necessary Being?

Snapshots from the life of an AGN

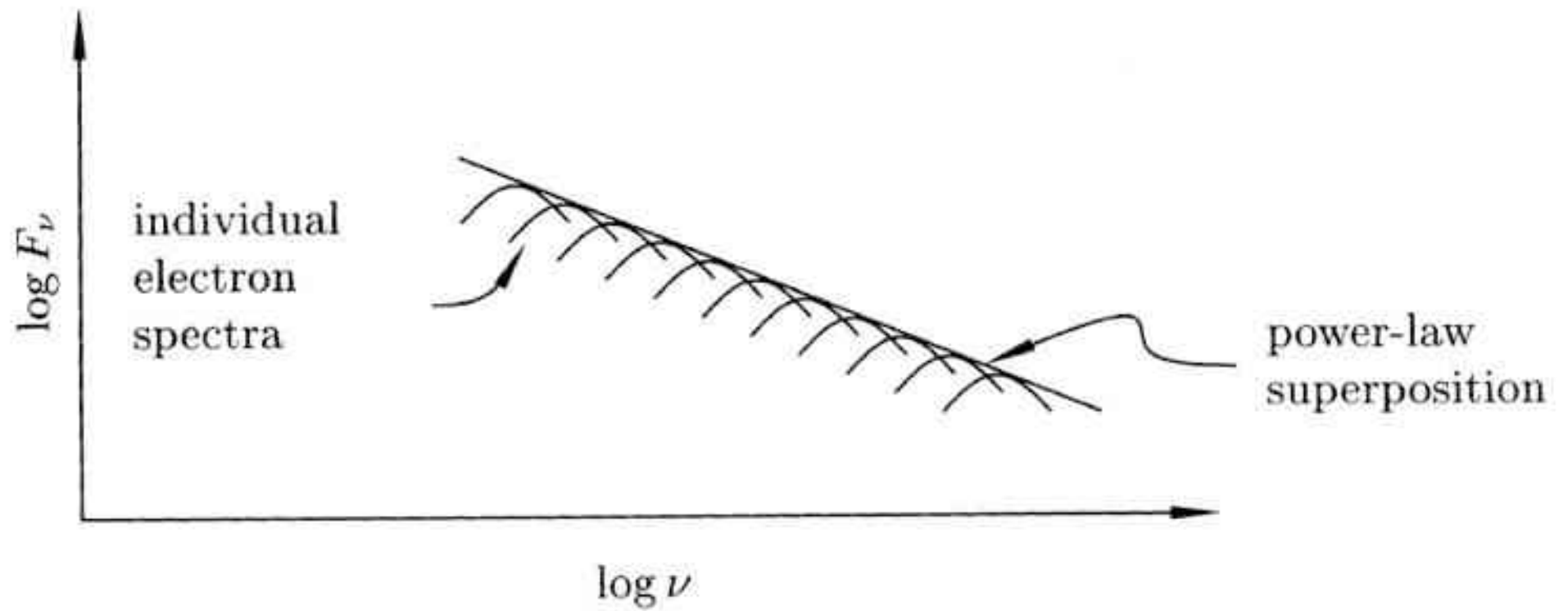
A.3 Equations...

“Synchrotron Emission”

(A.1) Rusen Lu

(A.2) Marios Karouzos

(A.3) Chin-Shin Chang



Snapshots from the life of an AGN

B.2 Milestone in....

“The accretion disk”

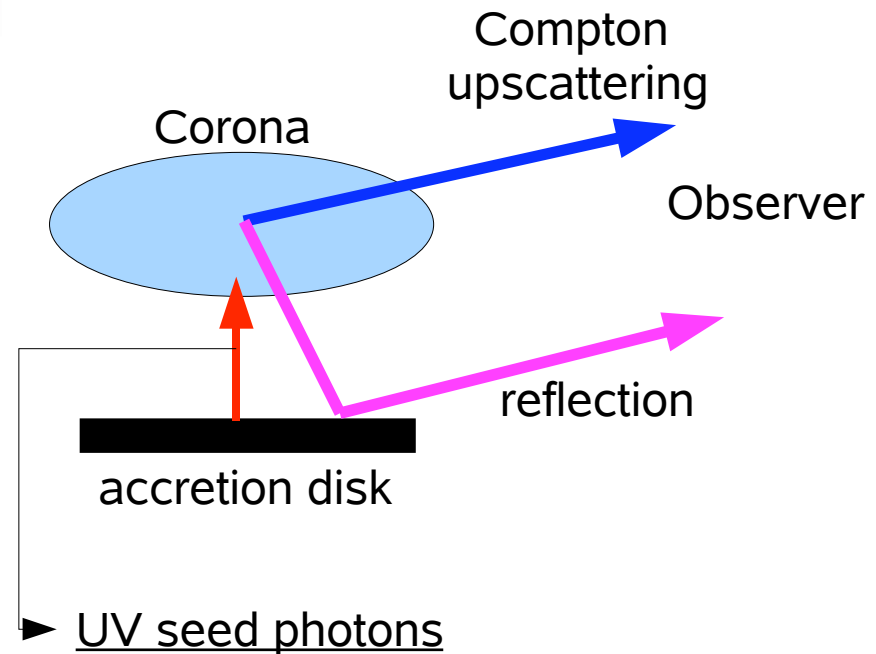
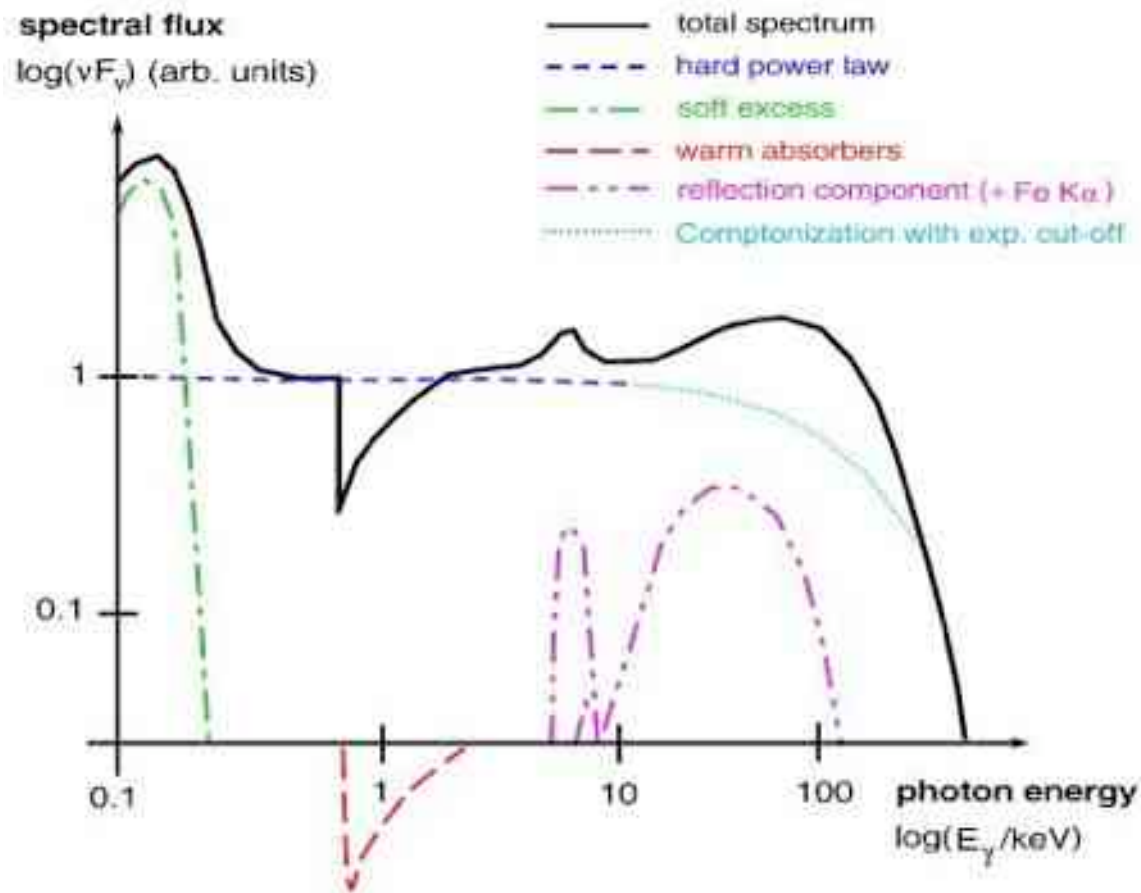
(B.1) Marios Karouzos

(B.2) Chin-Shin Chang

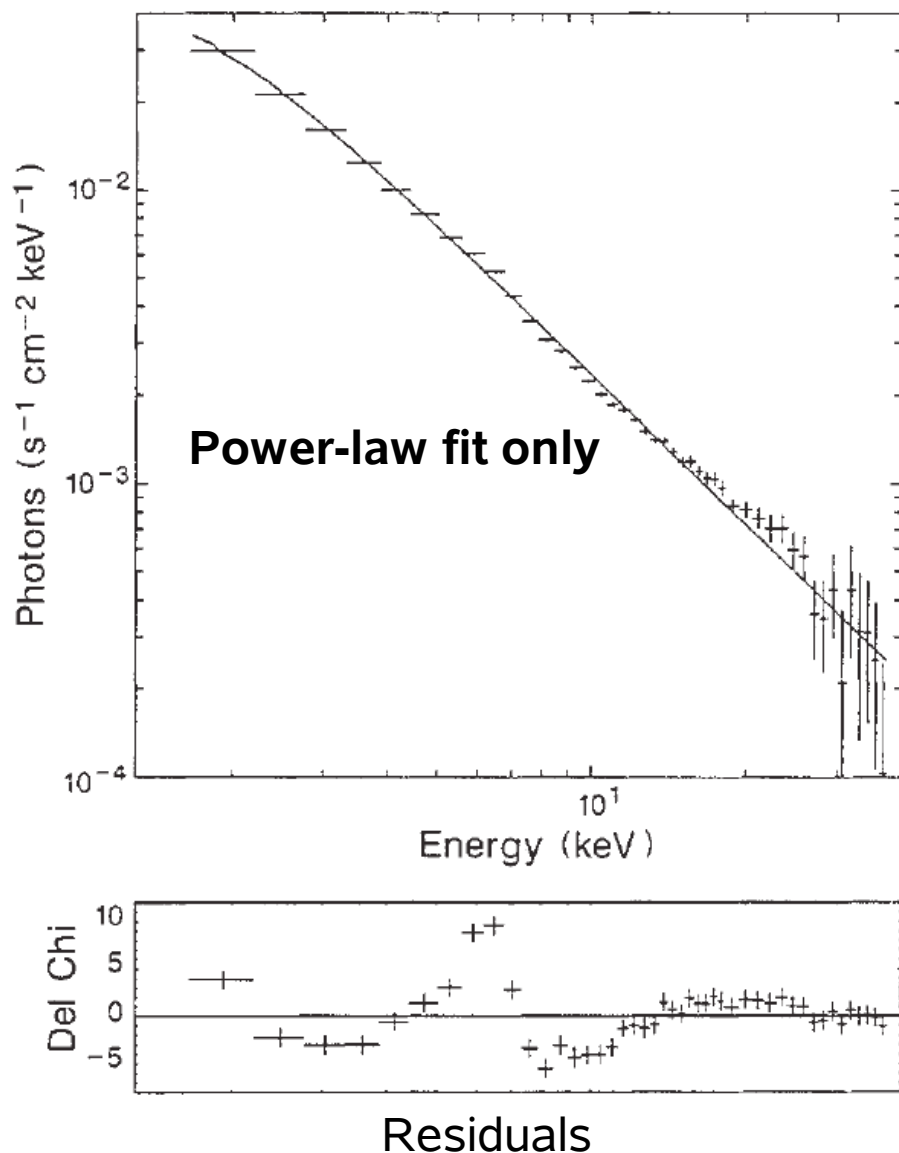
(B.3) Rusen Lu

X-ray observational evidence of AGN accretion disk

X-Ray: spectra and mechanism



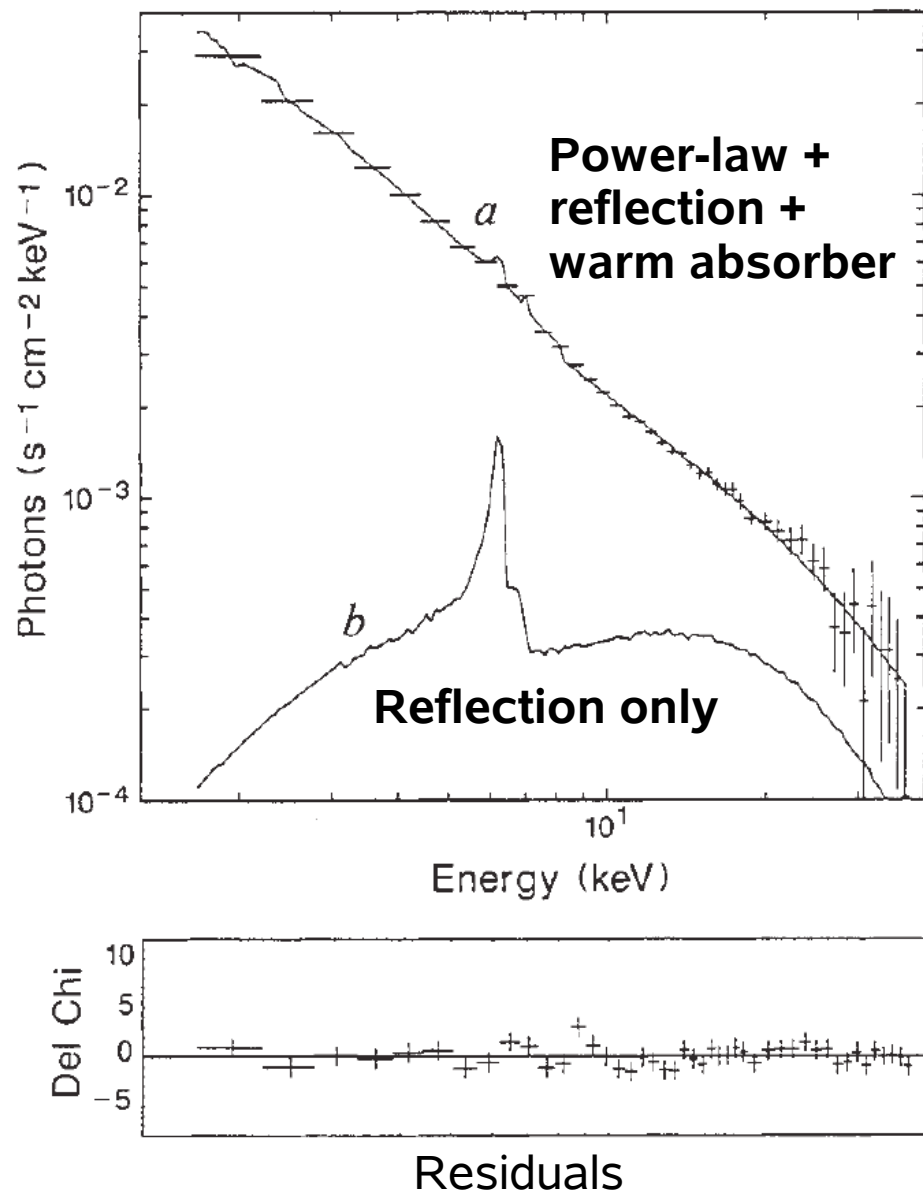
First evidence of accretion disk



- Exosat & Ginga satellites observations
- Power-law fit residuals show an excess around 6-7 keV
- Possible iron line

Pounds et al., 1990, *Nature*, 344,132

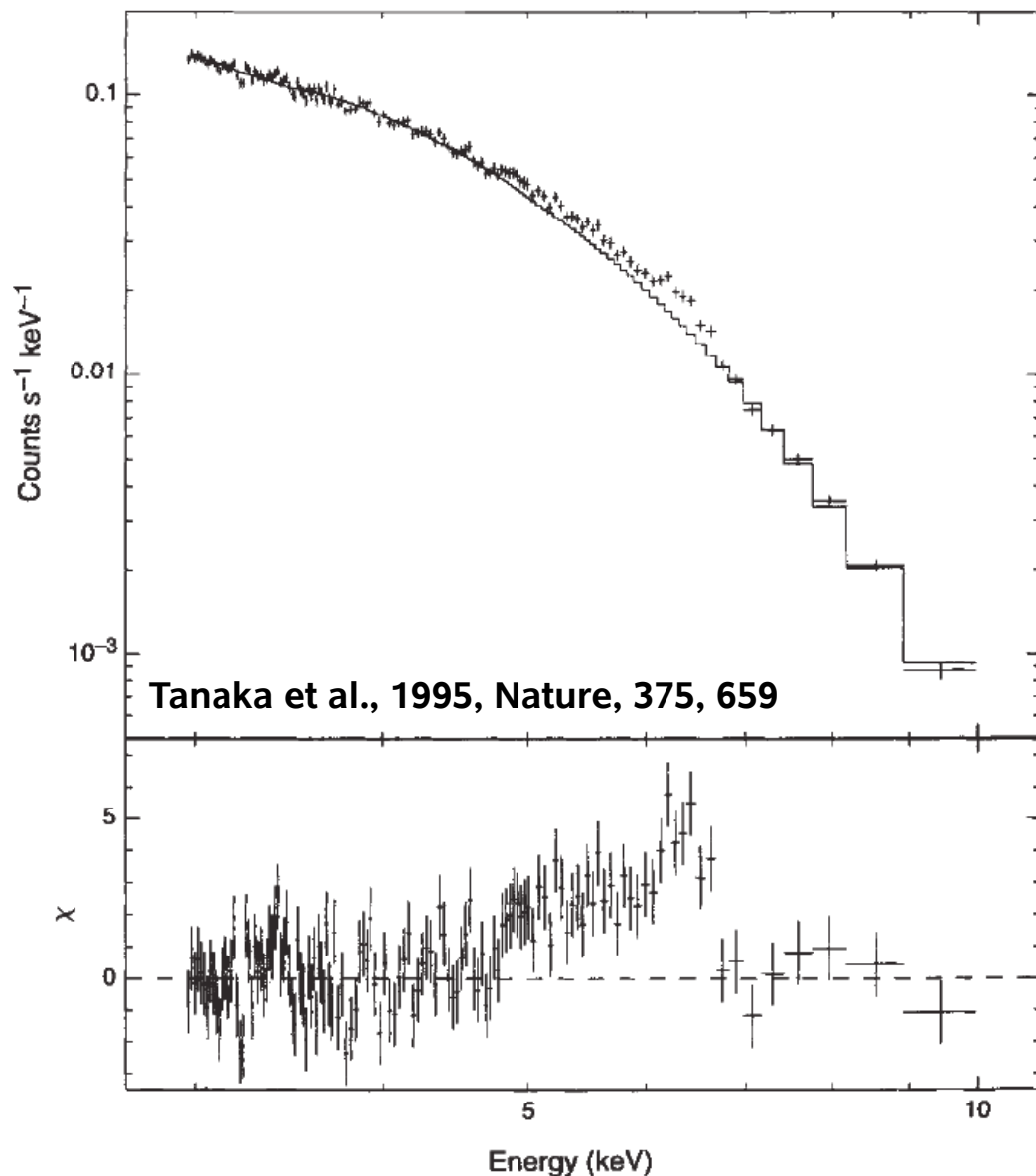
First evidence of accretion disk



- Fit greatly improved by adding reflection component (+ Iron K- α line)
- Reveal cold, dense matter within 1000 gravitational radii
- Quantitative evidence for the reflected continuum component from this cold matter

Pounds et al., 1990, Nature, 344, 132

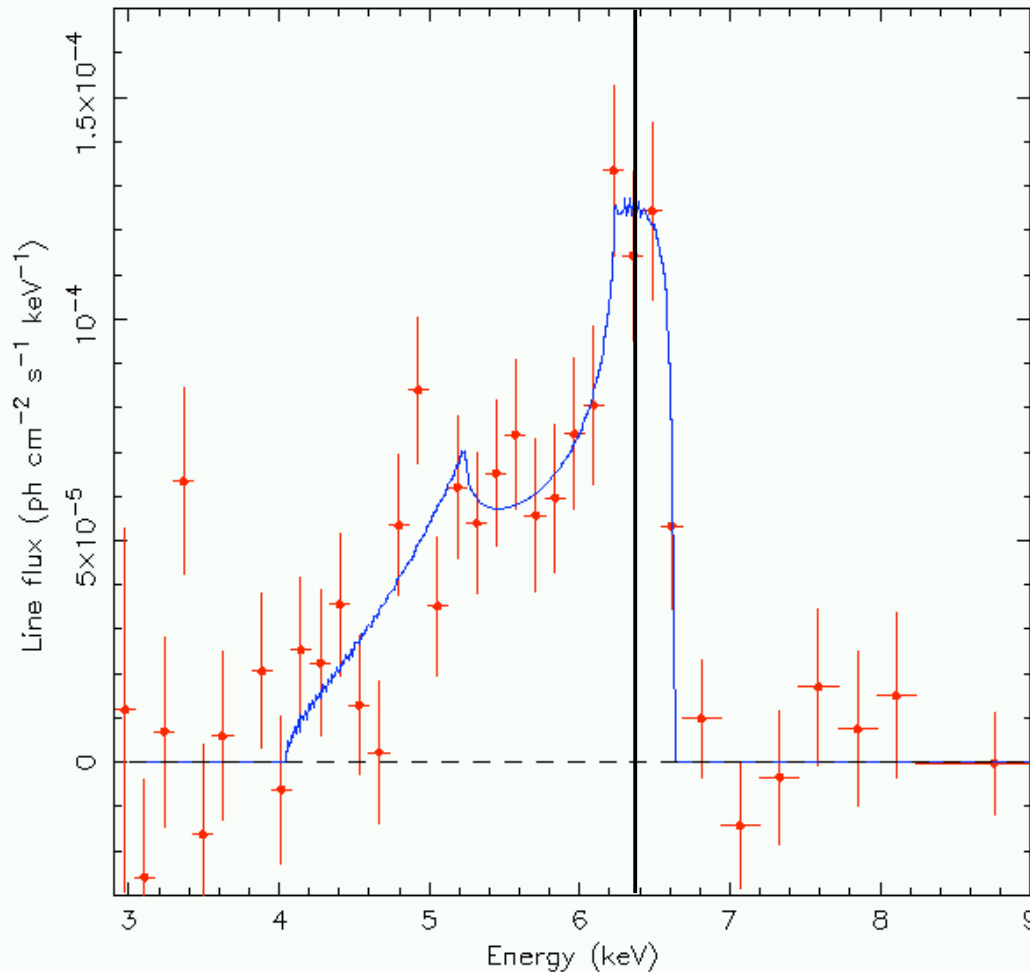
Further evidence of accretion disk



- ASKA observation of MCG-6-30-15
- Power-law + continuum reflection model: residual showed iron-line broadening

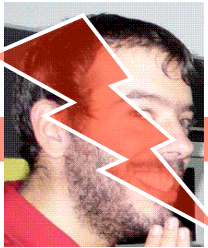
Iron line broadening

Rest frame
iron line center

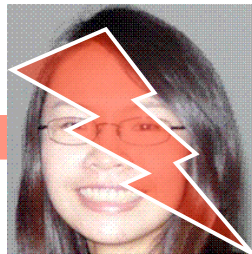


Tanaka et al., 1995, Nature, 375, 659

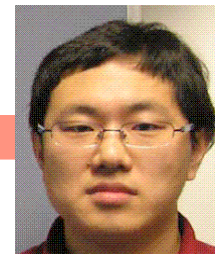
- The broad iron K- α line shows extensive red wing
- Suggests a Doppler and gravitational shifts close to a central black hole
- Best-fit line model: an externally-illuminated accretion disk orbiting a Schwarzschild black hole (Fabian et al., 1989, MNRAS, 238, 729)



2009/09/15



Chin-Shin Chang



IMPRS Retreat 2009 Braunfels

Snapshots from the life of an AGN

C.1 Introduction

“Superluminal motion”

(C.1) Chin-Shin Chang

(C.2) Rusen Lu

(C.3) Marios Karouzos

"Awesomely weird...utterly fascinating...[an] entrancing web
from which escape is hardly desirable." *Washington Post Book World*

SUPERLUMINAL

A NOVEL OF
INTERPLANETARY
CIVIL WAR



TONY DANIEL

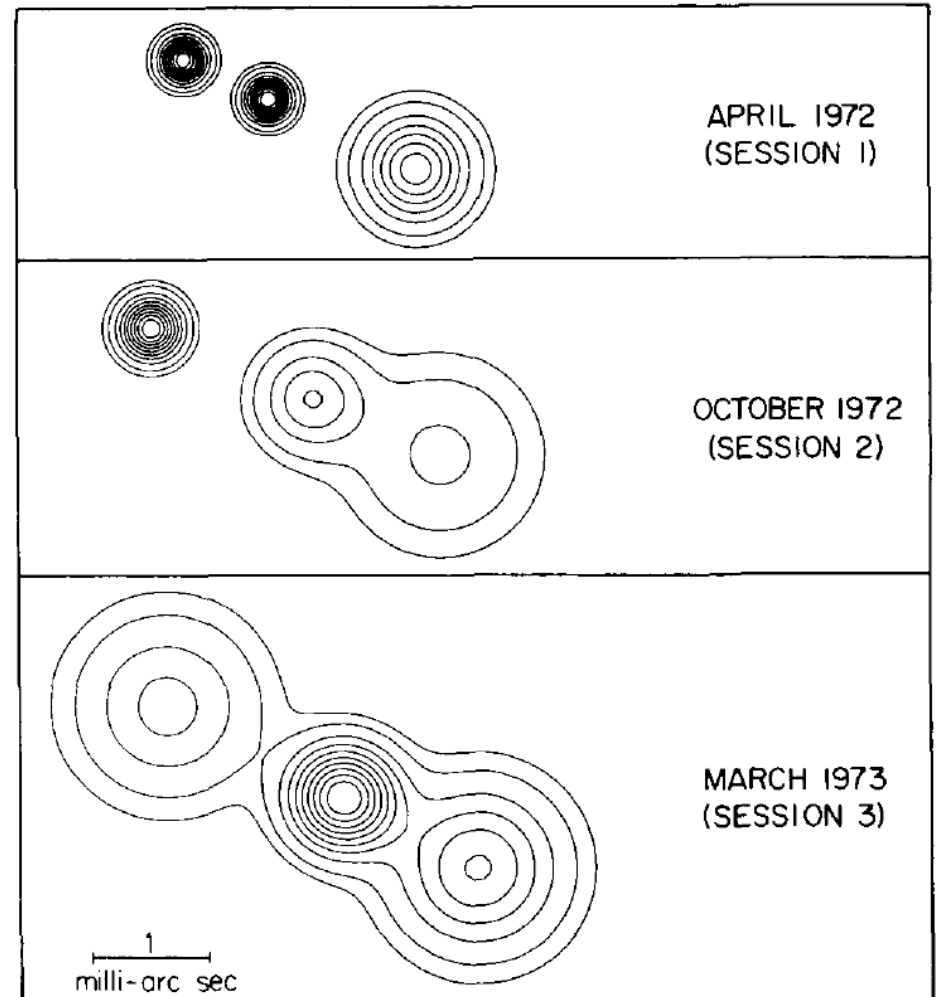
AUTHOR OF METAPLANETARY

MOTION

Introduction

3C 273

- Very Long Baseline Interferometry (VLBI) observations starting from the 70s
- compact extragalactic sources made up of two or more components, which have speed faster than light $\sim 2 - 4c$



Cohen 1975

People were very excited and
started to figure out why...

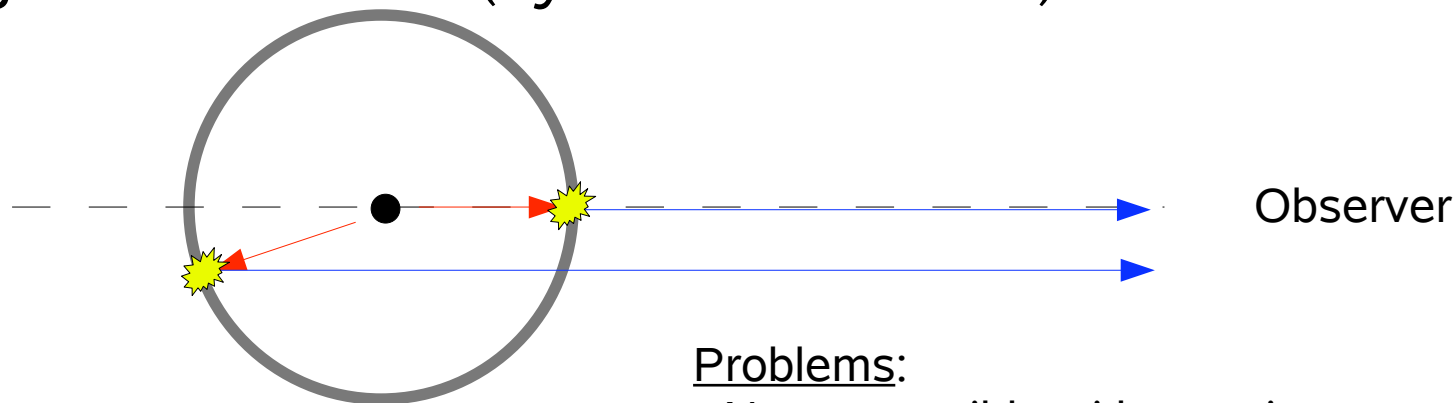
Let's take a look at some models on
debate back then

Theoretical models

- Overestimate of distance
- Random fluctuations (Dent 1972)
 - Christmas tree model

Problem: expansions/contractions should be 50-50% statistically

- Light-echo model (Lynden-Bell 1977):

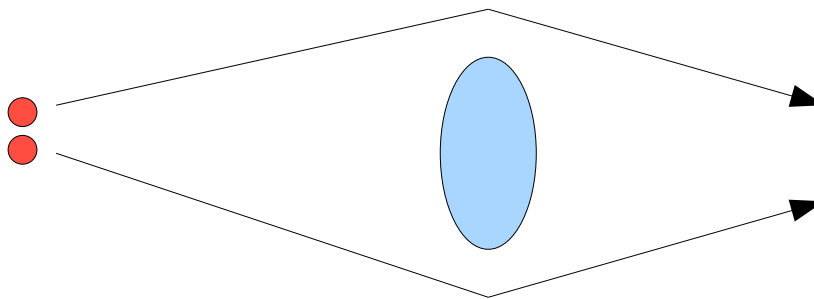


Problems:

- Not compatible with core-jet structure
- Requires $H_0 > 100$

Theoretical models

- Phase effects
 - non-constant expansion velocities
 - frequency-dependent structure
- Gravitational lens
 - a subluminally moving source with a foreground galaxy could result in superluminal motion (Chitre&Narlikar 1979)



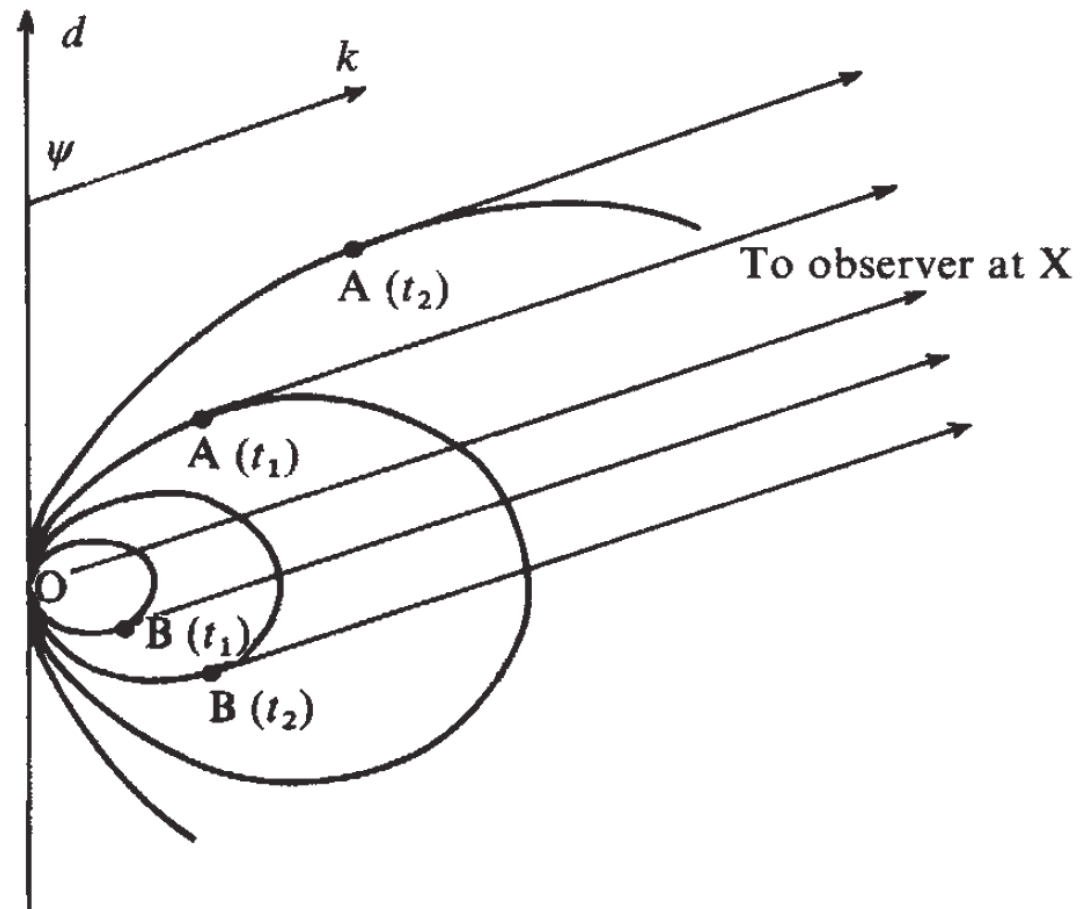
Observer

Problem:

- no foreground object which could act as lens was observed

Theoretical models

- Dipole field model
 - a burst of charged particles move along the field lines, forming a shell, which expands with relativistic velocities
- Opposite sides of the magnetic field tend to cancel out – in agreement with observation (weak circular polarization)



Milgrom 1978, Nature 274, 349

$$H_0 < 60 \text{ km/s/Mpc}$$

Theoretical models

Relativistic bulk motions

- Relativistic free expansion (Vitello & Salvati 1976)

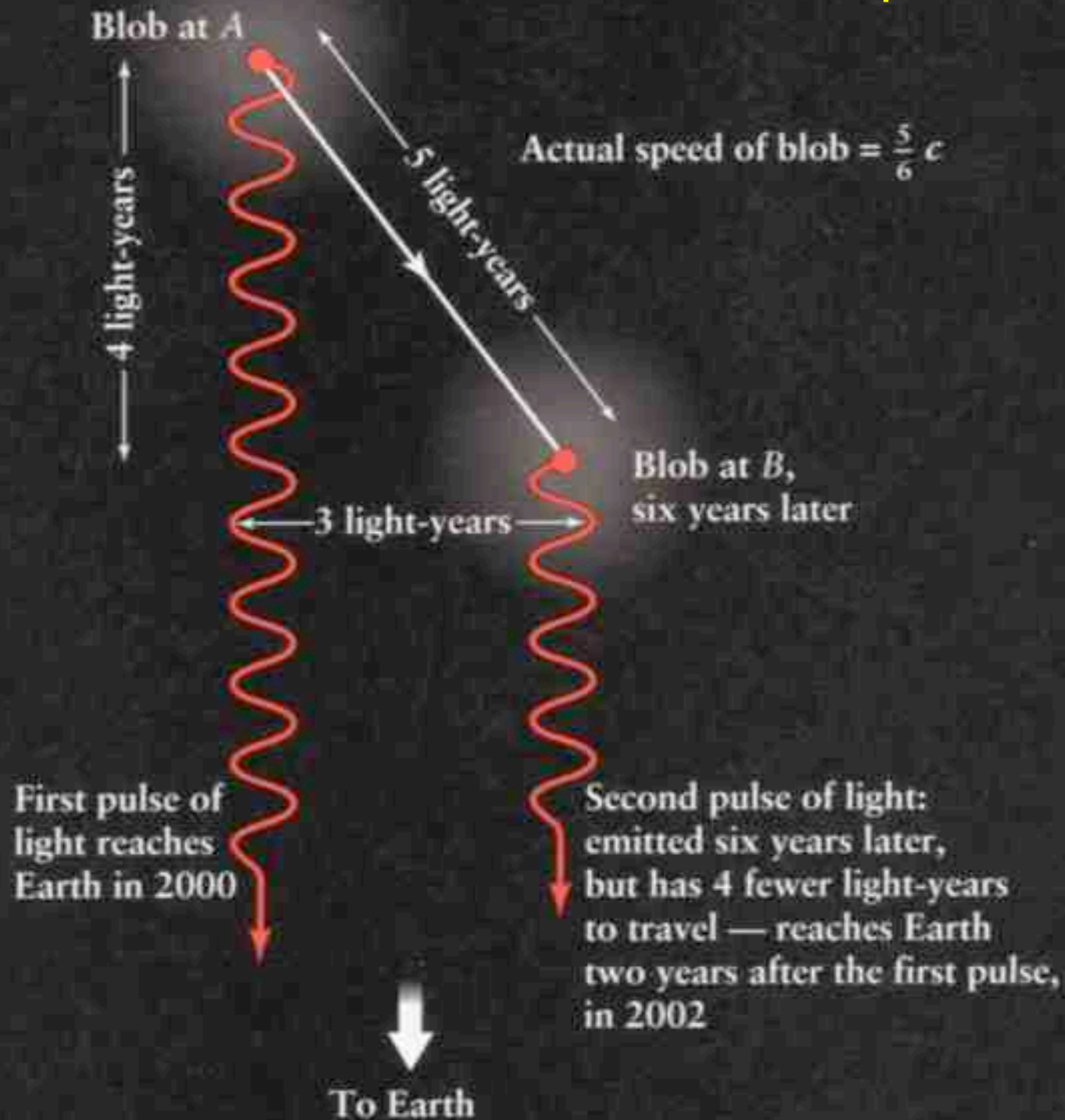
expansions constrained along one dimension can produce superluminal motion.

Problem: difficult to obtain two comparable components

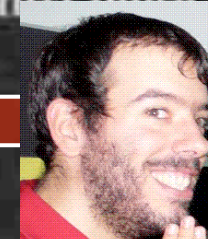
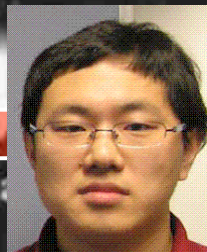
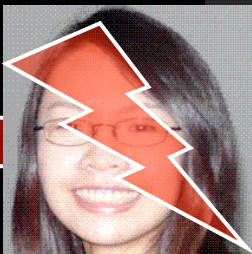
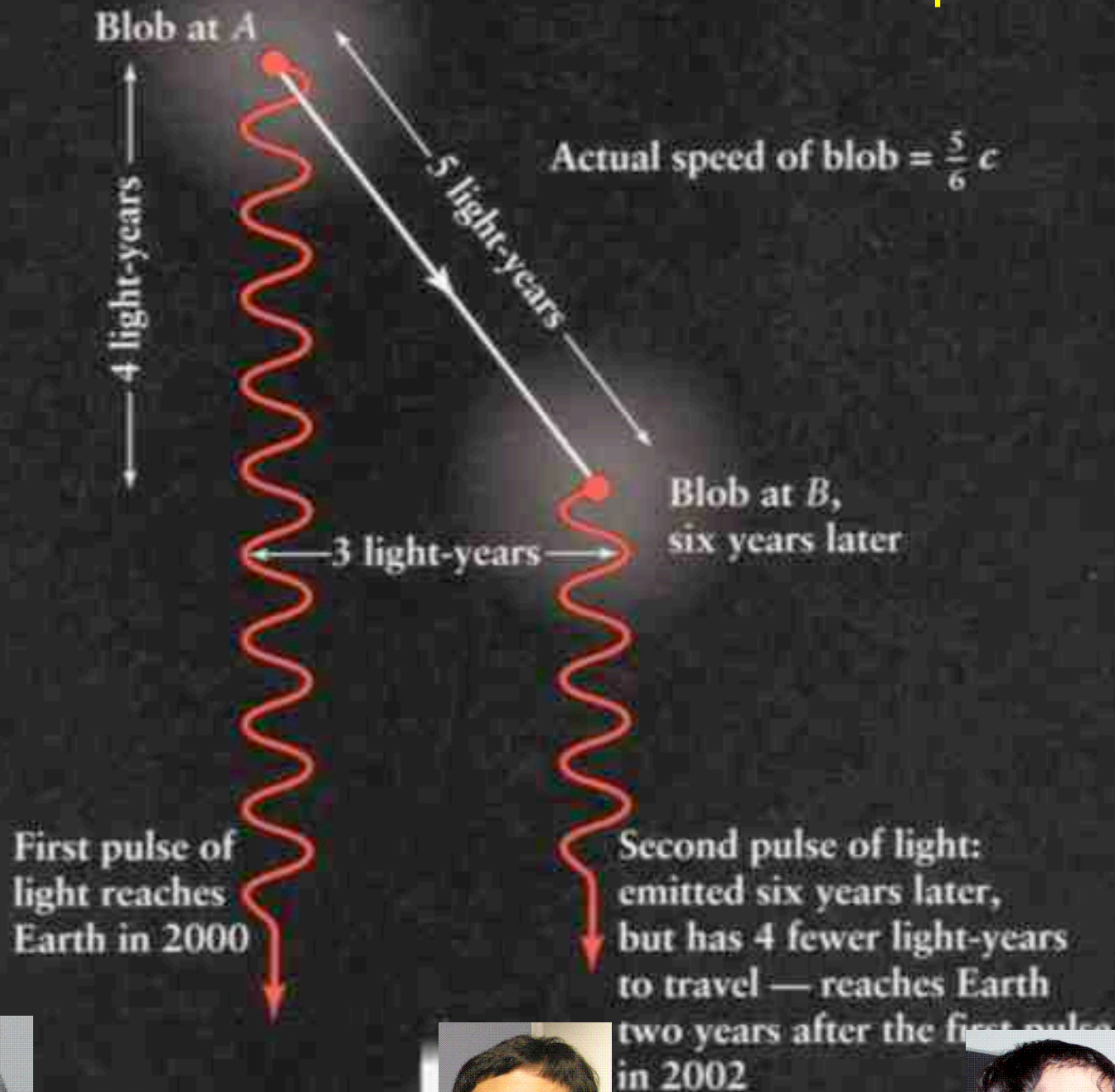
- Relativistic blast-waves
 - a large energy release in an ambient medium could lead to a relativistic blast-wave
 - Marscher (1978) and Shapiro (1979): isotropic explosion in a disk-confined ambient medium \rightarrow two superluminal radio components could be produced

Problem: blast waves should decelerate/accelerate, contradicts 3C 345 observation

Current picture



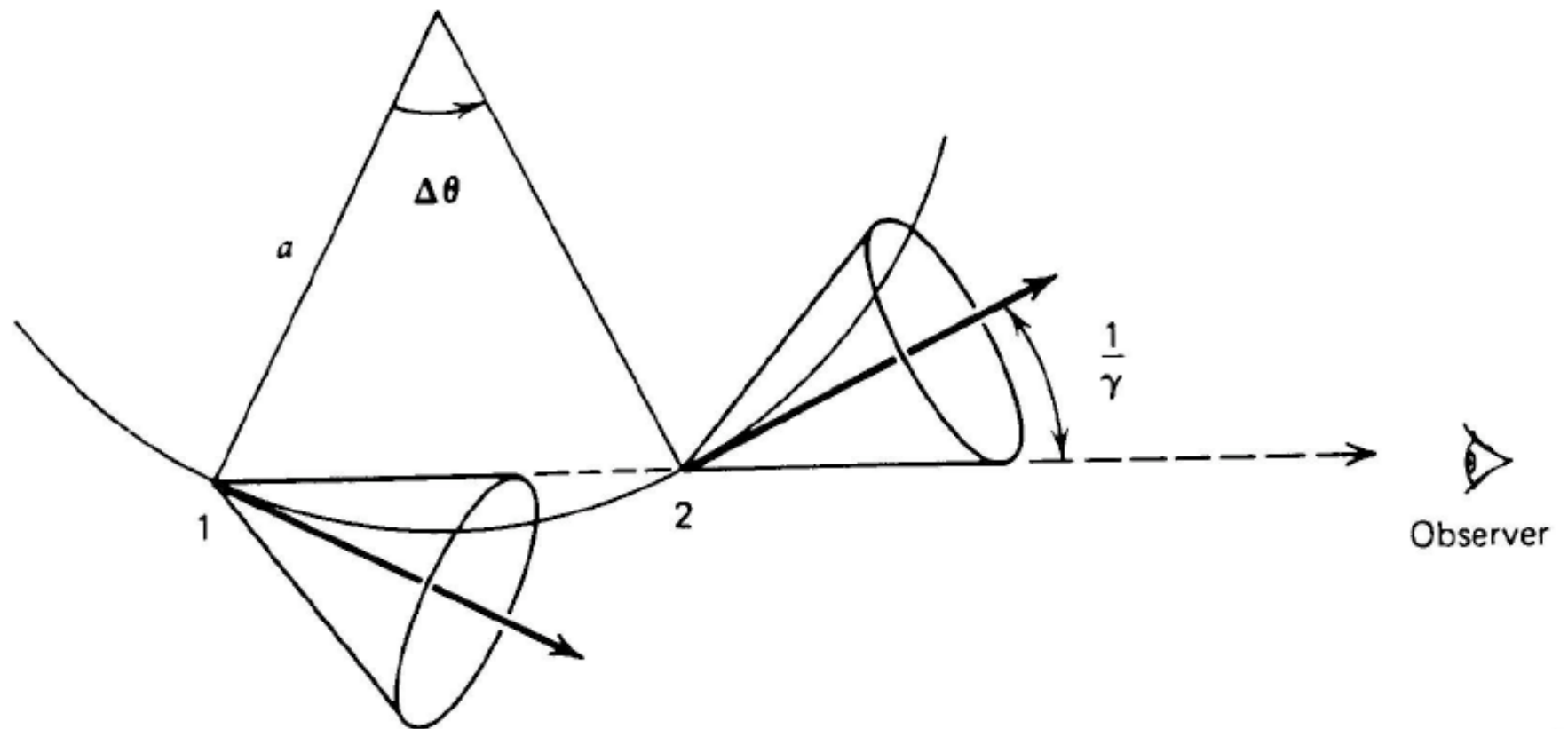
Current picture



To E

References

- Marscher & Scott, 1980, PASP, 92, 127
- Milgrom & Bahcall, 1978, Nature, 274, 349



Rybicki & Lightman, Fig. 6.2



Snapshots from the life of an AGN

A.1 An introduction...

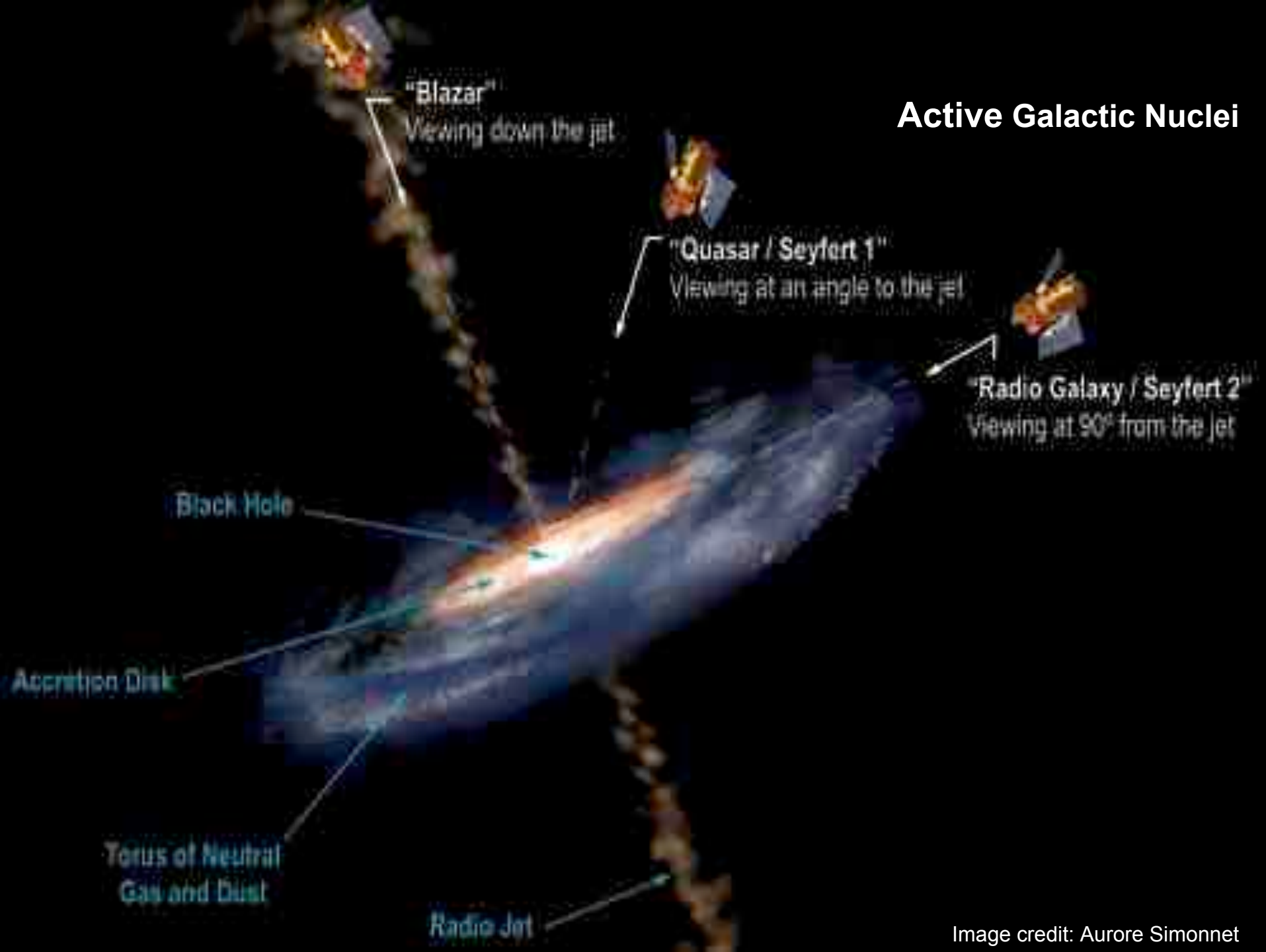
“Synchrotron Emission”

(A.1) Rusen Lu

(A.2) Marios Karouzos

(A.3) Chin Shin Chang

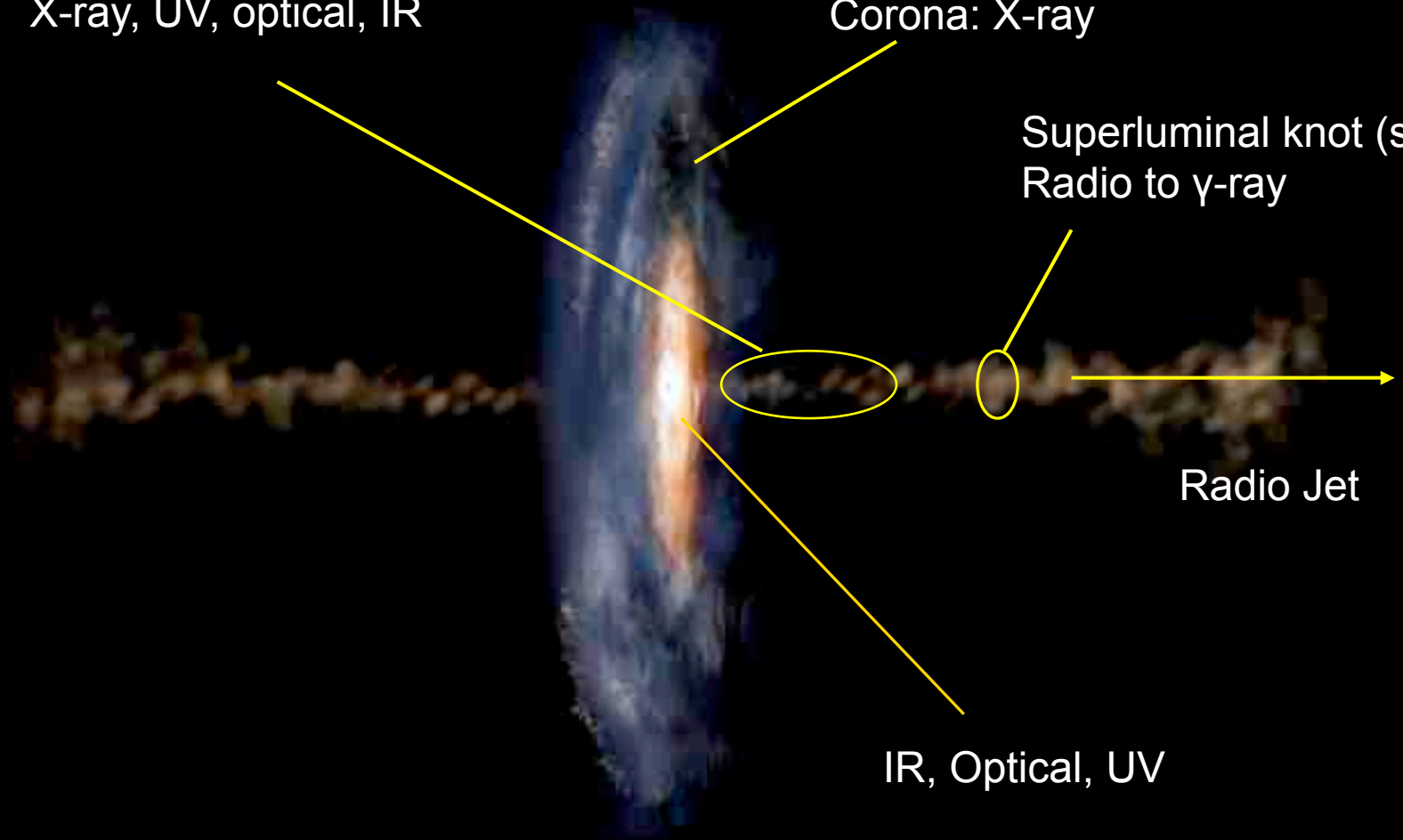
Active Galactic Nuclei



Acceleration, collimation:
X-ray, UV, optical, IR

Corona: X-ray

Superluminal knot (shock)
Radio to γ -ray



IR, Optical, UV

AGN across the spectrum



Radio

IR

Optical

X-ray

3C 273 jet

VLA

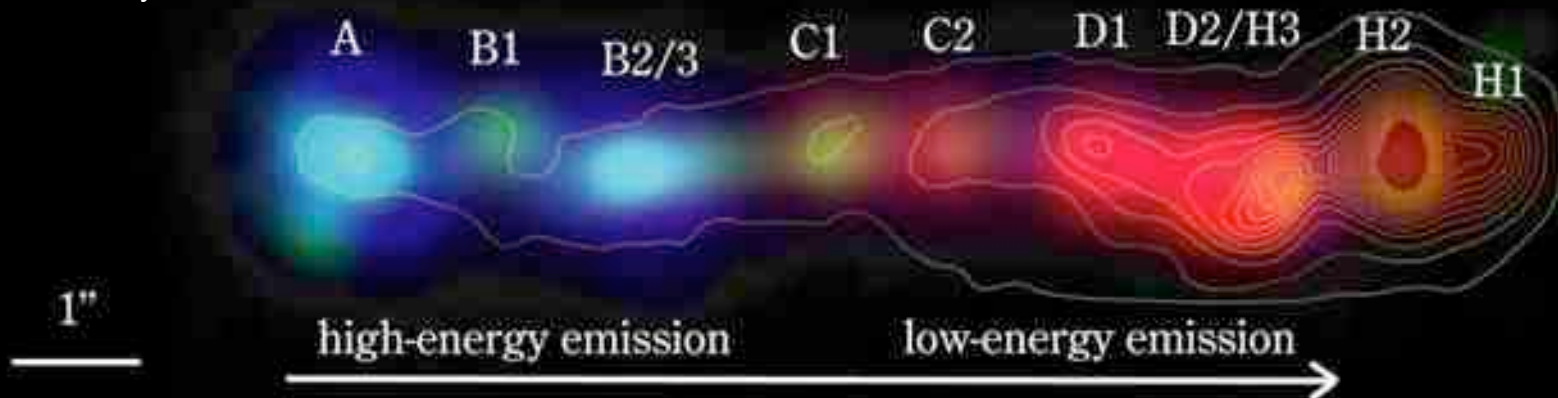
Spitzer*

Hubble

Chandra

(* deconvolved)

Credit: SST/Uchiyama



Radio & mm: Jet

IR: jet base

Optical: jet base + BH region

UV: jet base

X-ray: jet + BH region

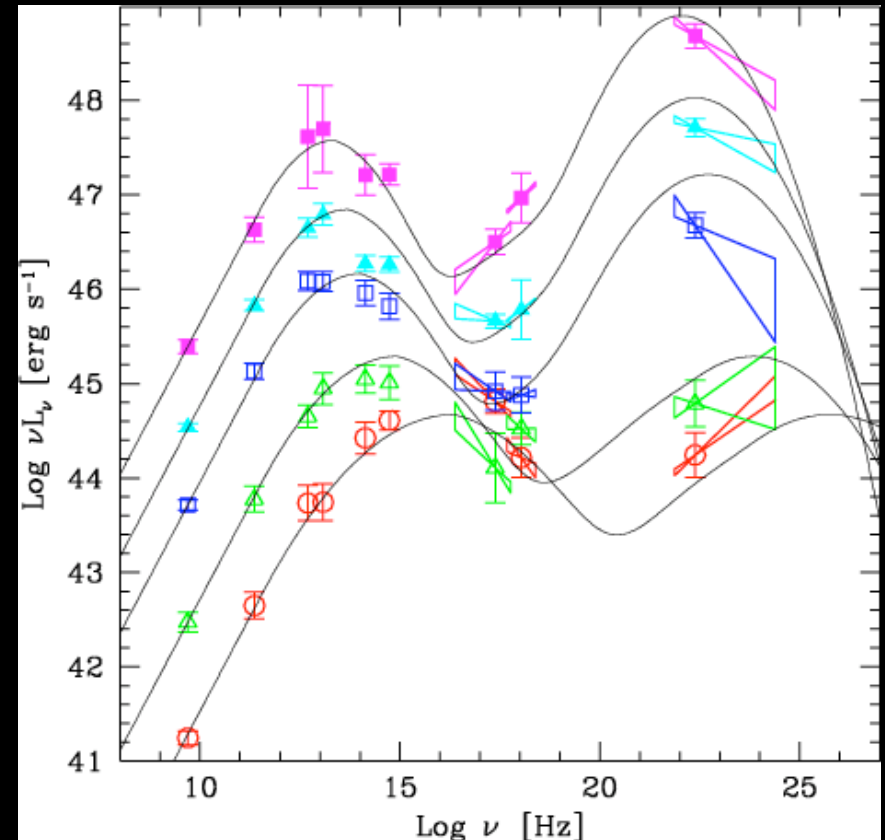
Gamma-ray: BH region + jet shocks

Emission mechanism of Blazars

SED: 2 peaks in μ -F(μ) plot

The first peaks in the UV-X-ray band for the HBL or in the NIR-optical band for the LBL and FSRQs.

The second peaks in the TeV band for the HBL and in the GeV band for the LBL.



Synchrotron and IC

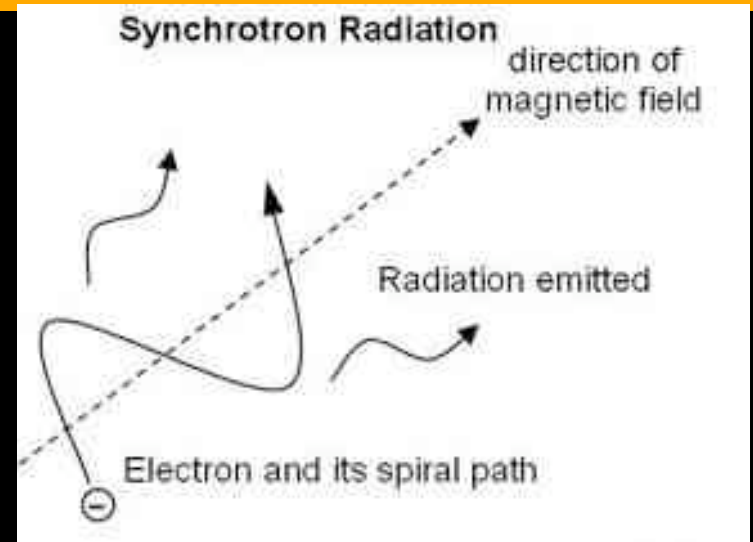
Named after its discovery in a synchrotron accelerator build in 1946_

Two of its characteristics include:

- (1) Non-thermal **power-law** spectrum
- (2) **Polarization**.

Energy loss:

$$P_{\text{syn}} = \frac{4}{3} \sigma_T c \beta^2 \gamma^2 U_B$$

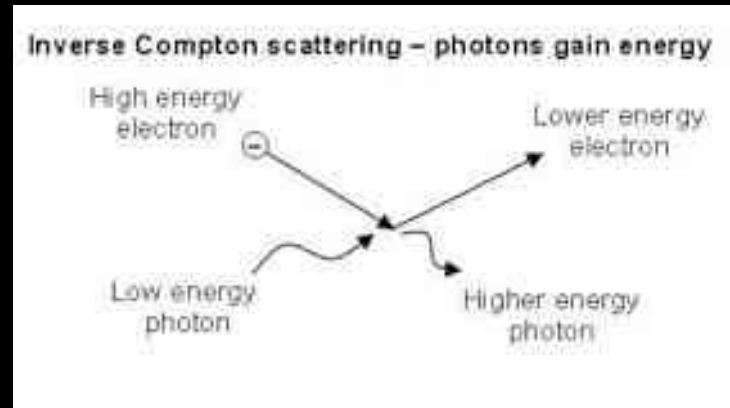


Average frequency of the up-scattered photo:

$$\frac{\langle \nu \rangle}{\nu_0} = \frac{4}{3} \gamma^2$$

Energy loss:

$$P_{\text{IC}} = \frac{4}{3} \sigma_T c \beta^2 \gamma^2 U_{\text{rad}}$$



Synchrotron and IC

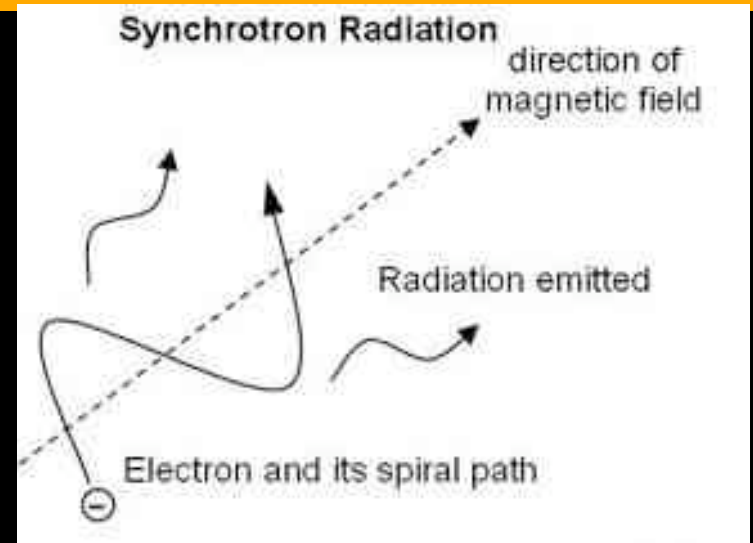
Named after its discovery in a synchrotron accelerator build in 1946_

Two of its characteristics include:

- (1) Non-thermal **power-law** spectrum
- (2) **Polarization**.

Energy loss:

$$P_{\text{syn}} = \frac{4}{3} \sigma_T c \beta^2 \gamma^2 U_B$$



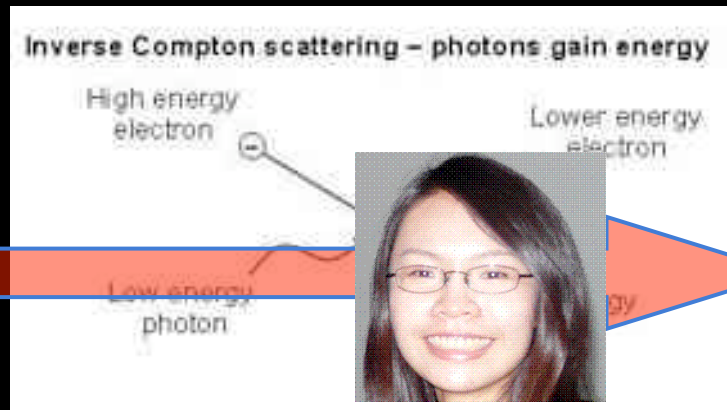
Road map:

Energy of the up-scattered photon:

$$\frac{\langle \nu \rangle}{\nu_0} = \frac{4}{3} \gamma^2$$

$$P_{\text{IC}} = \frac{4}{3} \sigma_T c \beta^2 \gamma^2 U_{\text{rad}}$$

Energy loss:



Snapshots from the life of an AGN

A.2 Milestone in...

“Superluminal motion”

(C.1) Chin Shin Chang

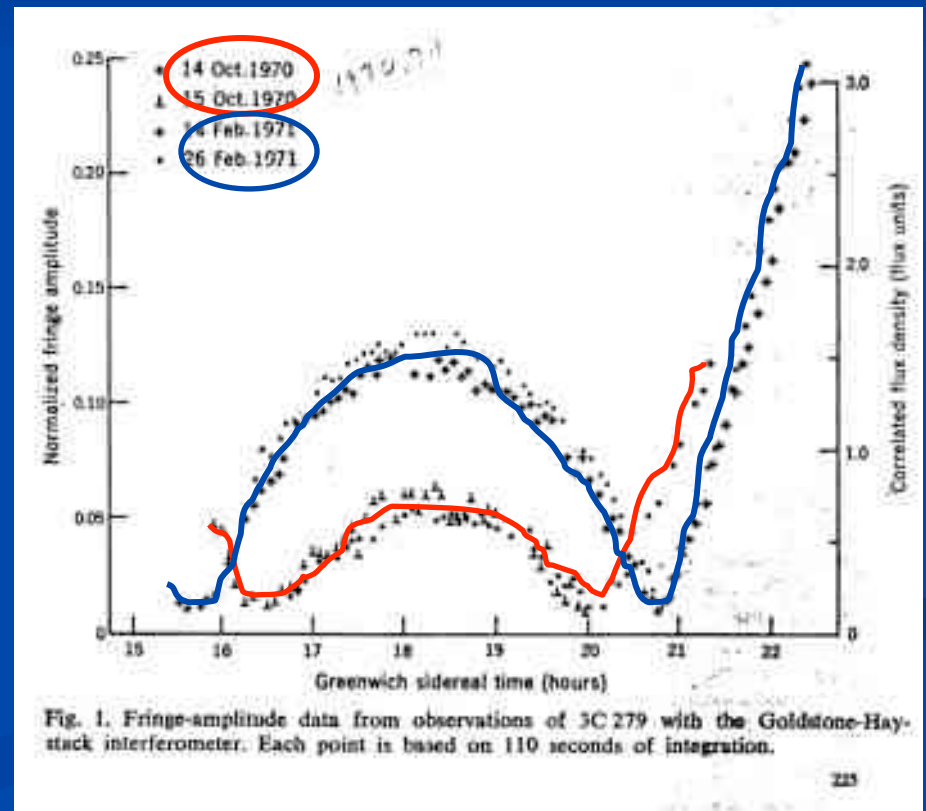
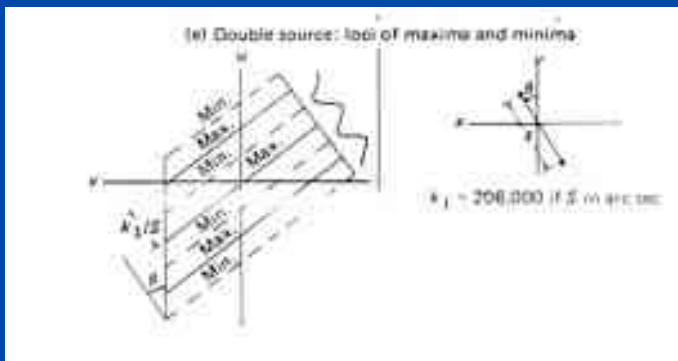
(C.2) Rusen Lu

(C.3) Marios Karouzos

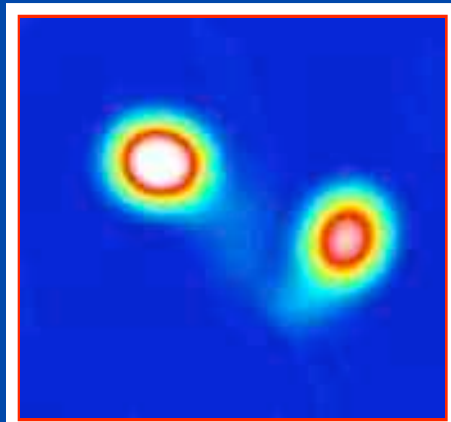
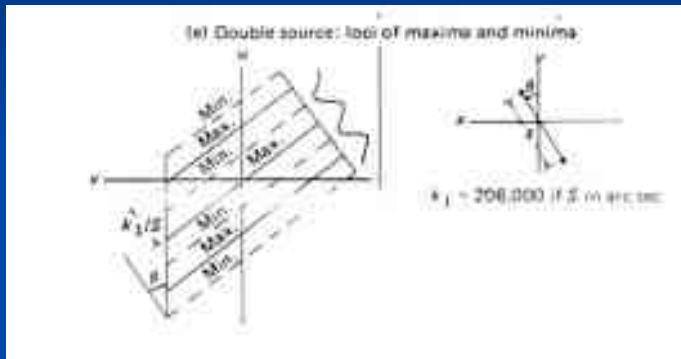
Superluminal motion

Discovery of superluminal motion in 3C 279
(Whitney et al. Science, 1971)

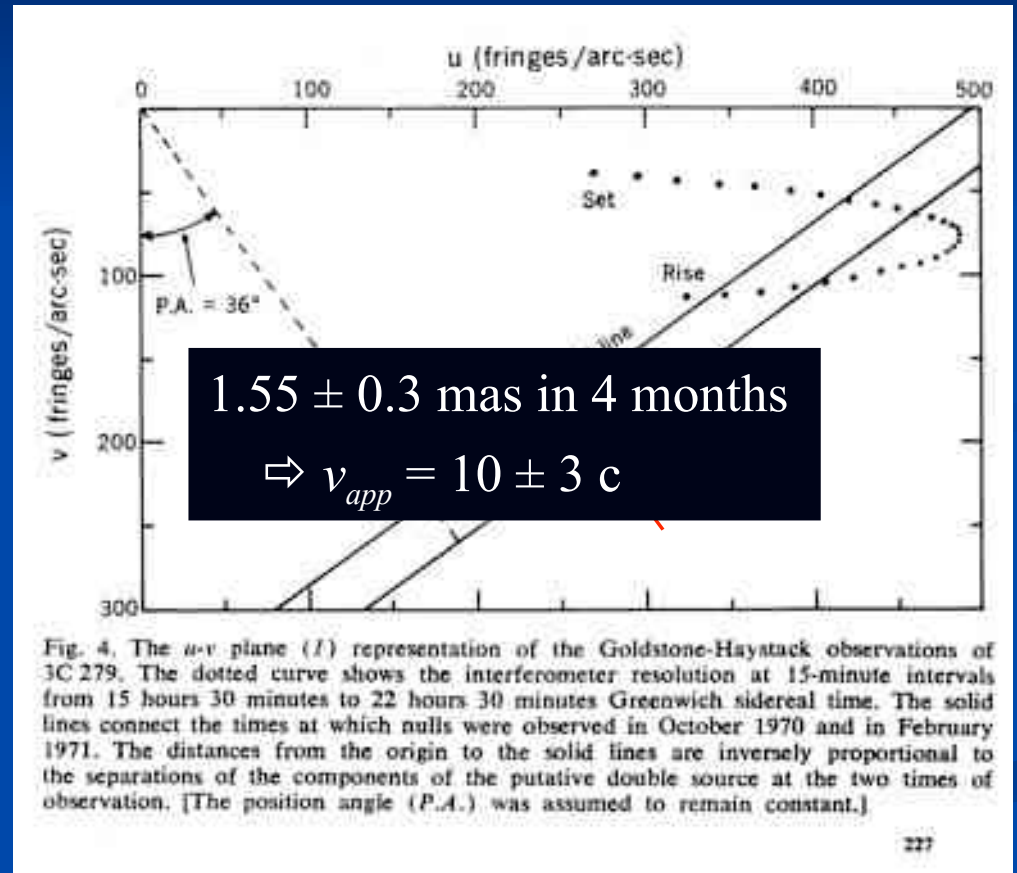
Single baseline observations:
(Goldstone-Haystack)
Freq.: 7.8 GHz



Superluminal motion



3C 279, VSOP@5GHz



Superluminal motion

1970s:

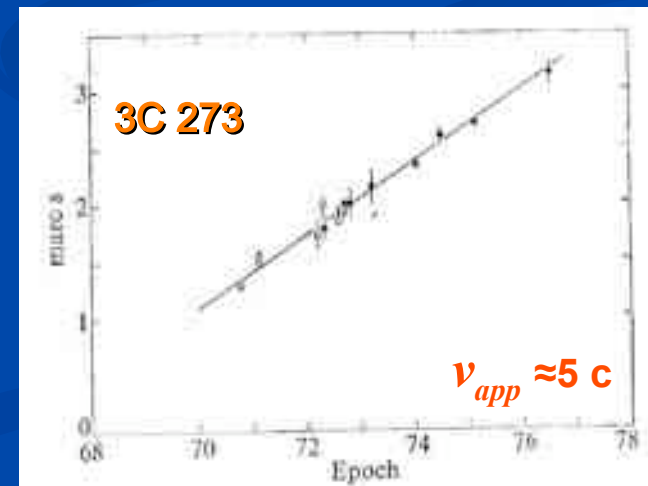
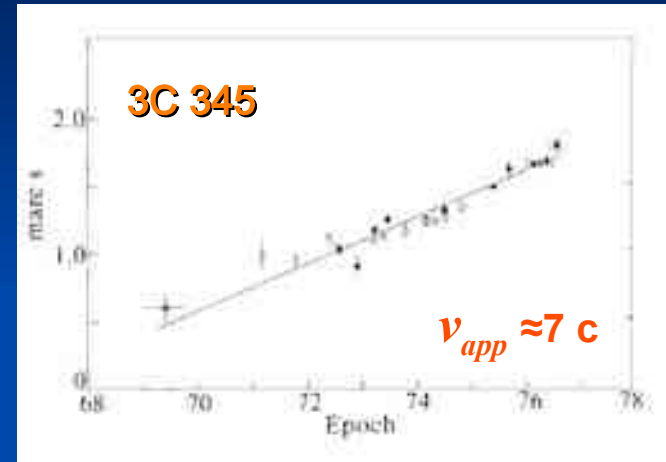
A few strong sources have repeated observations (3C120, 3C273, 3C 279, and 3C 345).

‘superluminal motion’ by comparing the amplitude patterns.

Late 70s:

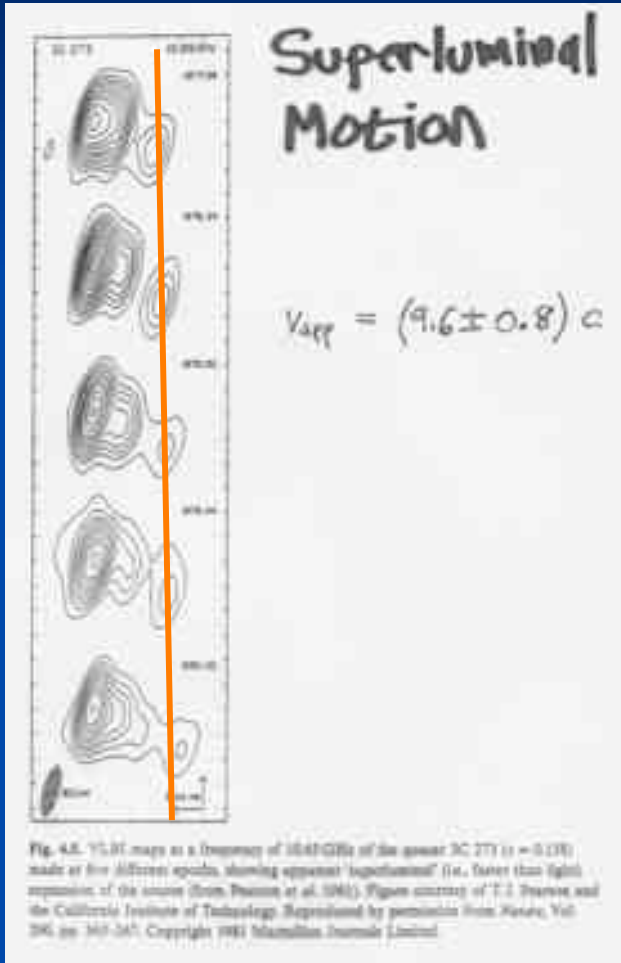
Map-making was in a stage of rapid development

“hybrid mapping technique”



Superluminal motion

(3C 273)



Development of “hybrid mapping” technique allows to map the brightness distribution!

=> First direct and unambiguous evidence!

The innermost part of the jet in 3C273:

The brightest (leftmost) one corresponds to the object at the center of the quasar.

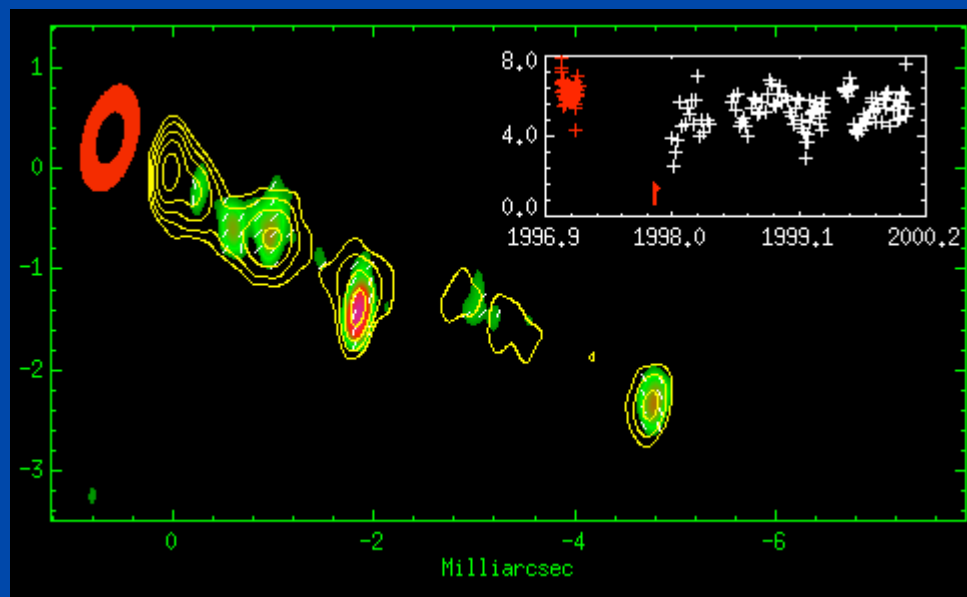
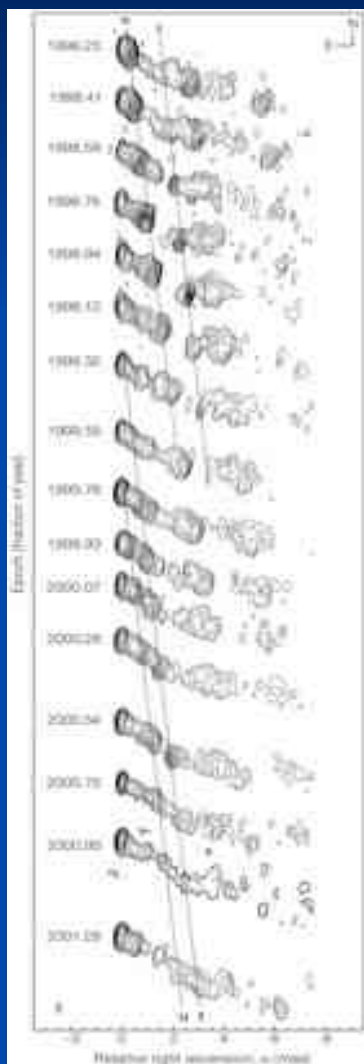
the rightmost knot looks to have moved about 30 light years in only three years. It moves at 10 times the speed of light

Superluminal motion

(3c 120)

16 epochs VLBA observations @7mm

$$v_{app} \approx 4-5 \text{ c}$$

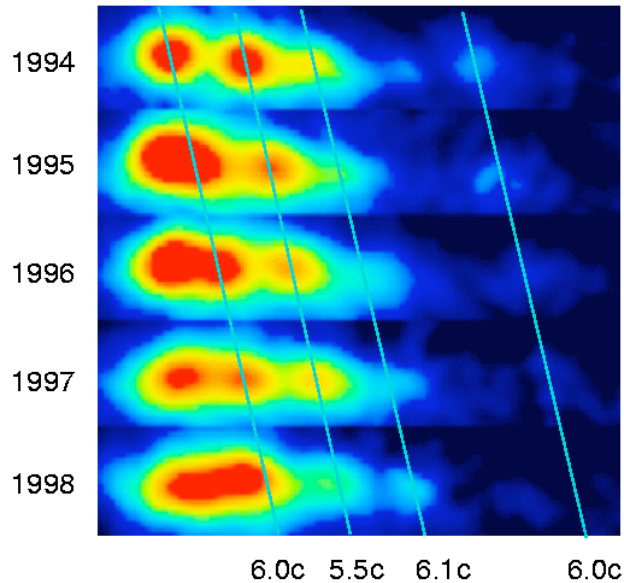
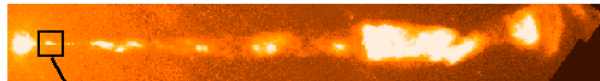


Superluminal motion

Optical superluminal motion

$$v_{app} \approx 6c$$

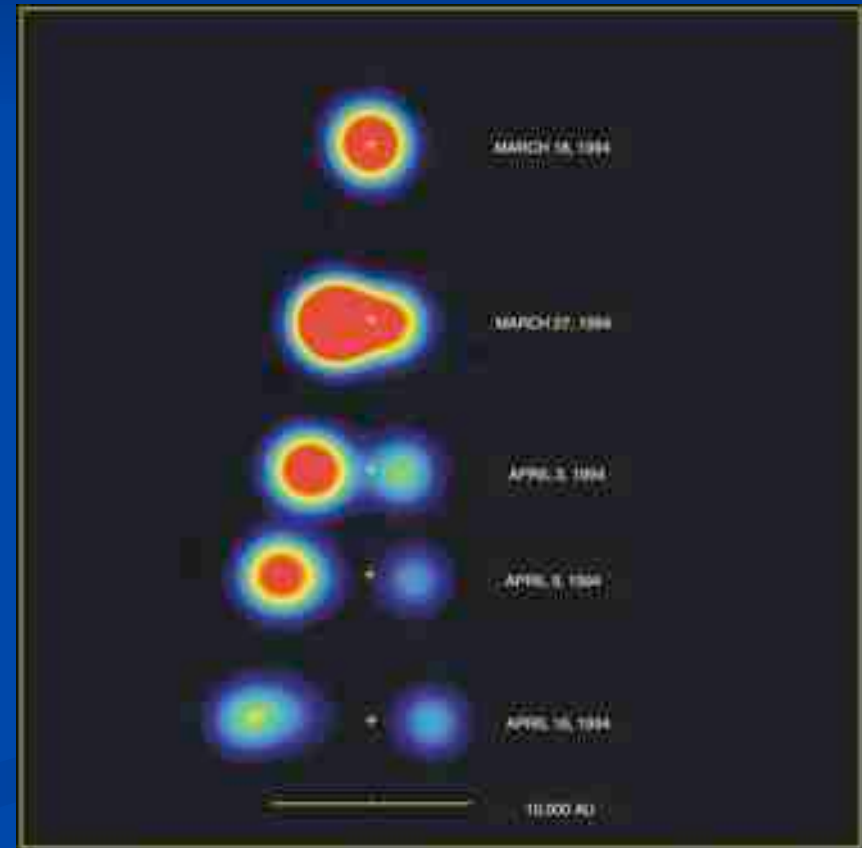
Superluminal Motion in the M87 Jet



Biretta et al. ApJ, 1999

Superluminal motion In the Galaxy (GRS 1915+105)

$$v_a \approx 1.25c; v_r = 0.65c$$



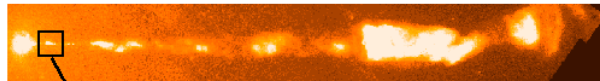
Mirabel and Rodriguez, Nature, 1994

Superluminal motion

Optical superluminal motion

$$v_{app} \approx 6c$$

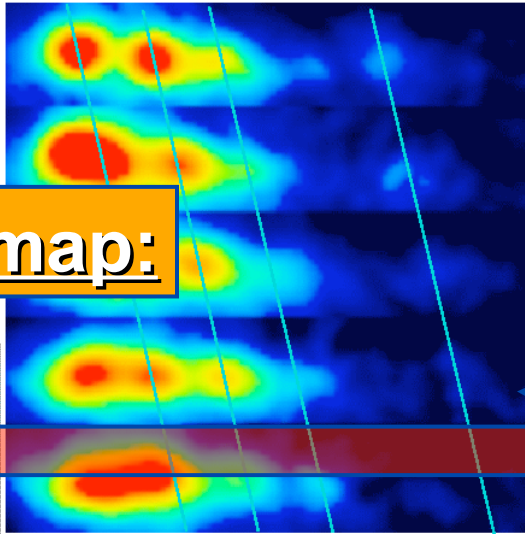
Superluminal Motion in the M87 Jet



1994

1995

Road map:



6.0c 5.5c 6.1c 6.0c

Superluminal motion In the Galaxy
(GRS 1915+105)

$$v_a \approx 1.25c; v_r = 0.65c$$



Snapshots from the life of an AGN

B.1 Introducing...

“The accretion disk”

(B.1) Marios Karouzos

(B.2) Chin Shin Chang

(B.3) Rusen Lu

Outline:

(making a long, long, long, long, long story quite short)

1. Introduction to the introduction
2. Accreting matter and extracting energy
3. Spherical and Bondi accretion
4. Non-adiabatic accretion
5. Accretion rate and the ADAF model
6. Observational evidence



© A. Marcher, COSMOVISION

Introduction

(...to the introduction)

SHORT INTERACTION

Hunting for the right picture...1

(or the screwed up selection algorithms of Google)



Hunting for the right picture...2

(or the screwed up selection algorithms of Google)



Hunting for the right picture...3

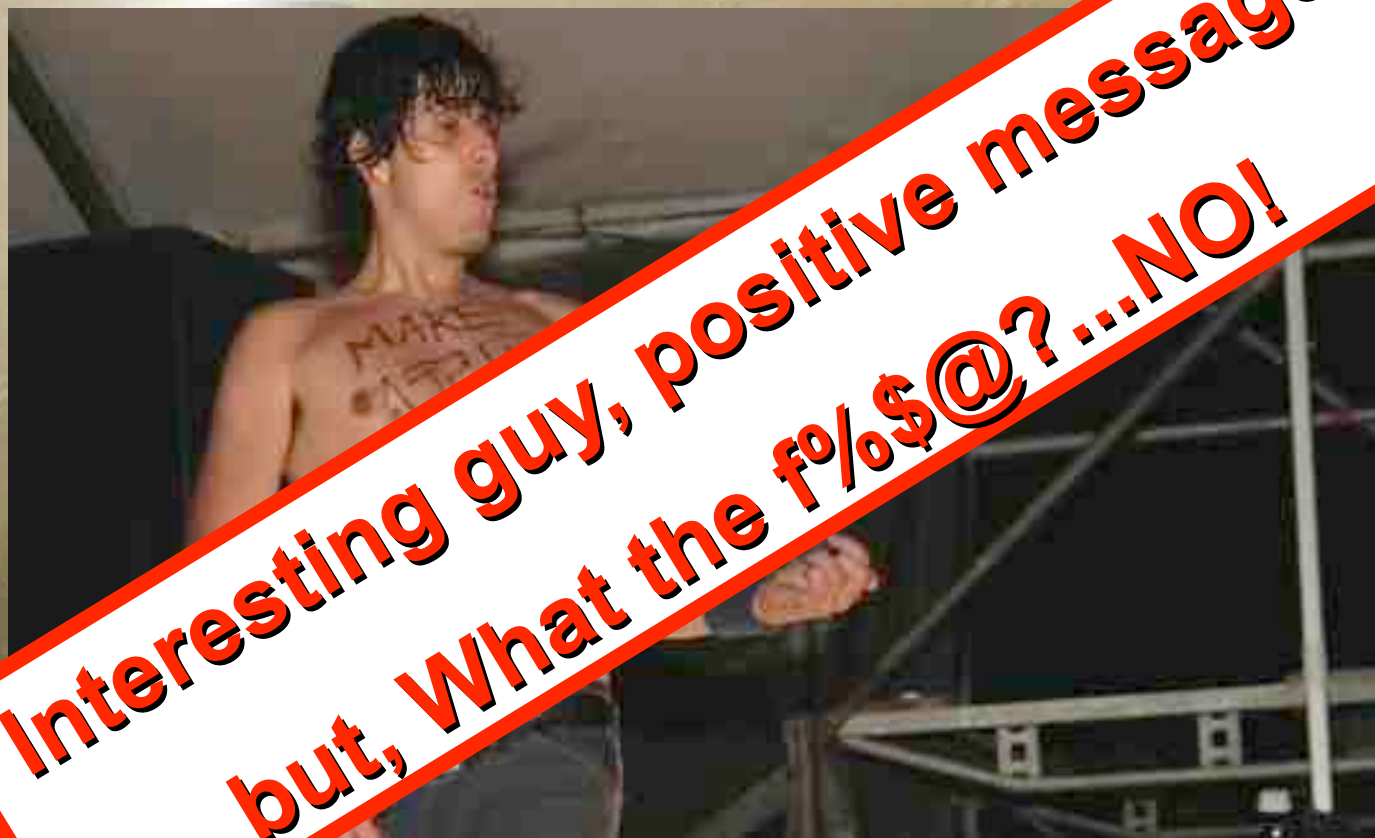
(or the screwed up selection algorithms of Google)



Jazz, nice! Not quite scientific...NO!

Hunting for the right picture...4

(or the screwed up selection algorithms of Google)



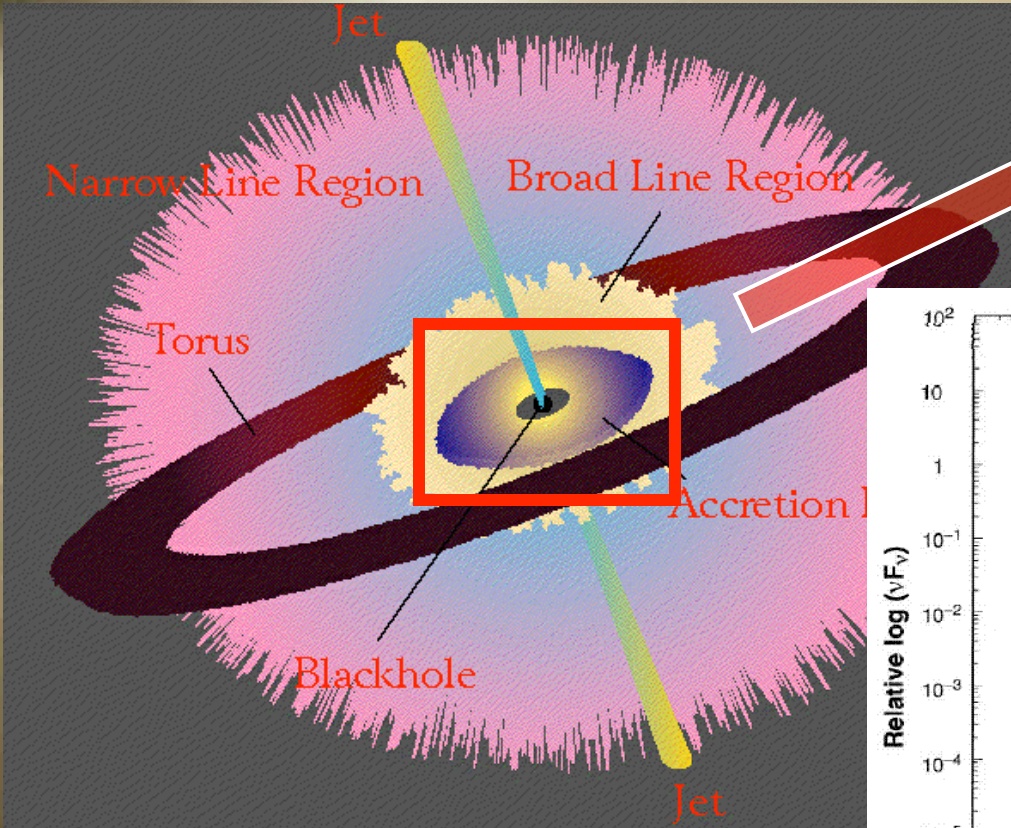
Hunting for the right picture...5

(or the screwed up selection algorithms of Google)



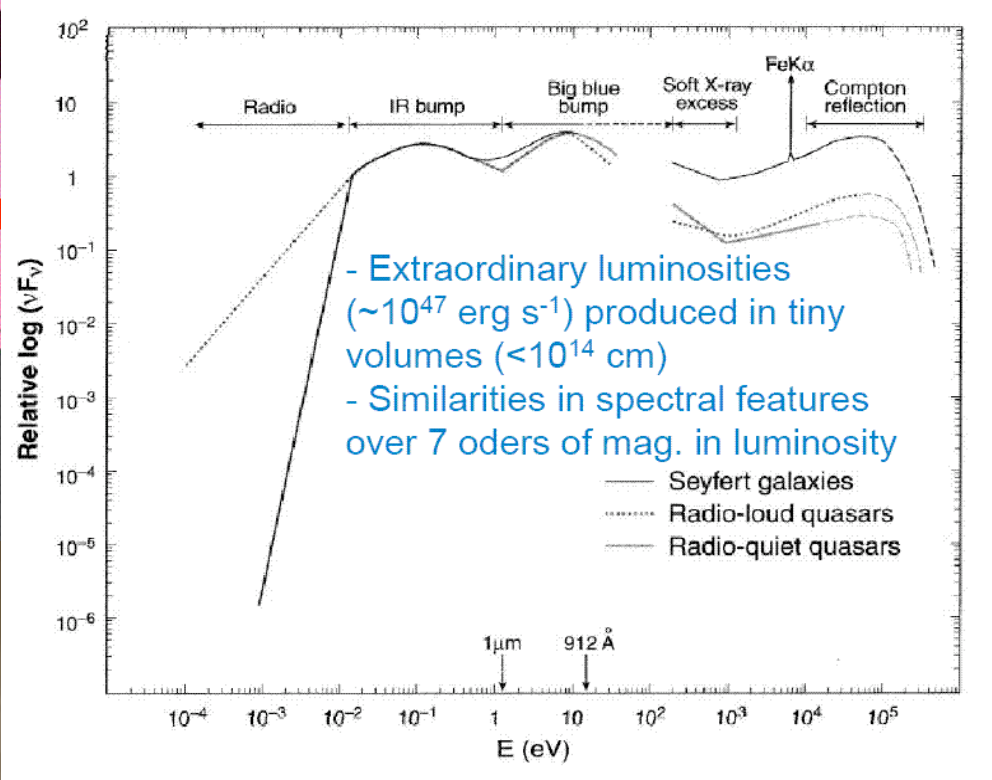
Introduction

(...to the introduction)



Accretion Disk

AGN SEDs



The Unified Scheme of AGN

Accreting matter

(...and energy interplay)

* depending on the spin of the BH

Powerful energy-producing mechanisms:

1. Nuclear fusion ($\epsilon \leq 0.8\%$)
2. Accretion ($\epsilon \sim 6 - 29\%$)*

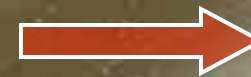
For most galaxies \rightarrow material has angular momentum (NOT free fall)

Mechanisms to extract energy:

- viscosity
- non-axisymmetric gravitational forces
- magnetic forces



Kinetic energy



Thermal energy

Intersection + Equalization of orbits \rightarrow Accretion Disk

*not the journal...

Spherical and Bondi accretion

(...simplifying Nature*)

Spherical accretion (simplest assumption):

- smooth
- time steady
- spherically symmetric



temperature of accreting gas very high
→ virialized



radiation pressure (trapped photons) high
→ support against gravity

Assumption valid for:
> Eddington luminosity

$$L_E = \frac{4\pi c G M \mu_e}{\sigma_T} = 1.51 \times 10^{38} \frac{M}{M_{sol}} \text{ergs}^{-1}$$

(see Rusen's B.3)

Spherical and Bondi accretion (cont.)

(...simplifying Nature*)

Equation of state (energy equation):

→ simplest case (Bondi 1952): adiabatic law

$$p \propto \rho^\gamma$$

We can derive the accretion rate:

$$\dot{M} = 4\pi\lambda(\gamma) \frac{(GM^2)\rho_\infty}{c_s^3}$$

where:

$\lambda(\gamma)$ is a function of γ

ρ_∞ is the density at infinity

c_s the speed of sound at infinity

From the above:

1. we have a **scale** for the accretion rate (for certain M and f_∞)
2. accretion is **regulated** by equation of state (γ)

* for astrophysical plasma $\gamma = 5/3$ (no heating/cooling)

Non-adiabatic accretion

(...now it gets interesting!)

We need to approximate the conditions of the flow:

$$n_e = \frac{\dot{M}}{4\pi r^2 \mu_e u} = 3.8 \times 10^{11} \left(\frac{\dot{M}}{M_{\text{sol}} \text{yr}^{-1}} \right) M_8^{-2} x^{-3/2} \text{cm}^{-3}$$

assuming Newtonian physics
+
infall at \sim free-fall speed

We can derive the **Thomson optical depth**, in terms of the Eddington accretion rate:

$$\tau_T = \frac{\dot{M} / \dot{M}_E}{x^{1/2}}$$

$$\frac{L}{L_E} \sim 1 \times 10^{-4} \left(\frac{\dot{M}}{\dot{M}_E} \right)^2$$

assuming a certain temperature profile
+
cooling mechanism (two-body collisions)

$$L \ll L_E$$

Non-adiabatic accretion (cont.)

(...now it gets interesting!)

Even for the more realistic case non-adiabatic accretion:
→ spherical assumption is not valid

photon trapping



ADAF

(see next slides)

thermal instability



disc disruption

(non-physical result)

Both problems arise from high efficiency ($L \sim L_E$)!

Accretion rate and ADAF

(...lets see what's really happening!)

Even for an initial spherical infall:

- > circular orbits of fixed angular momentum
- > interaction of neighboring orbits
- > mixing of angular momentum
- > co-planar orbits

an **accretion disk** is formed!

in most cases:
thickness \ll radius



Thin accretion disk

accretion rate regulates the morphology of the disk:

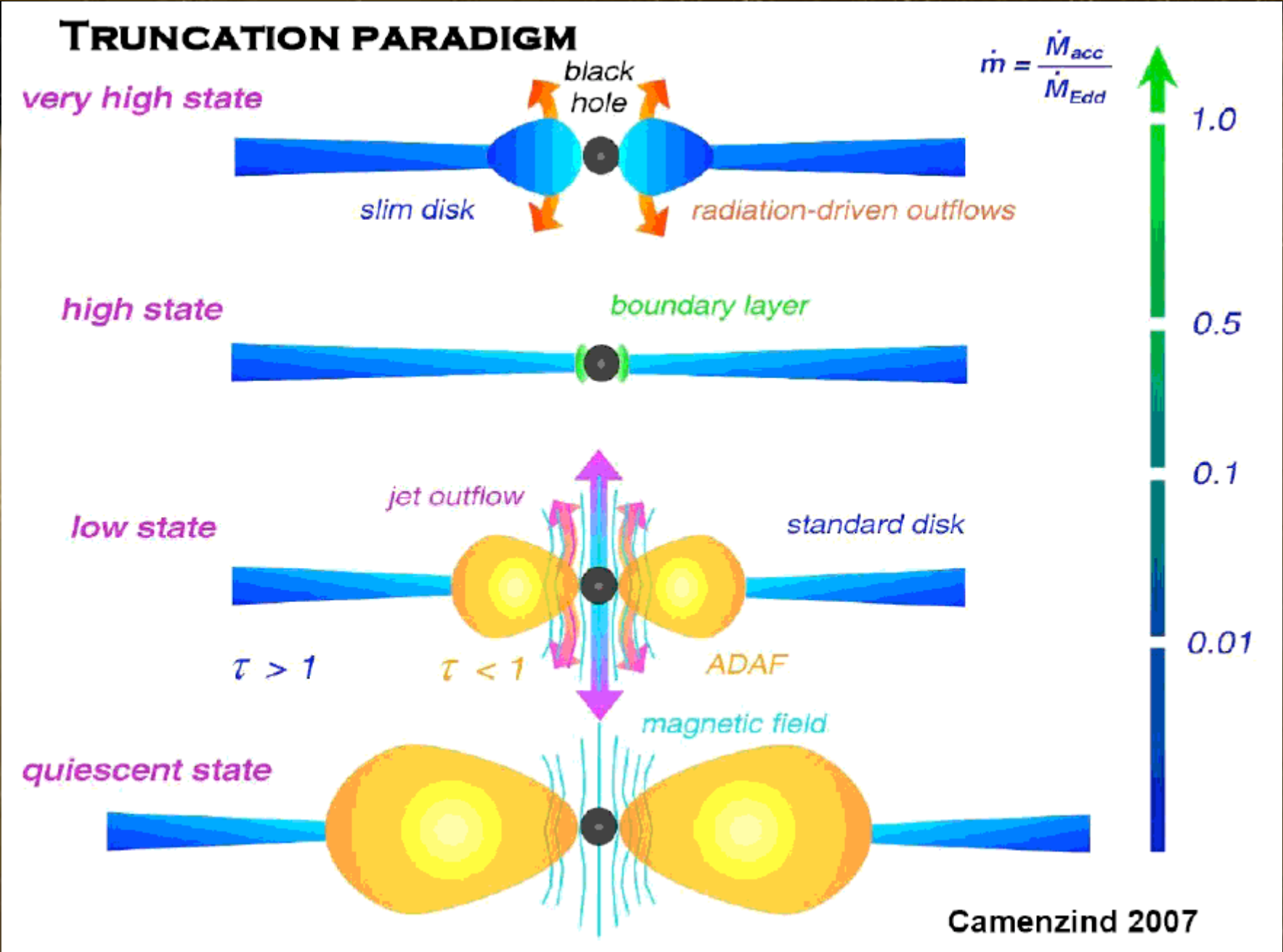
for $dM/dt \rightarrow (dM/dt)_E$



radiation pressure becomes important



thick disk

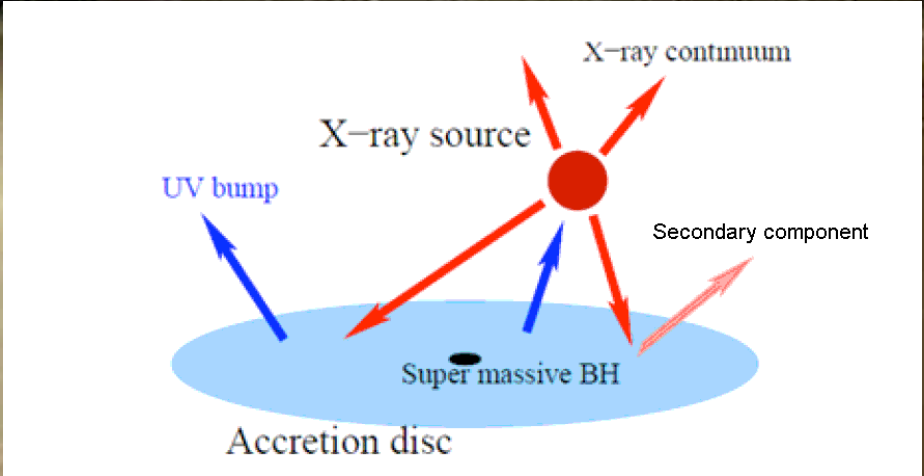


Observational tests

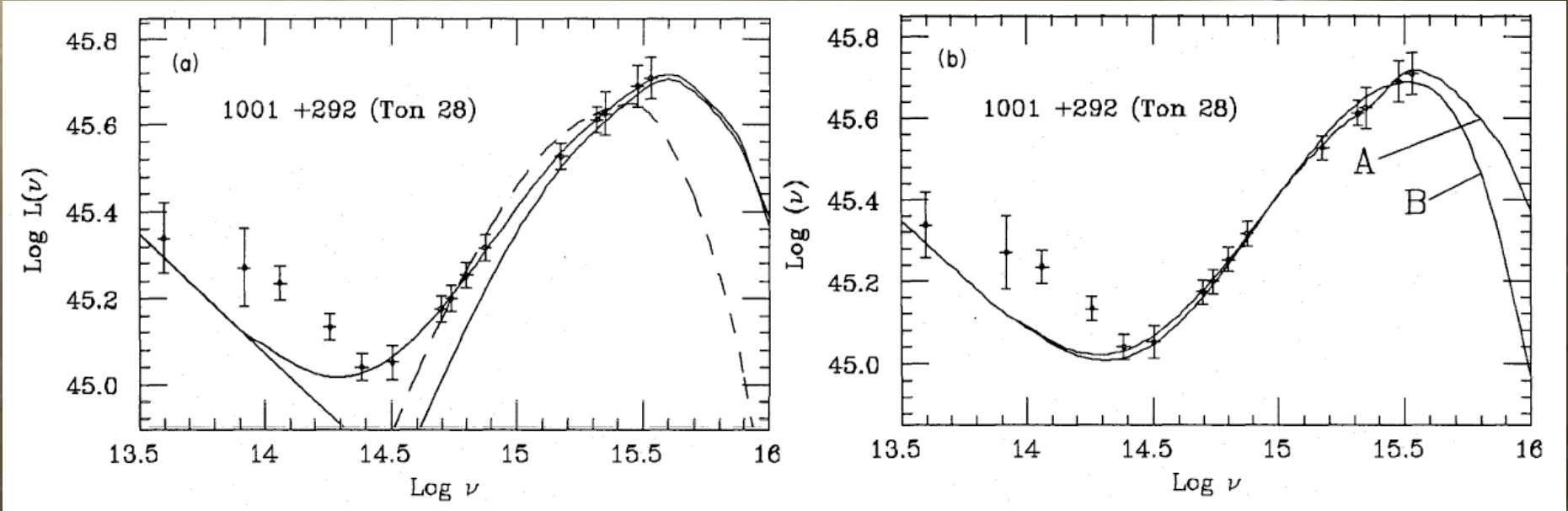
(...lets see!)

Big blue bump:

$$\frac{dF}{d \ln \lambda} \sim 10 eV$$



Points toward a thermally emitting surface (no specific geometry needed!)



Laor (1990)

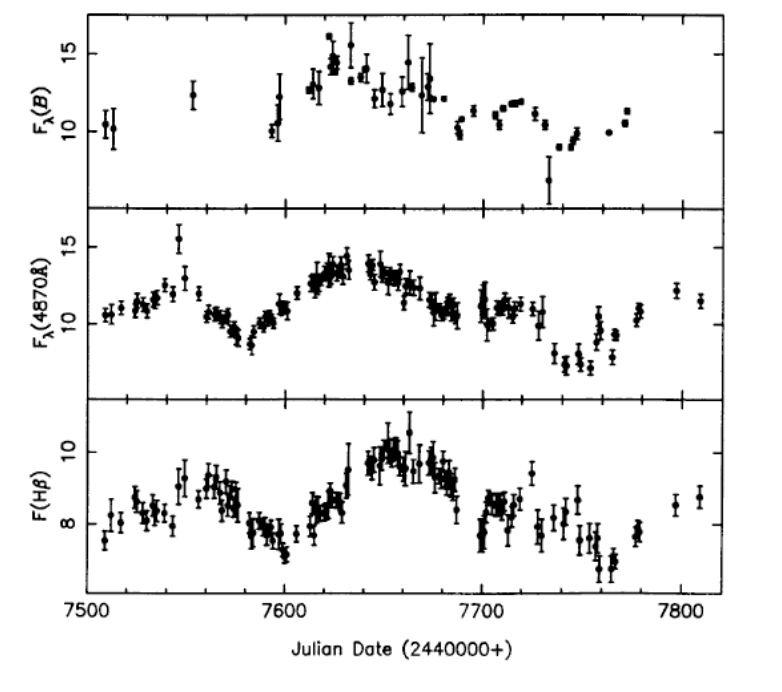
Observational tests (cont.)

(...lets see!)

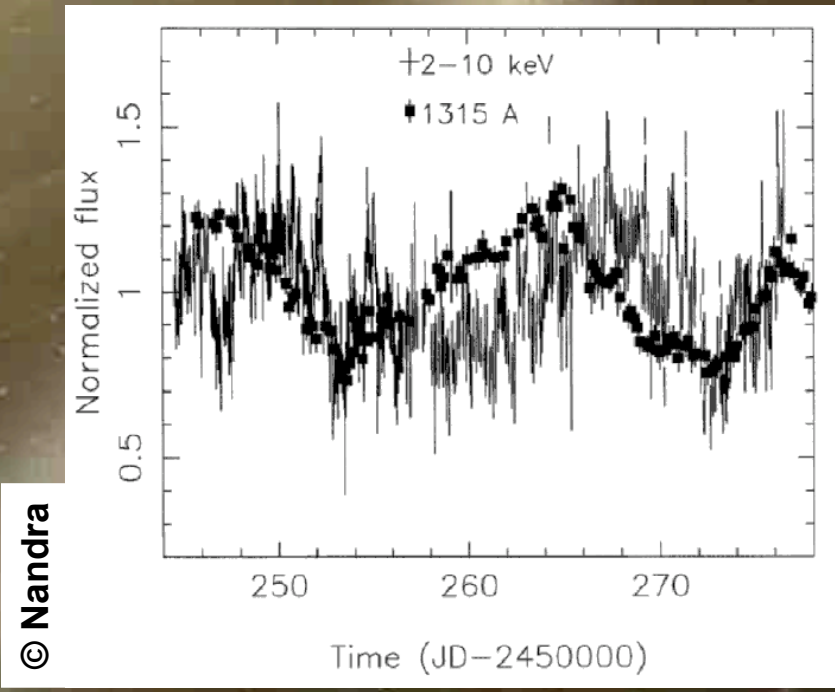
Variability:

timescales \rightarrow size of emitting regions (*light travel time*)
 \rightarrow physical nature of processes

frequency dependency \rightarrow tracing across the disk



Peterson et al. (1991)



© Nandra

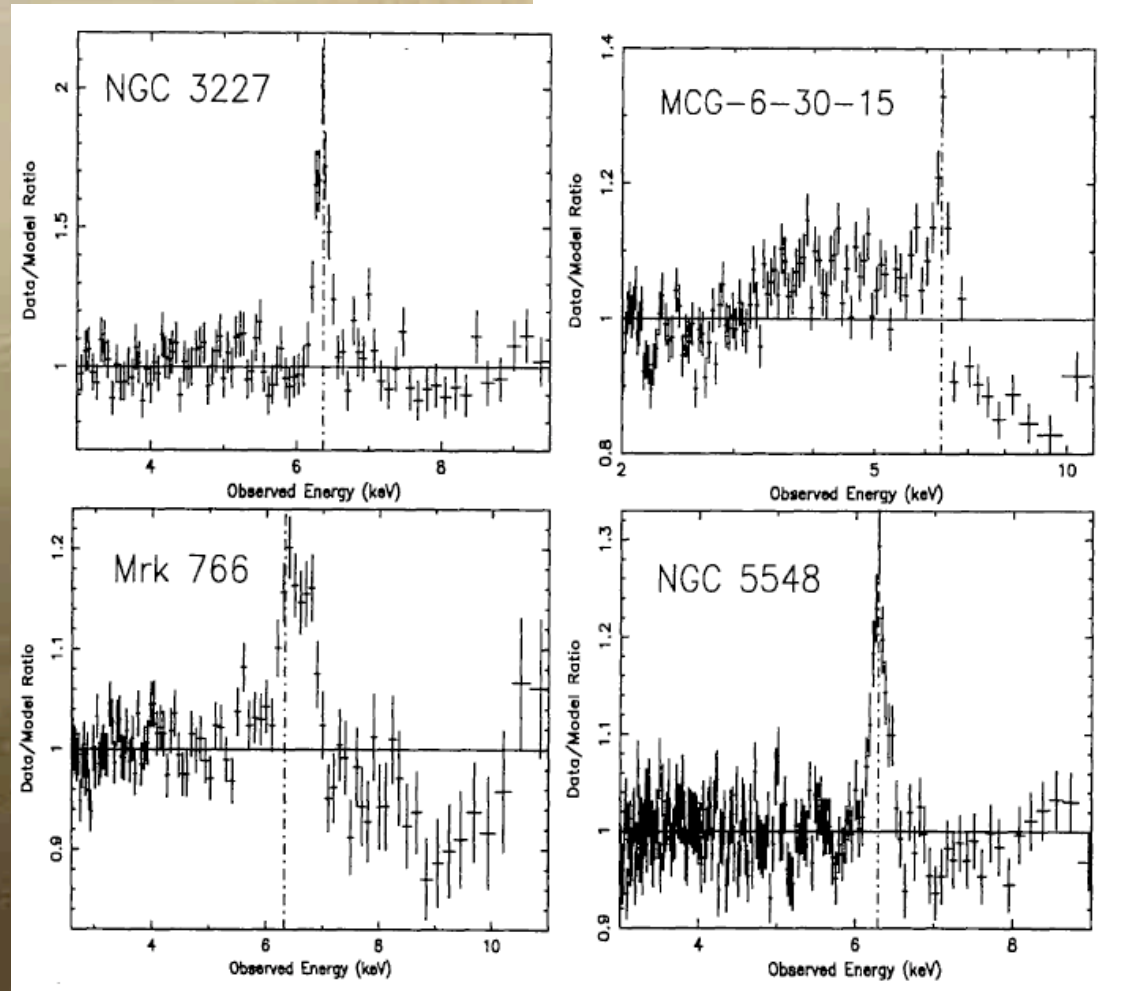
Observational tests (cont.)

(...lets see!)

The iron K line:

(see Chin Shin's B.2)

XMM line profiles; Reeves (2003)

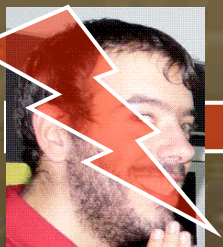


Summary

(...and passing the torch!)

- Accretion \rightarrow high enough ϵ to power AGN
- Spherical accretion \rightarrow first order approximation
 - > Bondi (adiabatic)
 - > non-adiabatic
- Accretion in disk geometry \rightarrow most probable
 - > geom. thin disks
 - > geom. thick disks
- Indirect observations
 - > Big Blue Bump
 - > Variability
 - > Iron K line

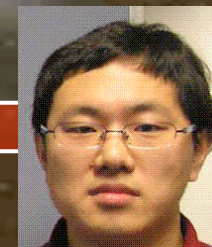
Road map:



Overview



Milestone



Equations

Snapshots from the life of an AGN

A.2 Milestone in...

“Synchrotron Emission”

(A.1) Rusen Lu

(A.2) Marios Karouzos

(A.3) Chin Shin Chang



THE POLARIZATION OF SYNCHROTRON RADIATION

K. C. WESTFOLD*

California Institute of Technology

Received February 14, 1959

ABSTRACT

The spectral distribution and polarization of radiation from an electron gyrating ultra-relativistically in a magnetic field are calculated. The result is used to calculate the principal emissivities of a distribution of high-energy electrons such as occurs in the Crab Nebula. It is shown that the degree of polarization of the emission increases with frequency, from two-thirds at radio frequencies to unity. The depolarizing factors affecting the intensity of the emergent rays are briefly discussed.

I. INTRODUCTION

The synchrotron process by which radiation is generated has assumed considerable importance since the recent studies by Oort and Walraven (1956), Pikelner (1956), and Woltjer (1958). These have virtually confirmed Shklovsky's (1953) hypothesis that the light from the Crab Nebula is due to radiation from high-energy electrons gyrating in a magnetic field. This process can now be invoked to account for the non-thermal emission from other radio stars and from the galactic halo.

The most useful calculations of the radiation from charged particles moving with velocities close to the velocity of light (ultra-relativistic velocities) are those of Schwinger (1949). His procedure was to calculate the radiant power emitted, via the rate at which the particle does work on the field of which it is the source. The field vectors were not required, so that the polarization of the emission was left undetermined.

On general grounds it is to be expected that radiation so intimately connected with a magnetic field would exhibit polarization. Indeed, it was the discovery of strong polarization in the optical emission from the Crab Nebula by Vashakidze (1954) and Dombrovsky (1954) that sealed the adoption of the synchrotron hypothesis. Woltjer (1957) has

K.C. Westfold, 1959, ApJ

The Motivation

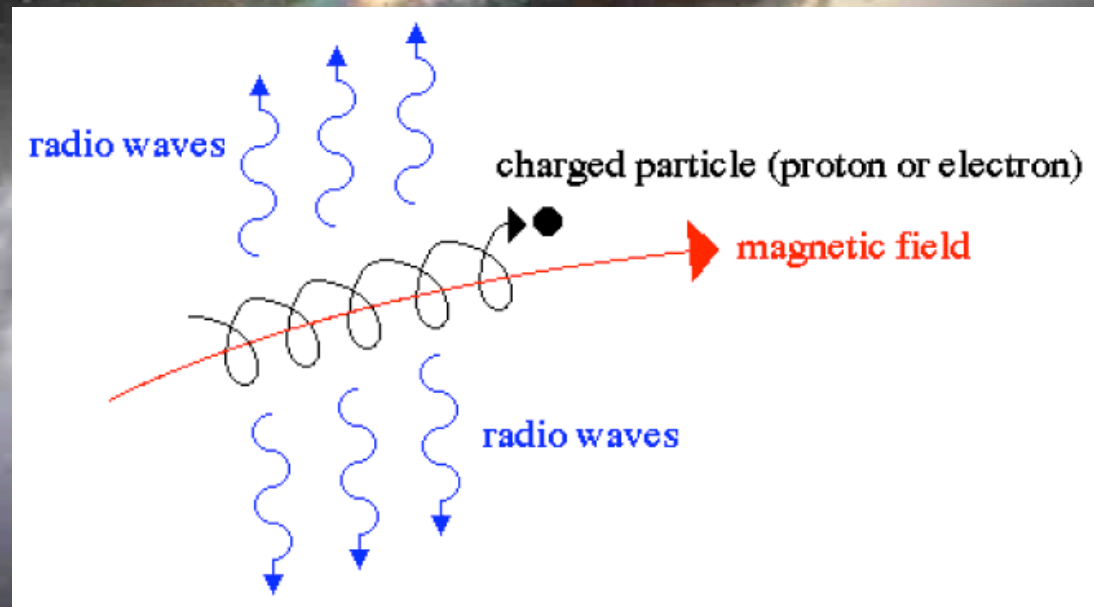
Polarization measurements (photographic plates)

Oort and Walraven (1956); Mean Polarization degree ~ 17%



The Paper

The **synchrotron process** by which radiation is generated has assumed considerable importance since the recent studies by Oort and Walraven (1956), Pikelner (1956), and Woltjer (1958). These have virtually confirmed Shklovsky's (1953) hypothesis that the light from the Crab Nebula is due to **radiation from high-energy electrons gyrating in a magnetic field**. This process can now be invoked to account for the **non-thermal emission from other radio stars** and from the galactic halo.



The general idea of the synchrotron process

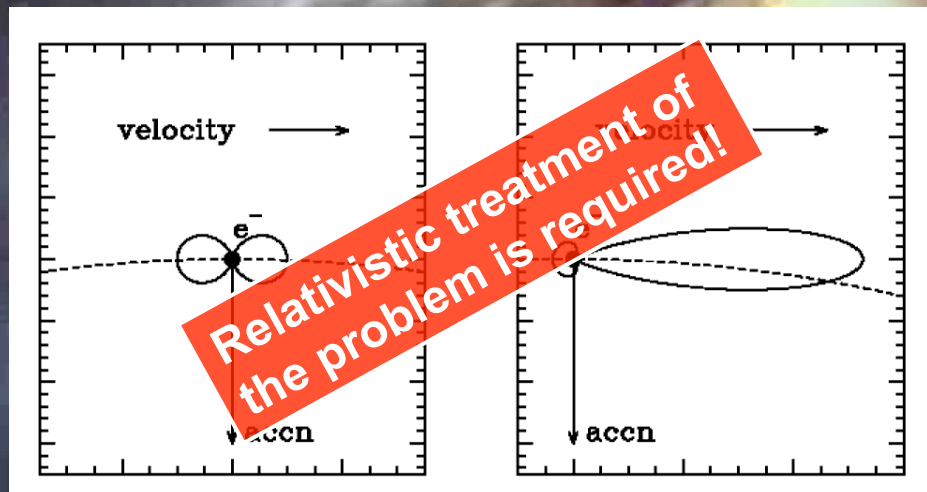
The gory details

On general grounds it is to be expected that radiation so intimately connected with a magnetic field would exhibit polarization. Indeed, it was the discovery of strong polarization in the optical emission from the Crab Nebula by Vashakidze (1954) and Dombrovsky (1954) that sealed the adoption of the synchrotron hypothesis.

For the proper interpretation of these measures it is essential that the polarization properties of the emission from a single electron should first be known.

We are dealing with relativistic particles, so that:

$$\gamma = \frac{1}{\sqrt{1 - \beta^2}}$$



The position vector

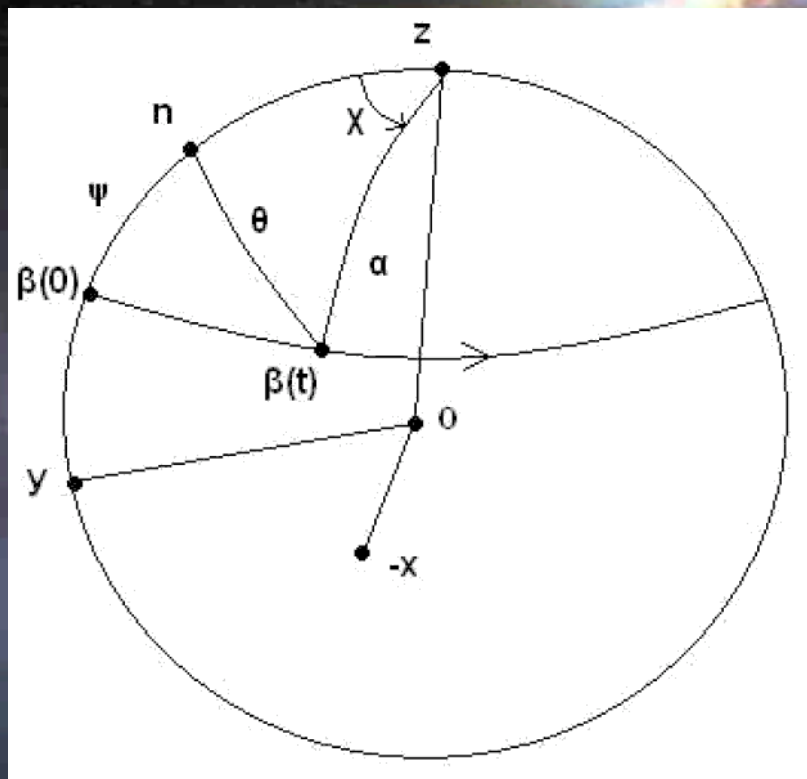
(and other things...)

assuming that $\gamma \sim \text{constant}$

$$\frac{\vec{r}}{c} = \frac{\beta}{\omega_B} \left[\underbrace{(\hat{x} \cos \omega_B t + \hat{y} \sin \omega_B t)}_{(A)} \sin a + \underbrace{\hat{z} \omega_B t \cos a}_{(B)} \right]$$

$$\vec{\omega}_B = \frac{e}{m} \sqrt{1 - \beta^2} \vec{B}_0$$

gyrofrequency



Index:

z: direction of B_0

n: line of sight vector

χ : position angle

α : angle between velocity and B_0

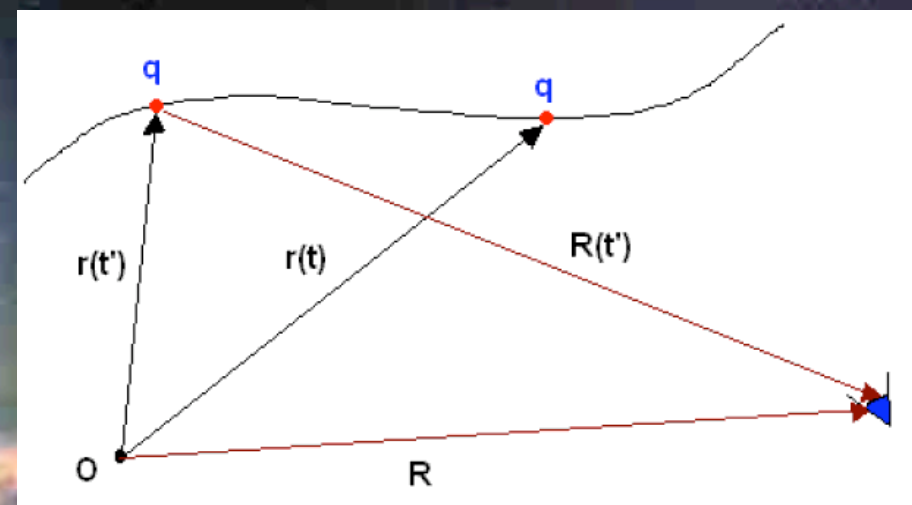
ψ : angle between velocity and n

The field equations

(hold onto your seats...)

$$\vec{E} = \frac{\mu e c}{4\pi R} \frac{\vec{n} \times [(\vec{n} - \vec{\beta}') \times \dot{\vec{\beta}}']}{(1 - \vec{\beta}' \cdot \vec{n})^3}$$

$$\vec{B} = \frac{1}{c} \vec{n} \times \vec{E},$$



Sketch of retarded * time

$$E_n(\vec{r}) = \frac{\omega_B}{2\pi} \int_0^{2\pi/\omega_B} \vec{E} \exp(in\omega_B t) dt$$

$$E_n = A(R, \omega_B) \cdot \int_0^{2\pi/\omega_B} \frac{\vec{n} \times [(\vec{n} - \vec{\beta}') \times \dot{\vec{\beta}}']}{(1 - \vec{\beta}' \cdot \vec{n})^2} \exp \left[in\omega_B \left(t' - \vec{n} \cdot \frac{\vec{r}}{c} \right) \right] dt'$$

* politically correct term: mentally challenged

Some assumptions

(of course...what else?)

We assume that:

- motion length scale \ll distance to observer
- $\gamma \gg 1 \rightarrow \gamma^{-1} \ll 1 \rightarrow \beta$ can be expanded
- \mathbf{n} is on the plane (\mathbf{B}_0, β_0)
- $\theta > \gamma^{-1}$ negligible \rightarrow integration over $\pm \infty$

$$E_n = \frac{\mu e c \omega_B}{4\sqrt{3}\pi^2 r} \exp\left(in\omega_B \frac{r}{c} \frac{n}{\sin \alpha}\right) \cdot \{E_2 \cdot \hat{\mathbf{x}} - E_1 \cdot (\hat{\mathbf{x}} \times \hat{\mathbf{n}})\}$$

$$Q_n = \frac{E_n \cdot \hat{\mathbf{x}}}{E_n \cdot \hat{\mathbf{x}} \times \hat{\mathbf{n}}}$$

complex polarization degree of the n^{th} E harmonic

Calculating the intensity

(and some guys called Stokes parameters...!)

$$I_f = R^2 \frac{c}{2\pi} |E_n|^2 \frac{dn}{df}$$

R: distance to observer
n: number of harmonic
f: frequency $O(\omega_B)$

$$f = n \cdot \frac{\omega_B}{2\pi}$$

$$I_f^{(1)} = \frac{3}{4\pi^2} \frac{e^3 B_0 \gamma}{mc^2} \left(\frac{f}{f_c} \right)^2 (1 + \gamma^2 \psi^2)^2 K_{2/3}^2(g_f)$$

$$I_f^{(2)} = \frac{3}{4\pi^2} \frac{e^3 B_0 \gamma}{mc^2} \left(\frac{f}{f_c} \right)^2 \gamma^2 \psi^2 (1 + \gamma^2 \psi^2) K_{1/3}^2(g_f)$$

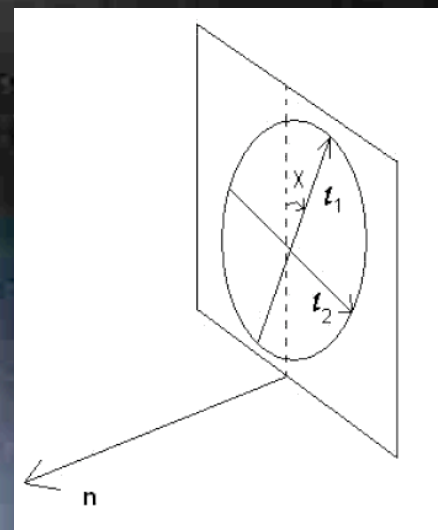
Stokes parameters:

$$I_f = I_f^{(1)} + I_f^{(2)}$$

$$Q_f = [I_f^{(1)} - I_f^{(2)}] \cos 2x$$

$$U_f = [I_f^{(1)} - I_f^{(2)}] \sin 2x$$

$$V_f = [I_f^{(1)} - I_f^{(2)}] \tan 2\beta$$





...and that was just for one freakin electron!

A population of electrons!

(in a nutshell...)

At a given field point the synchrotron radiation received from a small volume containing a distribution of ultra-relativistically gyrating electrons effectively originates in the group whose velocities have directions within the conical annulus for which α is within an angular distance $O(\xi)$ of θ , the angle between \mathbf{n} and \mathbf{B}_0 .

The contributed power depends on:

- the energy of the e^- : $E=E(E_0, \gamma)$
- the angle ψ

$$\eta_f^{(i)}(\vec{n}) = \frac{1}{4\pi} \int_0^\infty N\left(\frac{E}{E_0}\right) \left\langle P_f^{(i)}\left(\frac{f}{f_c}\right) \right\rangle \frac{dE}{E_0},$$

Total emissivity:

$$\eta_f = \eta_f^{(1)} + \eta_f^{(2)}$$

Polarized emissivity:

$$\eta_f^{(p)} = \eta_f^{(2)} - \eta_f^{(1)}$$

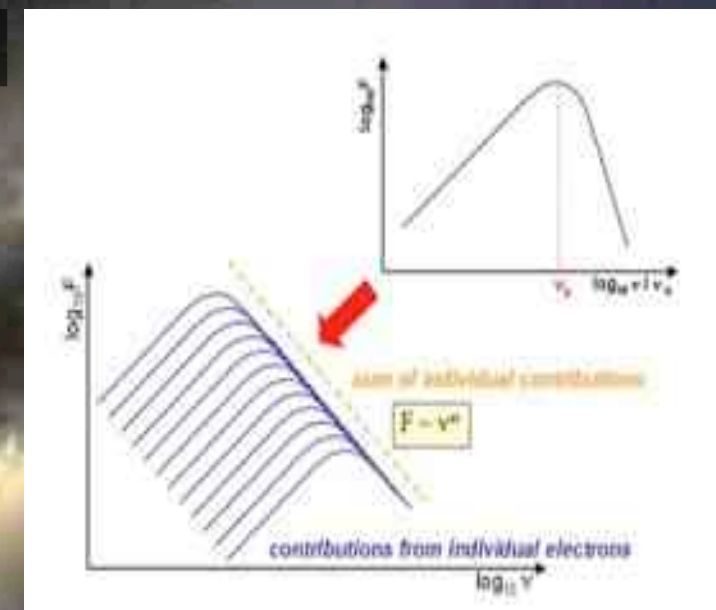
A power law...

(the simplest case!)

We can assume for the population of electrons:

$$N(x) = Ax^{-p} \quad \text{for} \quad \frac{E_1}{E_0} \leq x \leq \frac{E_2}{E_0}$$

$$N(x) = 0 \quad \text{for} \quad x < \frac{E_1}{E_0}, x > \frac{E_2}{E_0}$$



$$\eta_f(\vec{n}) = A \frac{\mu e^2 c}{8\sqrt{2}\pi} \left(\frac{3}{2}\right)^{\gamma/2} (f_{B_0} \sin \alpha)^{(p+1)/2} f^{-(p-1)/2} \left[G\left(\frac{f}{f_{c2}}\right) - G\left(\frac{f}{f_{c1}}\right) \right],$$

Direct dependency on: Lorentz factor, frequency, transverse B

Intensity and Stokes parameters

(hung on...almost there!)

Assuming an optically thin medium:
(and no depolarization effects)

$$I_f = \int \eta_f ds$$

$$\eta_f^{(1)} + \eta_f^{(2)} = \frac{\sqrt{3}}{16\pi} A \frac{e^3 B \sin \theta}{mc^2} \frac{p + \frac{7}{3}}{p + 1} \Gamma\left(\frac{3p - 1}{12}\right) \Gamma\left(\frac{3p + 7}{12}\right) \left(\frac{3eB \sin \theta}{2\pi mcf}\right)^{\frac{p-1}{2}}$$

$$\eta_f^{(1)} - \eta_f^{(2)} = \frac{p + 1}{p + \frac{7}{3}} (\eta_f^{(1)} + \eta_f^{(2)})$$

$$\begin{pmatrix} I_f \\ Q_f \\ U_f \\ V_f \end{pmatrix} = \frac{K f^{p+1}}{A \cdot B_{\perp}^{\frac{p+1}{2}}} \begin{pmatrix} \frac{p + \frac{7}{3}}{p + 1} \\ \cos 2\chi \\ \sin 2\chi \\ 0 \end{pmatrix}$$

!!Observer's frame!!

This refers to energy per unit length, frequency, time, surface, and solid angle

Summary...

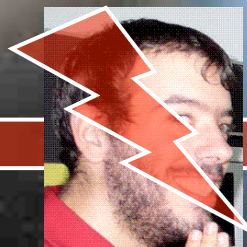
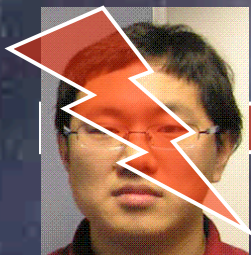
(yeap, it's over*!)

- We calculate Stokes parameters for 1 electron
- Polarization depends on the energy (γ)
- Also on the magnetic field power + structure
- Angle (β , B) is important
- Relativistic effects important
- Generalize for a population of electrons
- Polarization then depends on power law index!

Simple description:

- > constant B field
- > constant energy
- > constant geometry
- > optically thin medium

Road map:



Gamma – Ray Bursts

Ioannis Nestoras

IMPRS Retreat 15/09/2009

**International Max Planck Research School (IMPRS)
for Astronomy and Astrophysics.**

Outlook

Outlook

- What are gamma-ray bursts , (GRBs)??

Outlook

- What are gamma-ray bursts , (GRBs)??

Outlook

- What are gamma-ray bursts , (GRBs)??
- Type of GRBs

Outlook

- What are gamma-ray bursts , (GRBs)??
- Type of GRBs

Outlook

- What are gamma-ray bursts , (GRBs)??
- Type of GRBs
- Theoretical models for GRBs

Outlook

- What are gamma-ray bursts , (GRBs)??
- Type of GRBs
- Theoretical models for GRBs

Outlook

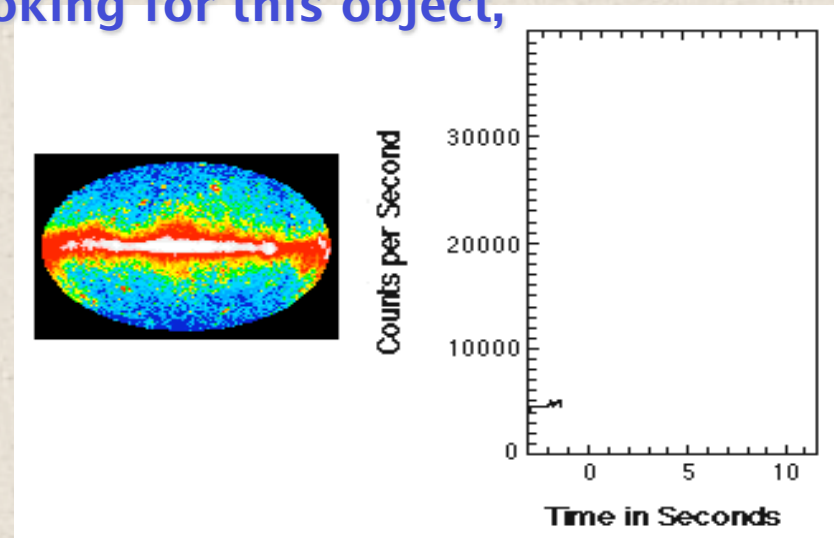
- **What are gamma-ray bursts , (GRBs)??**
- **Type of GRBs**
- **Theoretical models for GRBs**
- **Obsarvational data for GRBs**

So what are they exactly??

IMAGINE if you could see something that :

Emitted as much energy as nearly the entire universe for few seconds,
Allowed you to see billions of years into the past, from your own
backyard,

And, of all the world's great observatories looking for this object,
You saw it first...



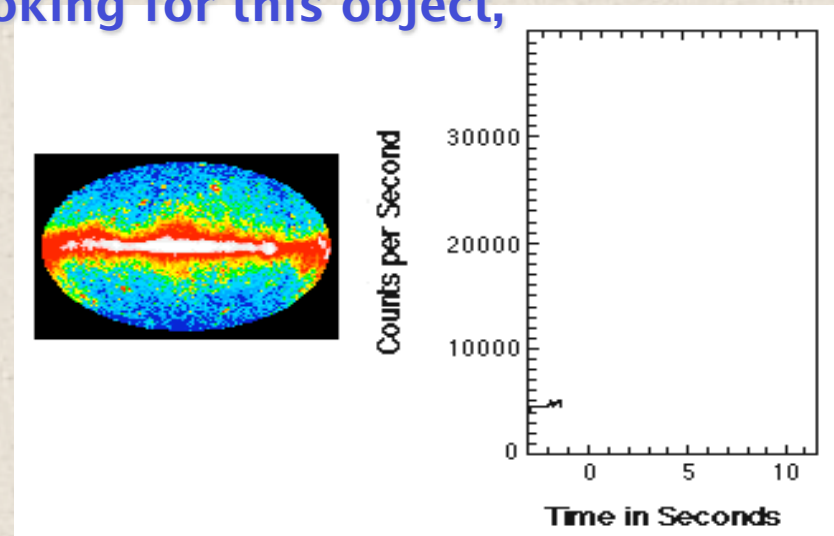
So what are they exactly??

IMAGINE if you could see something that :

Emitted as much energy as nearly the entire universe for few seconds,
Allowed you to see billions of years into the past, from your own
backyard,

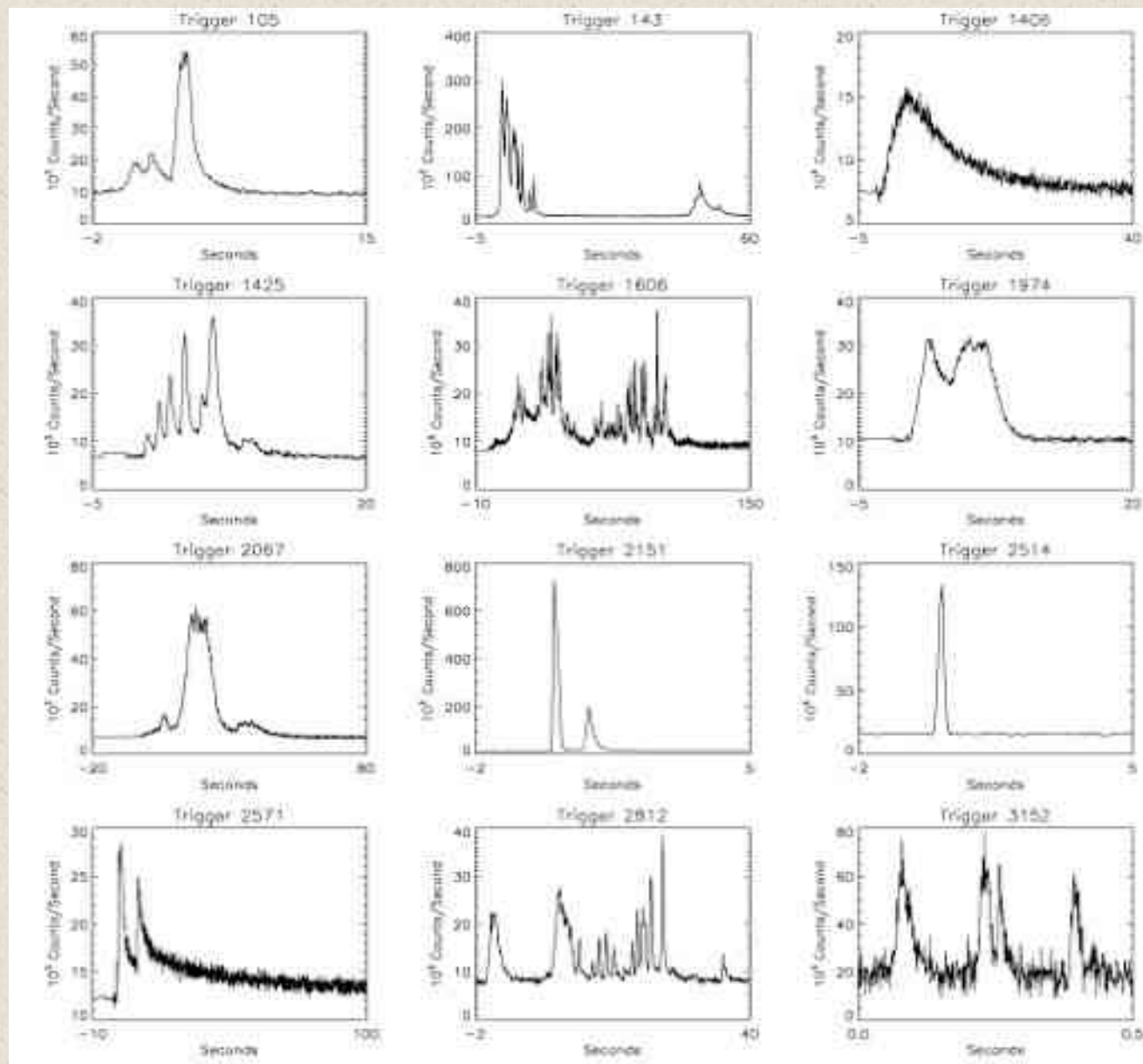
And, of all the world's great observatories looking for this object,
You saw it first...

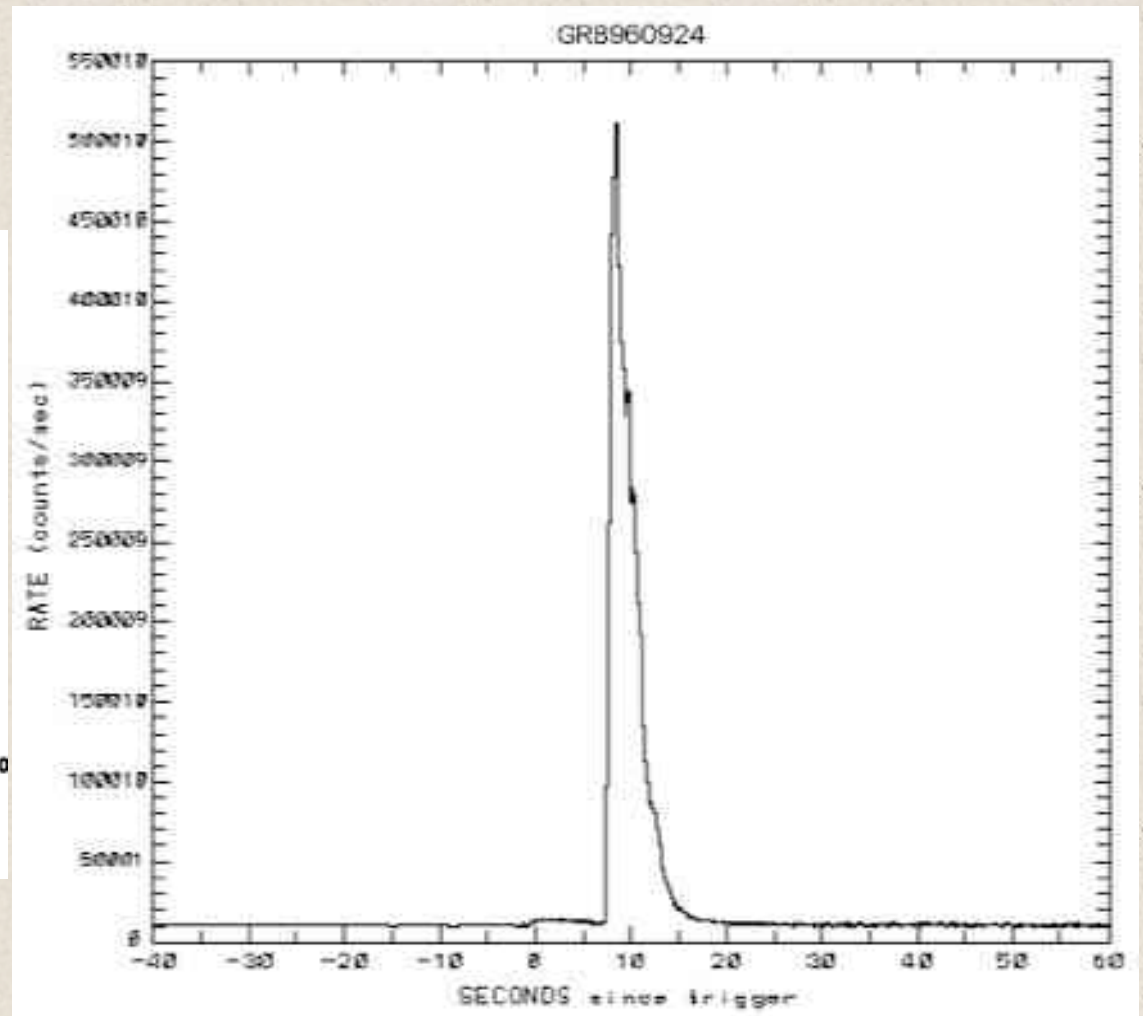
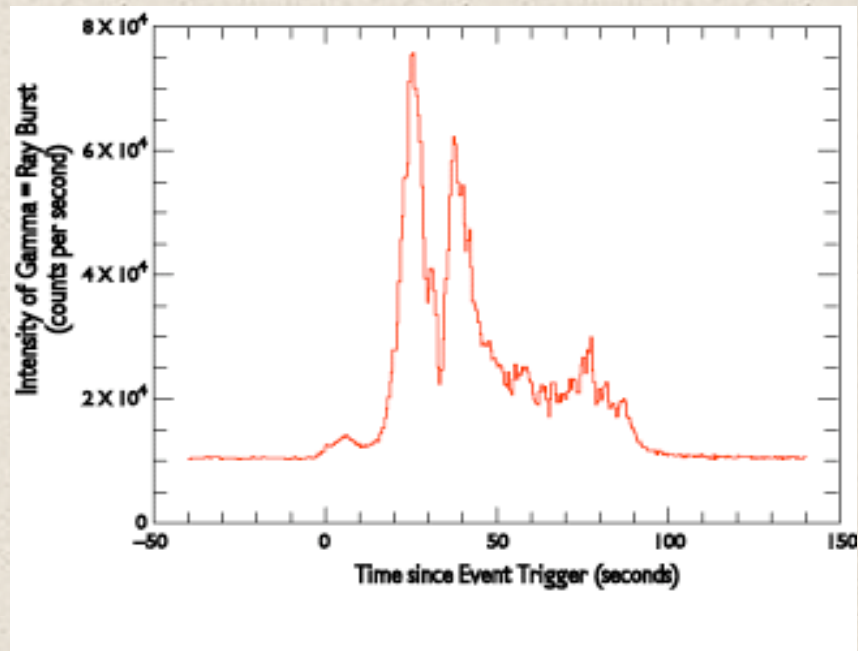
GRBs are objects that produce massive
emission of gamma rays for a period of ~ 0.1
to 100 seconds followed, in some cases, by
optical, radio, and/or x-ray afterglows



So what are they exactly??







GRB Characteristics

GRB Characteristics

- The distribution of GRBs in the sky is isotropical.

GRB Characteristics

- The distribution of GRBs in the sky is isotropical.
- The distances of GRBs are usally $z > 1$.

GRB Characteristics

- The distribution of GRBs in the sky is isotropical.
- The distances of GRBs are usally $z > 1$.
- The frequency of appearance is 1 – 2 per day.

GRB Characteristics

- The distribution of GRBs in the sky is isotropical.
- The distances of GRBs are usally $z > 1$.
- The frequency of appearance is 1 – 2 per day.
- There is no prediction of when and where a GRB will happen.

GRB Characteristics

- The distribution of GRBs in the sky is isotropical.
- The distances of GRBs are usally $z > 1$.
- The frequency of appearance is 1 – 2 per day.
- There is no prediction of when and where a GRB will happen.
- The typical duration of GRBs is $10^{-3} - 10^2$ sec.

GRB Characteristics

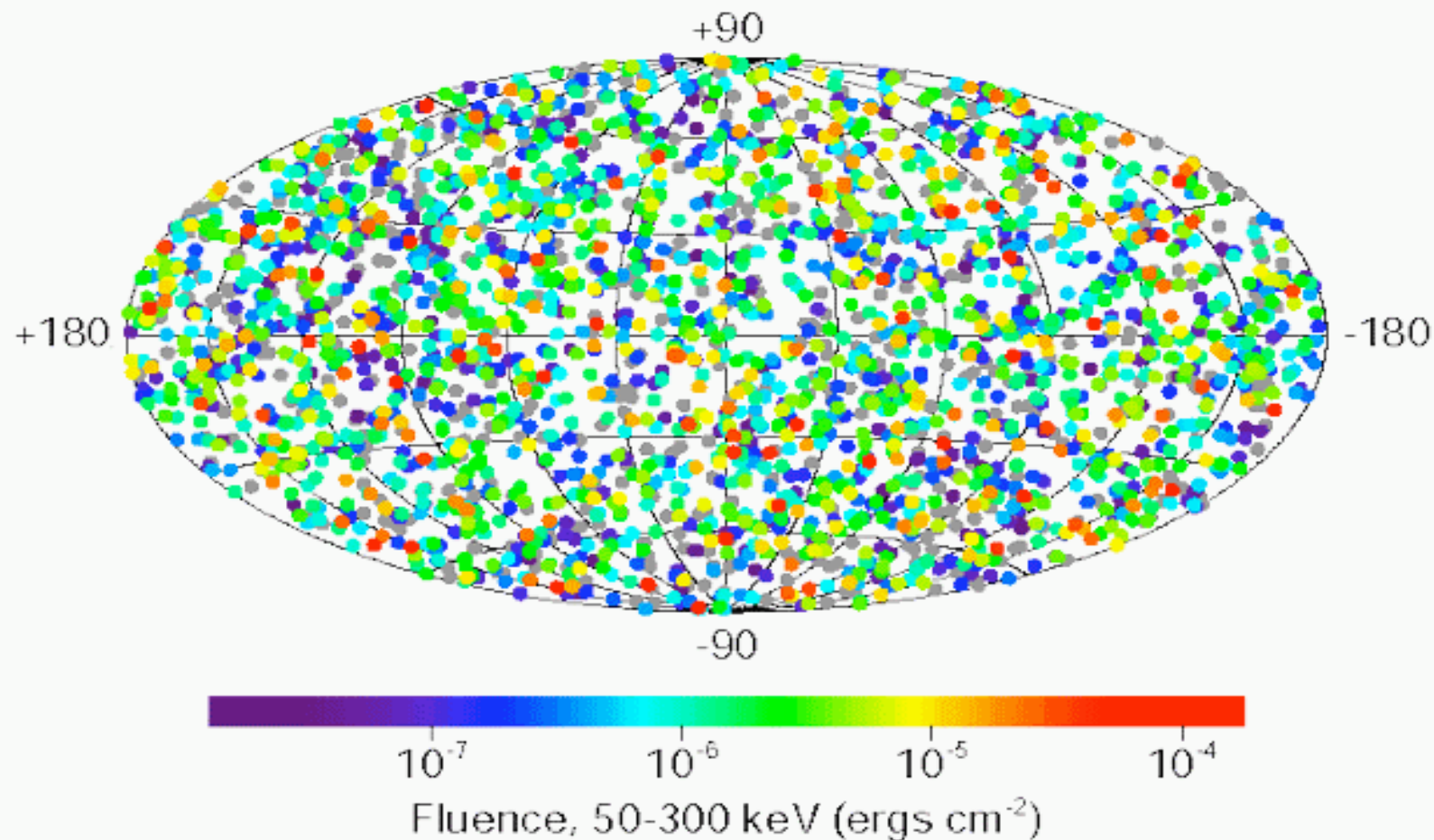
- The distribution of GRBs in the sky is isotropical.
- The distances of GRBs are usally $z > 1$.
- The frequency of appearance is 1 – 2 per day.
- There is no prediction of when and where a GRB will happen.
- The typical duration of GRBs is $10^{-3} - 10^2$ sec.
- The dimension of the central engine is of the order of $10^5 - 10^{10}$ m.

GRB Characteristics

- The distribution of GRBs in the sky is isotropical.
- The distances of GRBs are usally $z > 1$.
- The frequency of appearance is 1 – 2 per day.
- There is no prediction of when and where a GRB will happen.
- The typical duration of GRBs is $10^{-3} - 10^2$ sec.
- The dimension of the central engine is of the order of $10^5 - 10^{10}$ m.
- The power of a GRB is $> 10^{43}$ watts.

Distribution of GRBs

2704 BATSE Gamma-Ray Bursts



The power of GRBs

❖ Power of a single GRB $>10^{40}$ Joule/sec!!!!

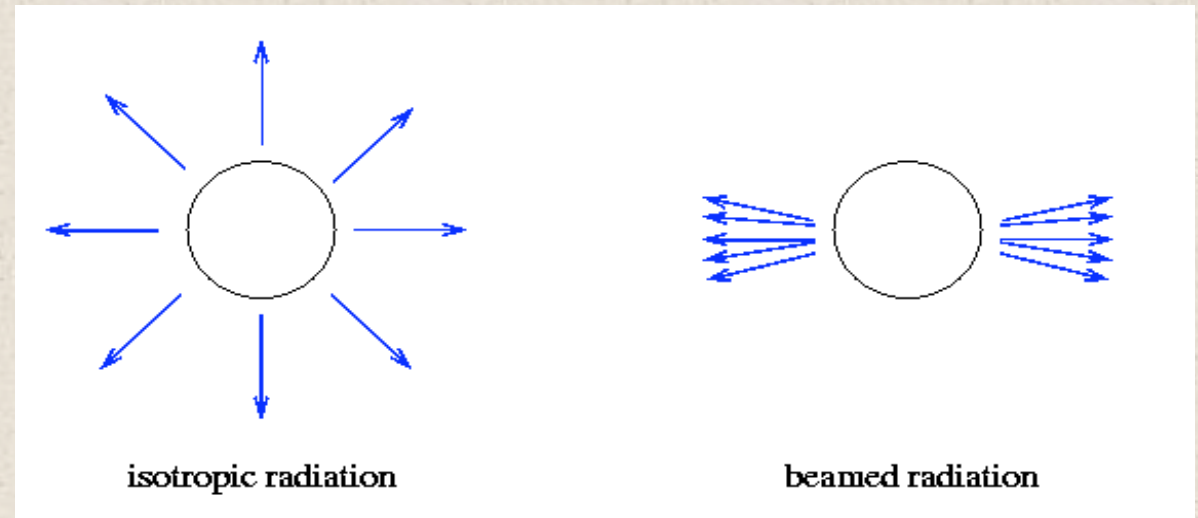
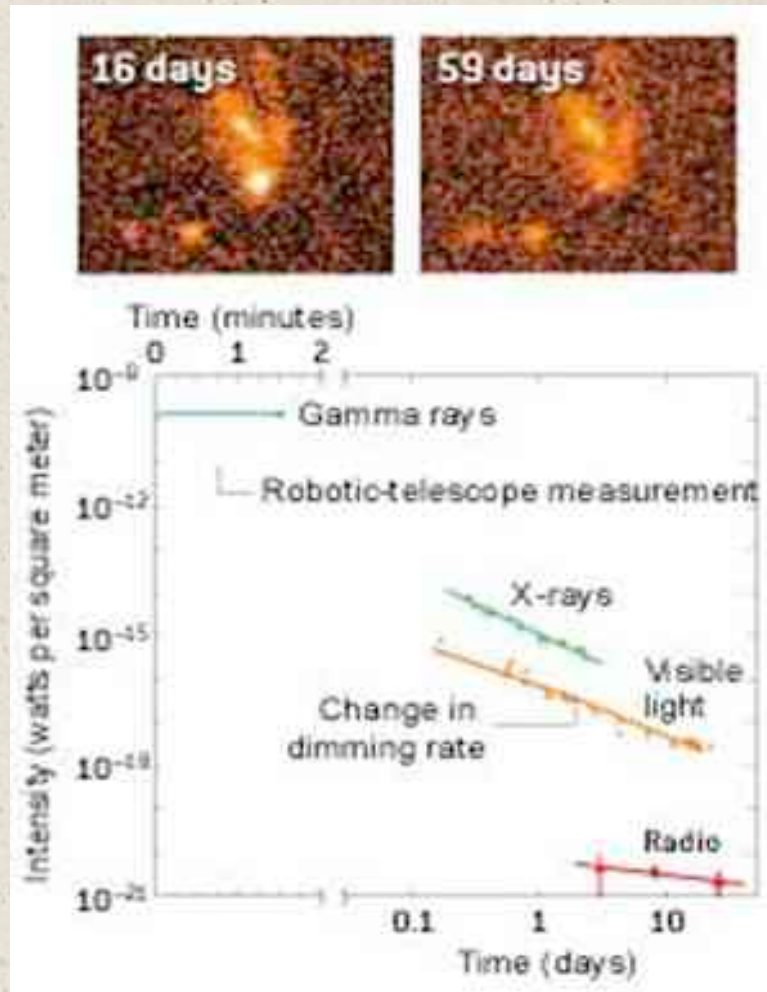
❖ Power of the Sun $L_{\text{H}}=3.8 \cdot 10^{26}$ Joule/sec

❖ Power of a Galaxy $L=10^{36}$ Joule/sec!!!

Beaming Effect

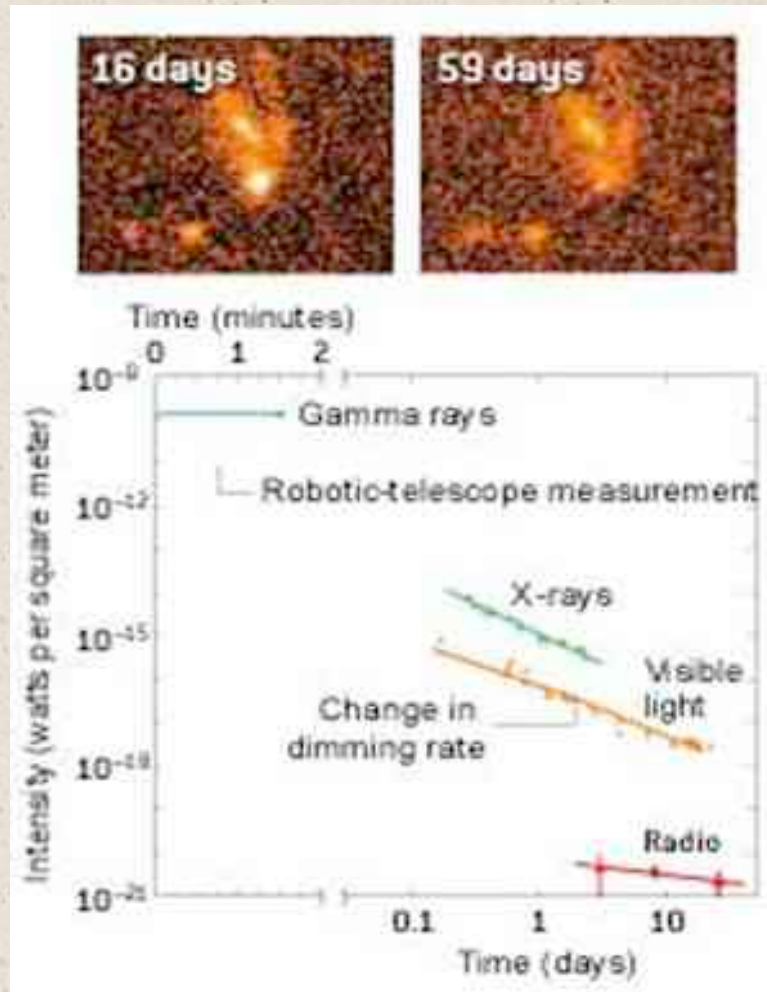
Beaming Effect

GRB990123



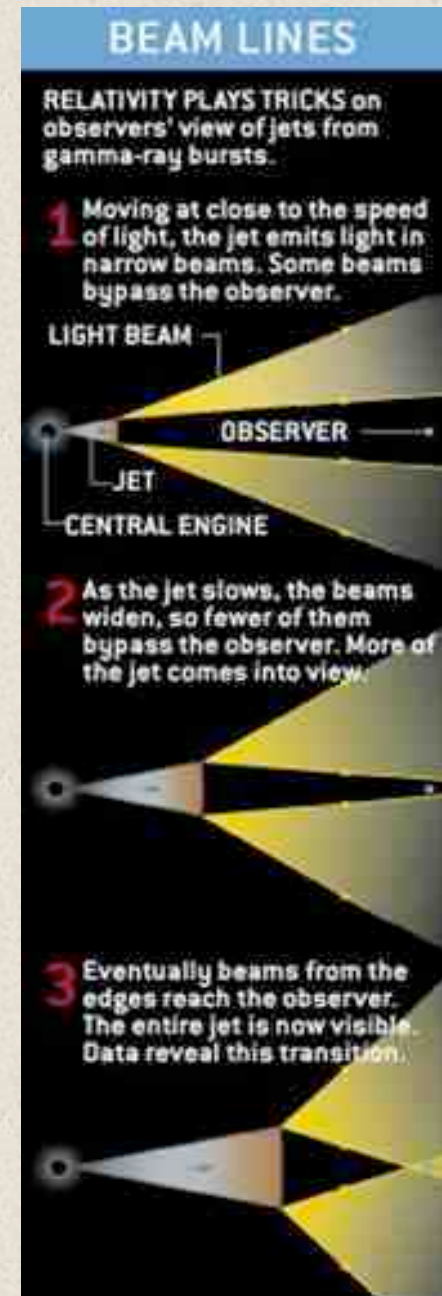
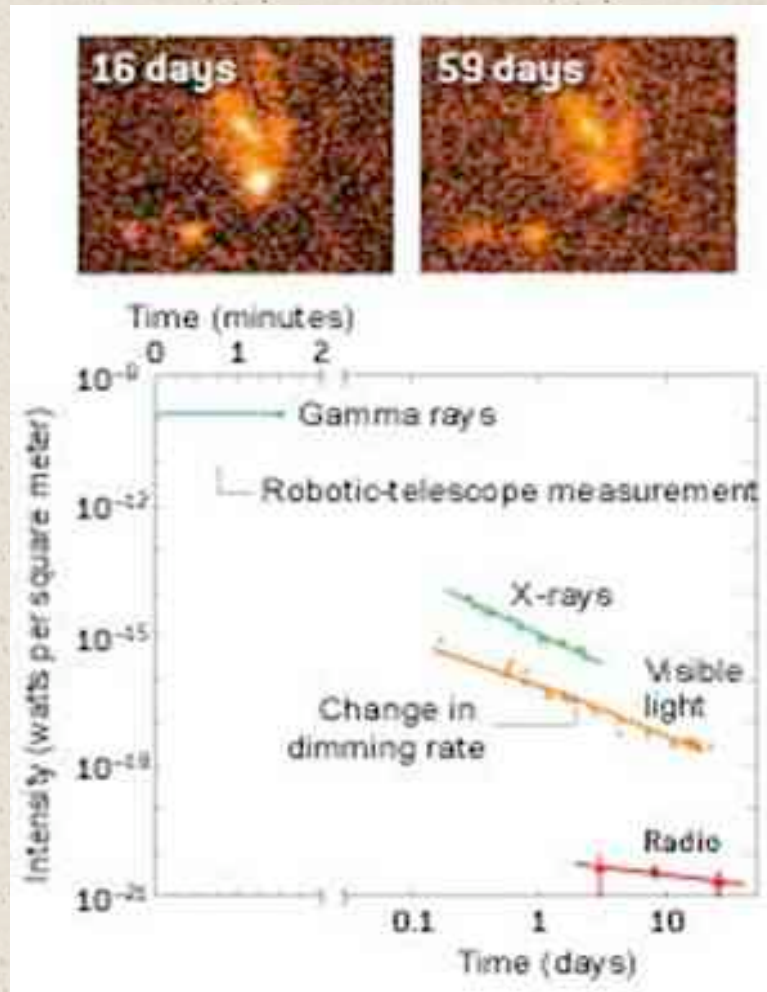
Beaming Effect

GRB990123



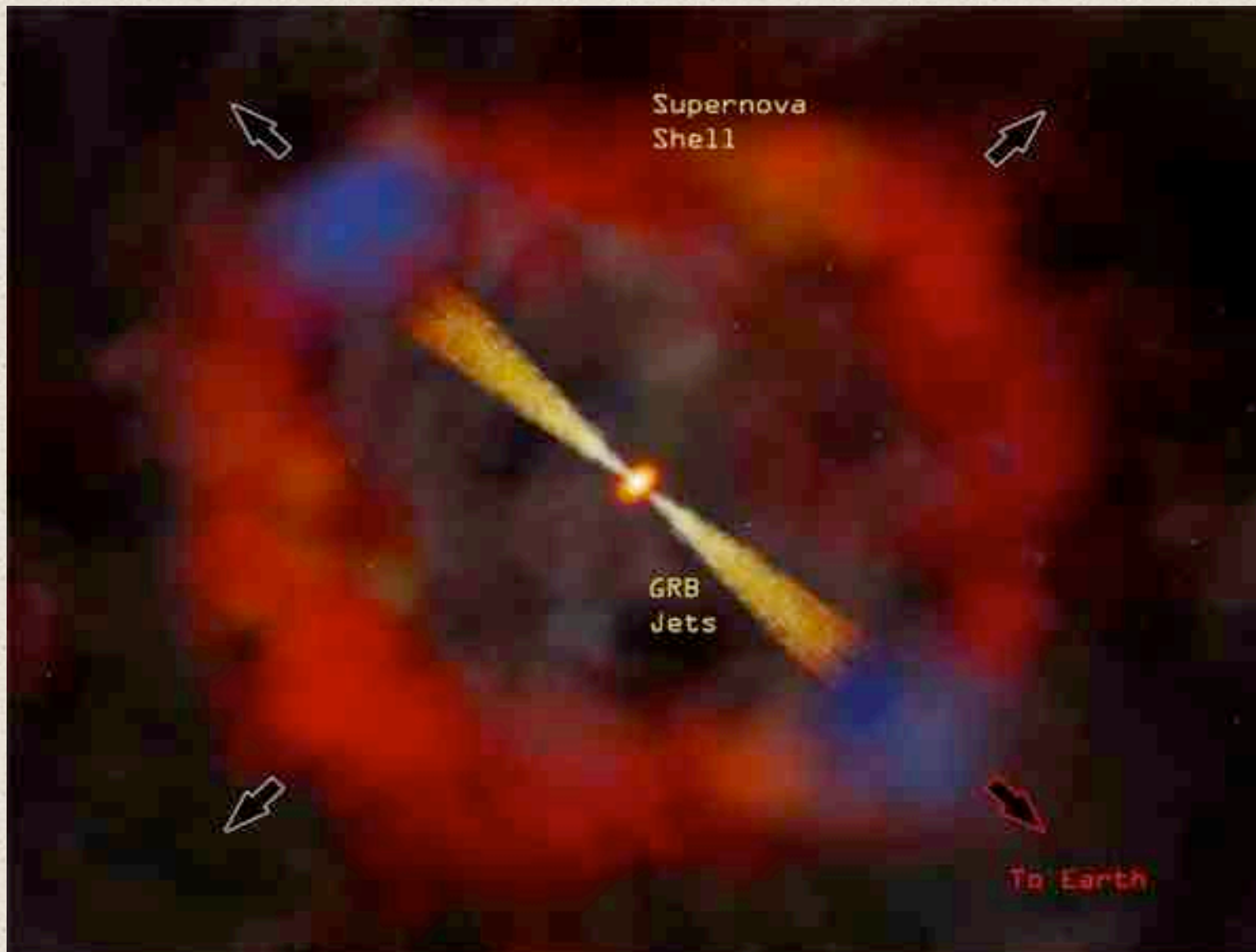
Beaming Effect

GRB990123



Beaming Effect

Beaming Effect



Beaming Effect

Beaming Effect

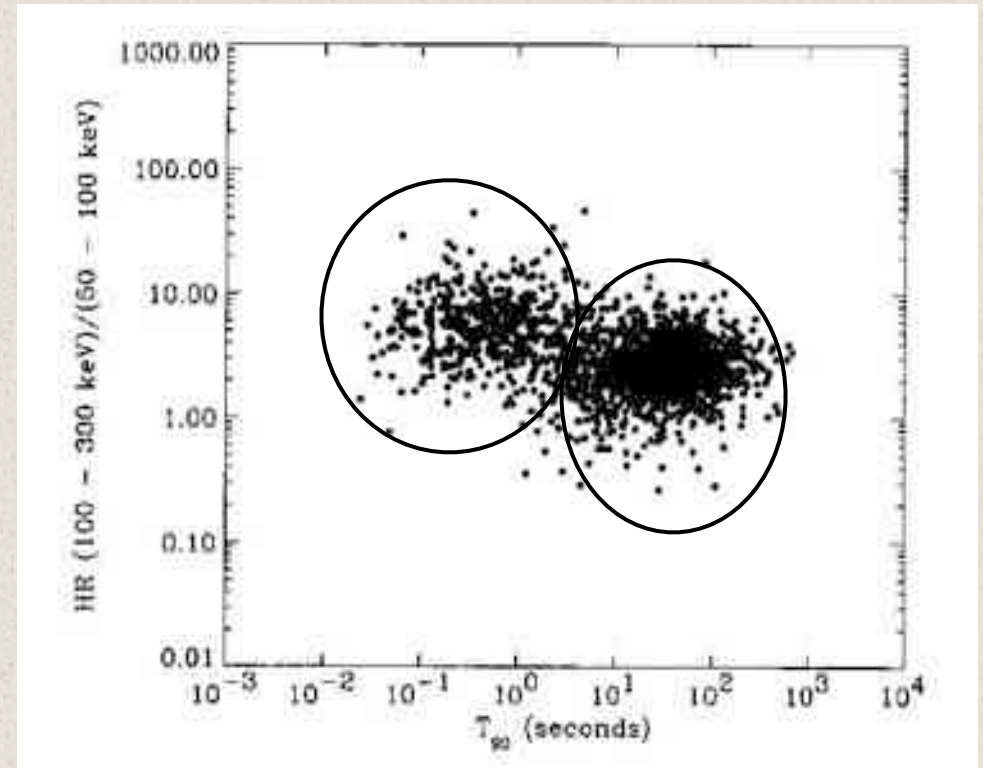


Type of GRBs

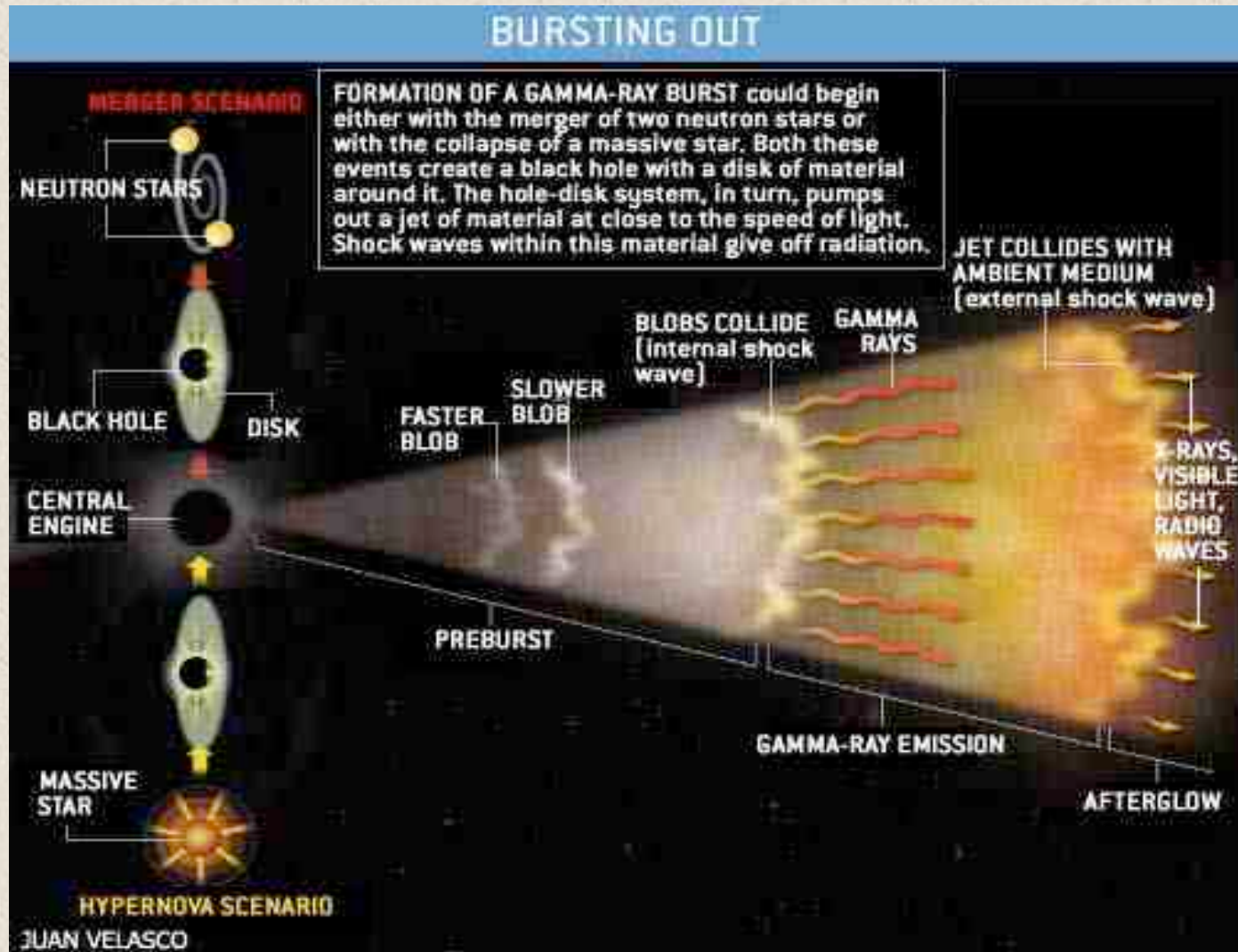
Burst Class (Subclass)	Percentage Of All Bursts	Duration of Initial Emission (sec)	Initial Gamma Ray Emission	X-Ray Emission	Visible Emission	Hypothetical Central Engine
Long (normal)	25	20	✓	✓	✓	Energetic explosion of massive star
Long (ghosts)	30	20	✓	✓	x	Energetic explosion of massive star
Long (x-ray flashes)	25	30	x	✓	x	Energetic explosion of massive star
Short	20	0.3	✓	?	?	Merger of pair of compact objects ?

Theoretical models of GRBs

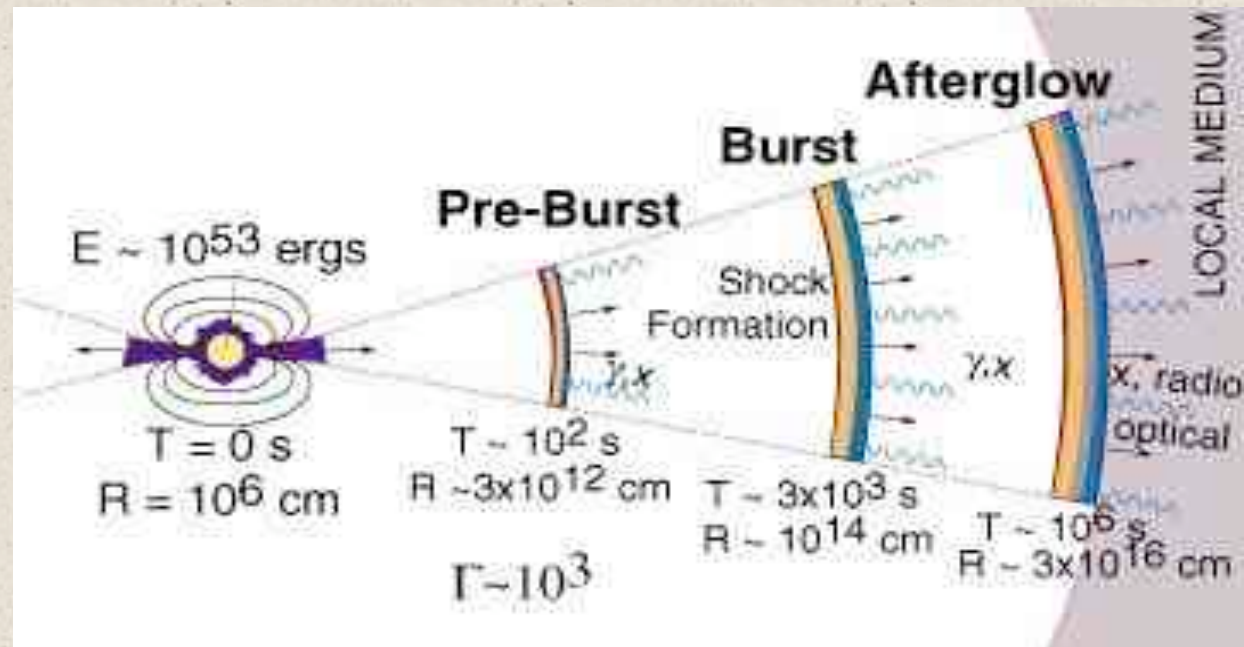
- Plots of “hardness ratio” versus burst duration showed a dumbbell-like distribution.
- Infers there may be two different types of GRB “engines”, thus multiple theories of GRB formation may be correct.



Theoretical models of GRBs



Theoretical models of GRBs



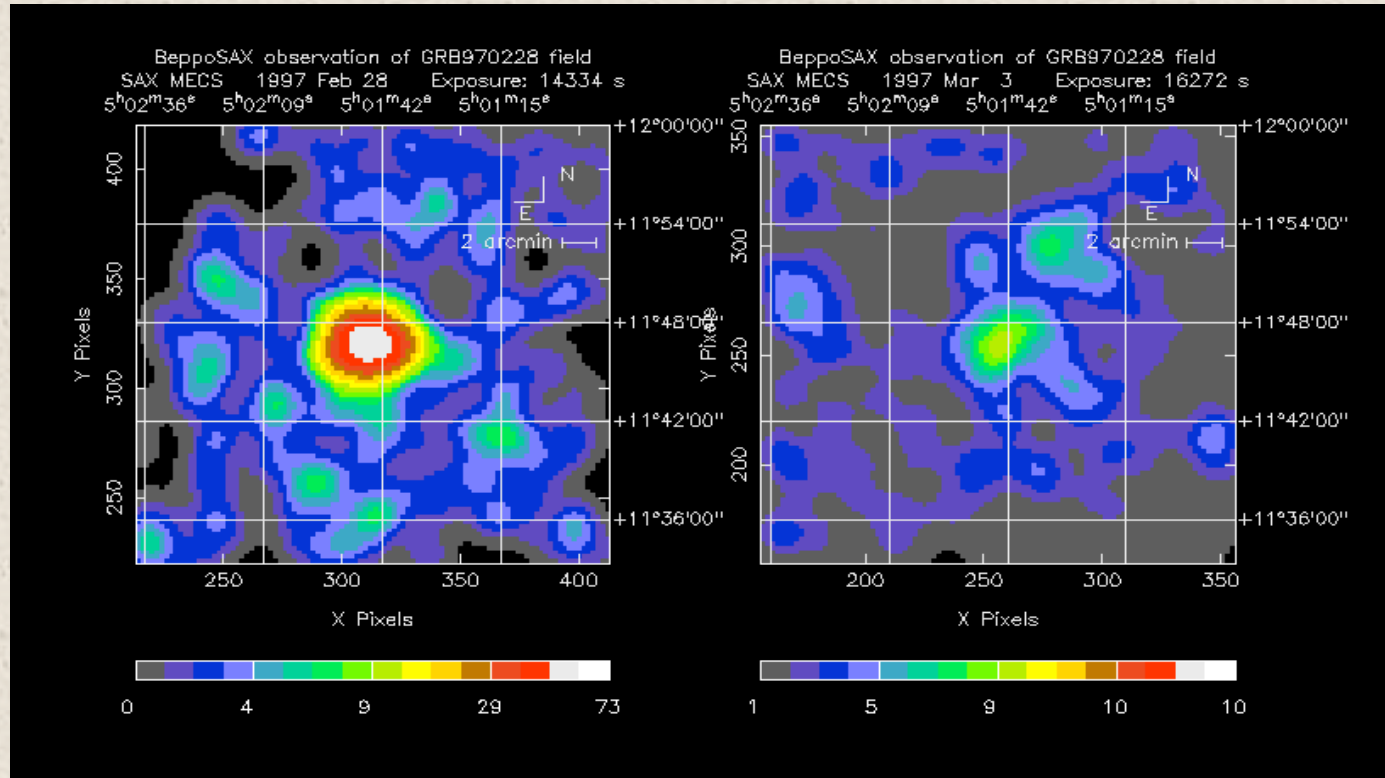
Theoretical models of GRBs



Observational data for GRBs

Observational data for GRBs

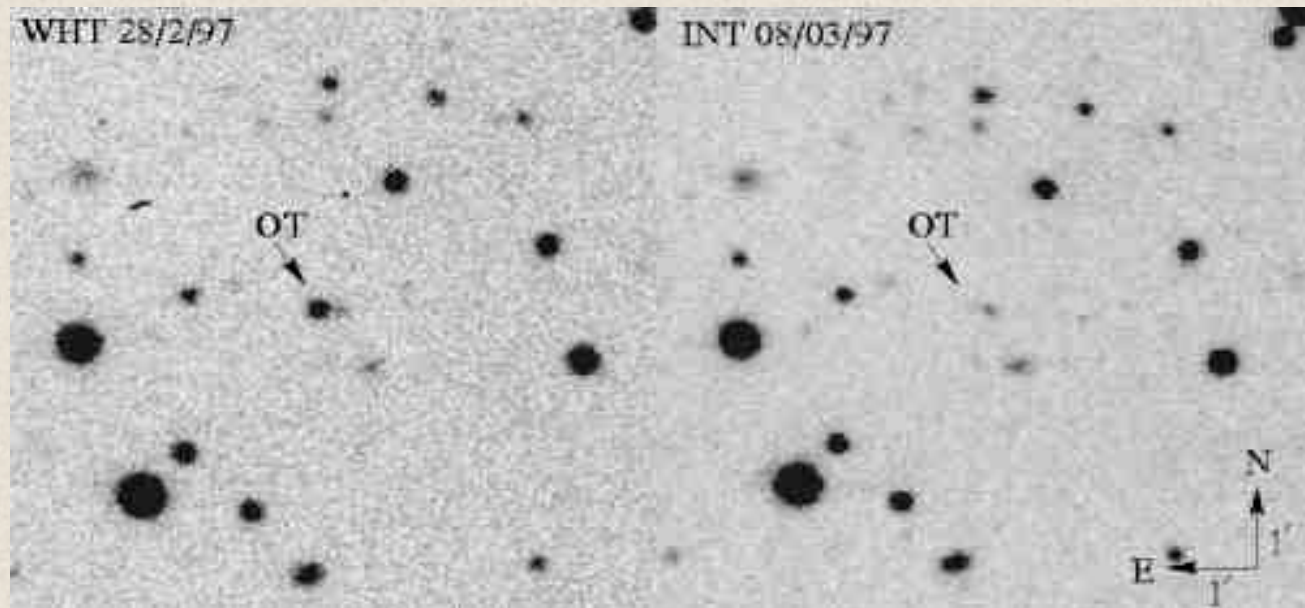
GRB970228



The first observation of an afterglow σ x-rays

Observational data for GRBs

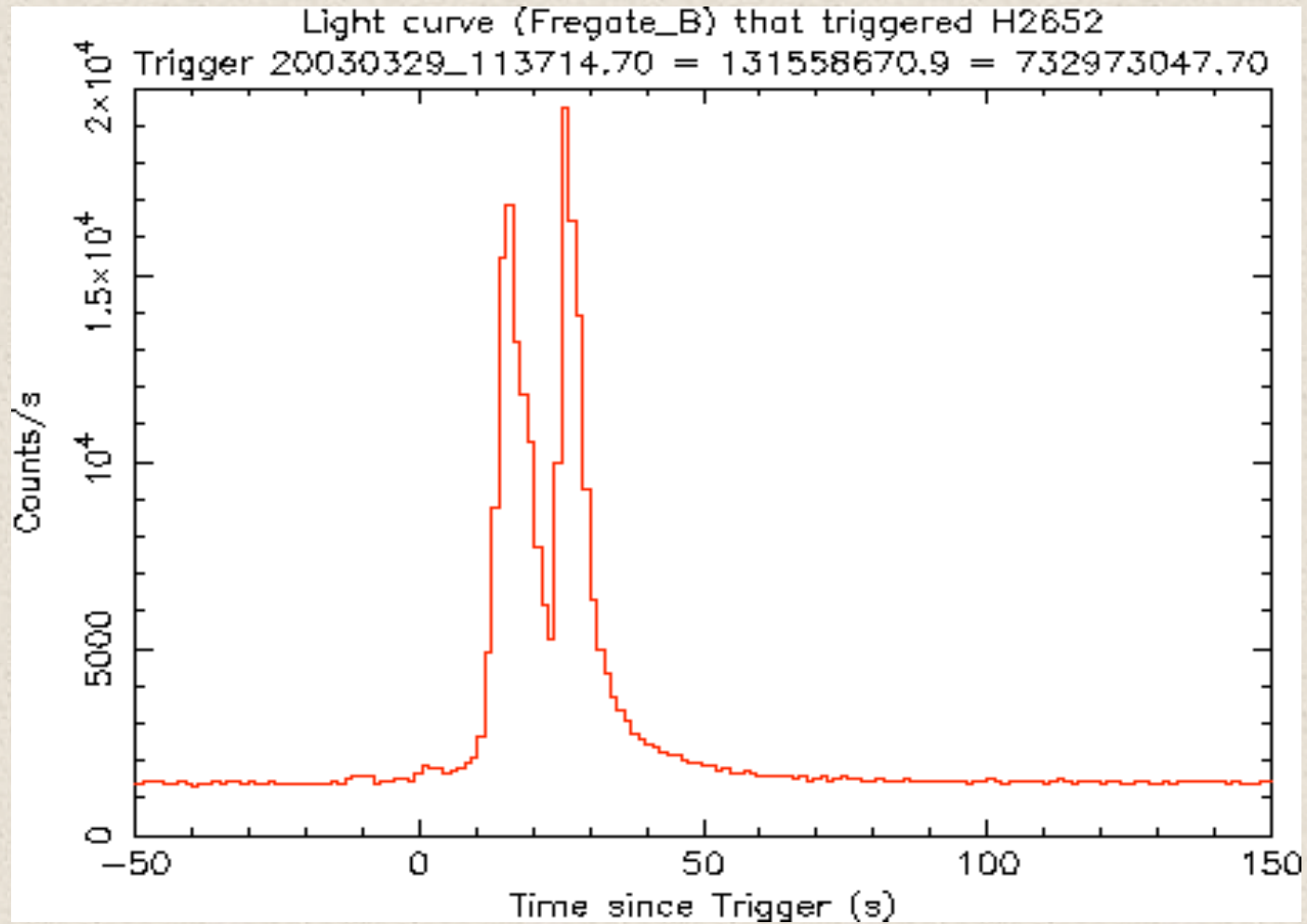
Observational data for GRBs



And in Optical...

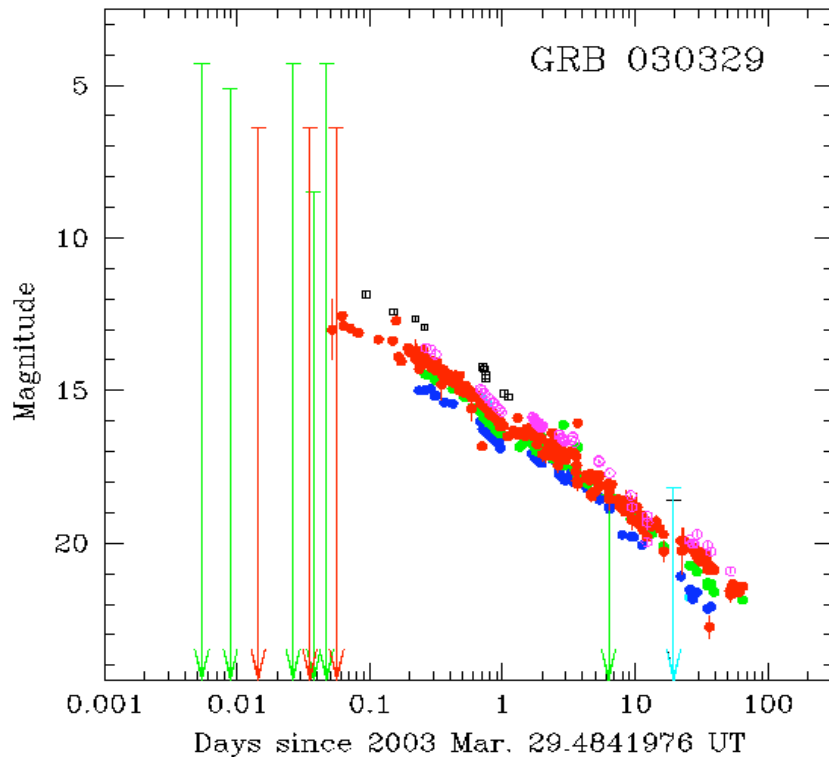
Observational data for GRBs

GRB030329



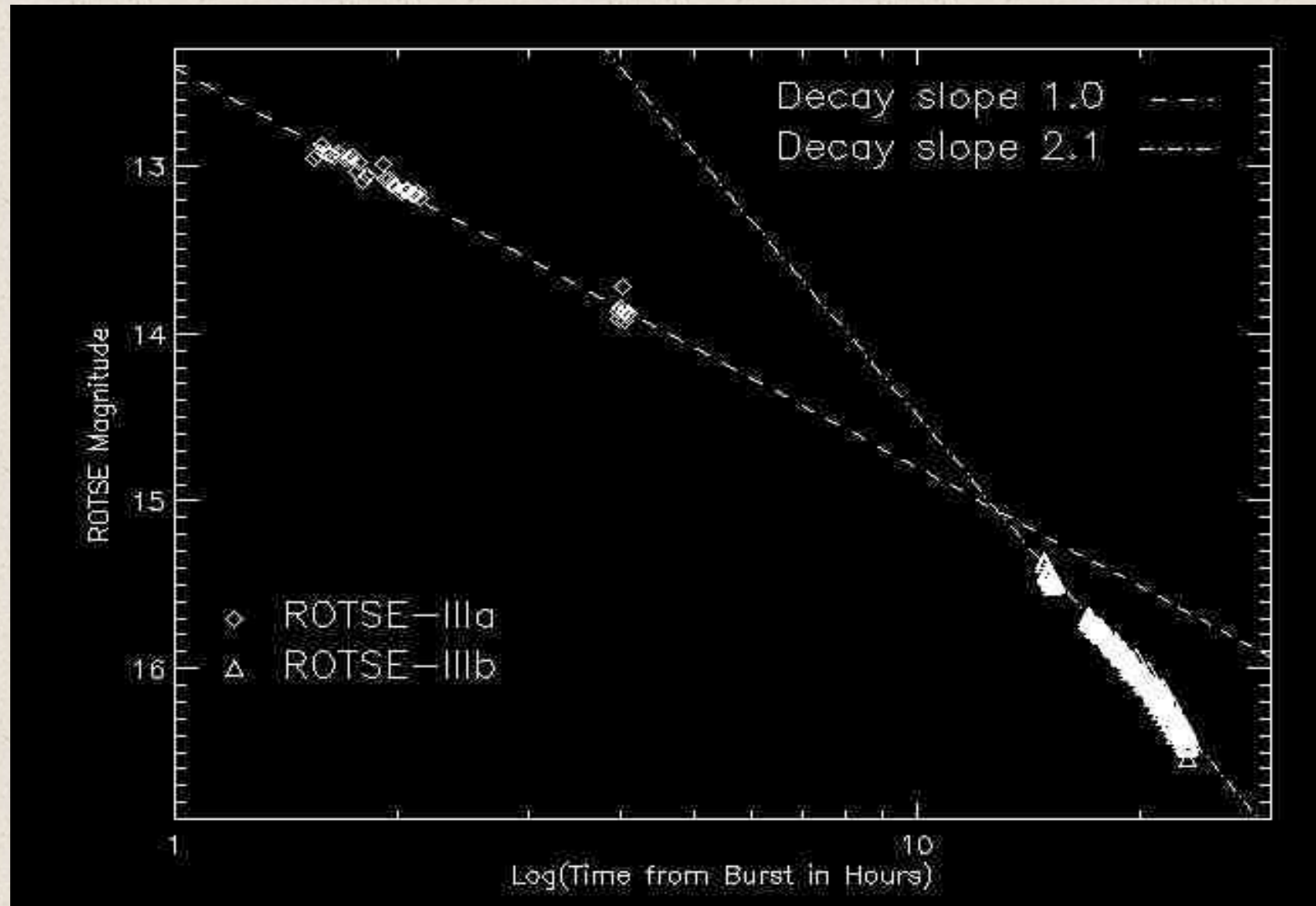
Observational data for GRBs

Observational data for GRBs



Observational data for GRBs

Observational data for GRBs

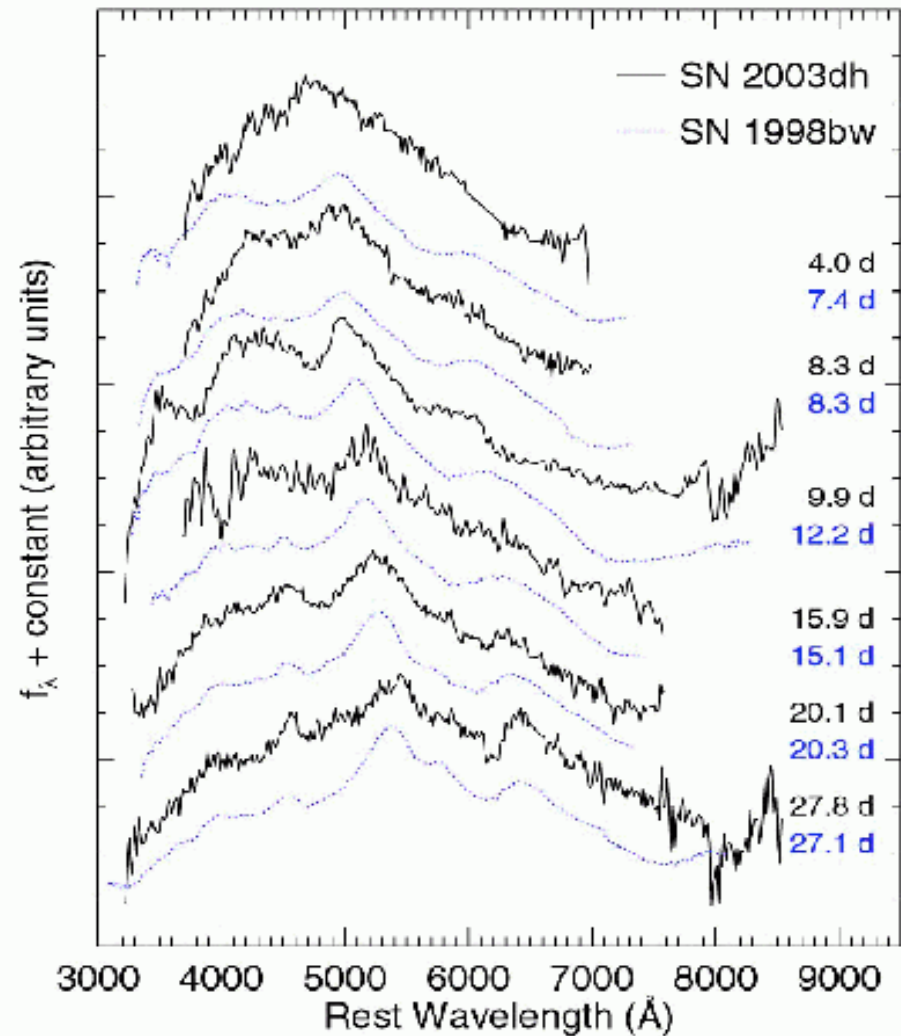


Observational data for GRBs

Connection of GRB980425
– SN 1998bw

and

Connection of GRB030329
– SN 2003dh



Radio (polarization) surveys of the Galaxy/Galactic plane

Xuyang Gao

IMPRS retreat 2009, Braunsfels 09-16-09

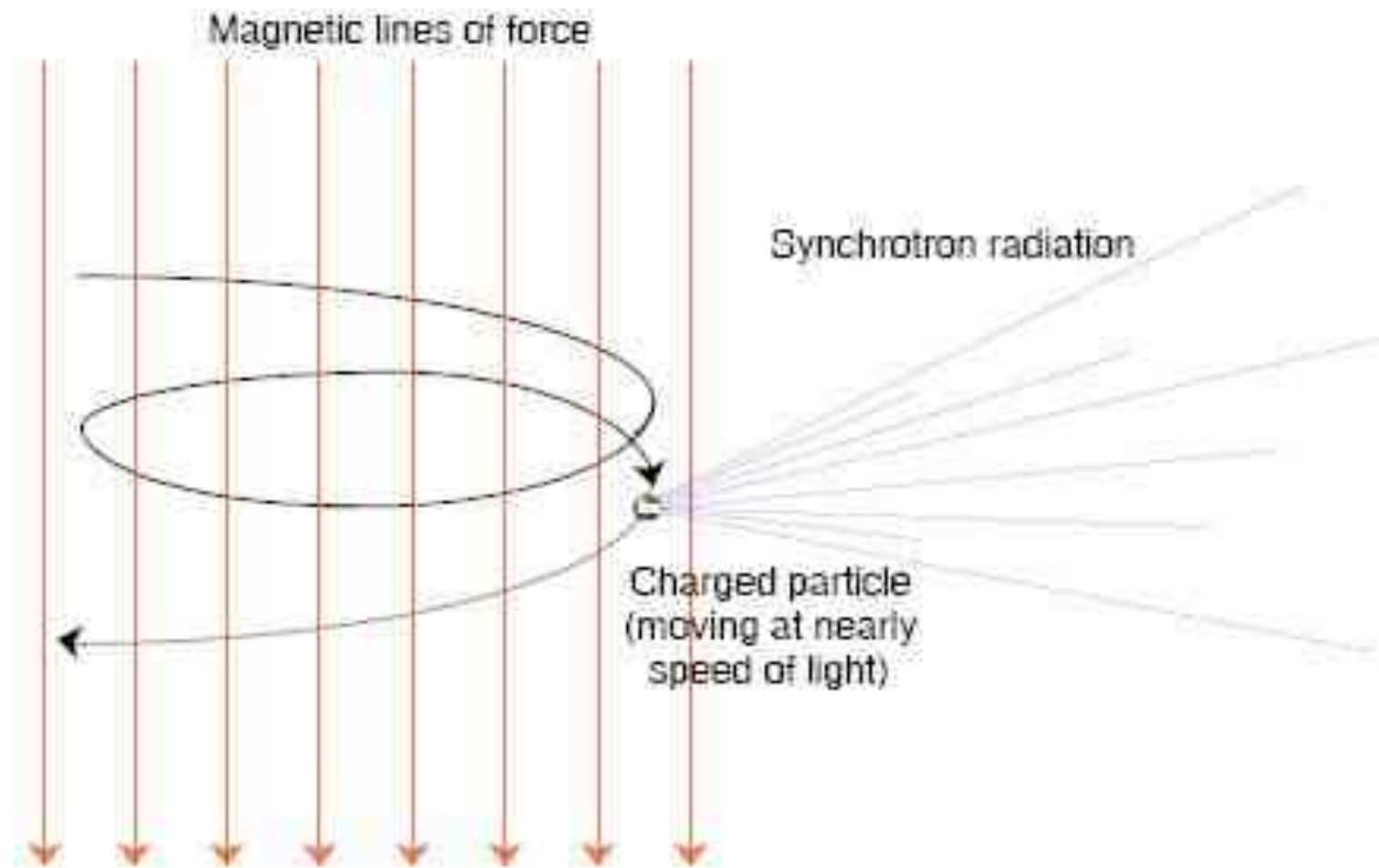
Why we do surveys of the Milky Way??

- Radio properties of SNRs, HII regions, FSs, ISM etc
- Foreground of CMB polarization
- Magnetic field in the Galaxy

Why we do surveys of the Milky Way??

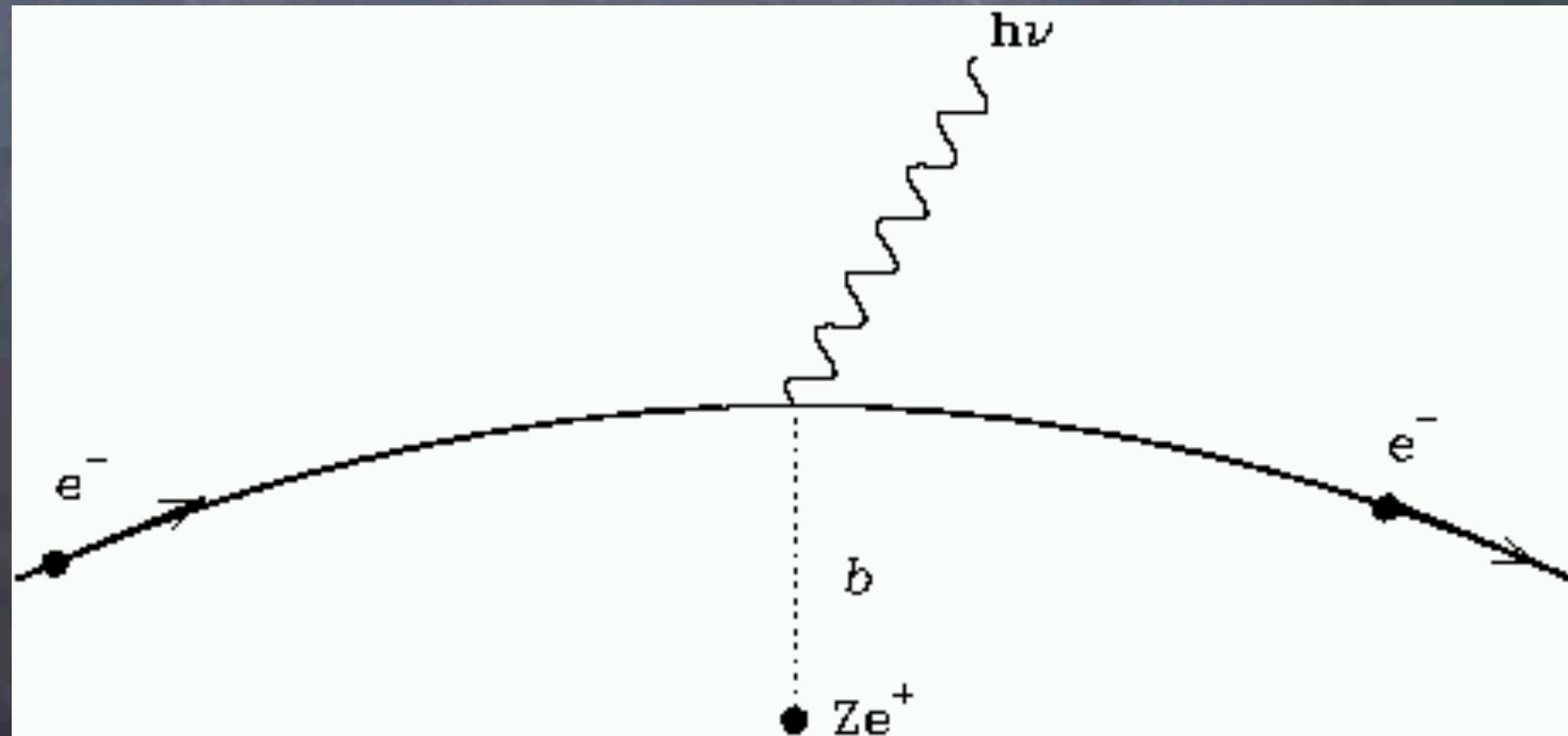
- Radio properties of SNRs, HII regions, FSs, ISM etc
- Foreground of CMB polarization
- Magnetic field in the Galaxy

Emission of Synchrotron Radiation



←
shell type SNRs

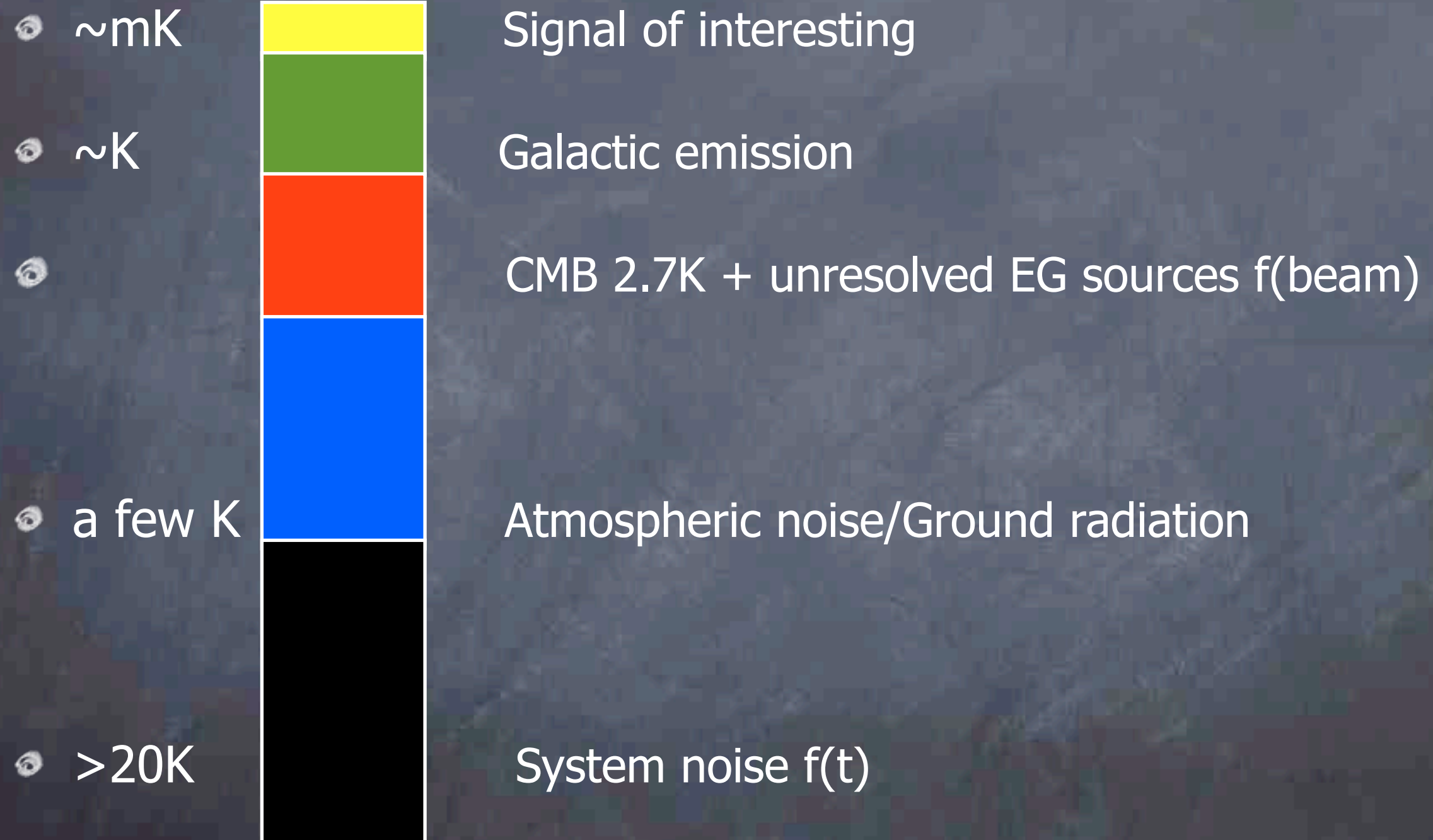
HII regions →



Why we do surveys of the Milky Way??

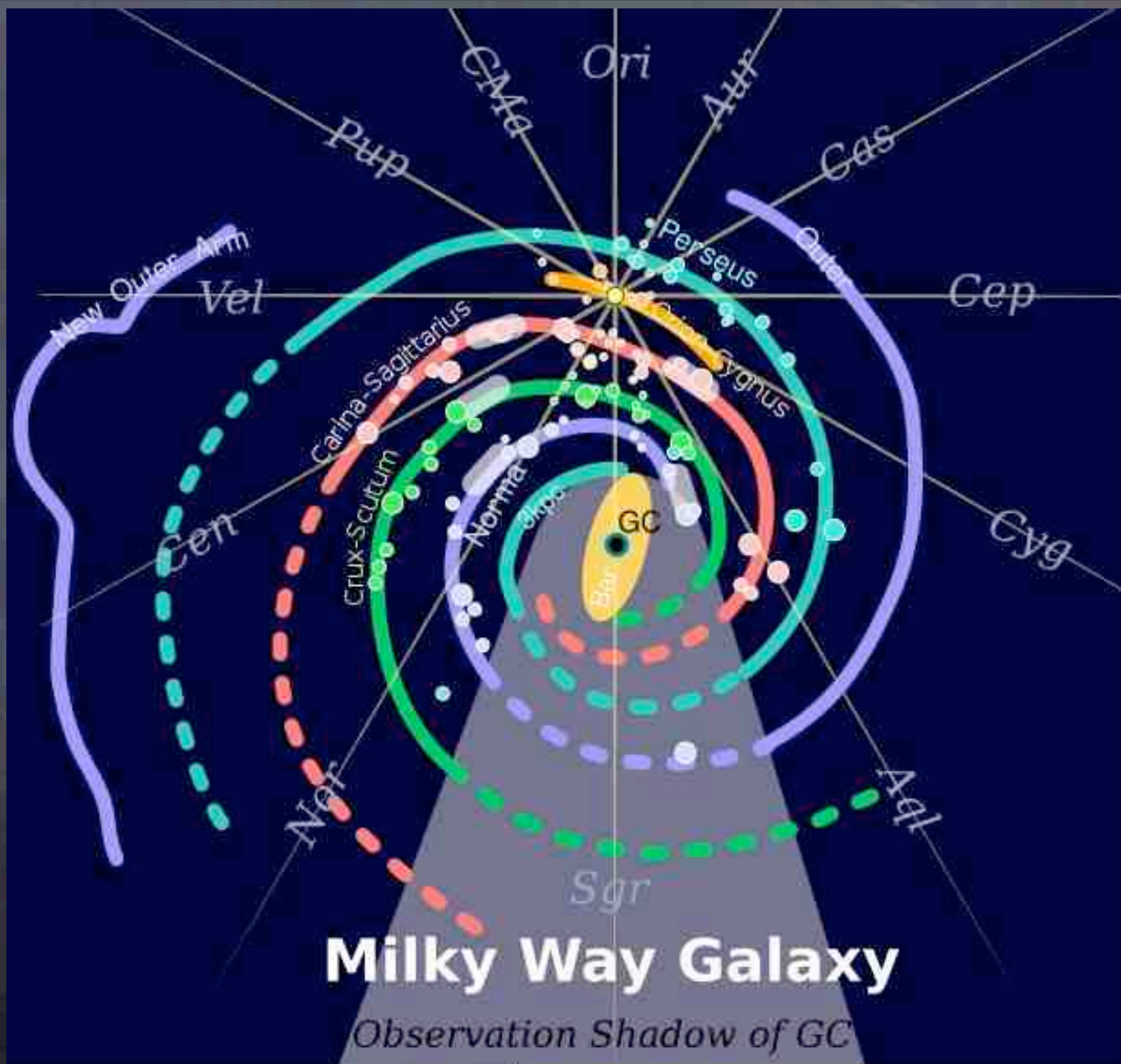
- Radio properties of SNRs, HII regions, FSs, ISM etc
- Foreground of CMB polarization
- Magnetic field in the Galaxy

Centimeter wavelengths :



Why we do surveys of the Milky Way??

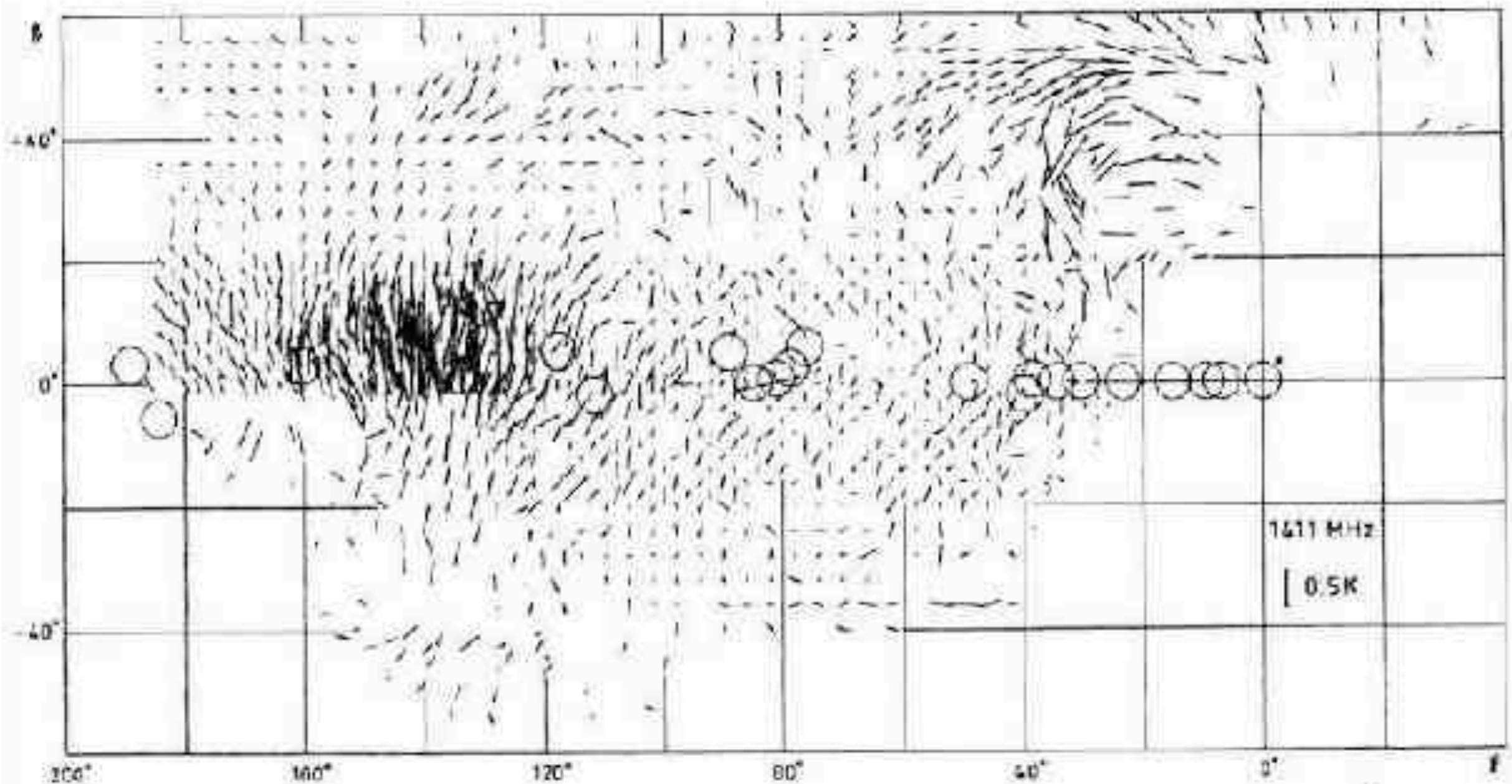
- Radio properties of SNRs, HII regions, FSs, ISM etc
- Foreground of CMB polarization
- Magnetic field in the Galaxy



History of polarization survey

- Cambridge 7.5-m dish 408MHz (Wielebinski et al. 1964)
- Leiden Dwingeloo 25-m telescope 408MHz (Berkhuijsen et al. 1963)
- Parks 64-m telescope 30MHz (Mathewson et al. 1965)
- Dwingeloo 610MHz
- 408MHz and 620MHz in southern sky

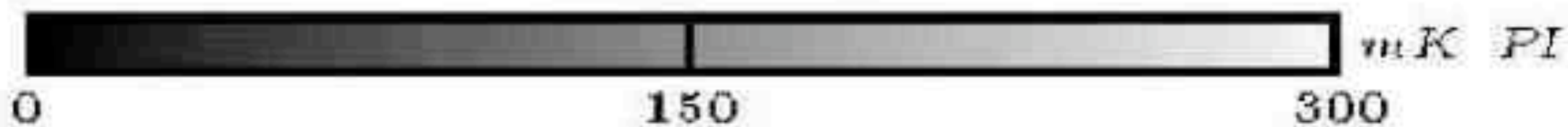
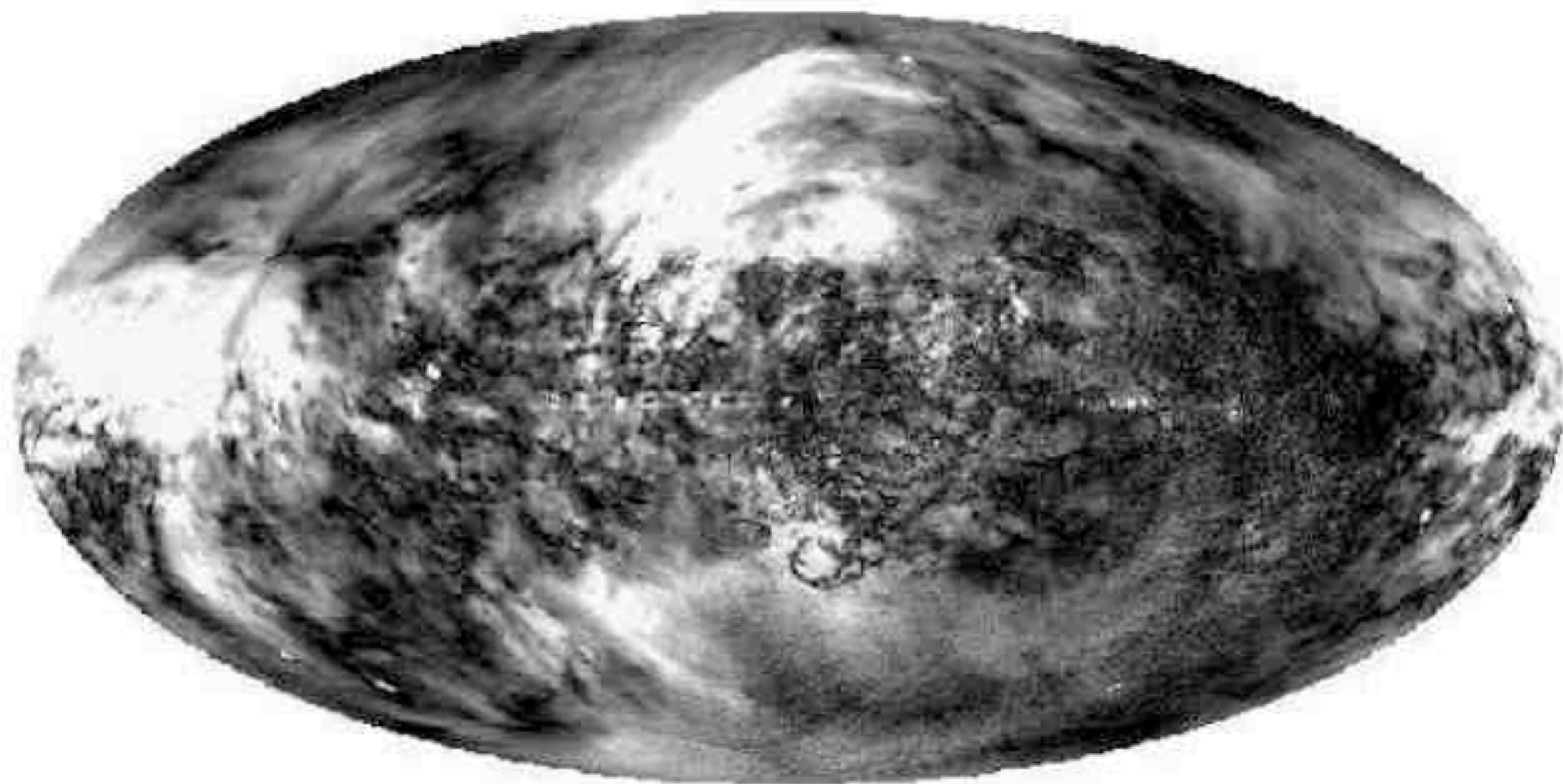
Leiden-Dwingeloo 1.411GHz polarization survey



Nowadays.....

- Effelsberg 1.4GHz, 2.7GHz survey
- CGPS/SGPS 1.4GHz survey
- EMLS 1.4GHz survey
- Parks 2.4GHz survey
- Sino-German 4.8GHz survey
- Nobeyama 10GHz survey
- WMAP
-

1.4 GHz Polarized Intensity



Property of synchrotron emission

• Intensity:
$$I_\nu \sim N_e B_\perp^{\frac{\gamma+1}{2}} \nu^{\frac{-(\gamma-1)}{2}}$$

• Polarization percentage:
$$p = \frac{\gamma + 1}{\gamma + \frac{7}{3}}$$

Faraday Rotation

$$RM(\text{rad m}^{-2}) = 0.81 \int_L n_e(\text{cm}^{-3}) B_{\parallel}(\mu\text{G}) dL(\text{pc})$$

$$\psi = \psi_0 + RM \lambda^2$$

Depolarization

$$U = U_1 + U_2 = E^2 (\cos(2\beta_1) \sin(2\chi_1) + \cos(2\beta_2) \sin(2\chi_2))$$

$$Q = Q_1 + Q_2 = E^2 (\cos(2\beta_1) \cos(2\chi_1) + \cos(2\beta_2) \cos(2\chi_2))$$

- Depth depolarization
- Bandwidth depolarization
- Beam depolarization

About our own survey

Longitude: 87d 10' 40.44"E
Latitude: 43d 28' 16.14"N
Altitude: 2029 m

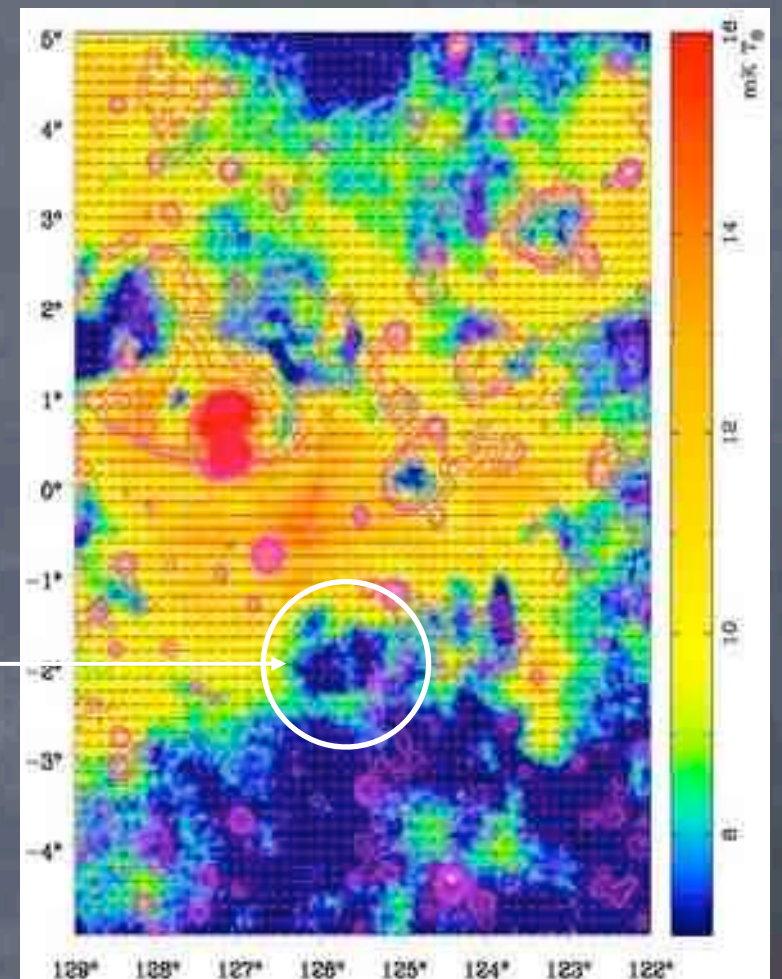
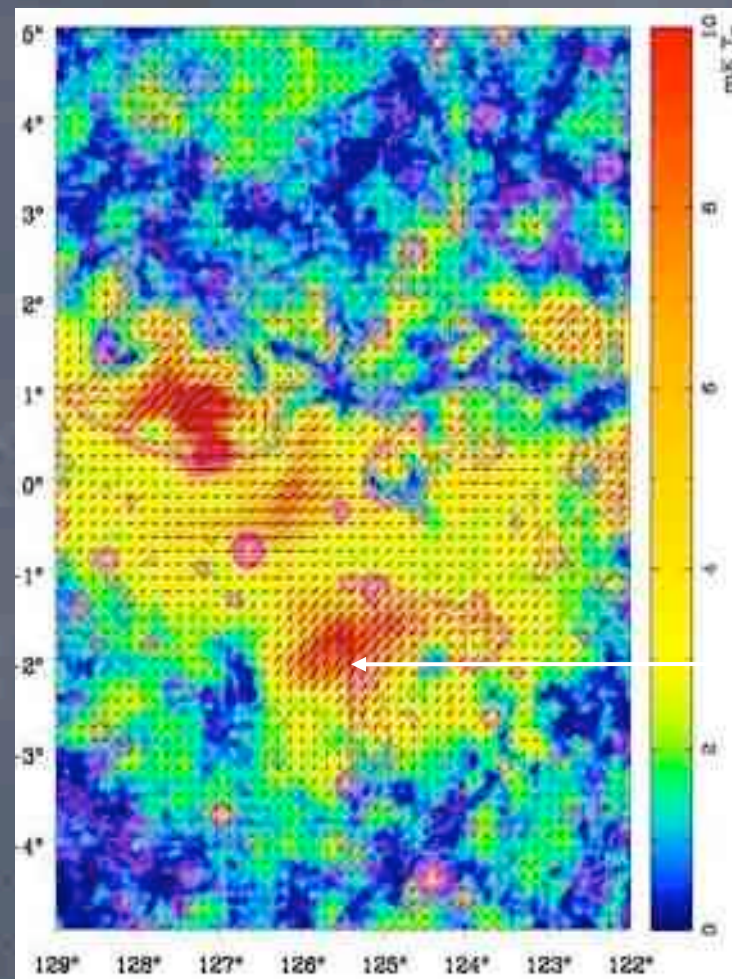
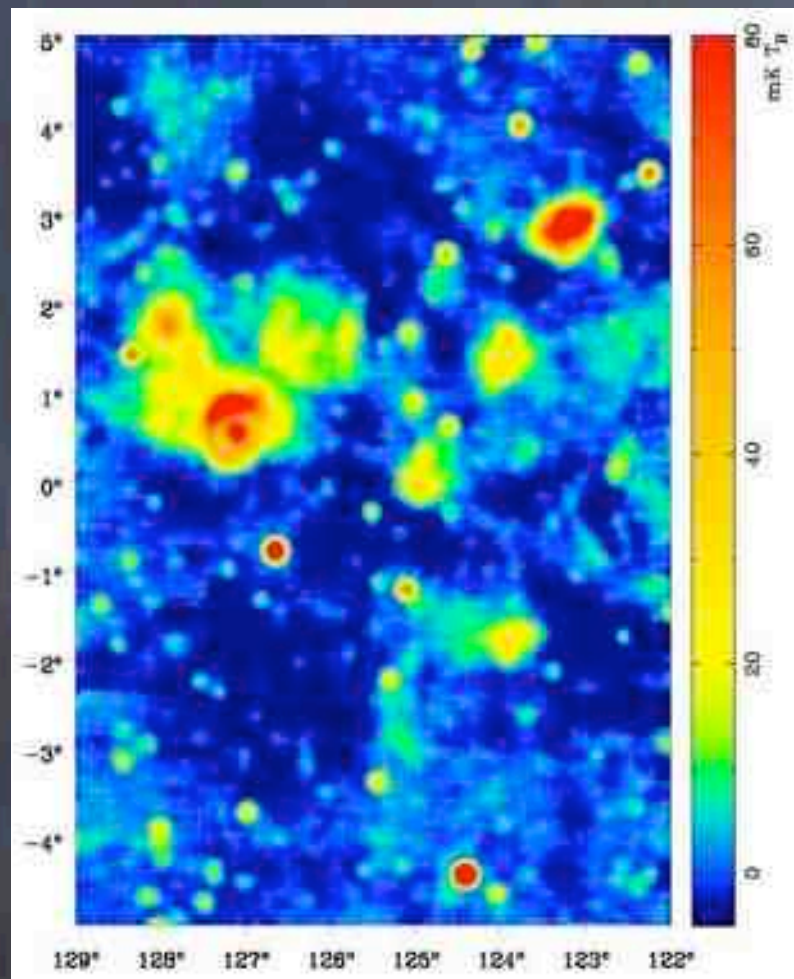
- Urumqi 25m telescope, located in Nanshan, Urumqi, China
- Survey started in Sept 2004
- 5GHz receiver constructed at MPIfR, almost the same as mounted in Effelsberg
- -5 to 5 deg in Galactic latitude, 10 to 230 deg in Galactic longitude
- Broad-band mode(600 MHz) and Narrow-band mode(295MHz)

Parameters of survey

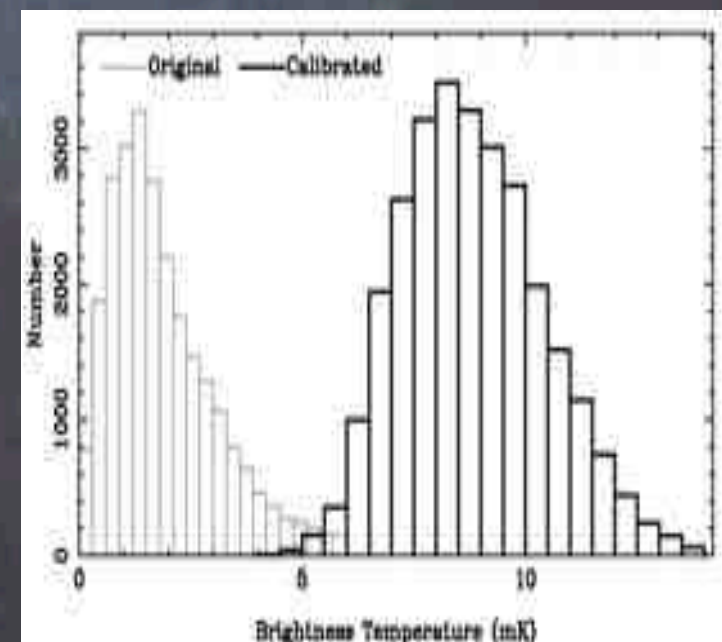
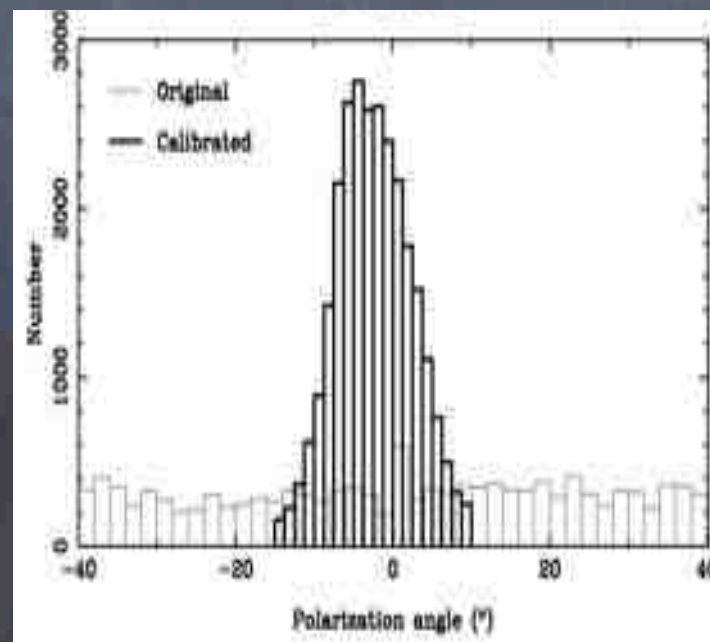
System Temperature	22 K T_a
Telescope Beamwidth	9.5'
Subscan Separation	3'
Scan Velocity	4'/s
Scan Direction	GL and GB
Theoretical rms-noise for total intensity (1s)	1.4 mK T_b
Theoretical rms-noise for Q/U (1s)	1.0 mK T_b
Central Frequency	4800/4963MHz
Bandwidth	600/295MHz
Aperture Efficiency	62
Beam Efficiency	67
$T_b[K]/S[Jy]$	0.164
Calibrator(Polarized/Non-polarized)	3C286/3C295

Sun et al. 2007

The first survey region

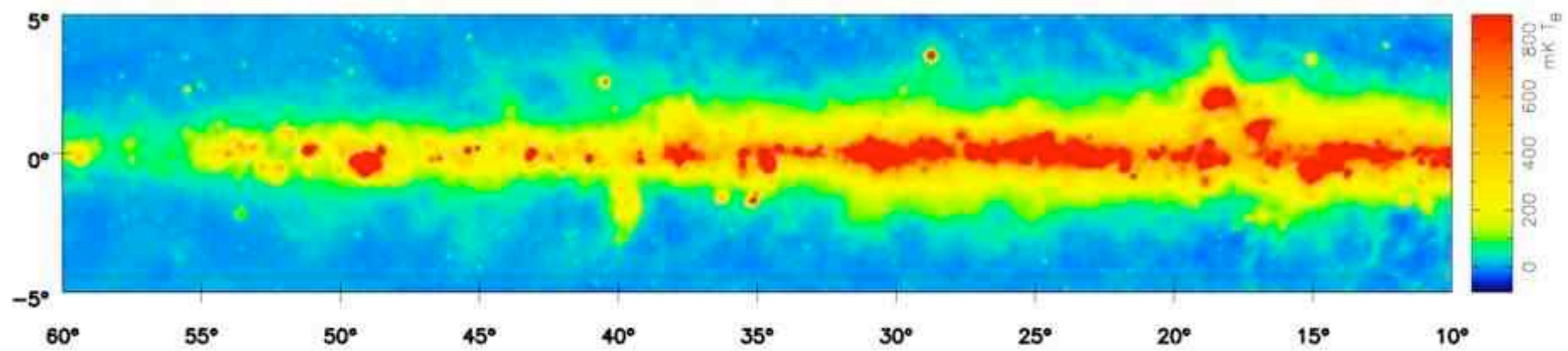


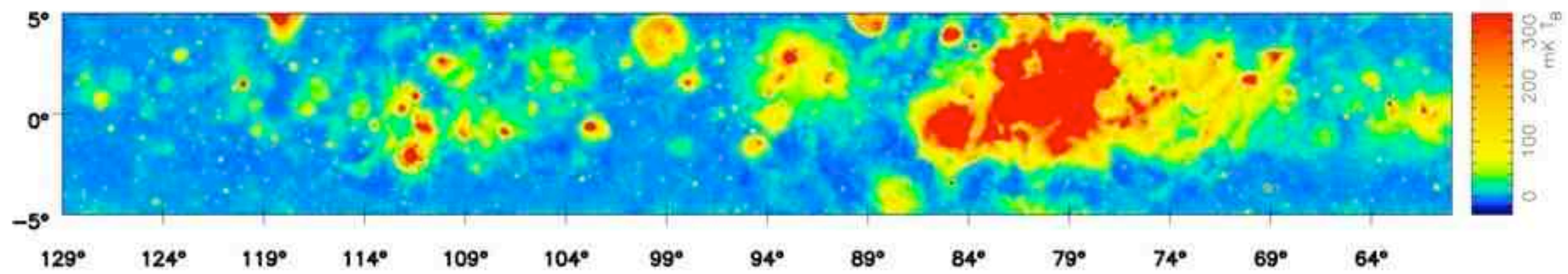
2 New HII regions: G124.0+1.4 and G124.9+0.1
 2 Faraday Screens: G125.6-1.8 and G124.9+0.1, HII as FS
 Rule out the spectral curvature of SNR 126.2+1.6
 Sun et al. 2007

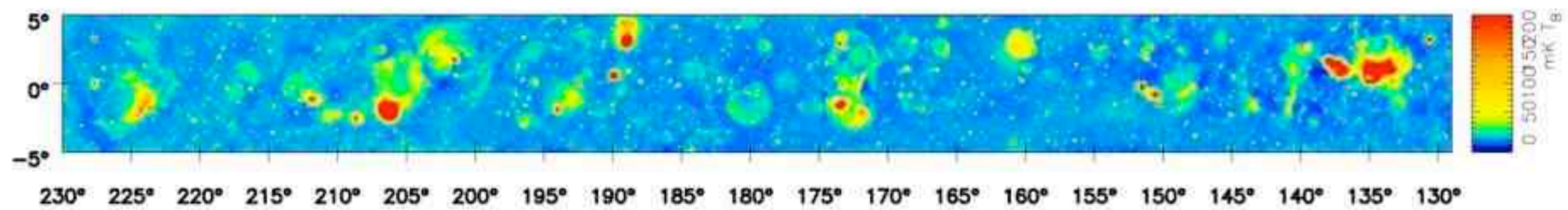


five years after the project
started

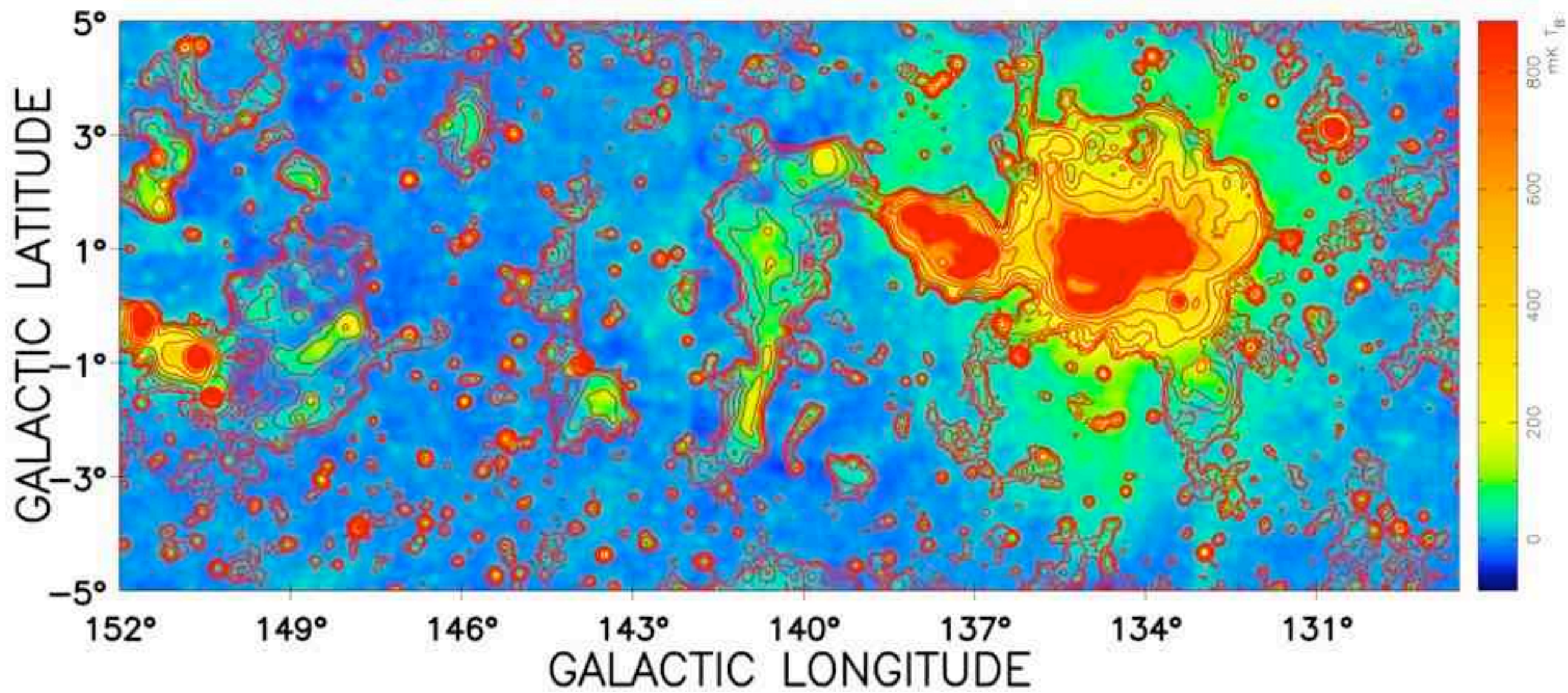
...



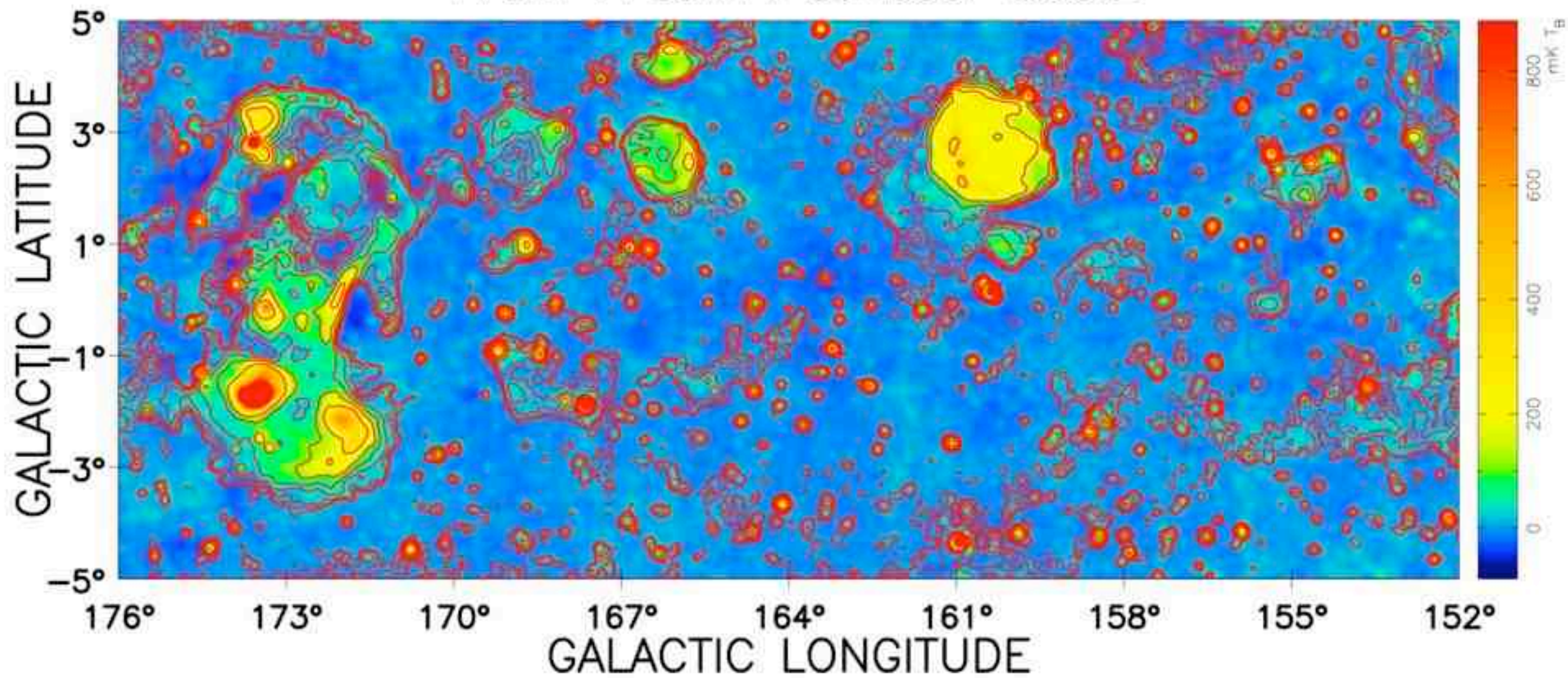




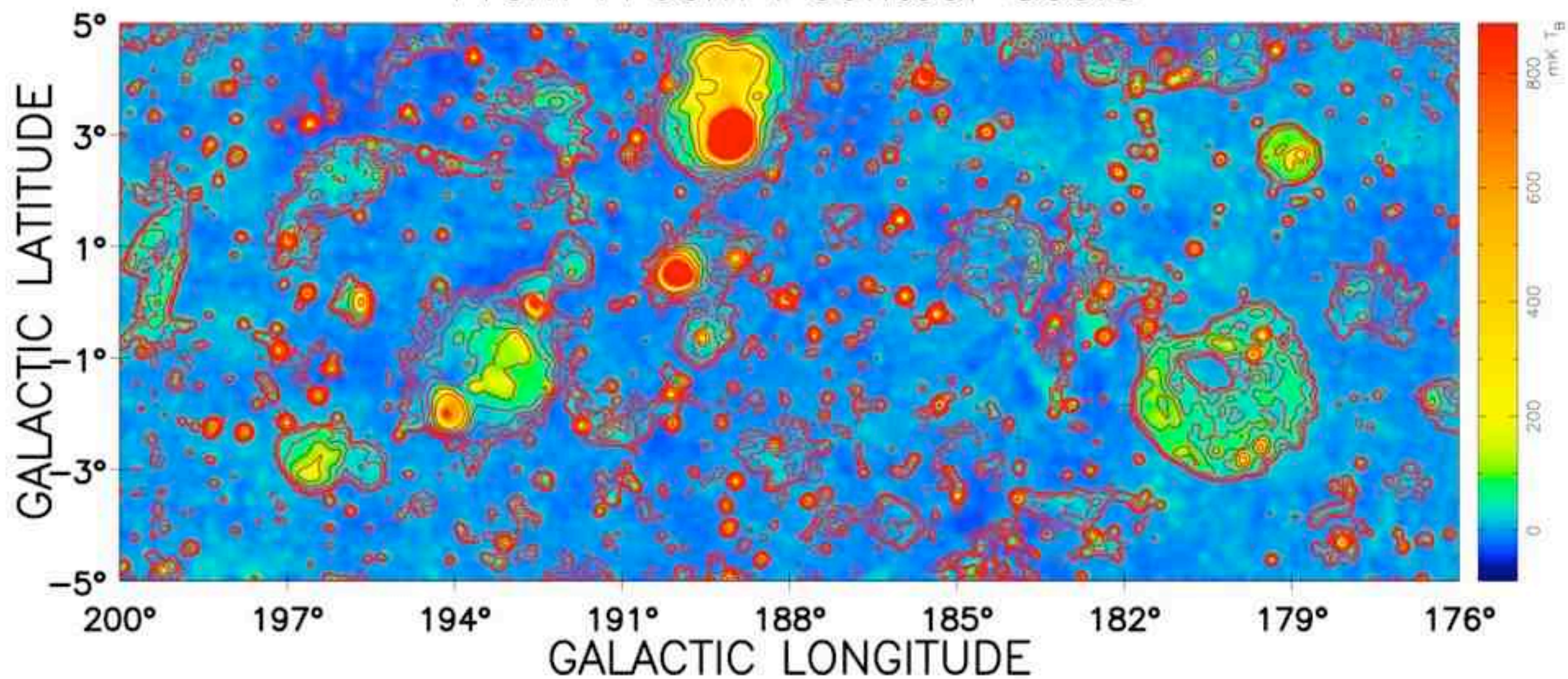
11cm I+6cm I contour Sec.1

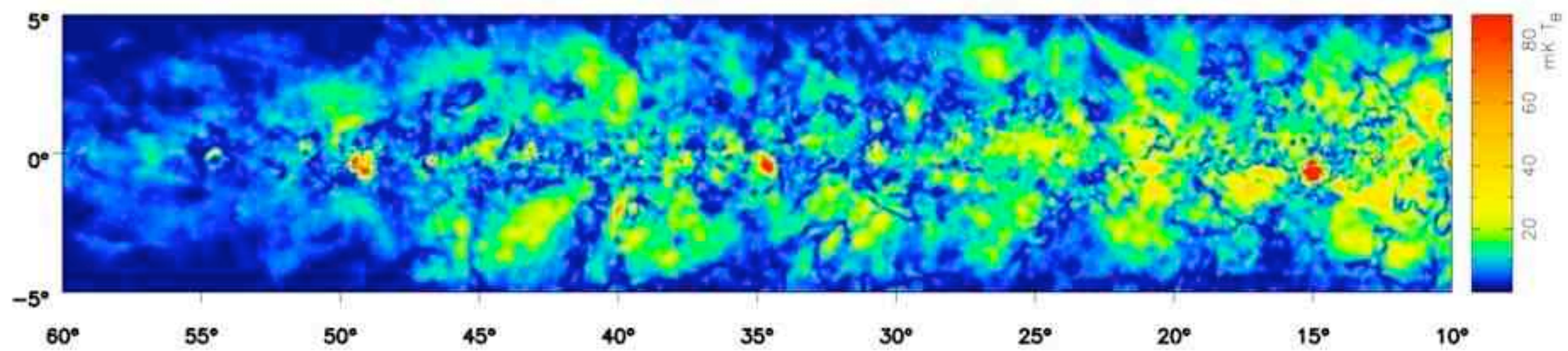


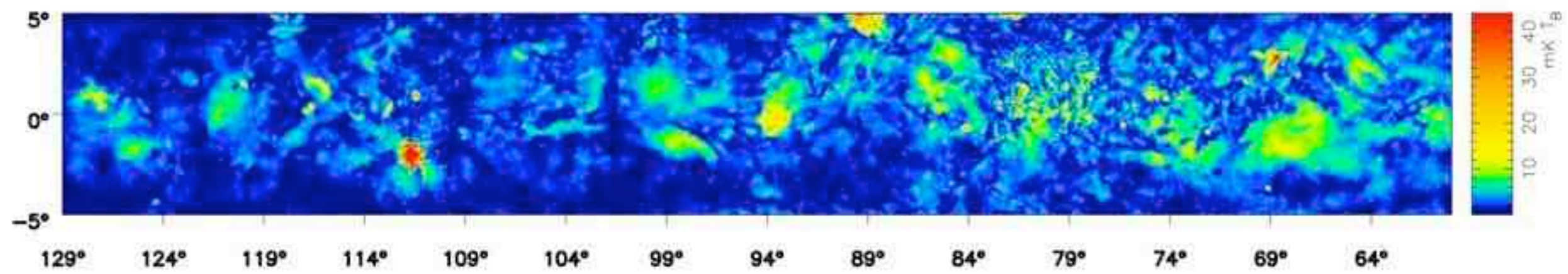
11cm I+6cm I contour Sec.2

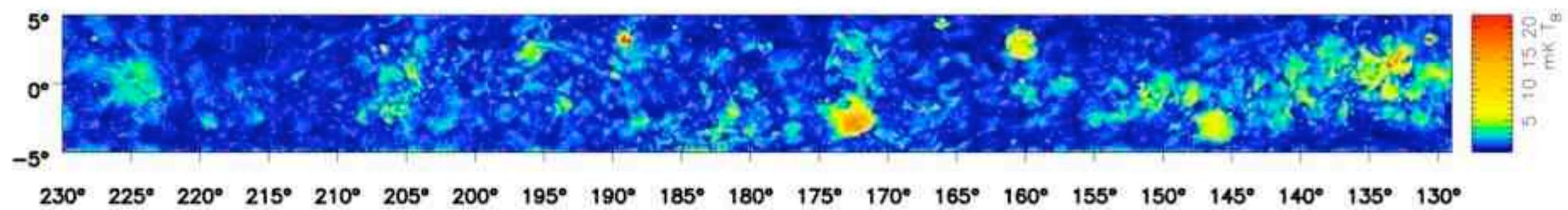


11cm I+6cm I contour Sec.3



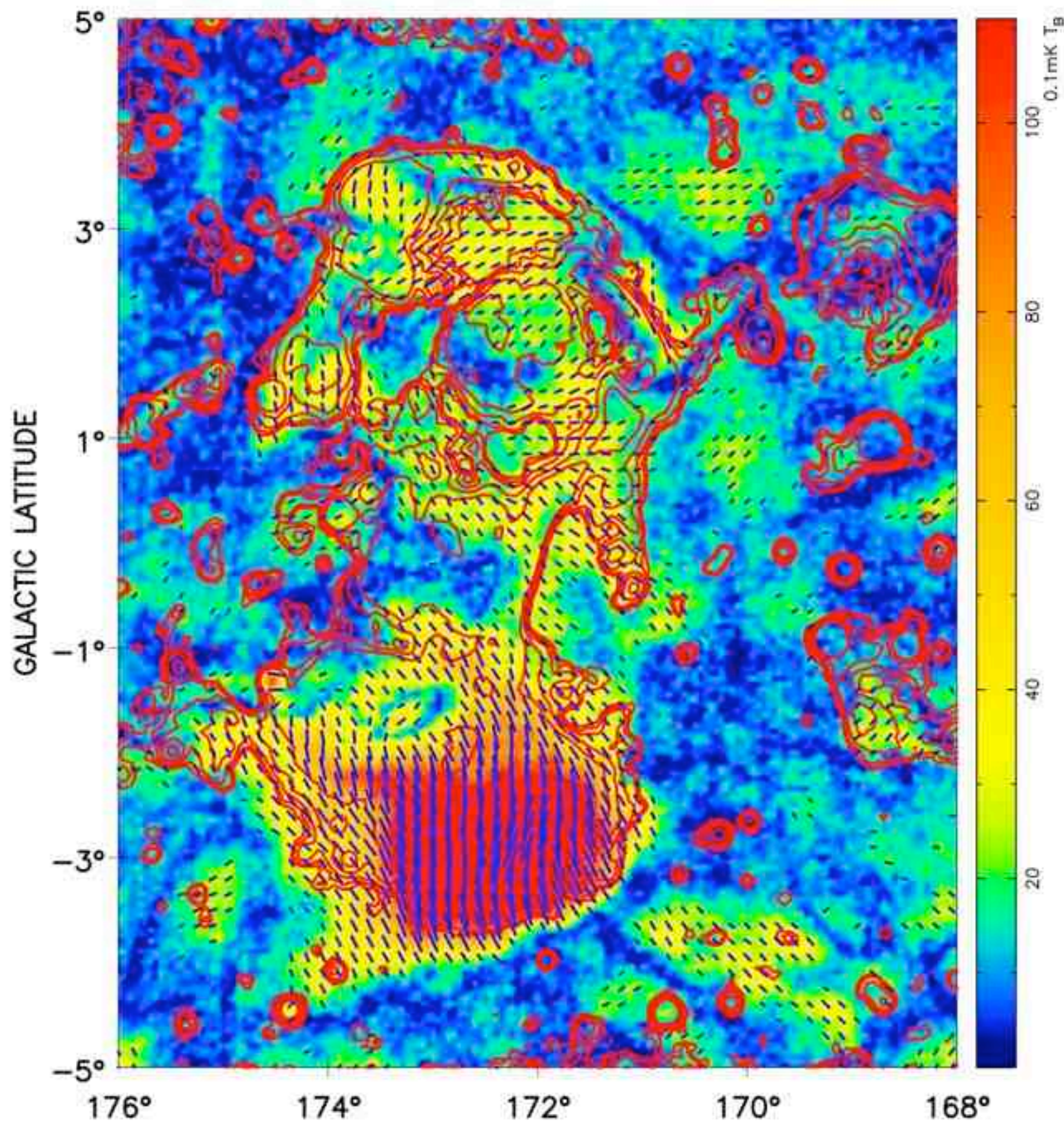




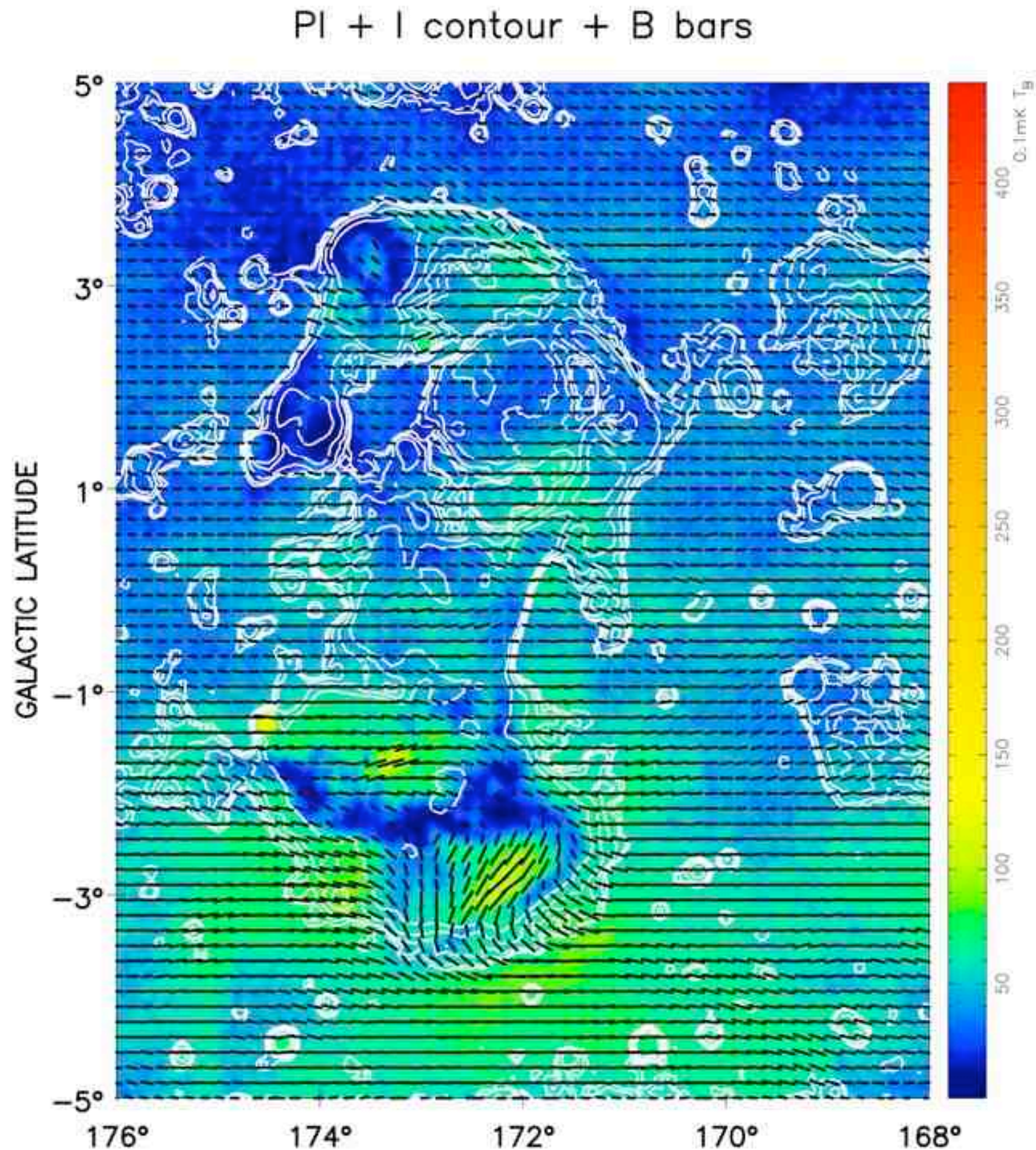


Zero-level restoration by WMAP extrapolation

PI + I contour + B bars

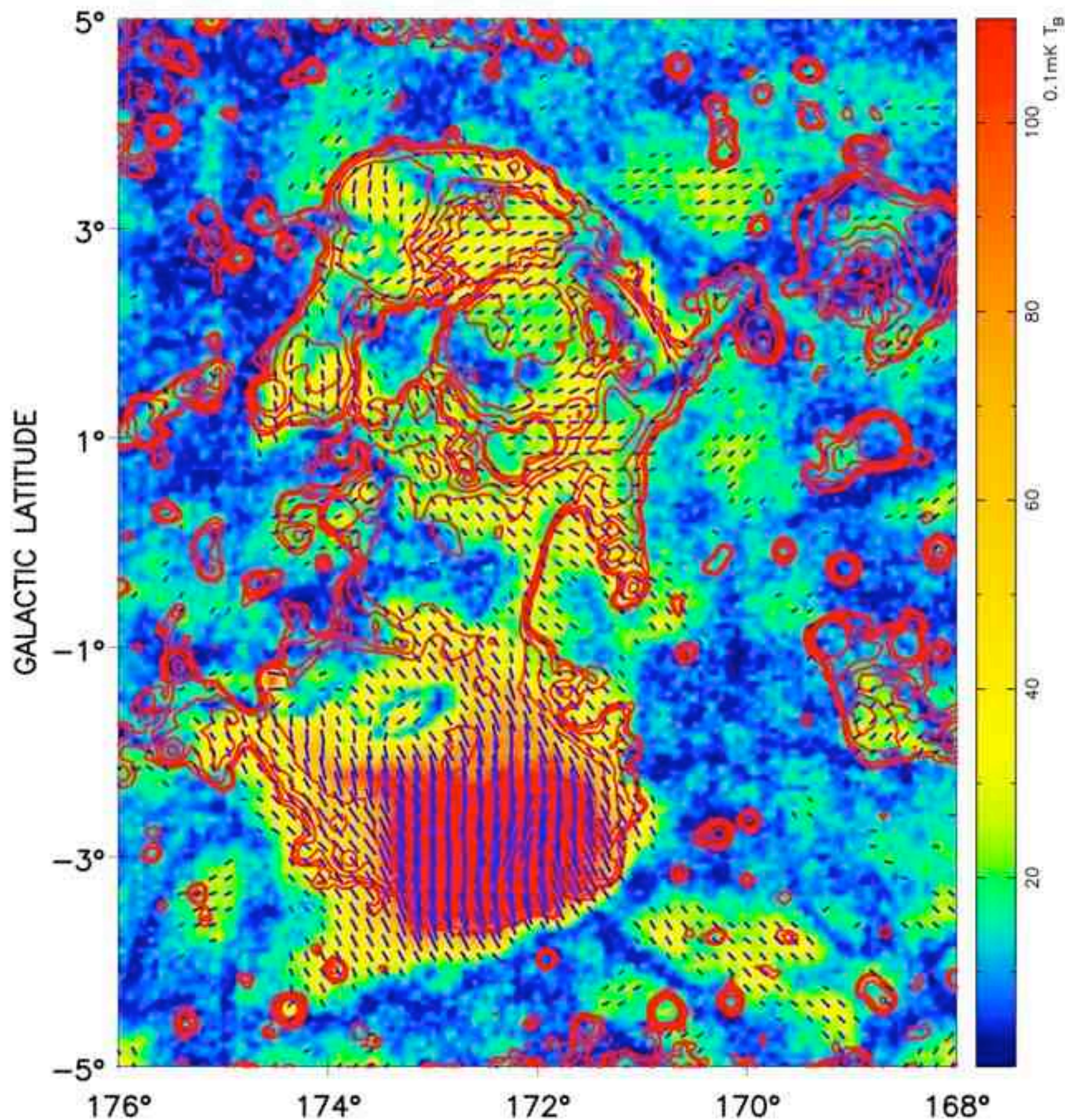


Zero-level restoration by WMAP extrapolation

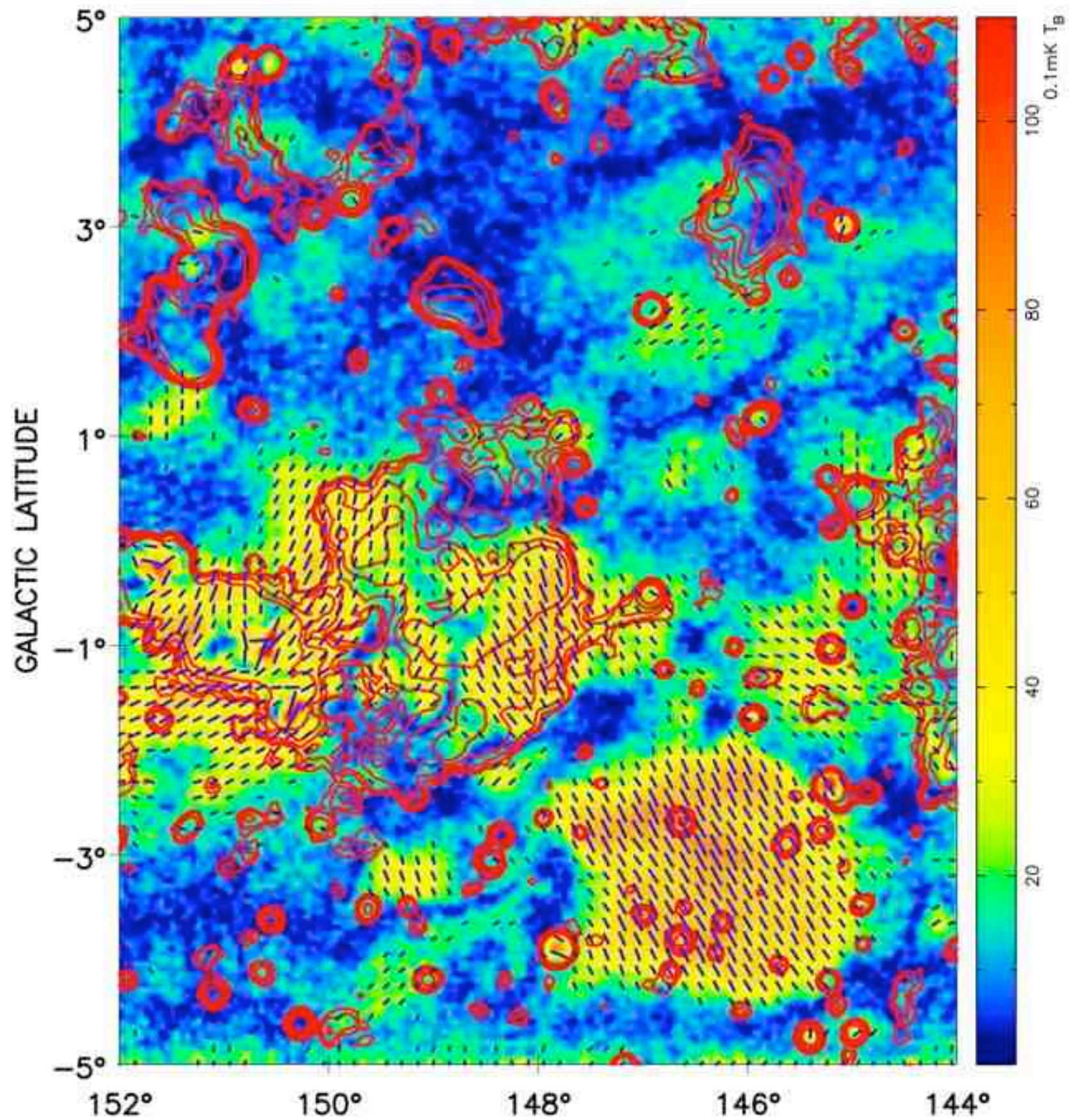


Zero-level restoration by WMAP extrapolation

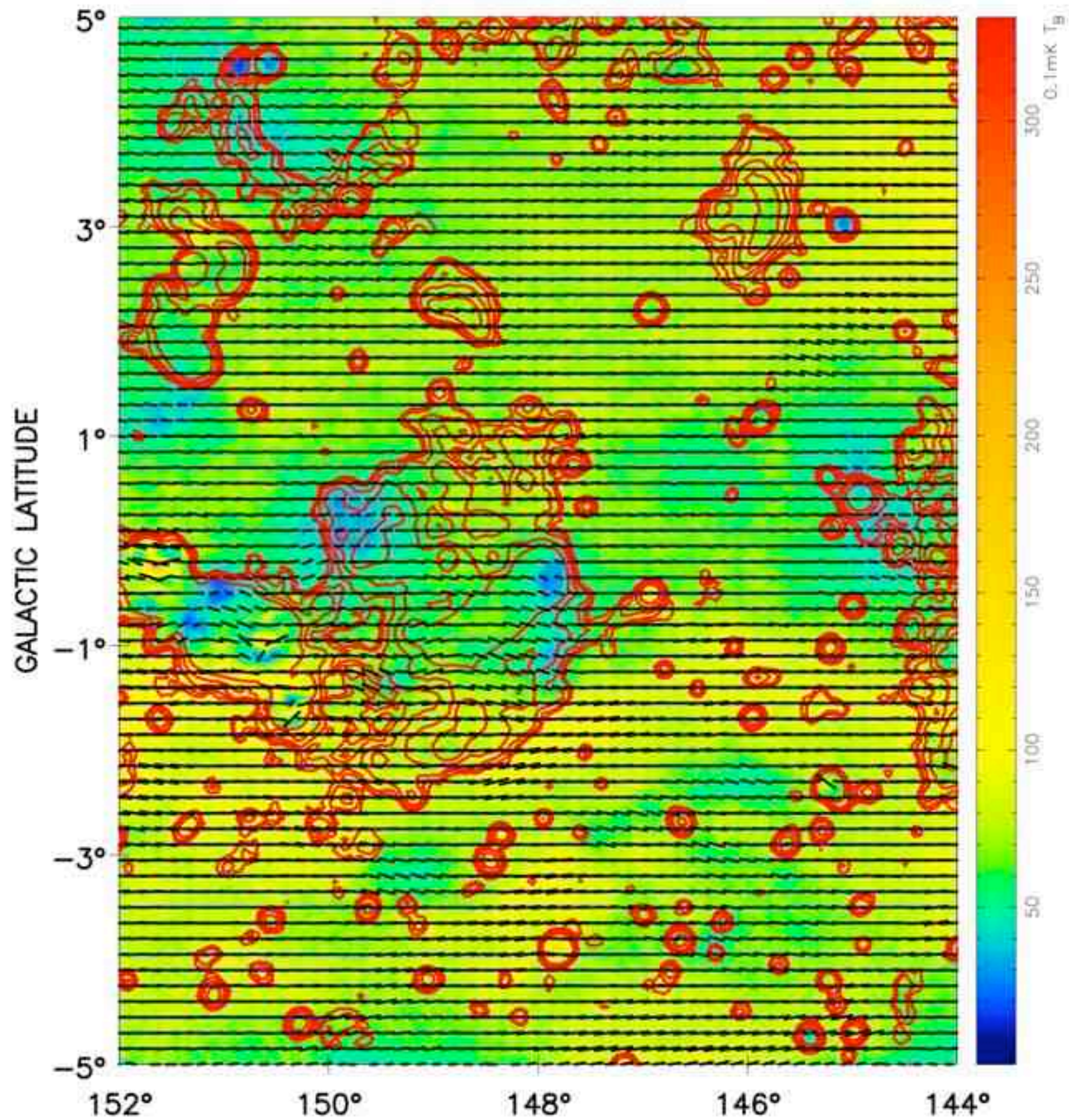
PI + I contour + B bars



PI + I contour + B bars



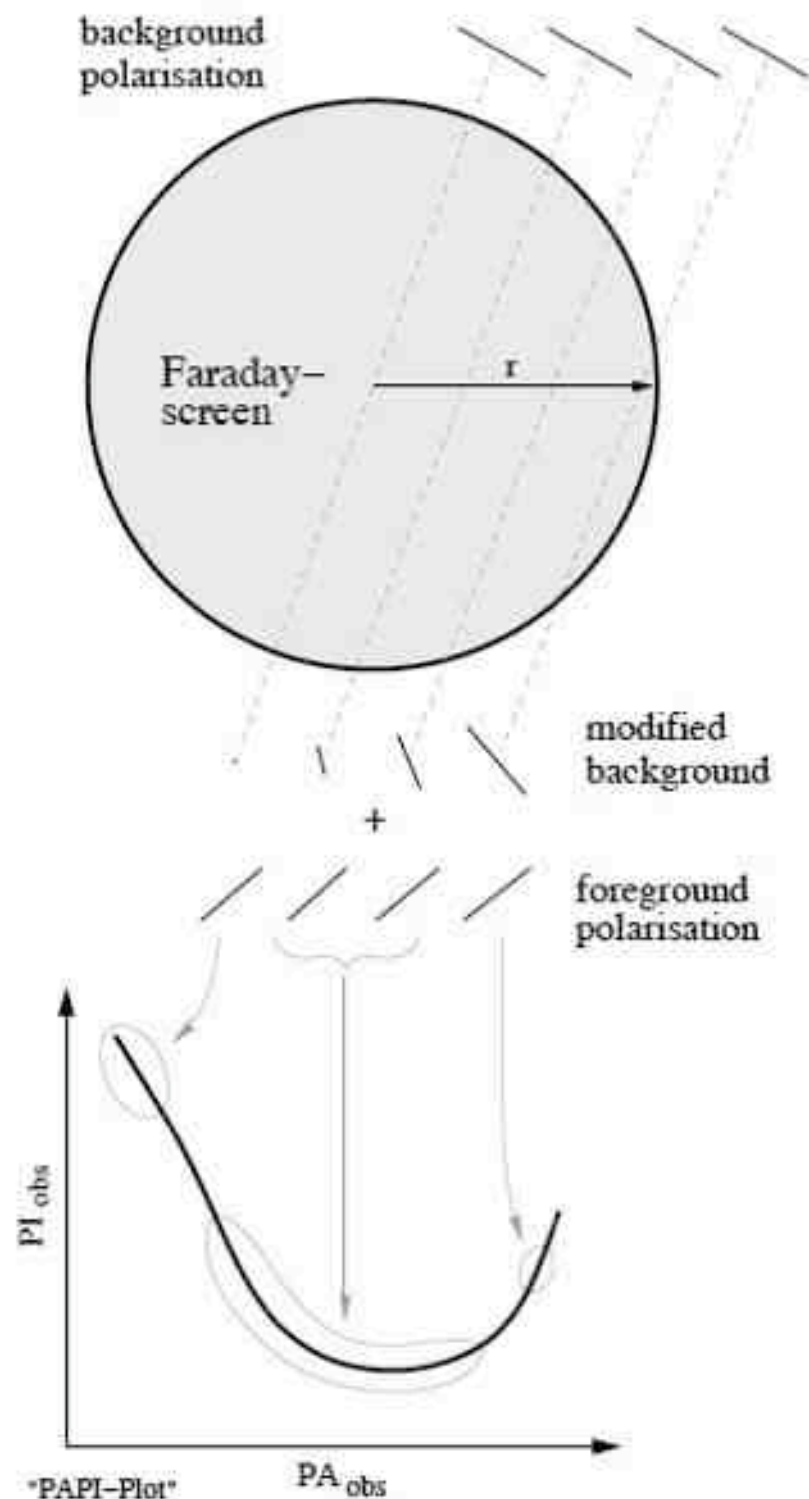
PI + I contour + B bars



Faraday Screen

- Diffused ionized gas
- HII regions
- Possibly HI clouds
- Surface of molecular clouds

Model of FS



$$\frac{PI_{on}}{PI_{off}} = (f^2(1-c)^2 + c^2 + 2fc(1-c)\cos 2\psi_s)^{1/2}$$

$$\psi_{on} - \psi_{off} = \frac{1}{2} \arctan \left(\frac{f(1-c)\sin 2\psi_s}{c + f(1-c)\cos 2\psi_s} \right)$$

f depolarization factor
c foreground PI ratio

谢谢=Danke

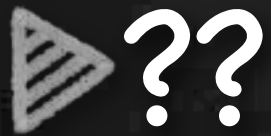
Chemistry in Star Formation Region

Fang-Chun Liu

IMPRS retreat 2009

Outline

Outline



Outline

Why?

Why Chemistry?

Why Chemistry?

- ▶ Chemistry controls critical physical parameters: the fractional ionization and cooling of the gas.

Why Chemistry?

- ▶ Chemistry controls critical physical parameters: the fractional ionization and cooling of the gas.
- ▶ Chemistry is a very powerful diagnostic, both of the current and the past physical conditions of the forming protostar.

Why Chemistry?

- ▶ Chemistry controls critical physical parameters: the fractional ionization and cooling of the gas.
- ▶ Chemistry is a very powerful diagnostic, both of the current and the past physical conditions of the forming protostar.
- ▶ Chemistry (initial composition and later process) affects the chemical composition of the objects that eventually form the star and planetary system.

Why Chemistry?

- ▶ Chemistry controls critical physical parameters: the fractional ionization and cooling of the gas.
- ▶ Chemistry is a very powerful diagnostic, both of the current and the past physical conditions of the forming protostar.
- ▶ Chemistry (initial composition and later process) affects the chemical composition of the objects that eventually form the star and planetary system.

★ Therefore, we need to study the chemistry properties and evolution in the star formation region.

How?

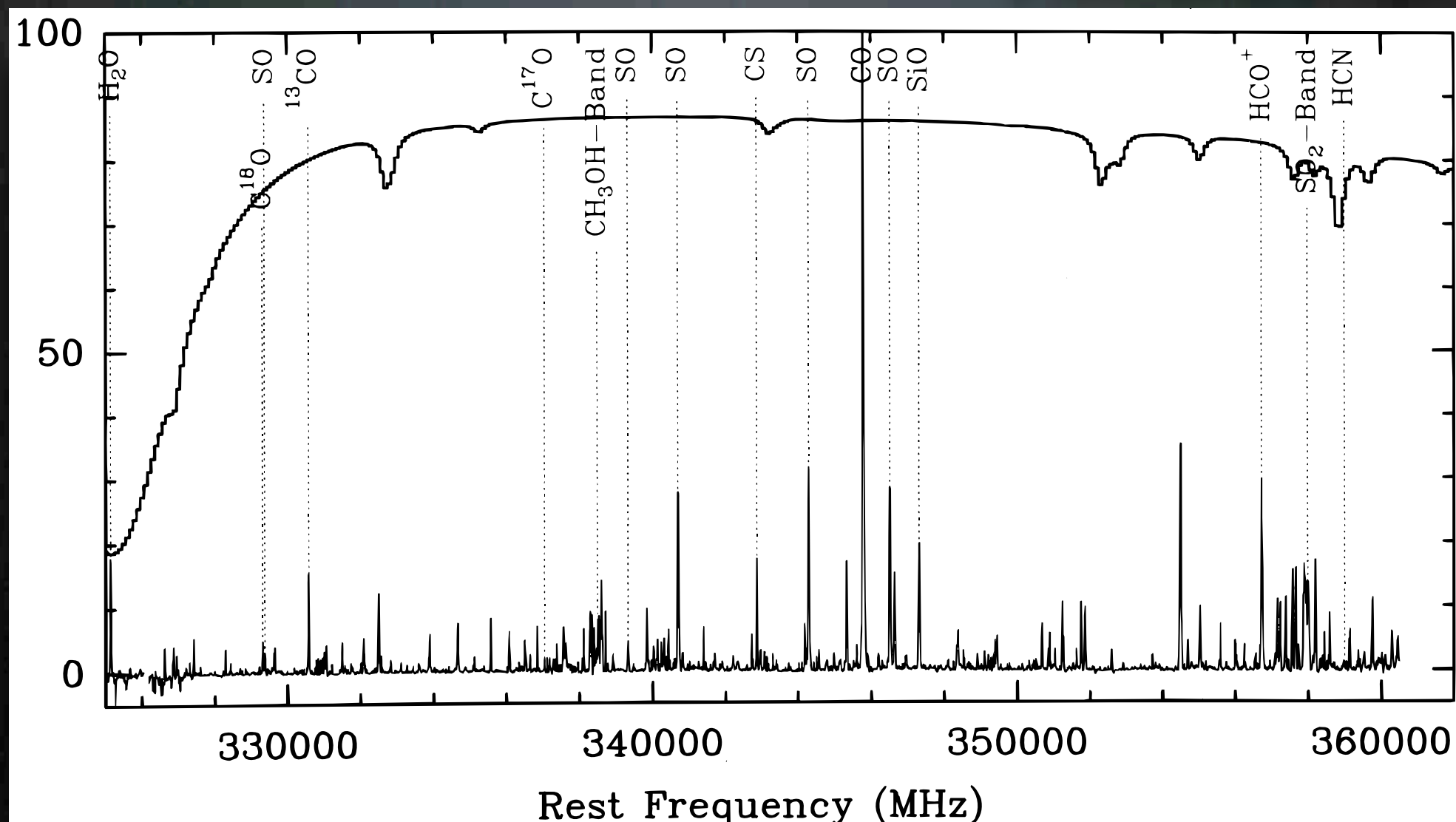
How?

-Observation Techniques

► (Sub)millimeter observations

1. Traditionally, most of the chemical information has been derived from (sub)millimeter observations due to the rotation transition.

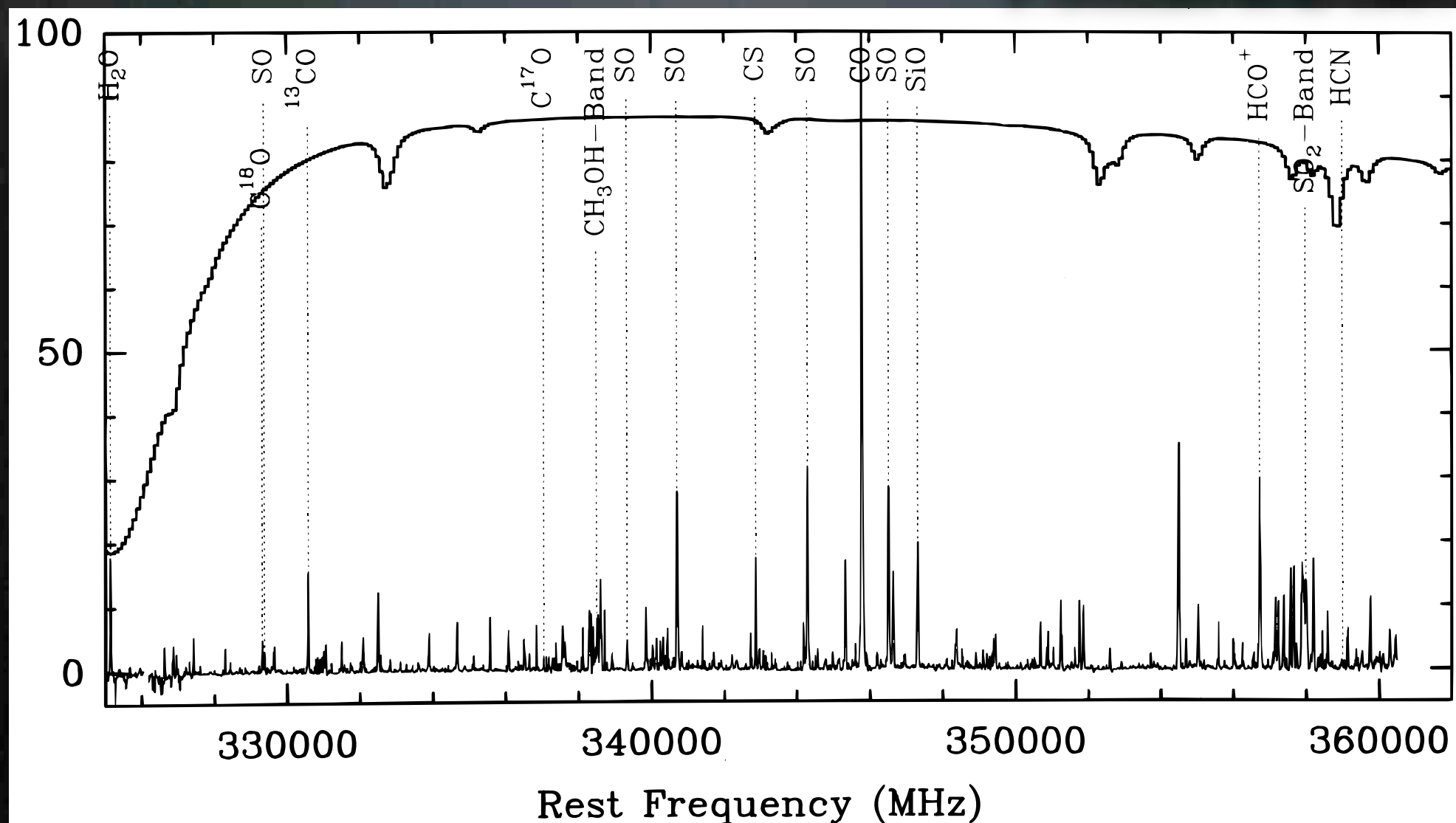
P. Schilke et al 1997



How?

-Observation Techniques

P. Schilke et al 1997

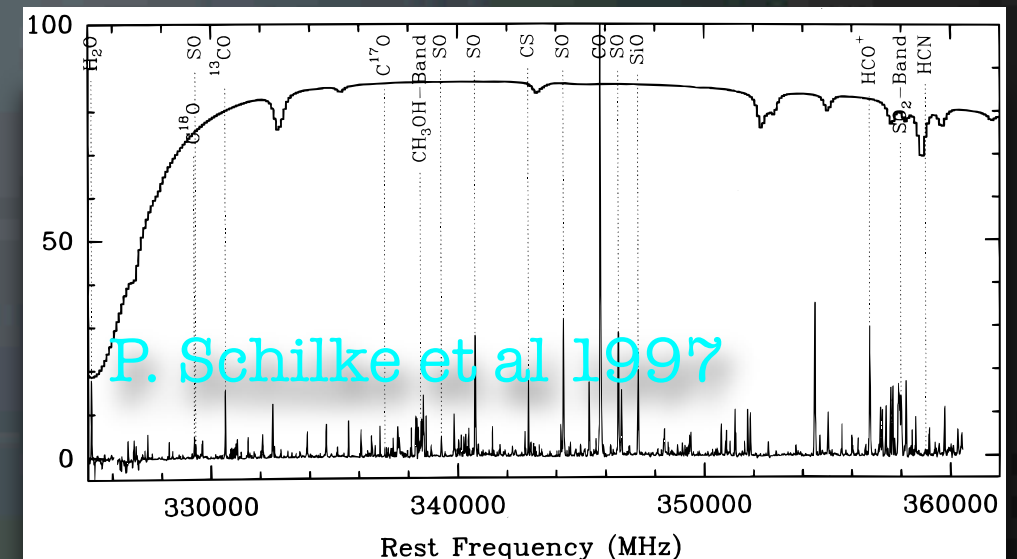


How?

-Observation Techniques

► (Sub)millimeter observations

1. Traditionally, most of the chemical information has been derived from (sub)millimeter observations due to the rotation transition.

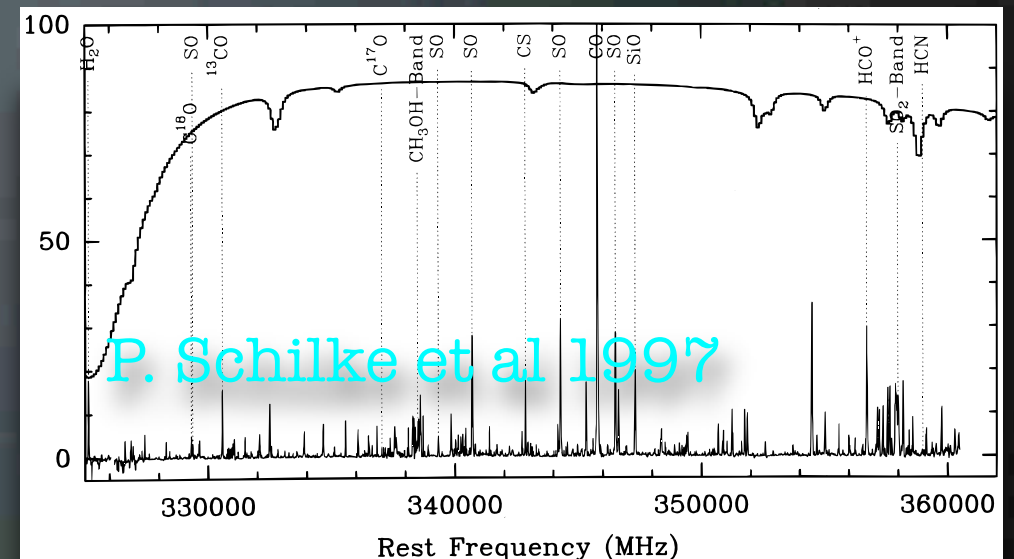


How?

-Observation Techniques

► (Sub)millimeter observations

1. Traditionally, most of the chemical information has been derived from (sub)millimeter observations due to the rotation transition.
2. They are not restricted to absorption/emission toward the source but can map the surroundings with high spectral resolution and resolution. (Kinematic Information and location)

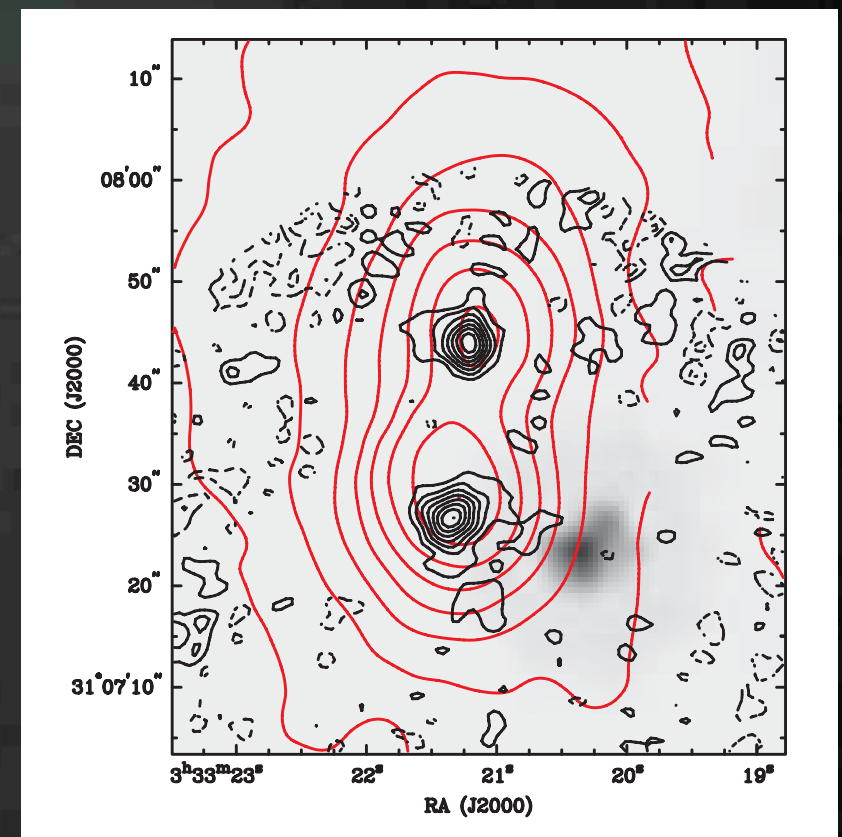
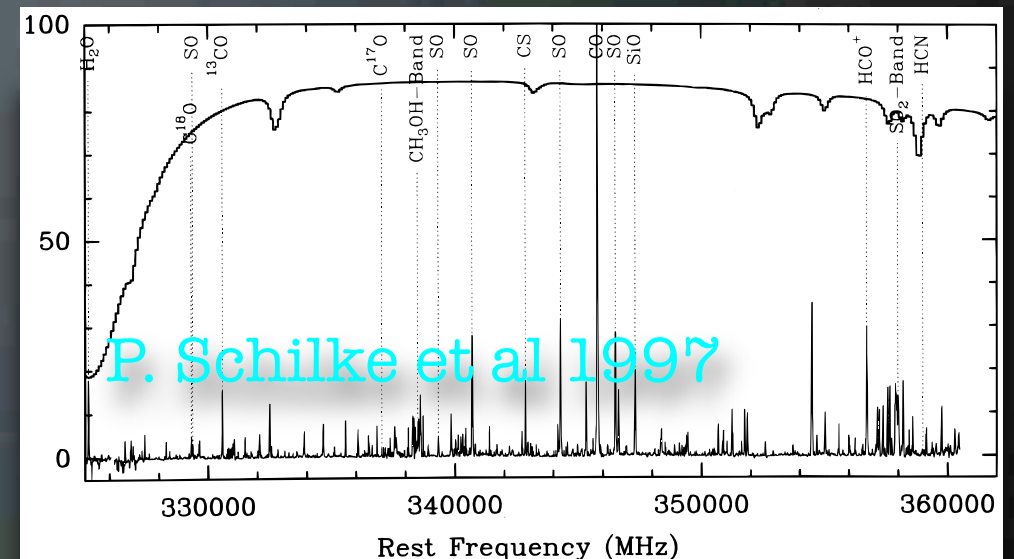


How?

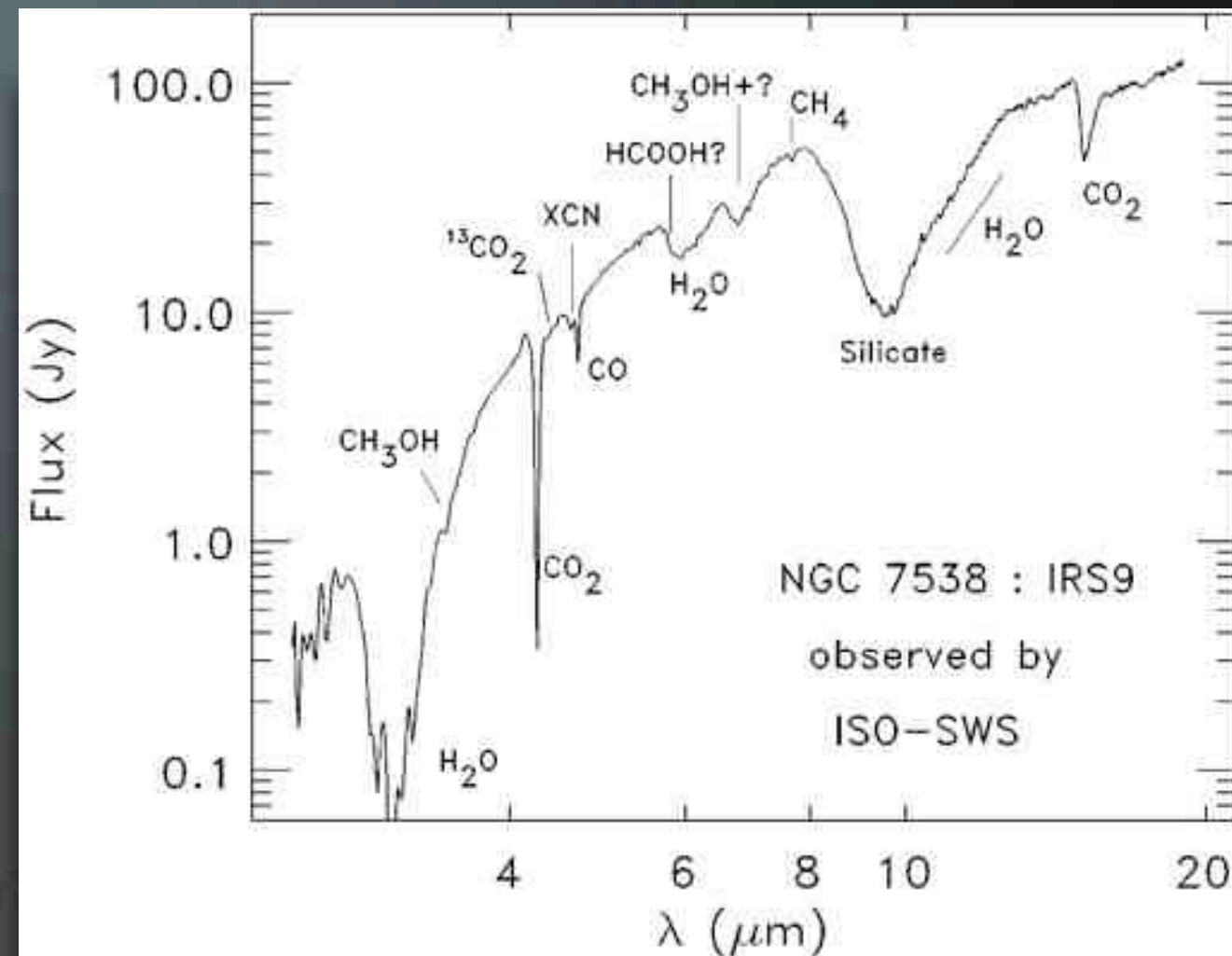
-Observation Techniques

► (Sub)millimeter observations

1. Traditionally, most of the chemical information has been derived from (sub)millimeter observations due to the rotation transition.
2. They are not restricted to absorption/emission toward the source but can map the surroundings with high spectral resolution and resolution.
(Kinematic Information and location)



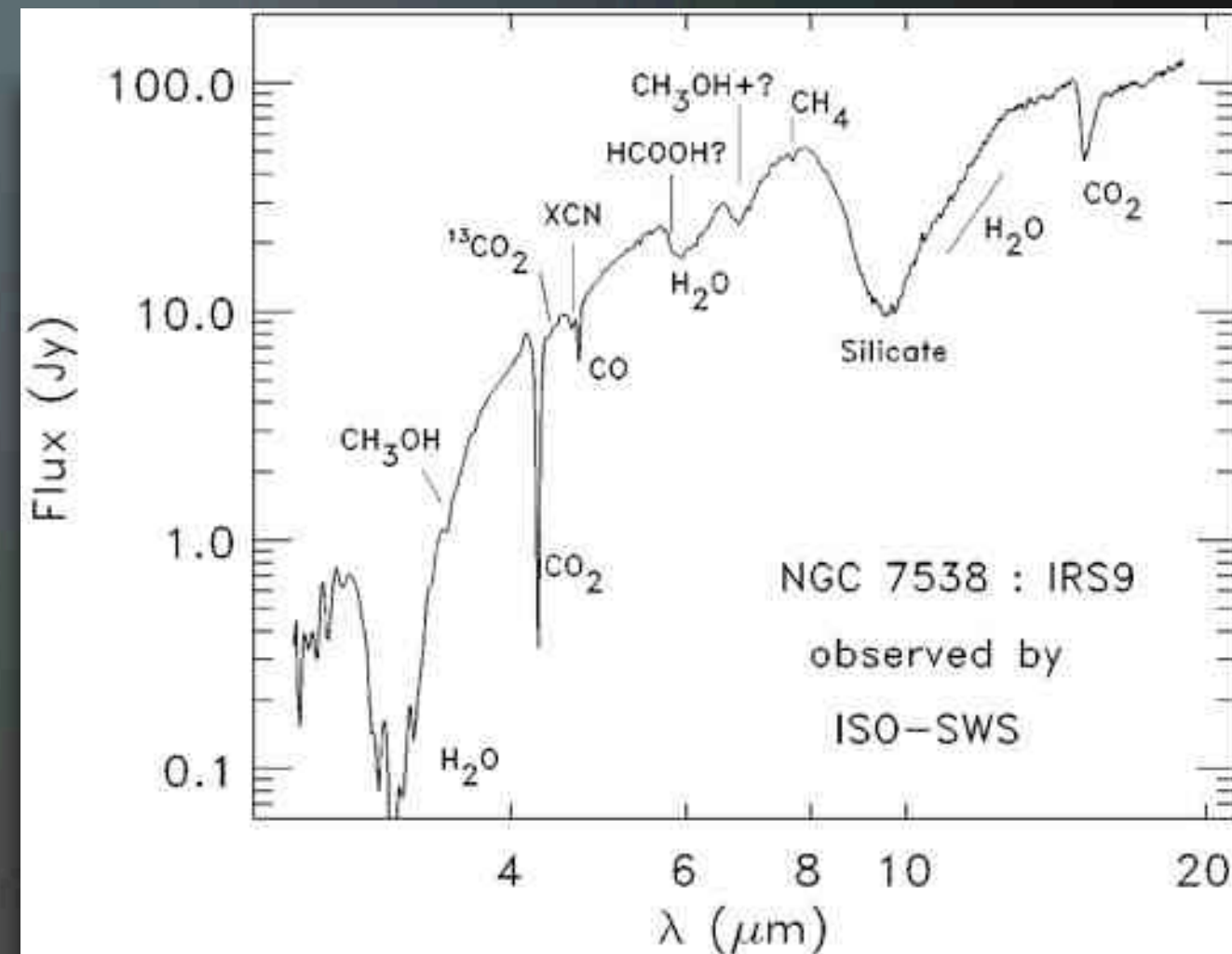
Infrared observations



van Dishoeck & Blake 1998

Infrared observations

► Infrared observations

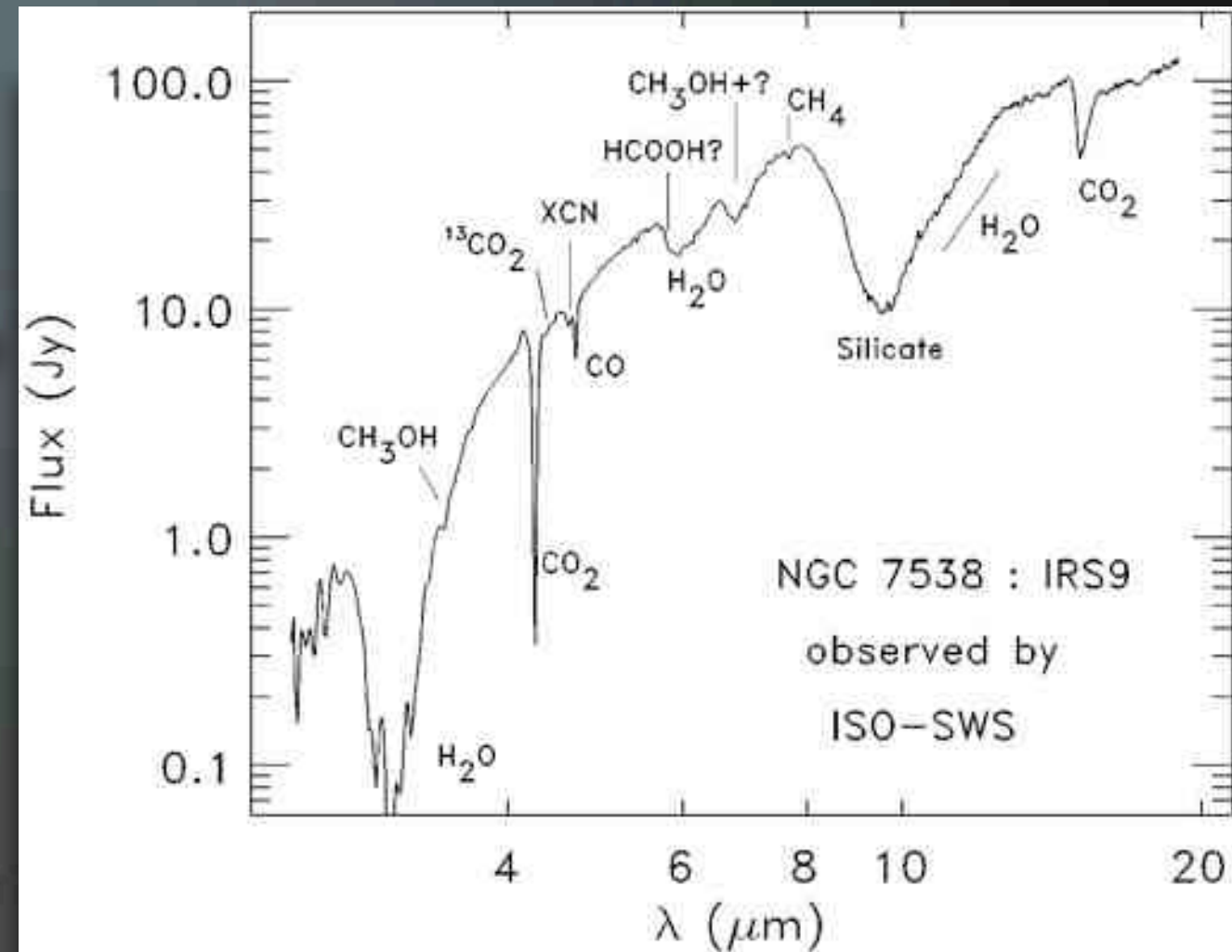


van Dishoeck & Blake 1998

Infrared observations

► Infrared observations

1. It can probe the absorption of material along the line of sight to the embedded young star.

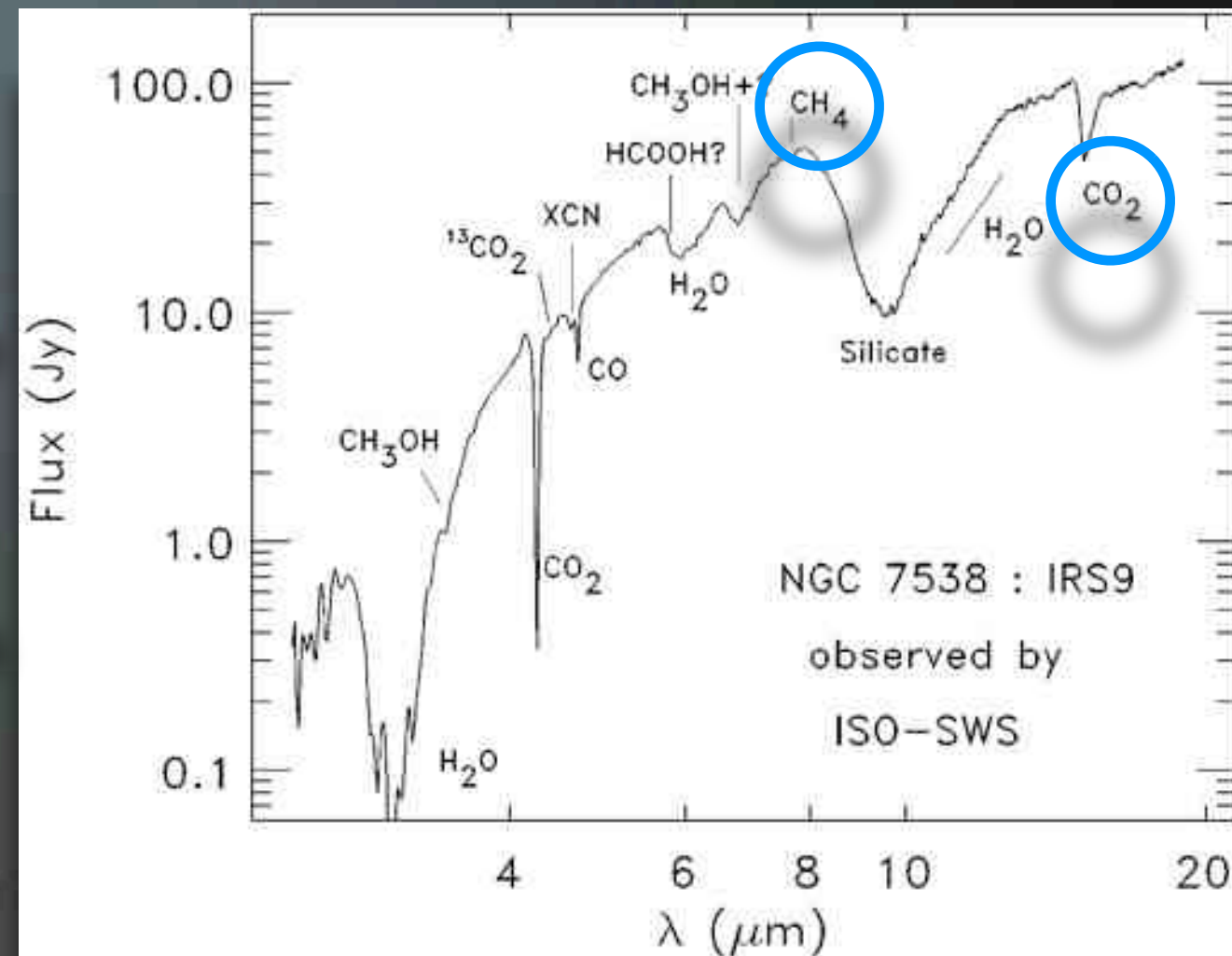


van Dishoeck & Blake 1998

Infrared observations

► Infrared observations

1. It can probe the absorption of material along the line of sight to the embedded young star.
2. Important molecules without a permanent dipole moment, such as H_3^+ , CO_2 , CH_4 , and C_2H_2 , possess strong infrared vibrational transitions.

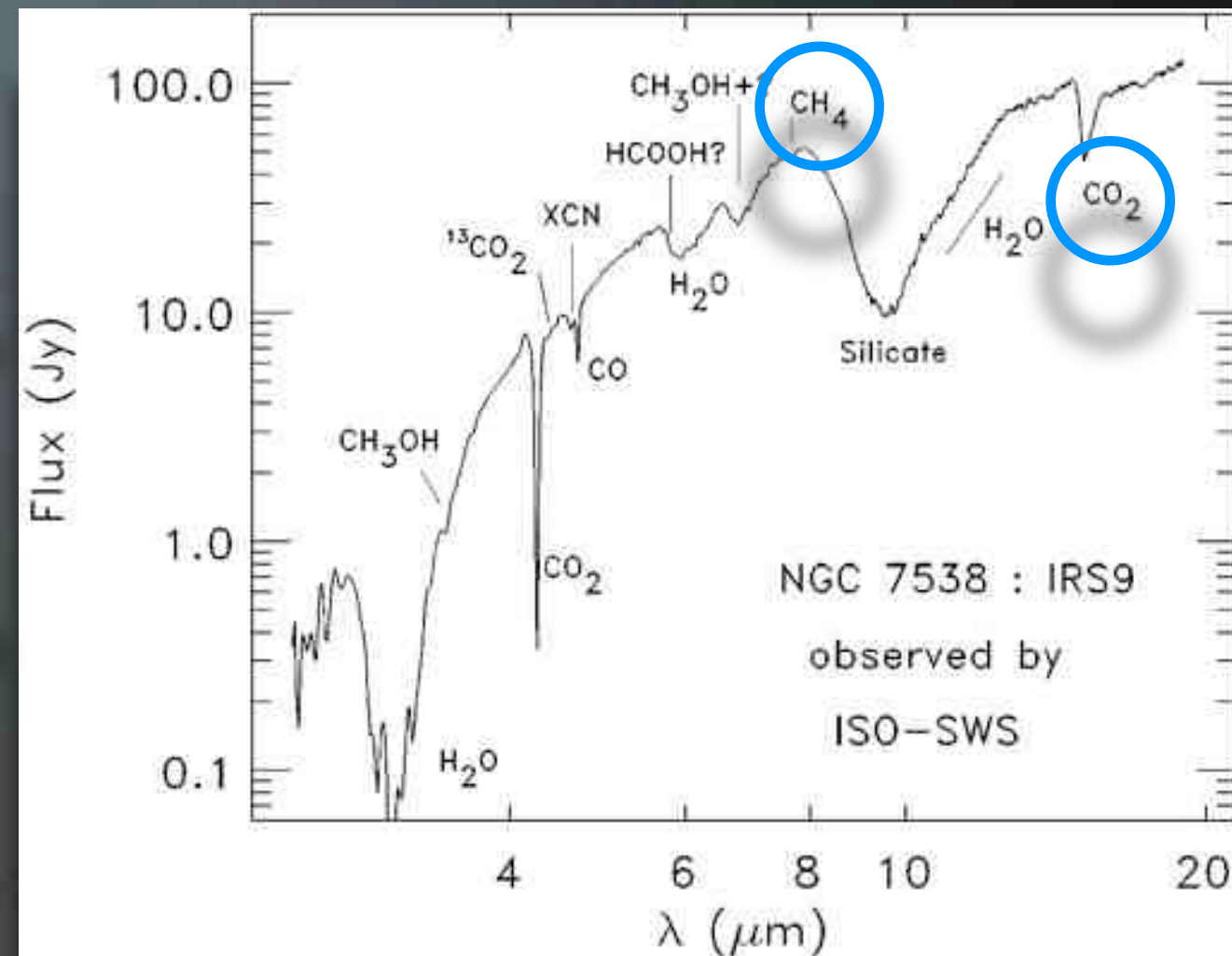


van Dishoeck & Blake 1998

Infrared observations

► Infrared observations

1. It can probe the absorption of material along the line of sight to the embedded young star.
2. Important molecules without a permanent dipole moment, such as H_3^+ , CO_2 , CH_4 , and C_2H_2 , possess strong infrared vibrational transitions.
3. Both gas-phase molecules and solid-state species can be detected at infrared wavelengths.



van Dishoeck & Blake 1998

How?

–Models

How?

–Models

▶ Two main fundamental models:

How?

–Models

► Two main fundamental models:

1. Gas-phase chemistry: molecules are form from the reaction in gas-phase. ex: HCO^+ formation.

How?

–Models

► Two main fundamental models:

1. Gas-phase chemistry: molecules are form from the reaction in gas-phase. ex: HCO^+ formation.
2. Grain-phase chemistry: molecules are form from the reaction in grain-phase. ex: H_2 formation.

What?

Outline

▶ why?

▶ How?

Outline

▶ why?

▶ How?

▶ Chemistry in

- Interstellar medium and the Hot Cores

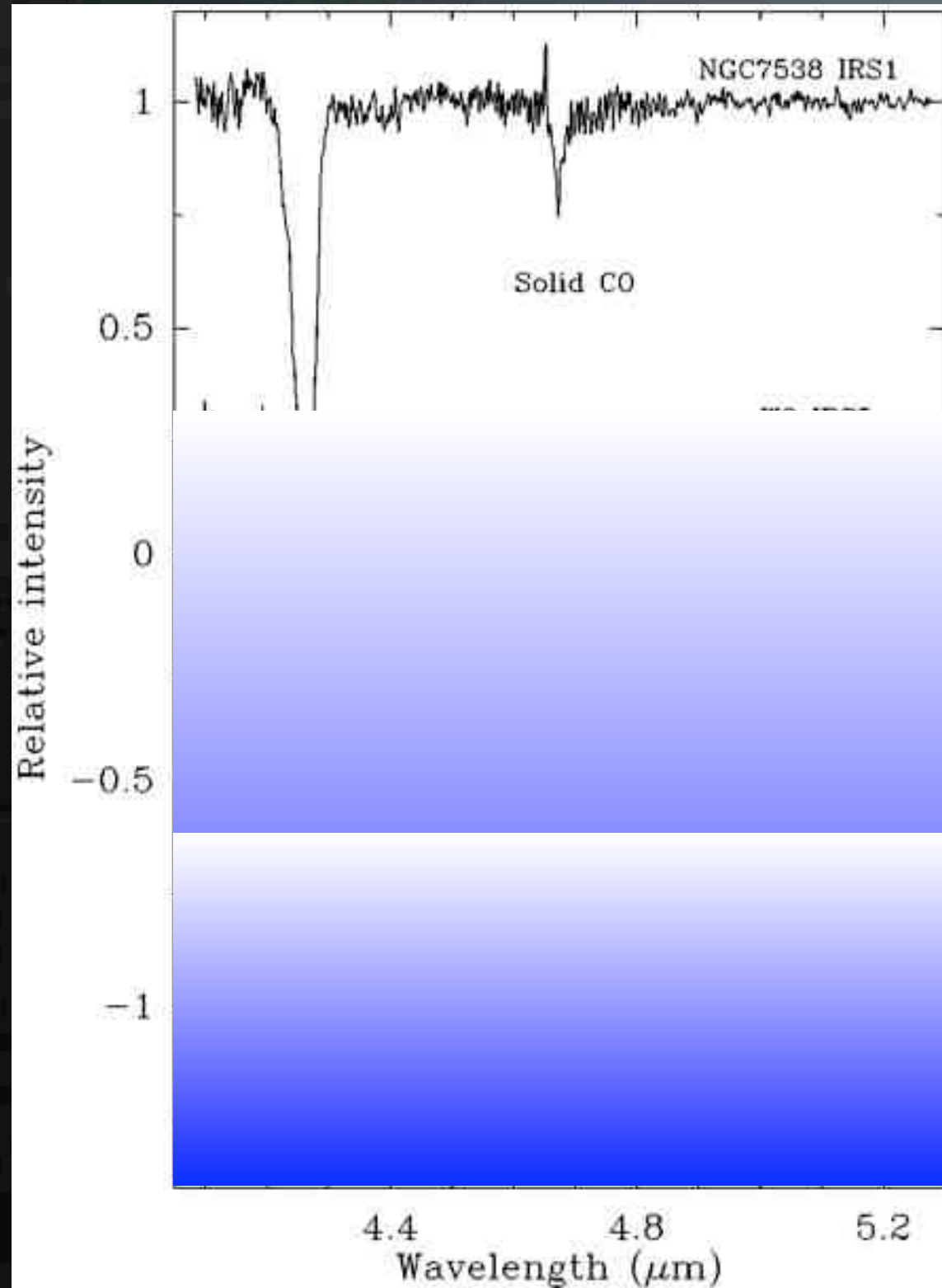
- Prestellar Cores and Young Protostars

About interstellar medium

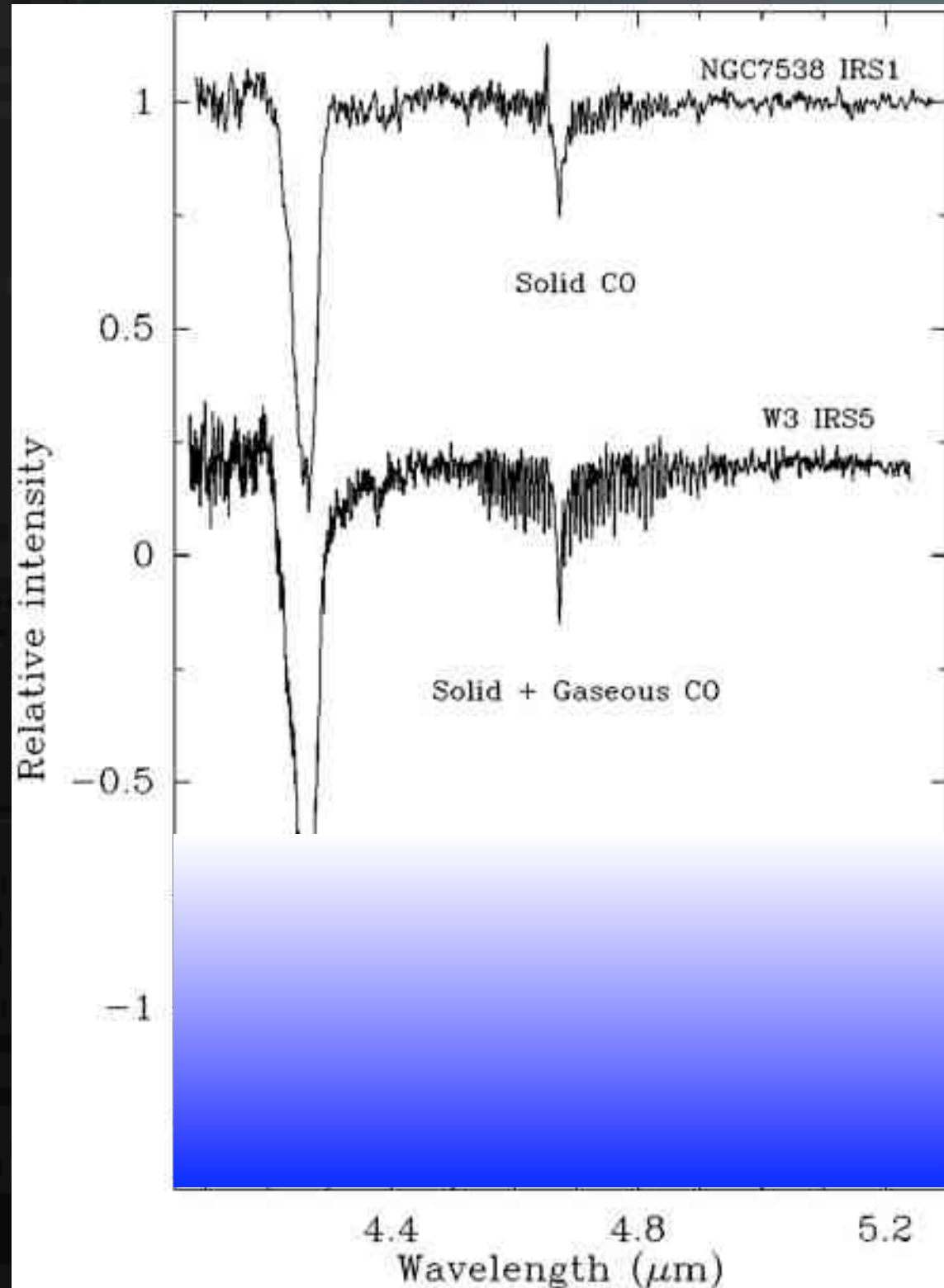


- ▶ Interstellar medium are the sites of a very rich chemistry, as evidenced by the detection of nearly 120 different molecules.
- ▶ The observed species range from single diatomic molecules in diffuse clouds to long, unsaturated carbon chains in dark pre-star-forming clouds and saturated organic species near massive YSOs.

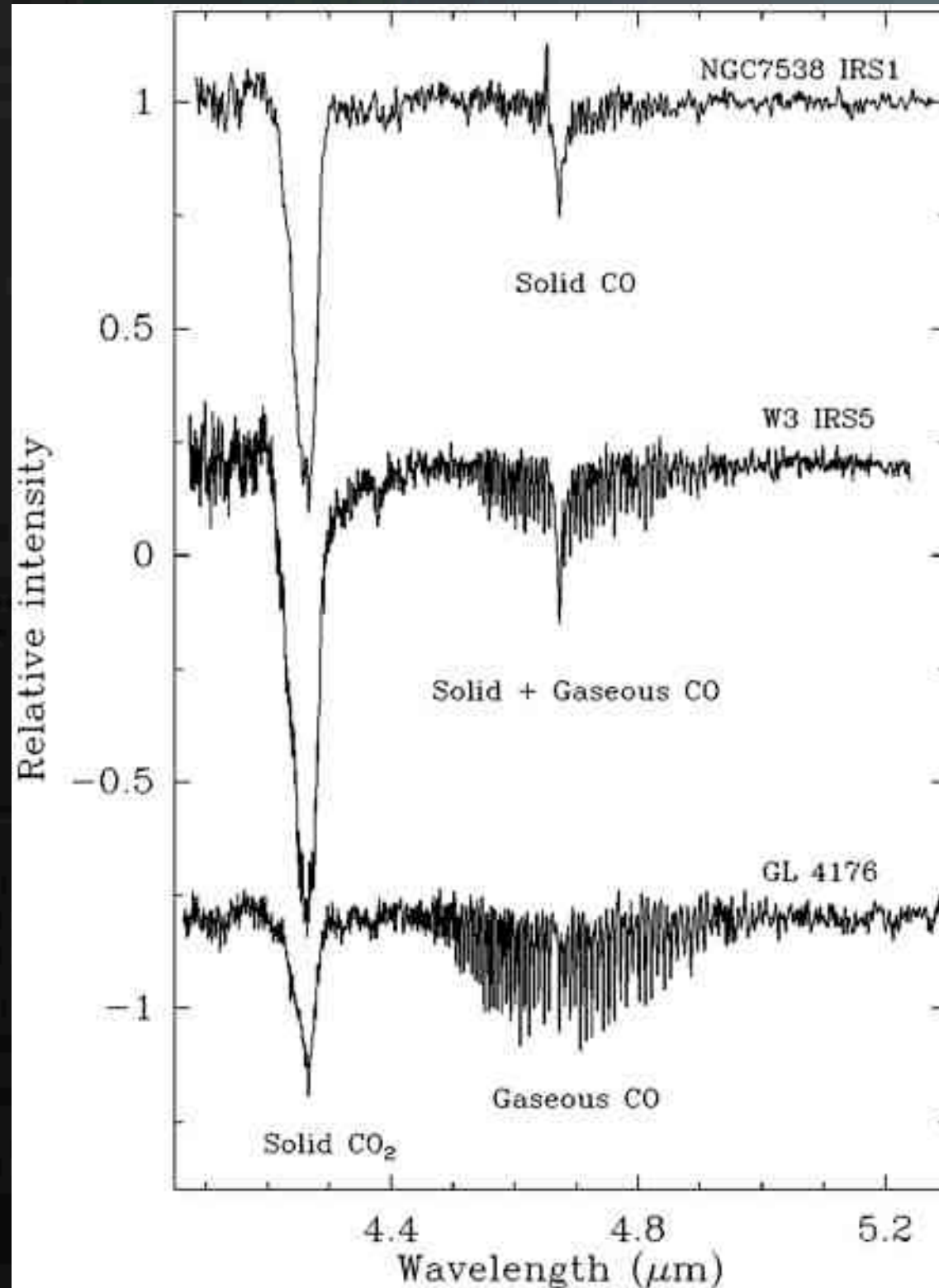
About the Hot cores



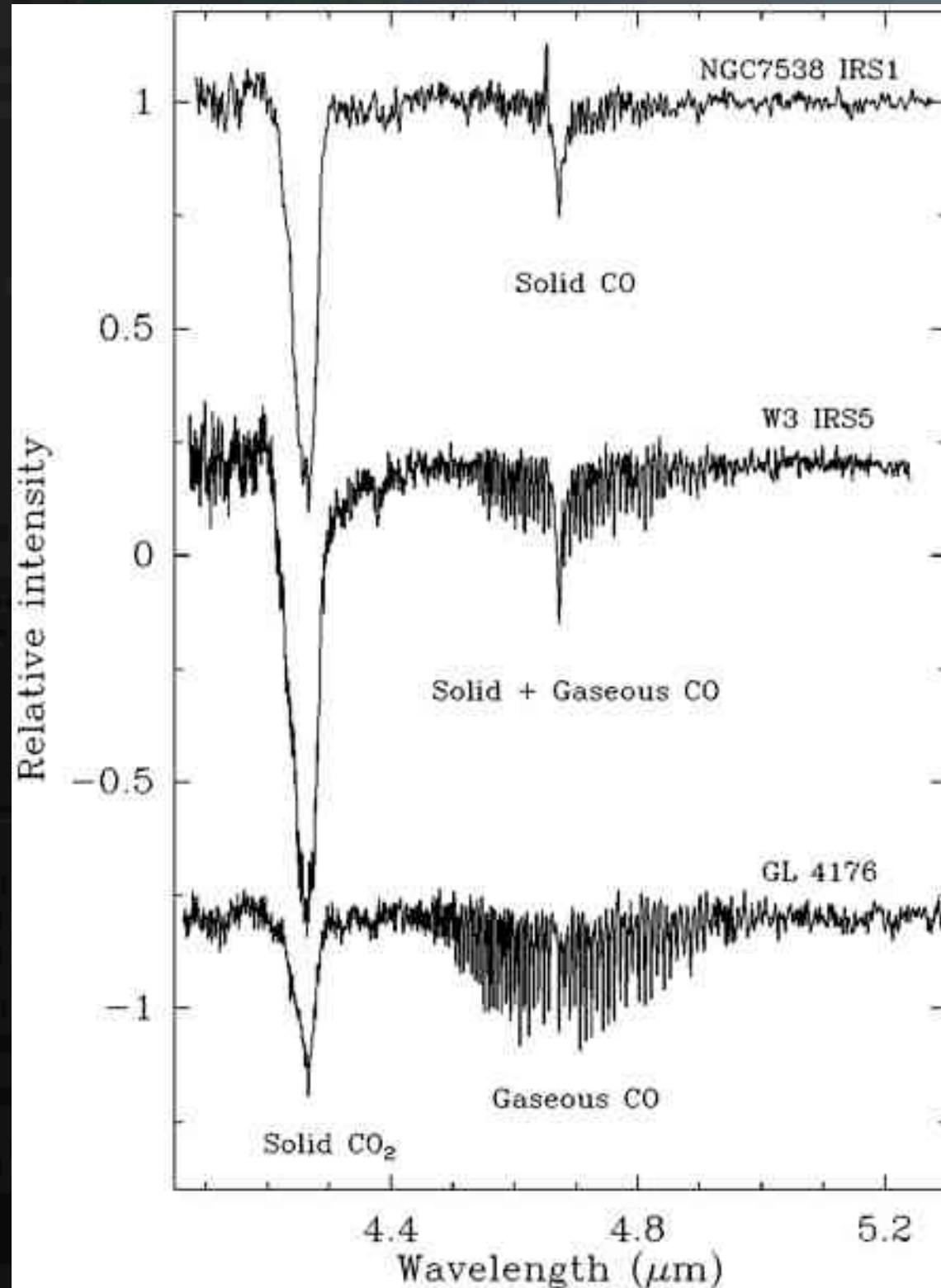
About the Hot cores



About the Hot cores

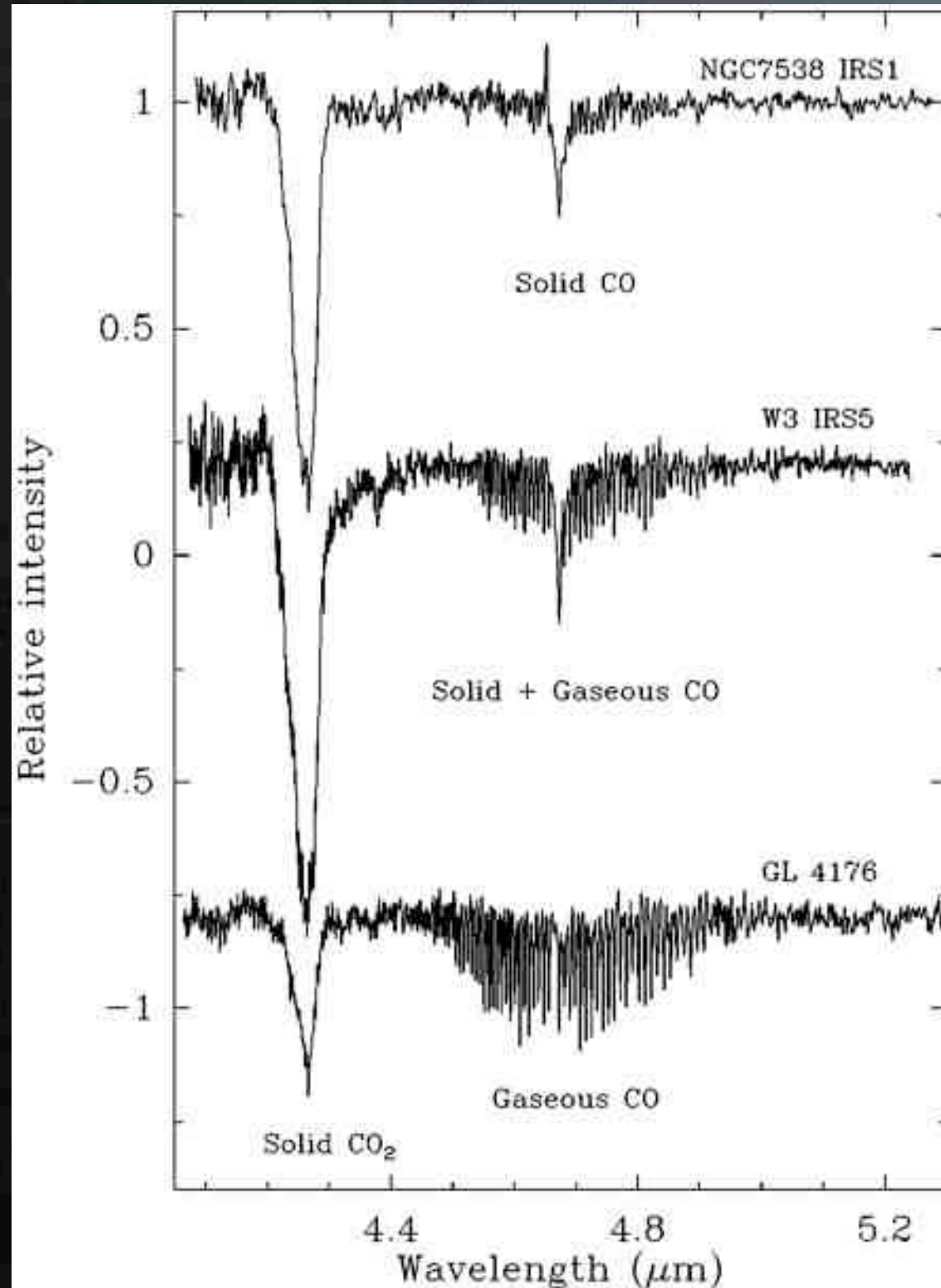


About the Hot cores



- The spectra of the solid-state CO₂ and solid- and gas-phase CO infrared absorption feature toward embedded massive YSOs, illustrating the evaporation of ices and development of a “hot core” region near W3 IRS5 and AFGL 4176.

About the Hot cores



► The spectra of the solid-state CO₂ and solid- and gas-phase CO infrared absorption feature toward embedded massive YSOs, illustrating the evaporation of ices and development of a "hot core" region near W3 IRS5 and AFGL 4176.

► The relative ratios of these features can be used as an indicator of the evolutionary state (van Dishoeck et al 1996, 1998).

Evolution

Outline

▶ why?

▶ How?

▶ Chemistry in

■ Interstellar medium and the Hot Cores

■ Prestellar Cores and Young Protostars

About Prestellar cores

Gravitational bounded cores

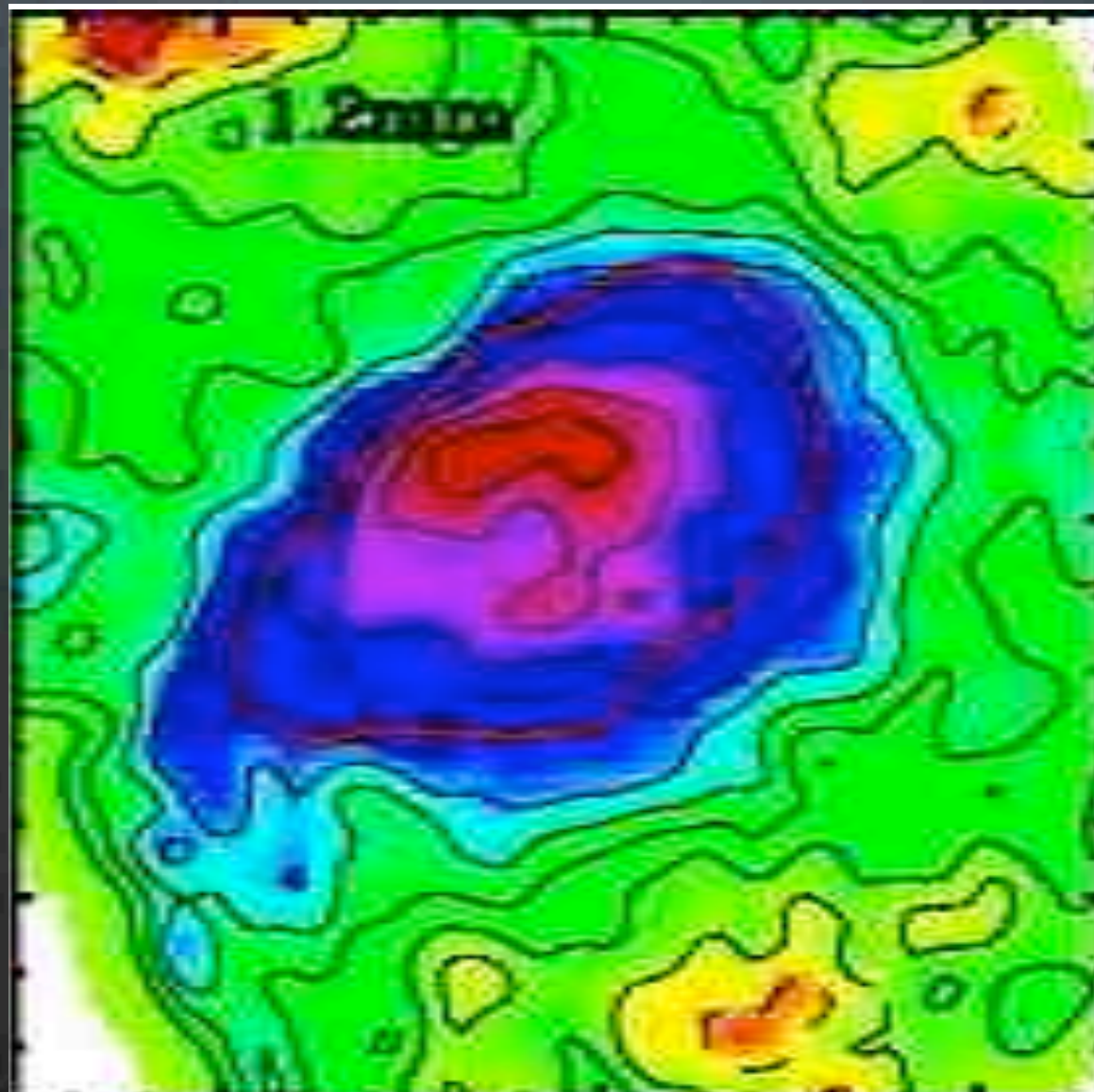
Central condensation
without protostellar objects
(No IR sources inside)

(Ward-Thompson et al. 1994).



L1498

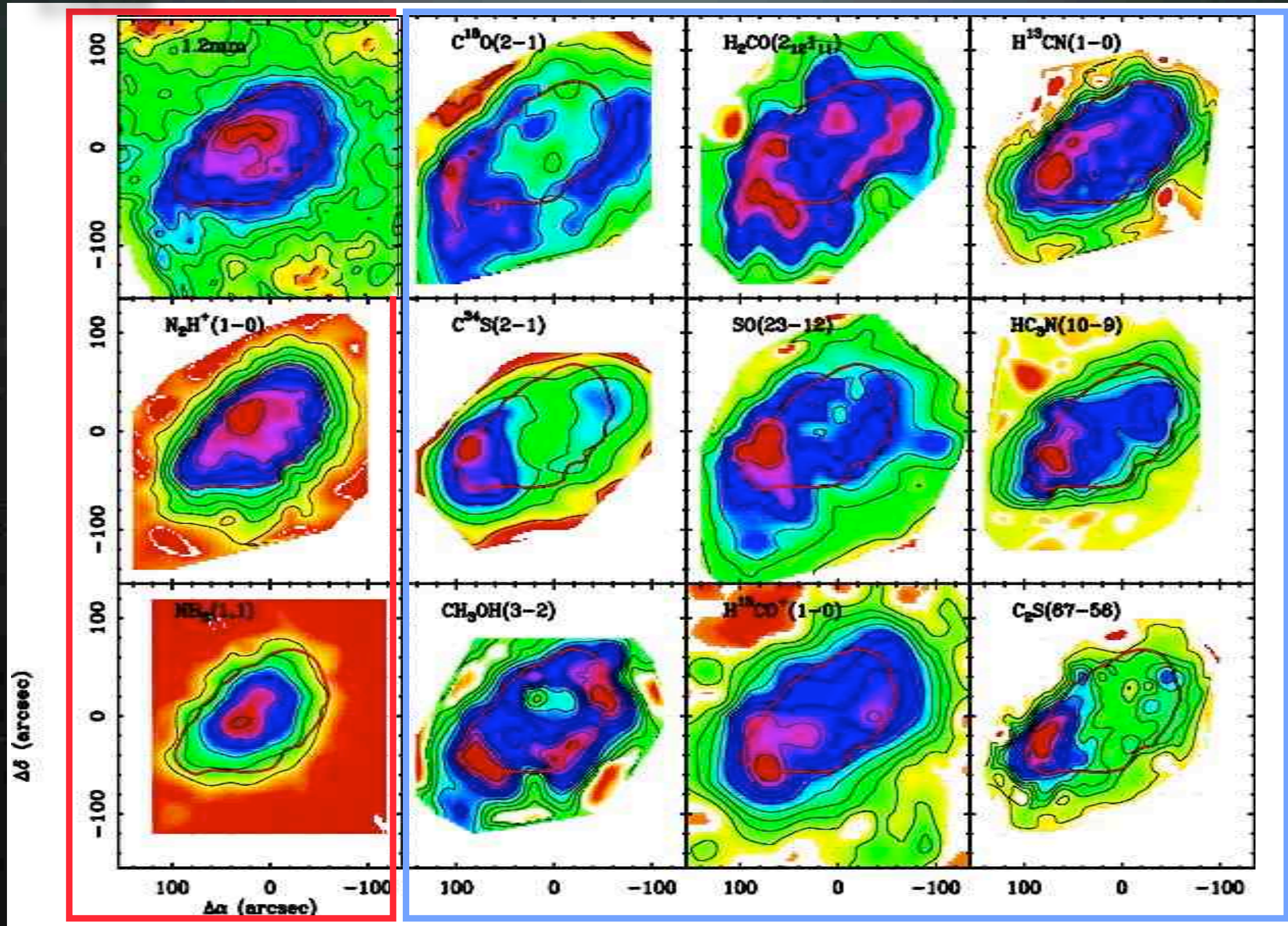
About Prestellar cores



Tafalla et al. 2006

L1498

About Prestellar cores

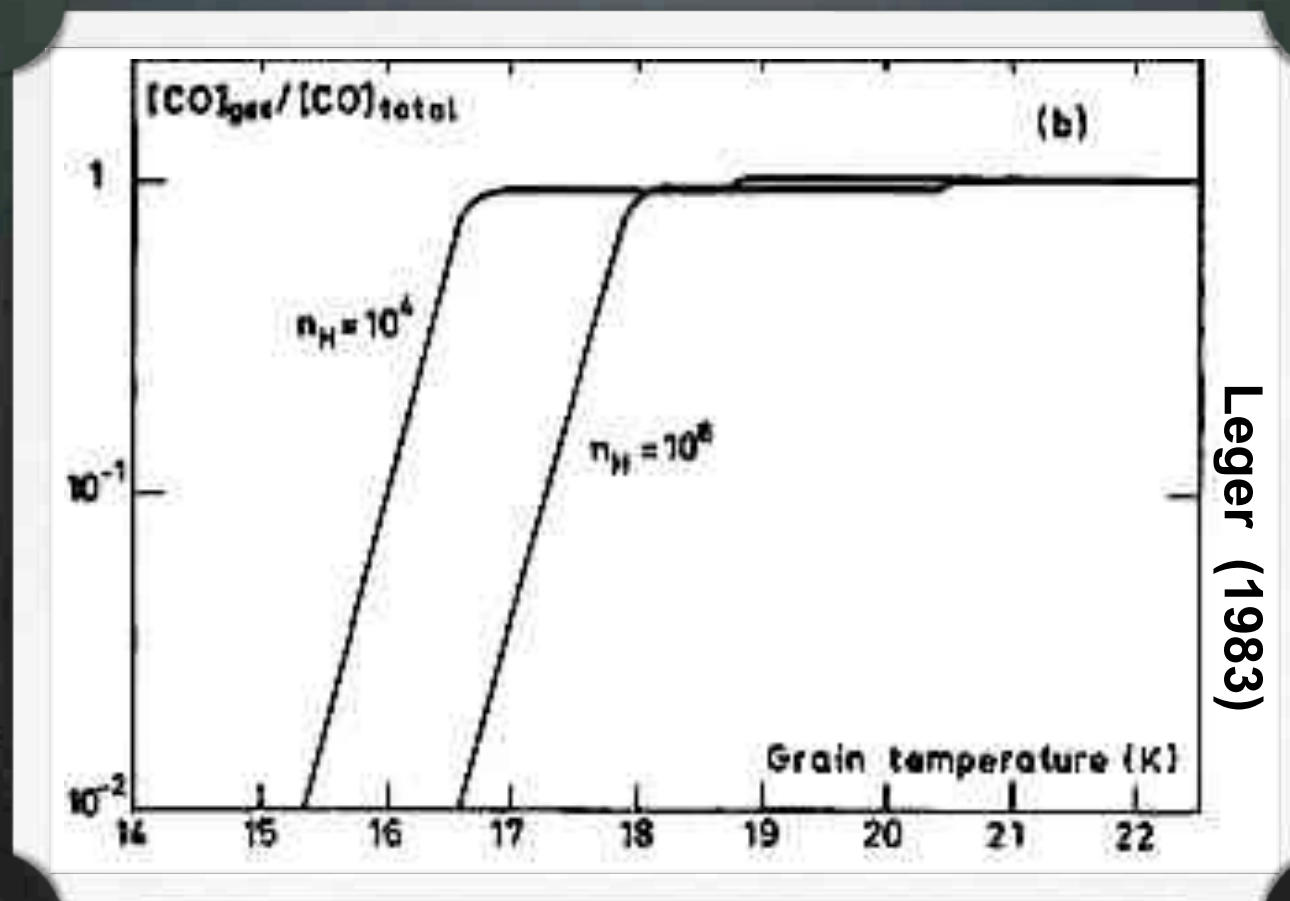


Tafalla et al. 2006

Depletion-Molecular freeze out

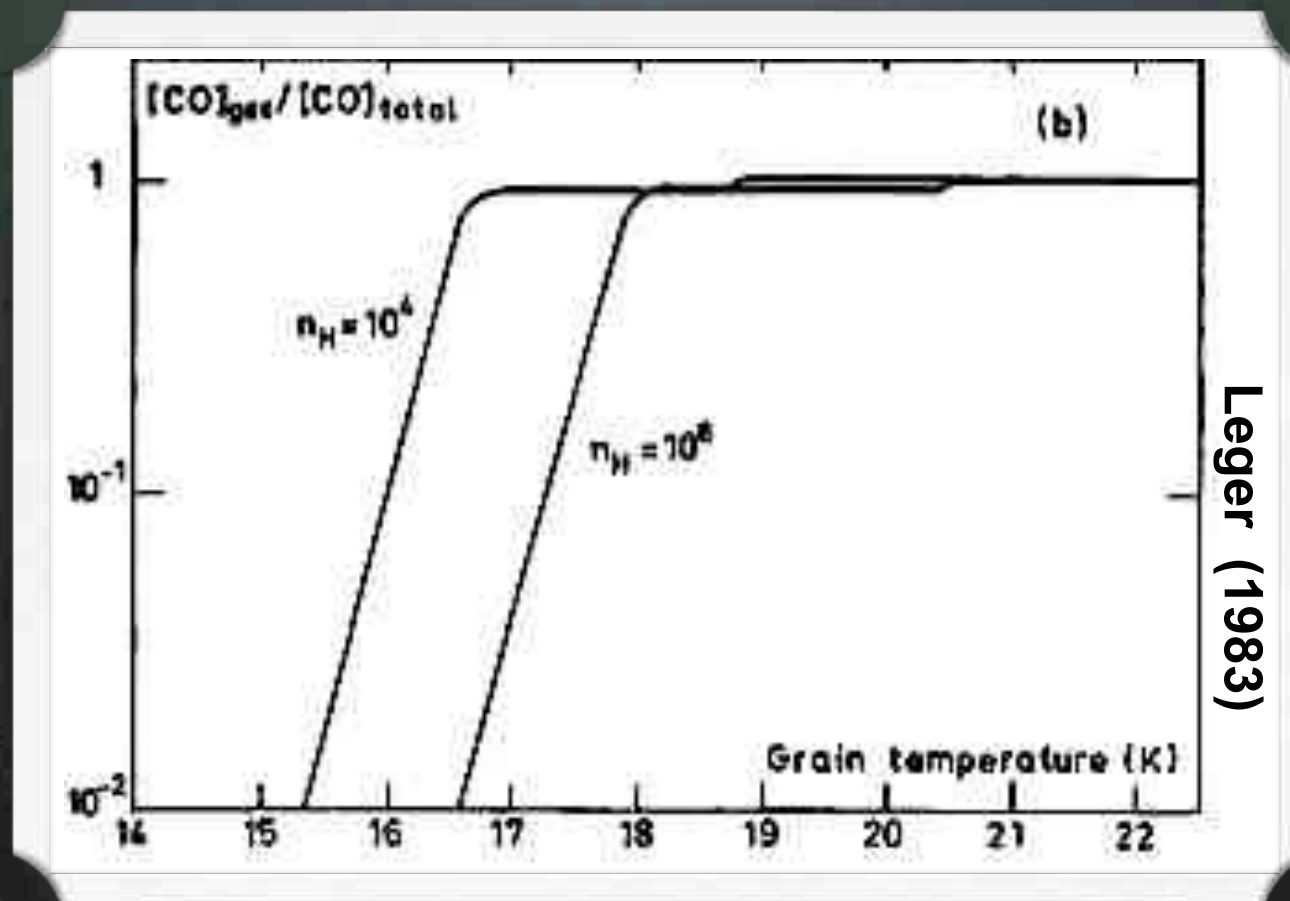
Depletion–Molecular freeze out

- ▶ Gas–grain equilibrium (sticking vs evaporation)
 - if $T_{\text{grain}} > T_{\text{freezeout}}$, most molecules in gas phase
 - if $T_{\text{grain}} < T_{\text{freezeout}}$, most molecules on grains



Depletion–Molecular freeze out

- ▶ Gas–grain equilibrium (sticking vs evaporation)
 - if $T_{\text{grain}} > T_{\text{freezeout}}$, most molecules in gas phase
 - if $T_{\text{grain}} < T_{\text{freezeout}}$, most molecules on grains

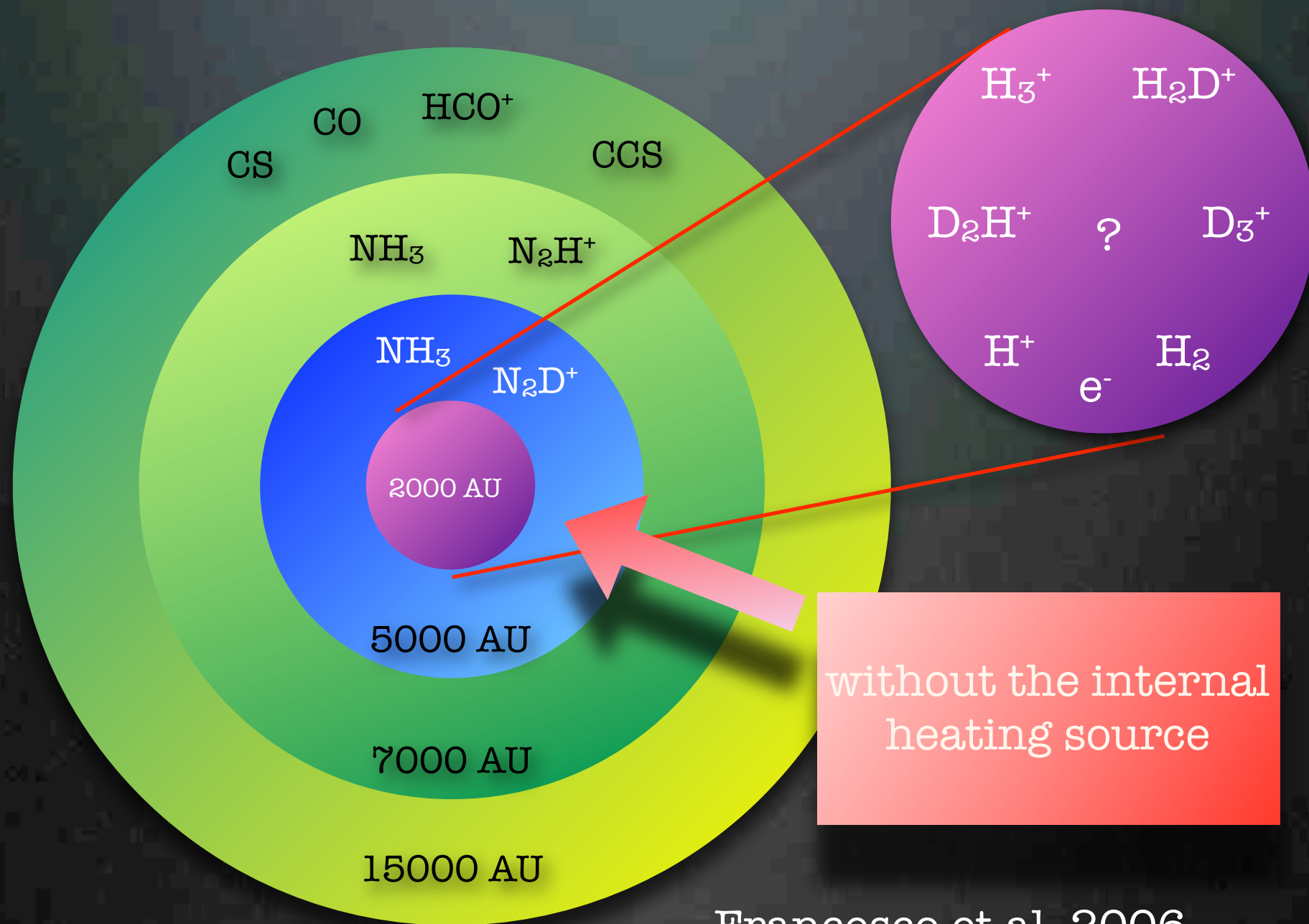


At low temperatures: molecules stick on grains and do not evaporate back to gas phase: freeze-out

Depletion–Molecular freeze out

- ▶ Most species disappear from gas phase at $\approx 5 \times 10^4 \text{ cm}^{-3}$
 - CO, CS, HCN, HCO^+ , H_2CO , C_2S , CH_3OH , SO, HC_3N , C_3H_2 , ...
 - poor tracers of core interior
- ▶ Only survivors
 - (H_2) , NH_3 , N_2H^+ , H_3^+ and D–isotopologues (i.e., H_2D^+)
 - only line tracers of internal core (dust in continuum)

About Prestellar cores



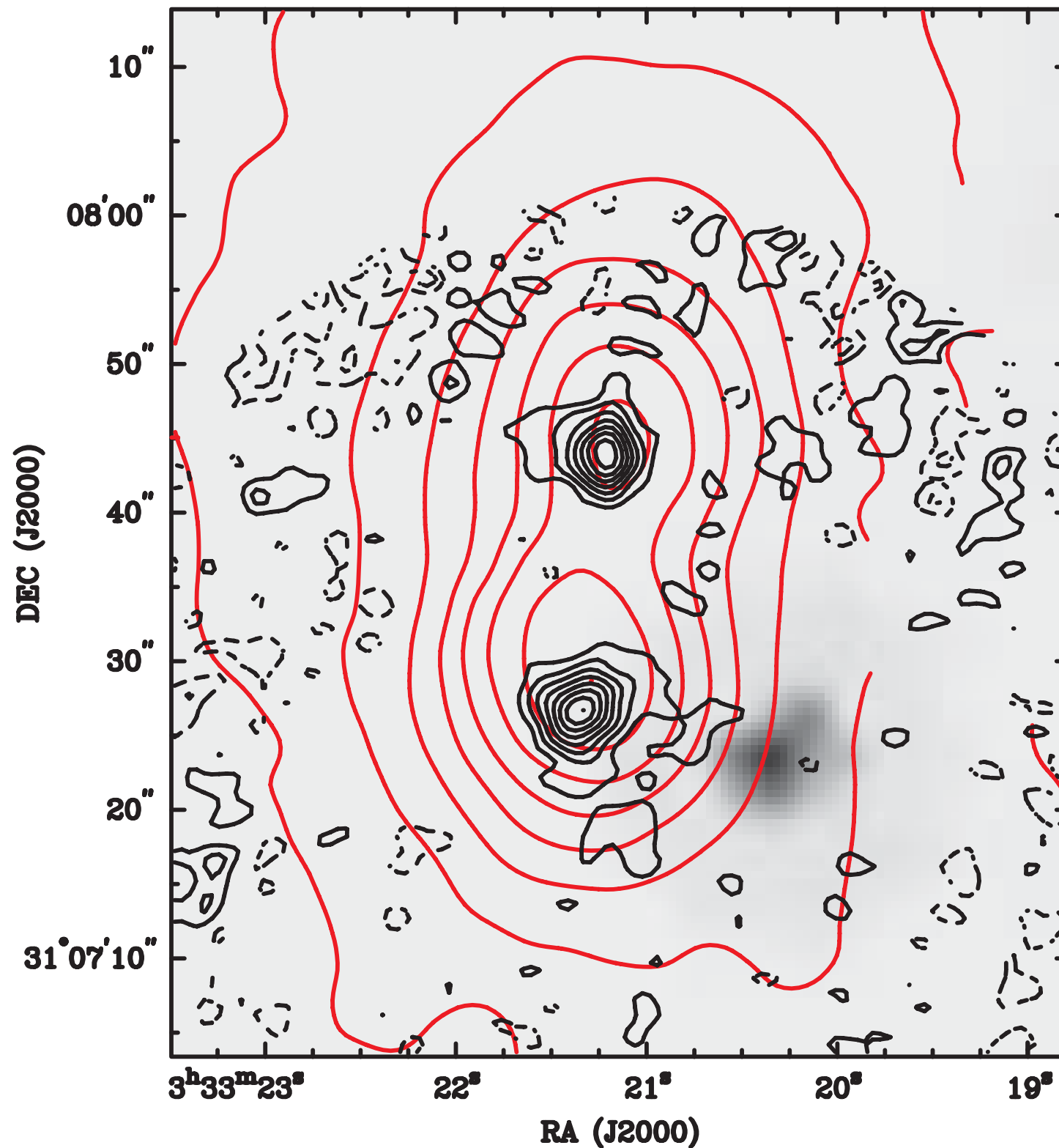
Francesco et al. 2006

About Prestellar cores

Barnard 1-b

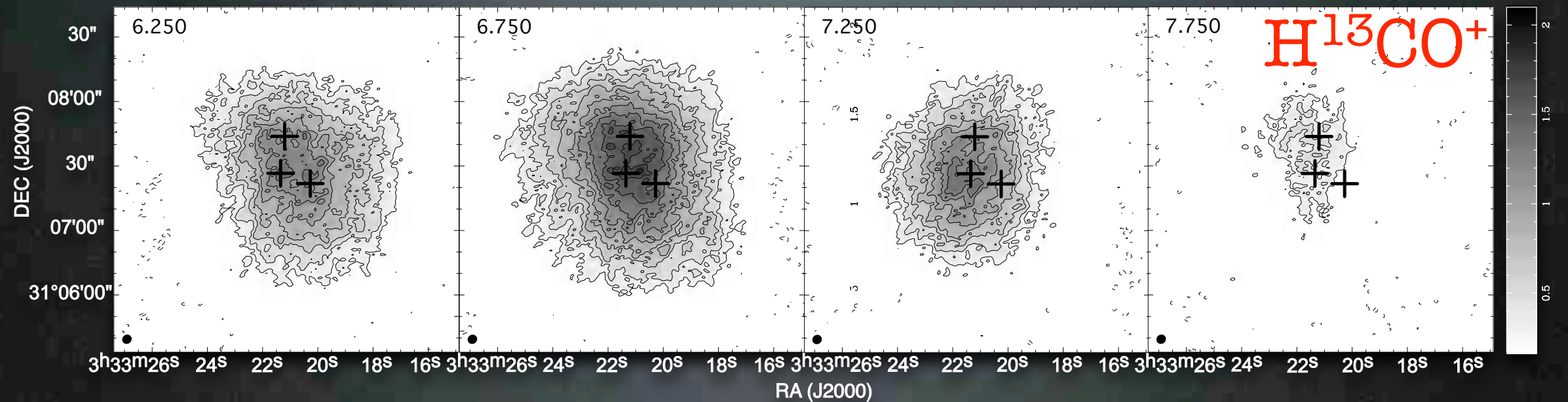
About Prestellar cores

Barnard



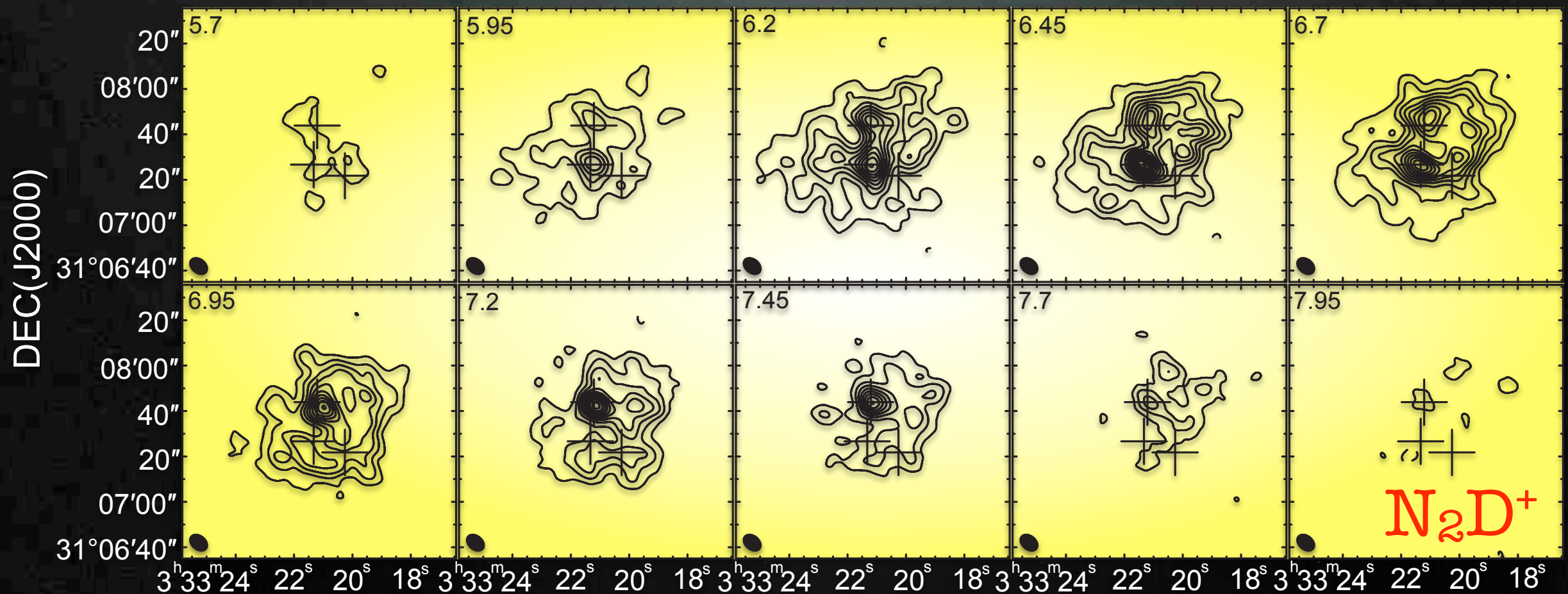
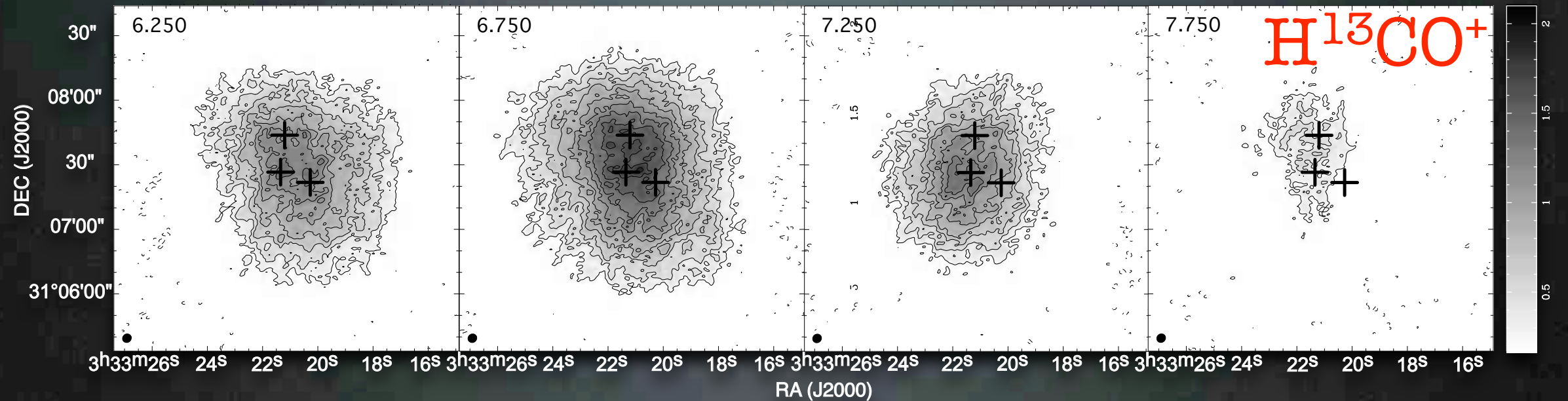
About Prestellar cores

Barnard 1-b

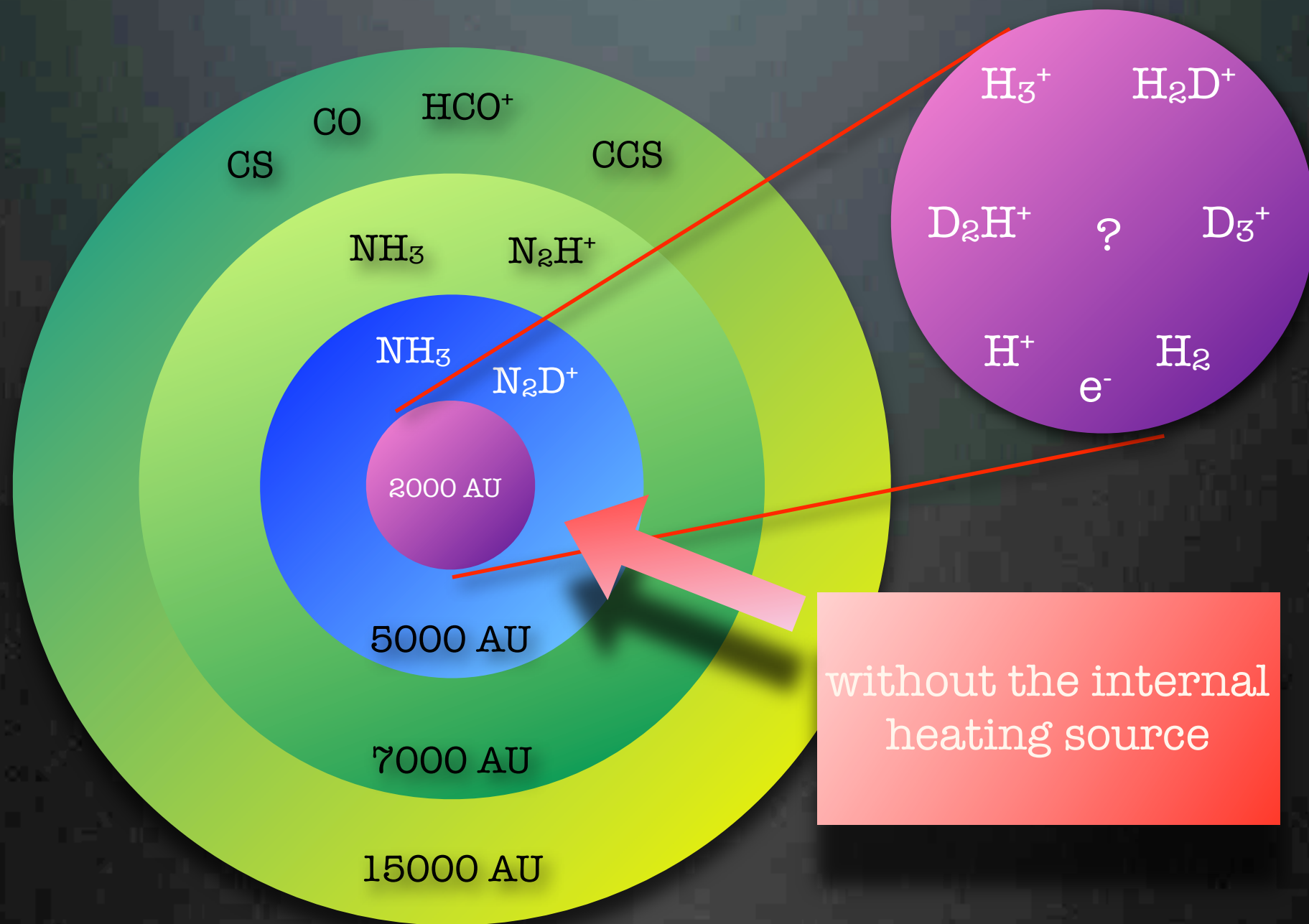


About Prestellar cores

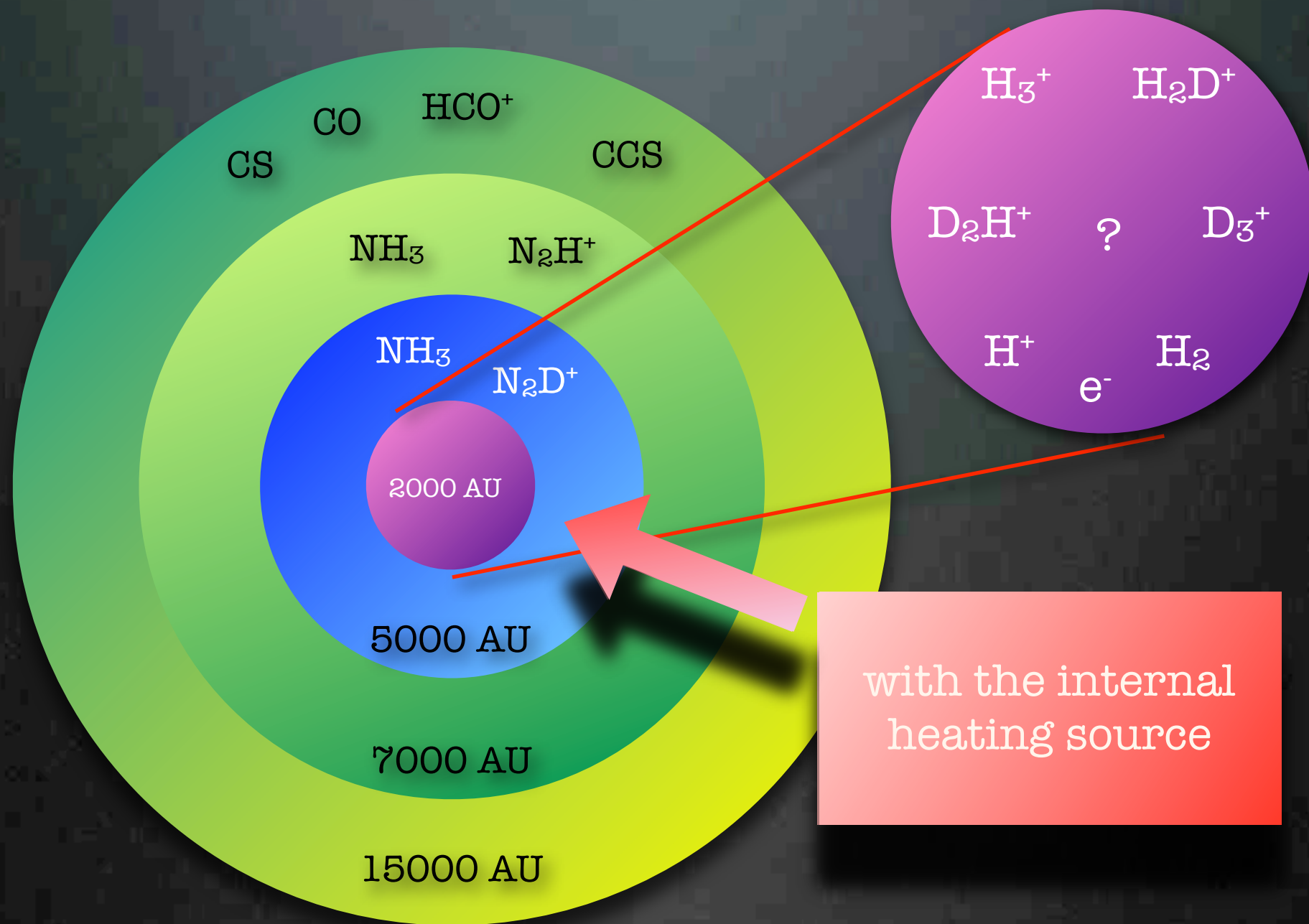
Barnard 1-b



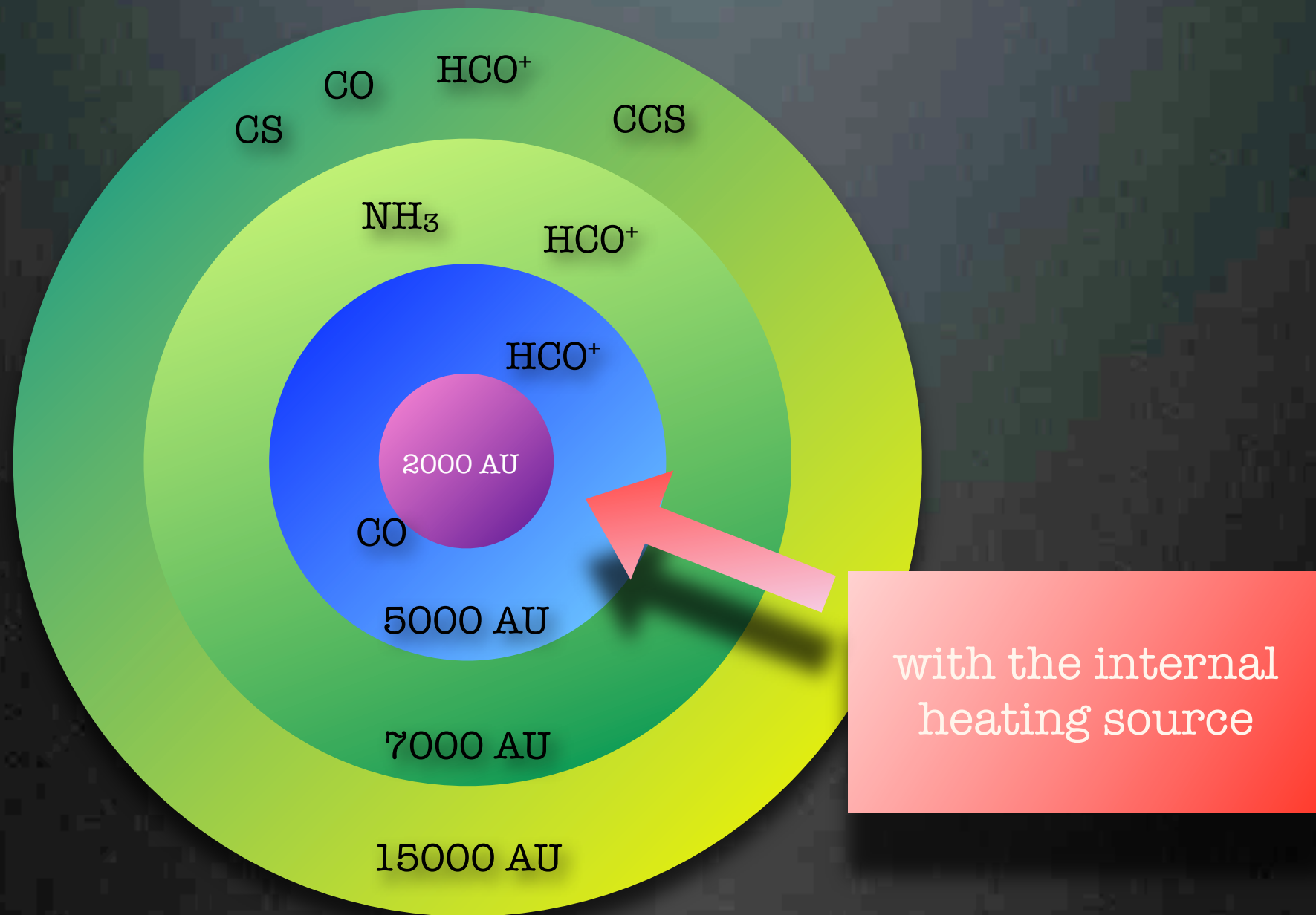
About Deeply Embedded Young Stellar Objects



About Deeply Embedded Young Stellar Objects

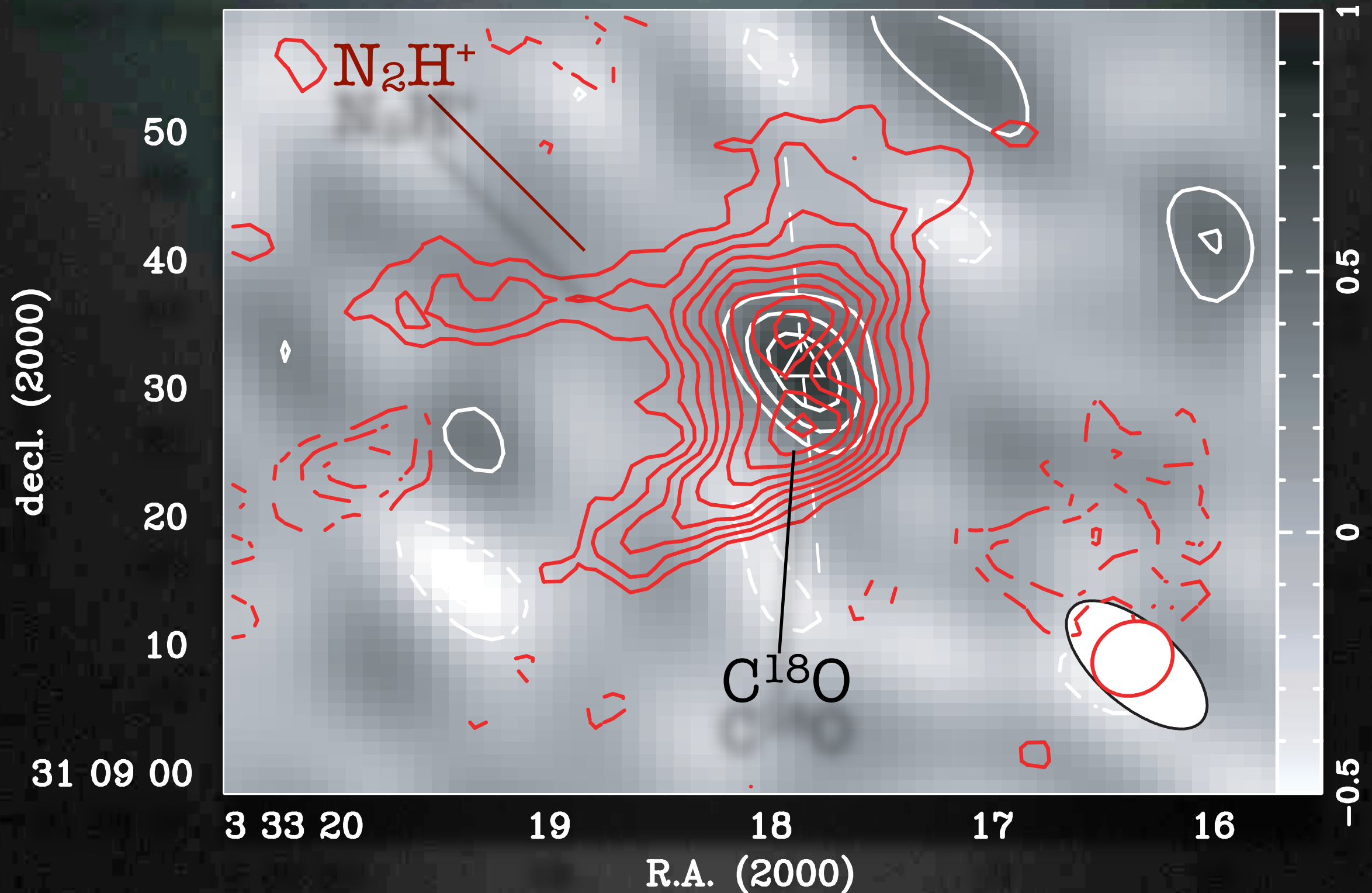


About Deeply Embedded Young Stellar Objects



About Deeply Embedded Young Stellar Objects

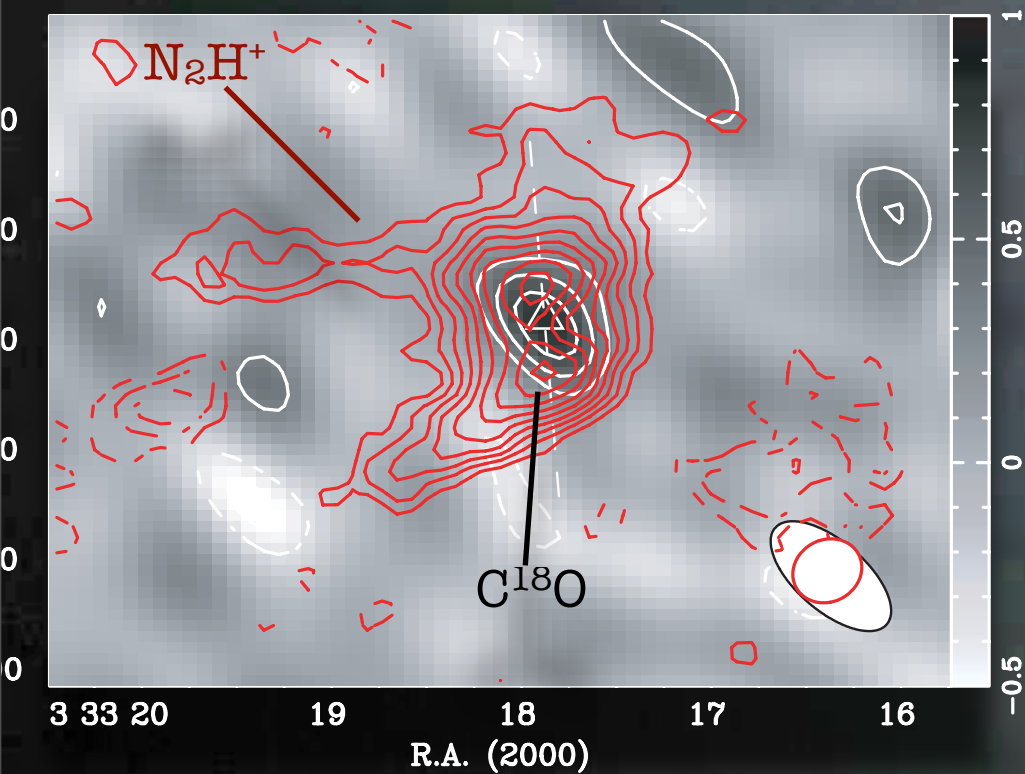
Barnard 1-c
class 0 source



Matthews et al. 2006

About Deeply Embedded Young Stellar Objects

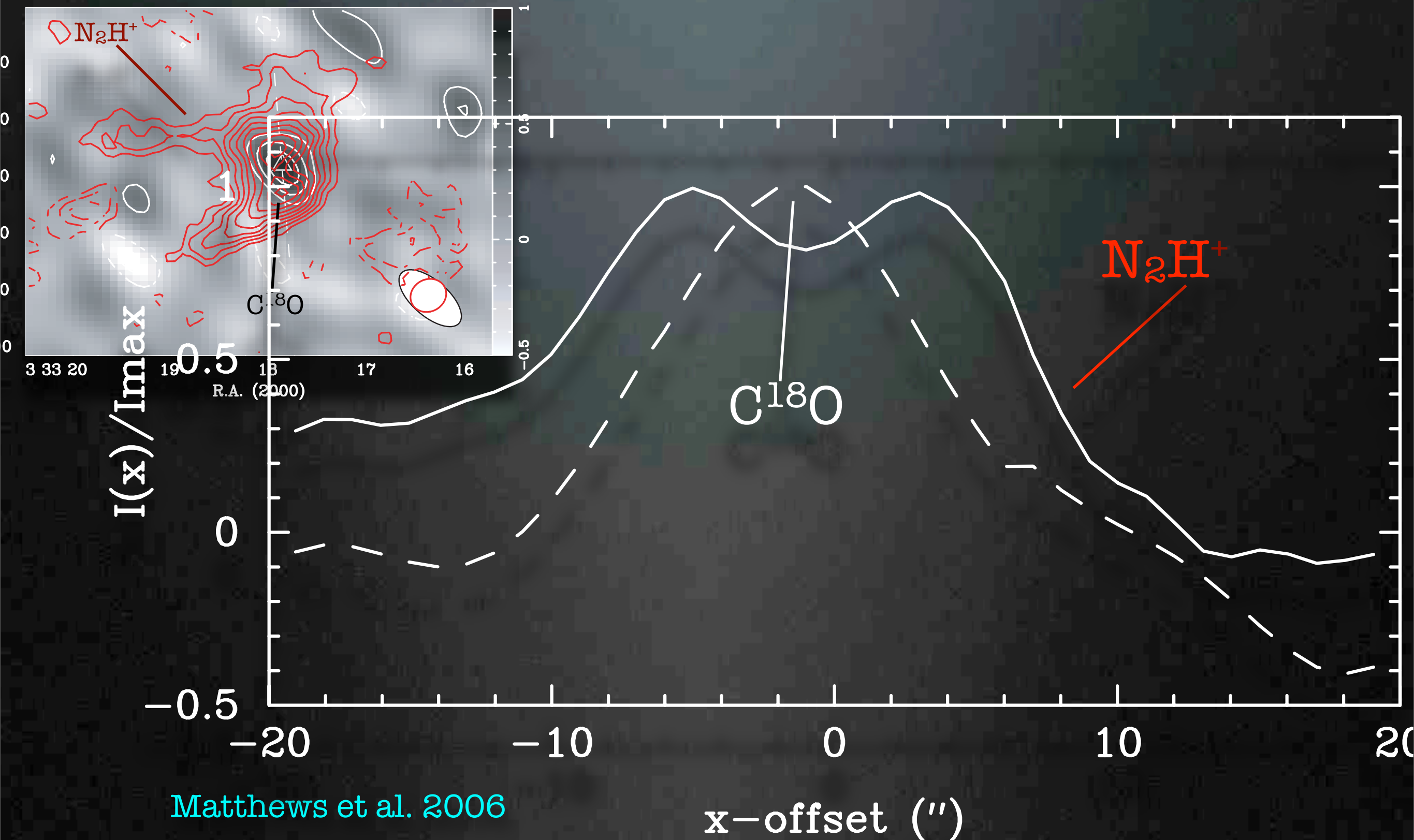
Barnard 1-c
class 0 source



Matthews et al. 2006

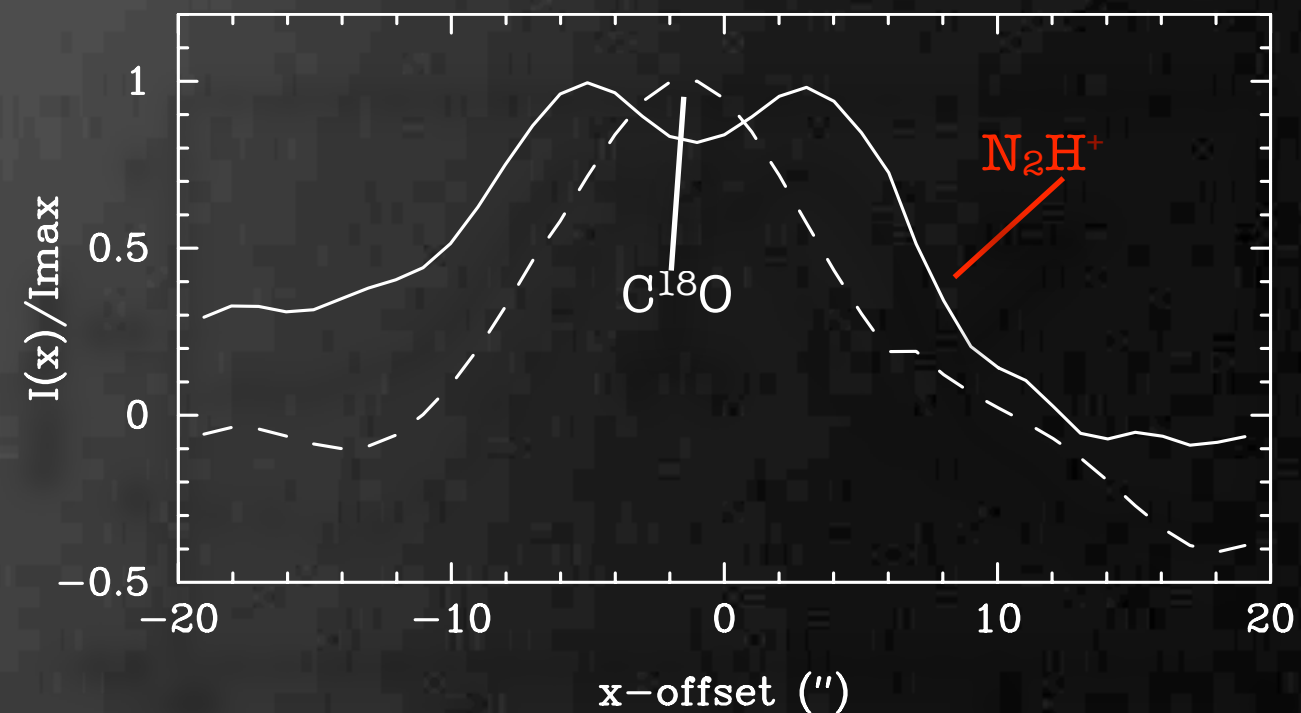
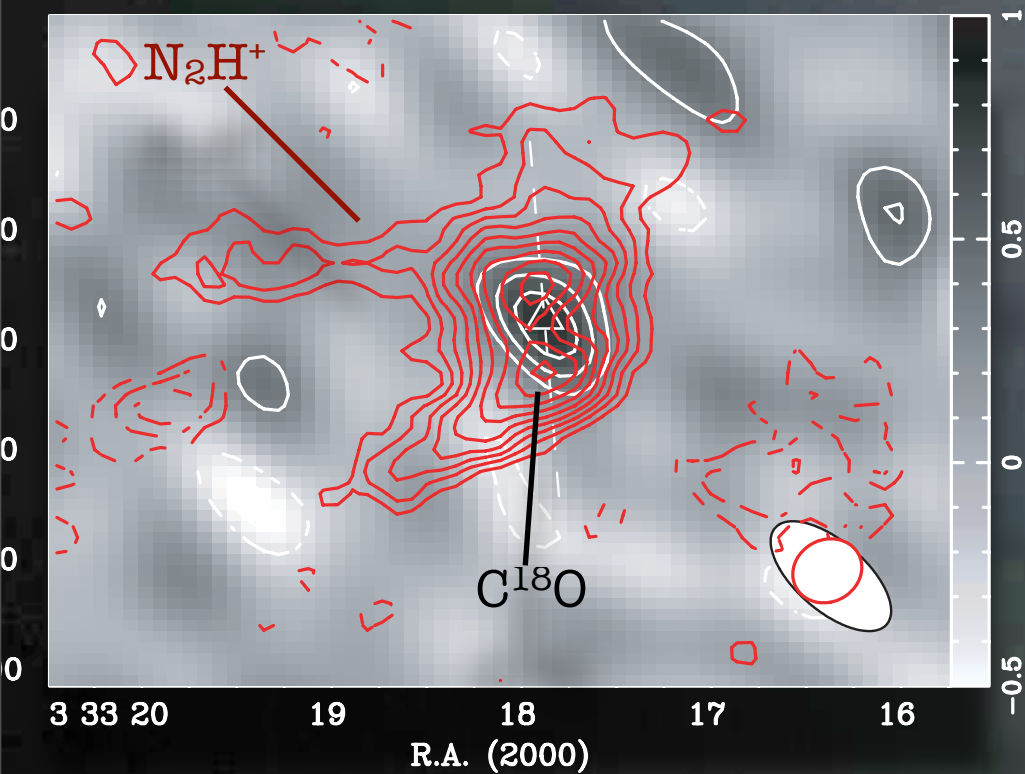
About Deeply Embedded Young Stellar Objects

Barnard 1-c
class 0 source



About Deeply Embedded Young Stellar Objects

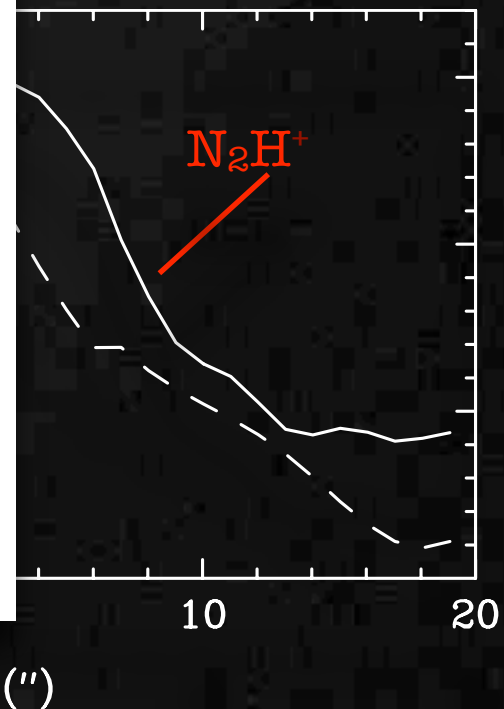
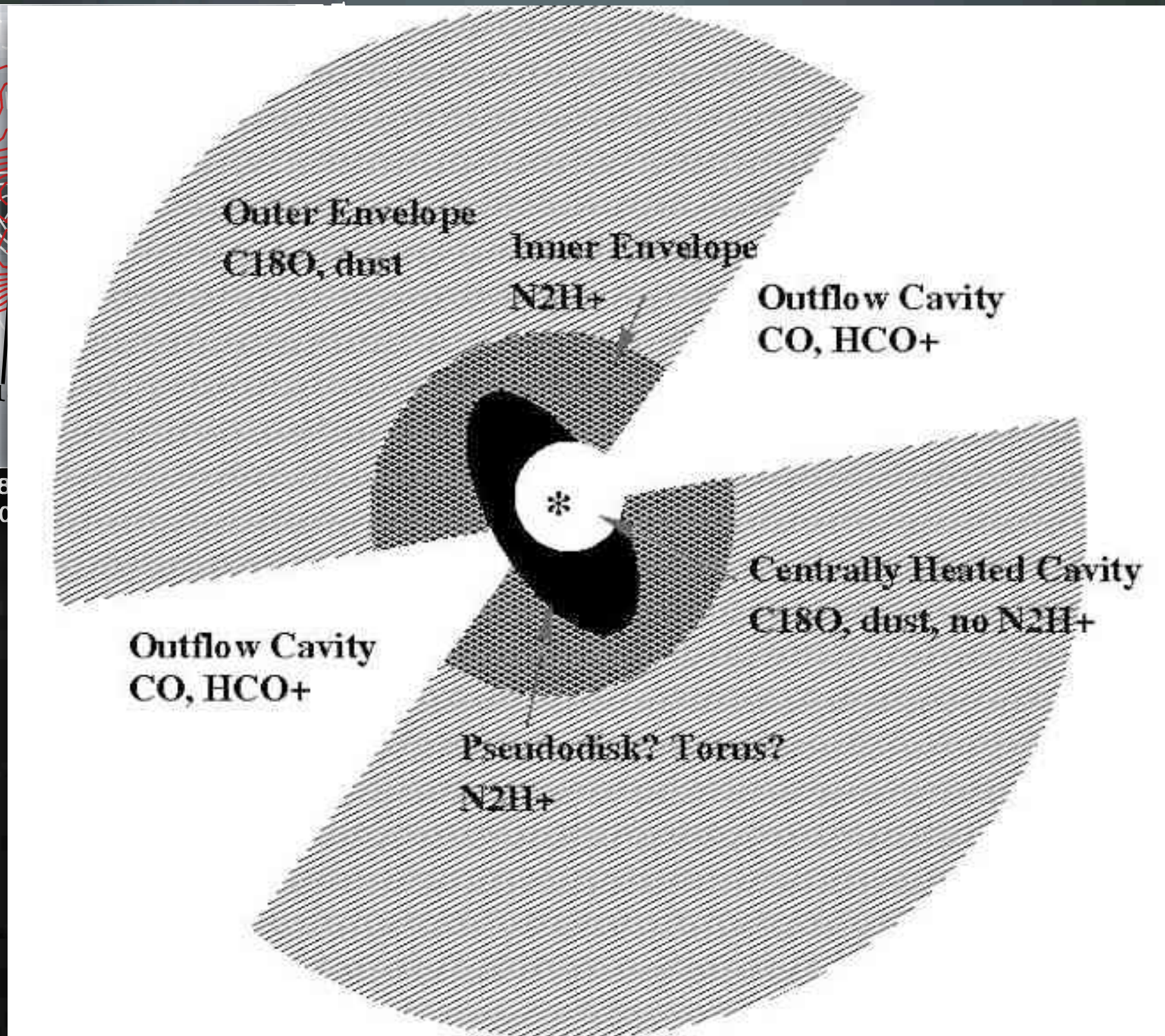
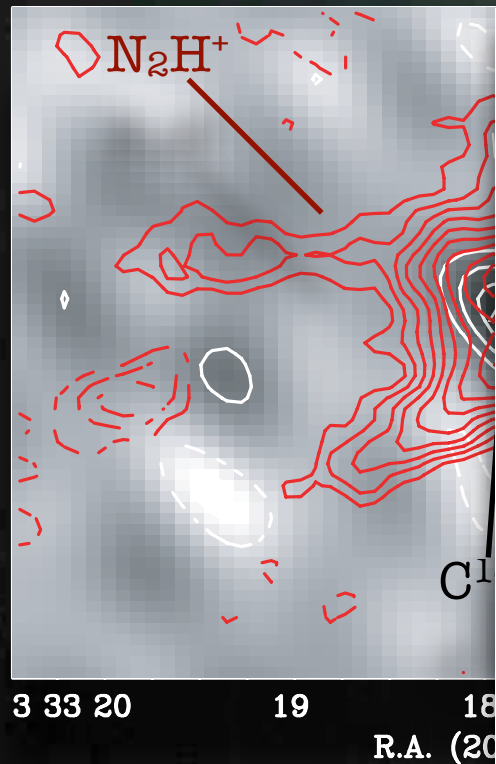
Barnard 1-c
class 0 source



Matthews et al. 2006

About Deeply Embedded Young Stellar Objects

Barnard 1-c
class 0 source



Matthews et al. 2006

About Deeply Embedded Young Stellar Objects



About Deeply Embedded Young Stellar Objects



1. The gas is heated by the collisions with the warm dust. This implies that within $r < 60$ AU of the young star, the infall gas is heated to 100 K, resulting in the sublimation of H_2O -rich ices into the gas.

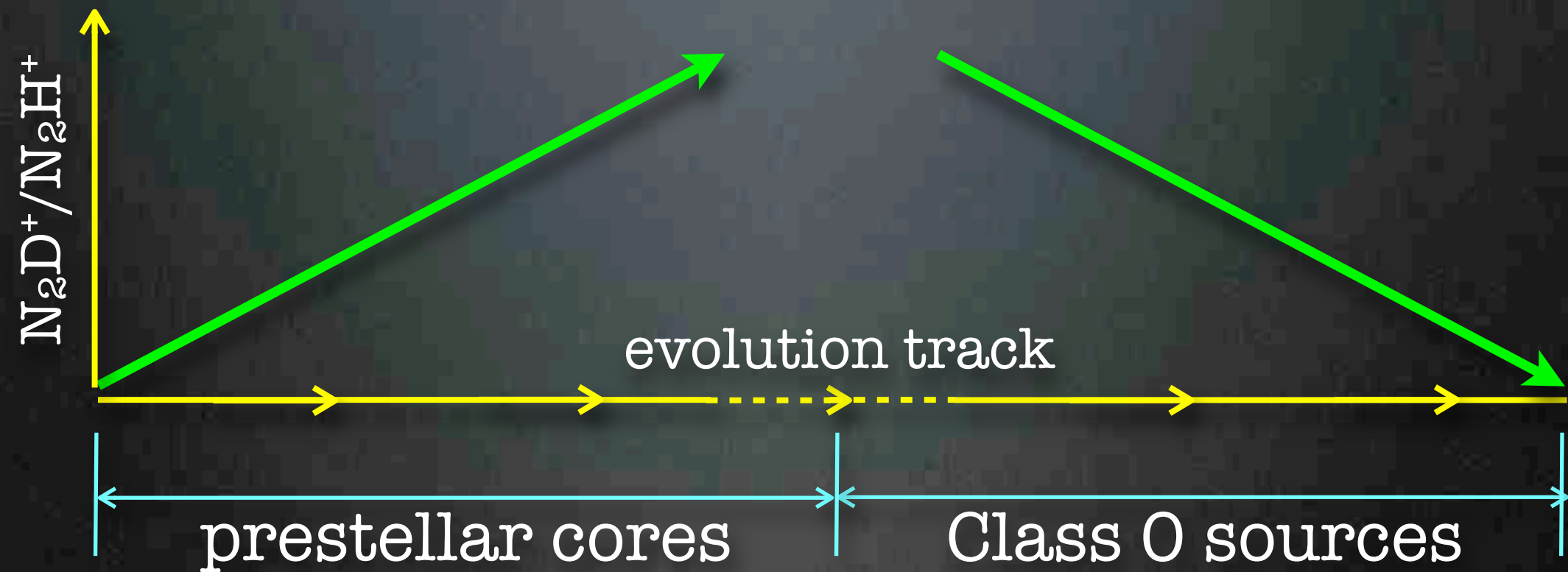
About Deeply Embedded Young Stellar Objects



1. The gas is heated by the collisions with the warm dust. This implies that within $r < 60$ AU of the young star, the infall gas is heated to 100 K, resulting in the sublimation of H_2O -rich ices into the gas.
2. In addition, once the gas is heated to 200–300 K, the gas-phase chemical reaction convert O and H_2 , resulting in high abundances of H_2O in the inner 10–100 AU.

Between prestellar and early protostar stage

Between prestellar and early protostar stage



Between prestellar and early protostar stage

Therefore, the understanding of chemistry lets us to study :

1. the initial condition of the star formation
2. the physical condition and kinematics of different sources with different evolutionary stages.

Future

- ▶ Higher angular resolution observations (lower beam dilution and good resolution) can not only help us to understand the chemistry properties itself more, but also help us to understand the physical condition around the star formation in detail.

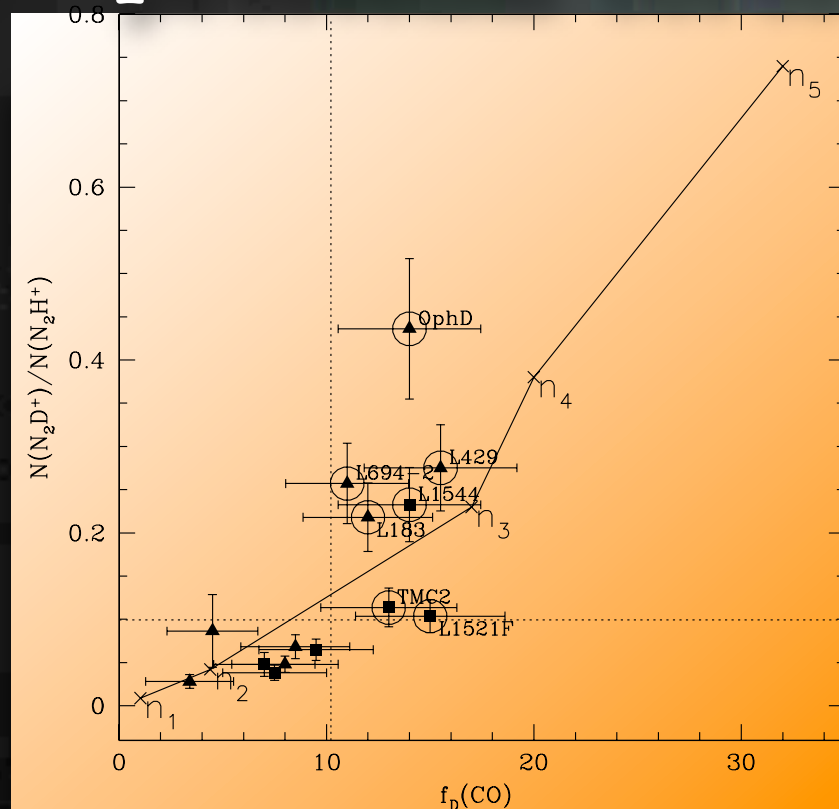
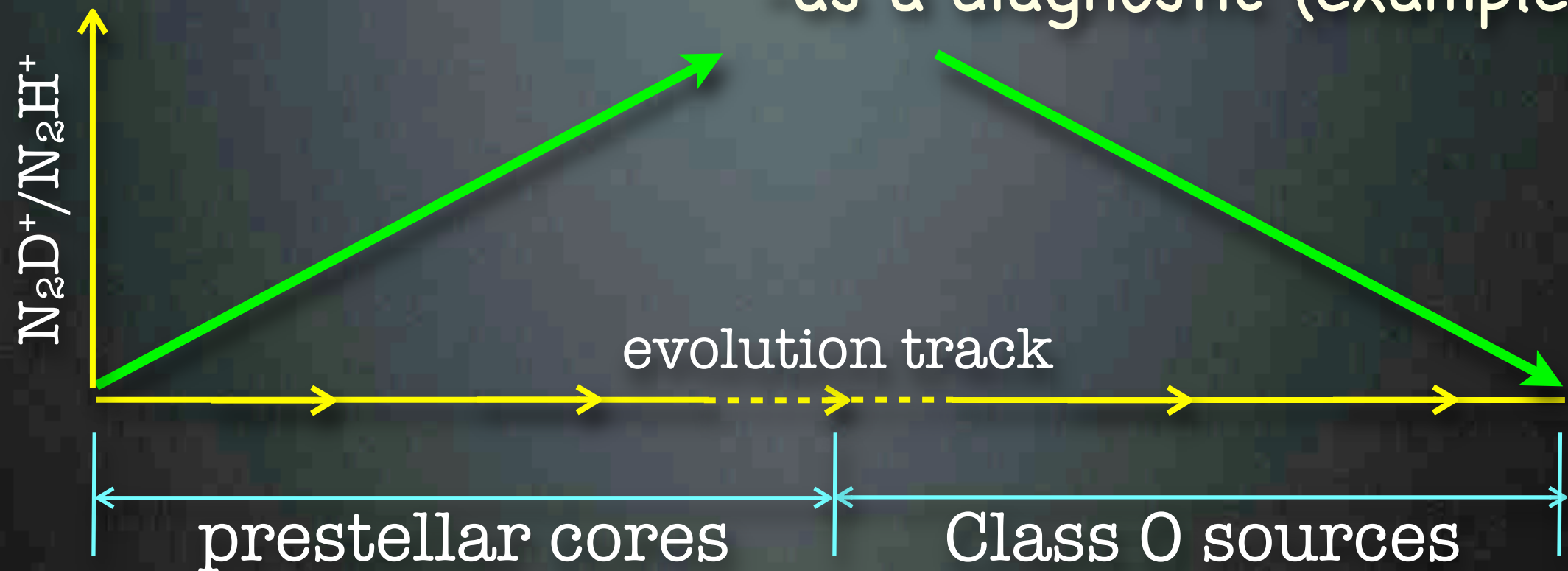


Thank you very much for your attention!

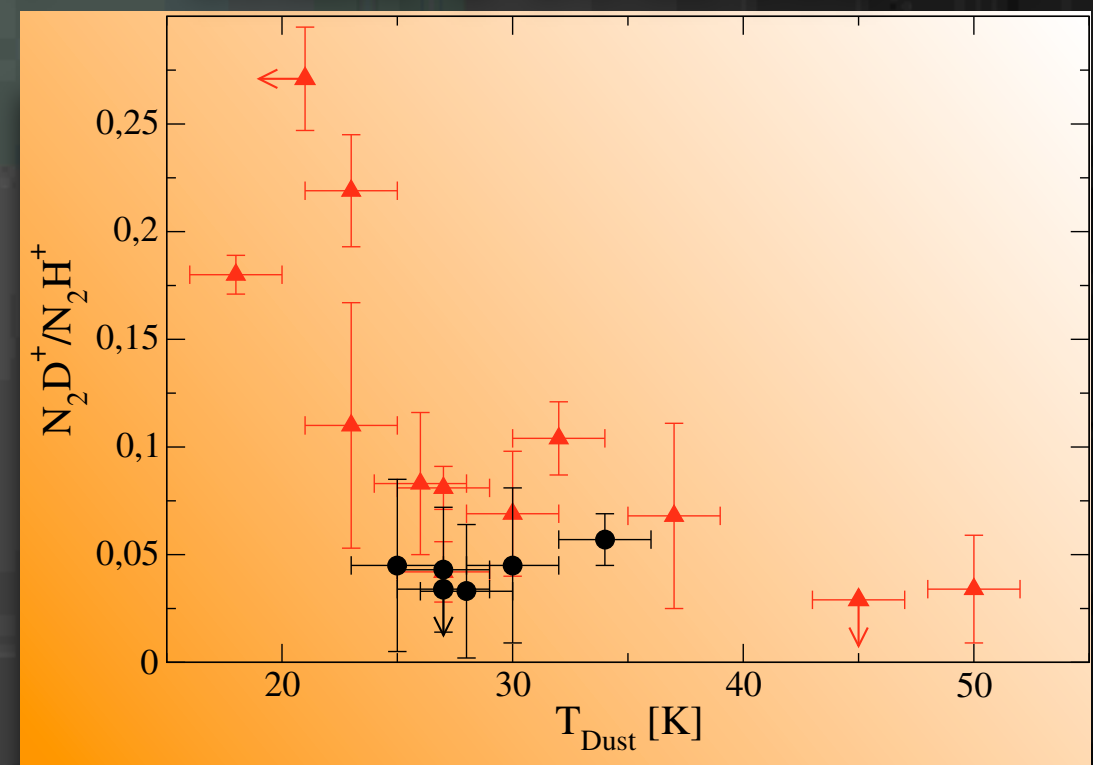


Why Chemistry?

-as a diagnostic (example)



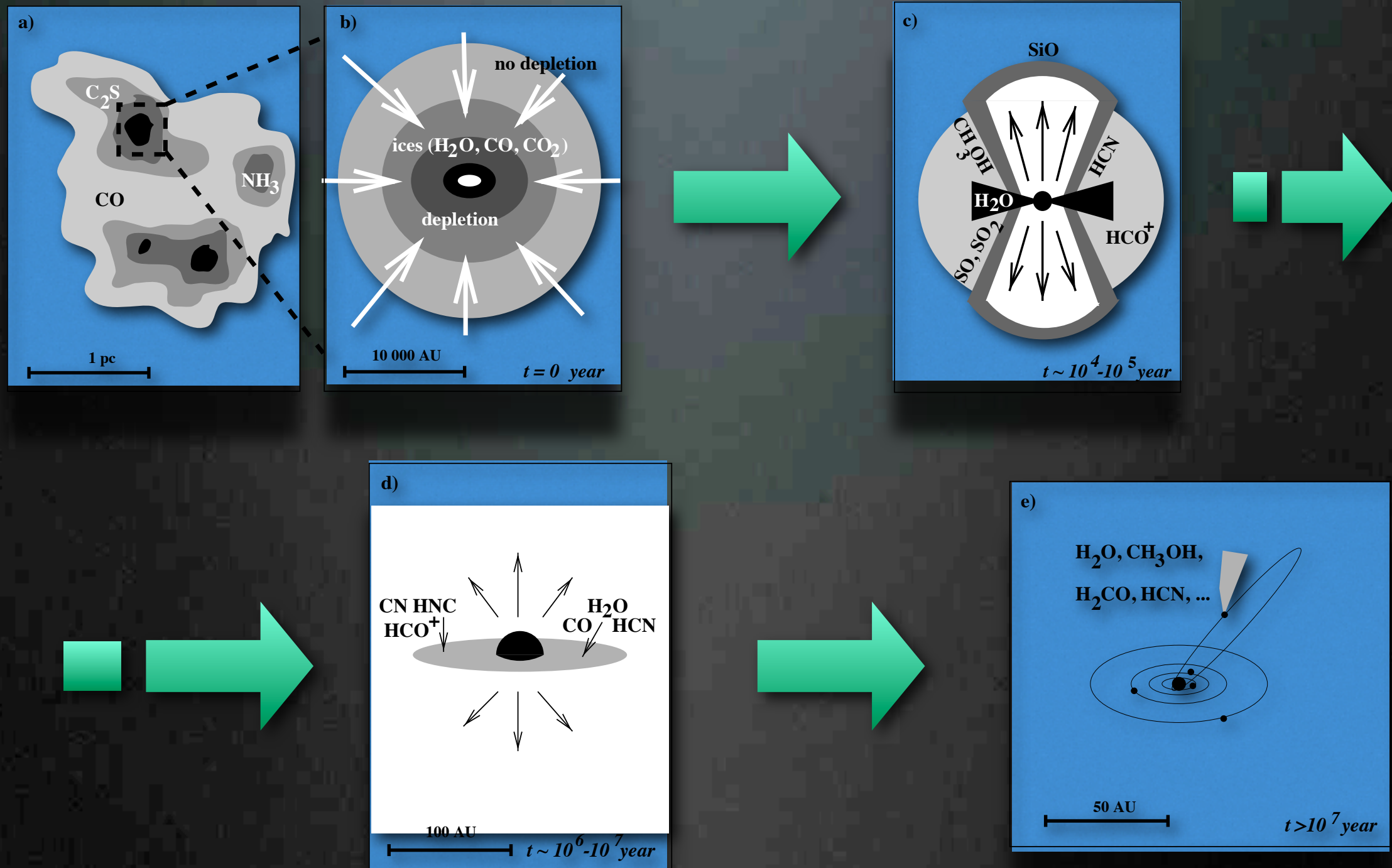
Crapsi et al. 2005



Emprechtinger et al. 2009

Why Chemistry?

-as a diagnostic

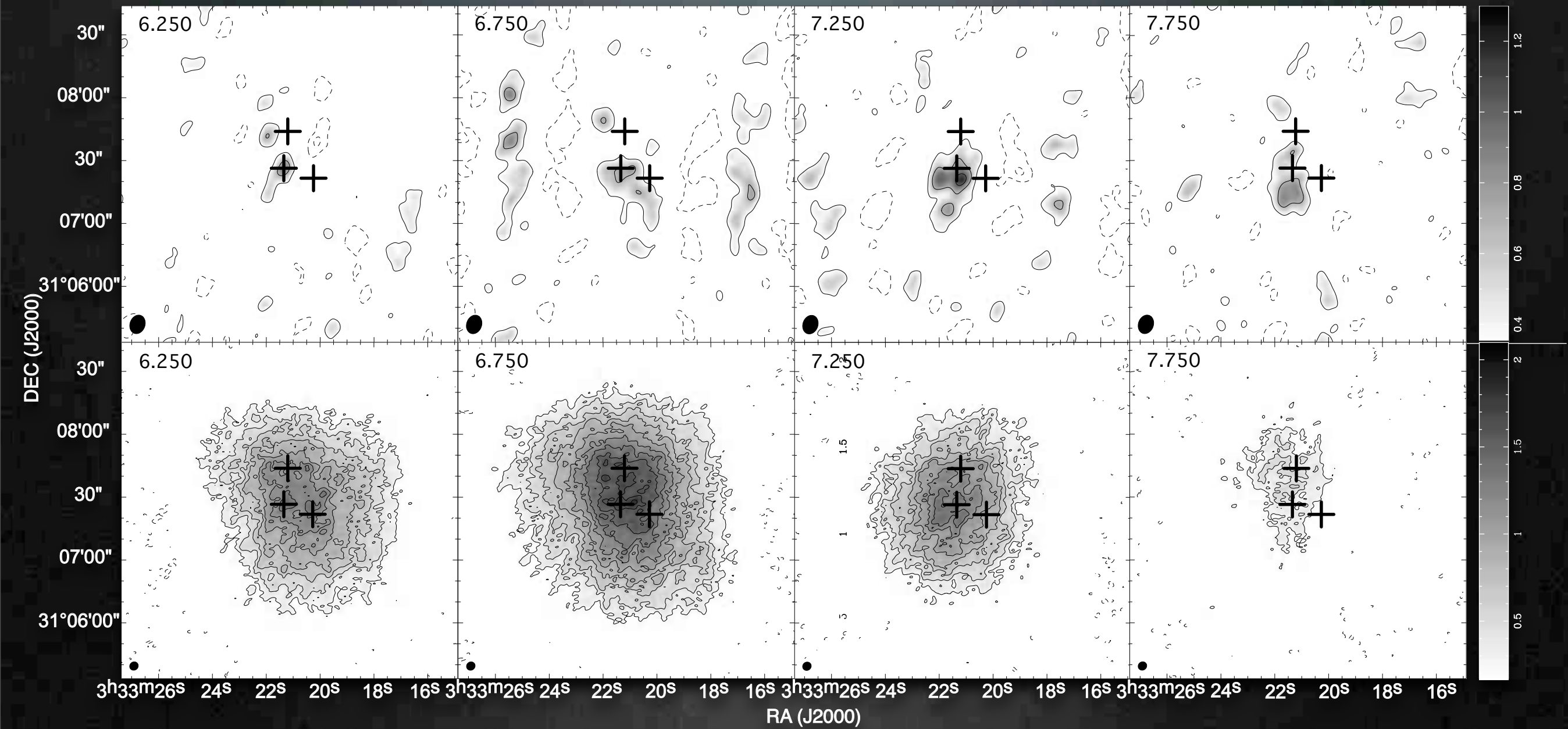


van Dishoeck & Blake 1998

Increased deuteration due to CO depletion

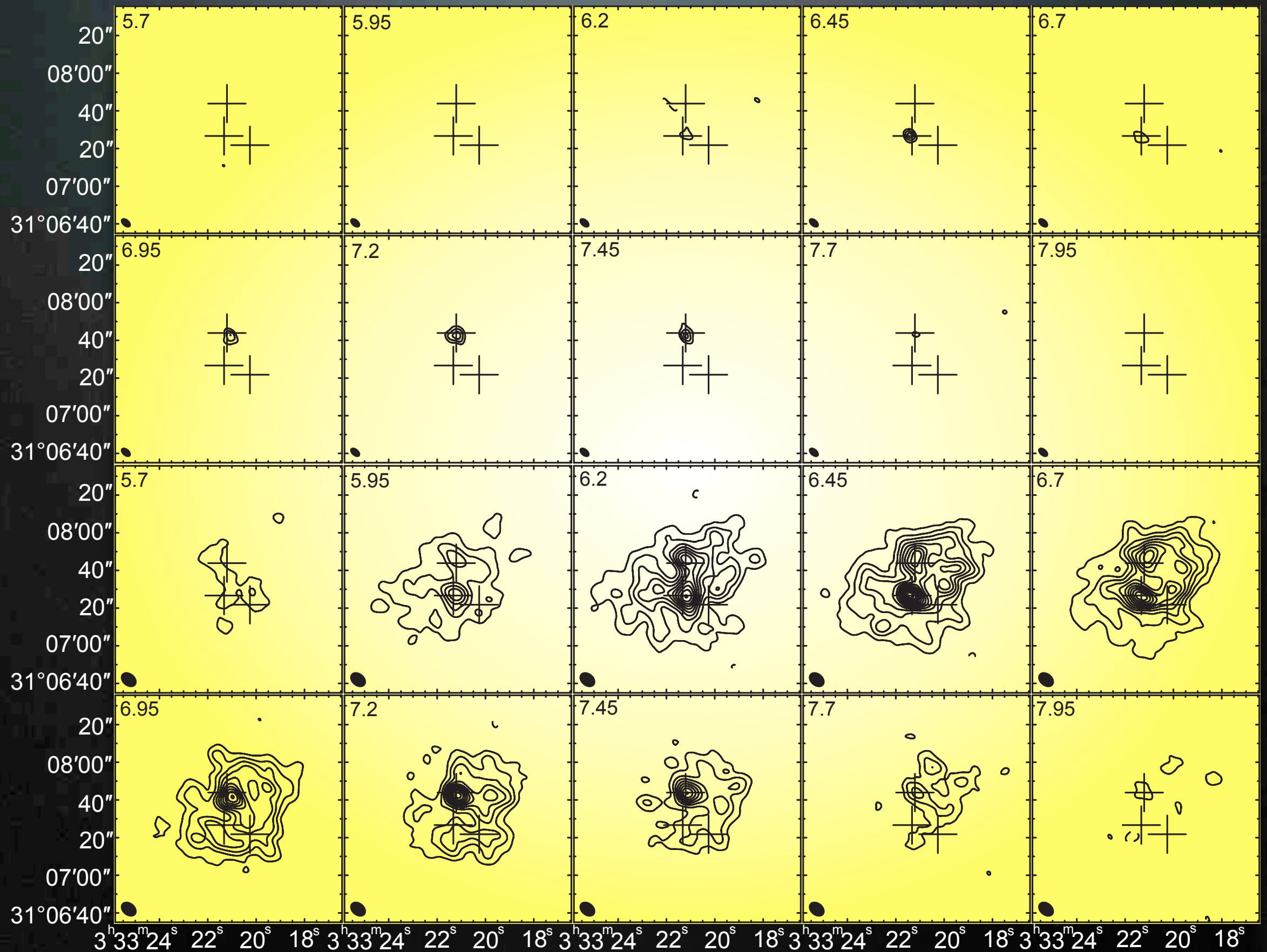
- CO depletion has profound consequences in core chemistry
 - triggers a number of second-order effects
- Deuterium fractionation of molecules is driven by
$$\text{H}_3^+ + \text{HD} \rightleftharpoons \text{H}_2\text{D}^+ + \text{H}_2 + 230 \text{ K}$$
- At low temperature (e.g., 10 K), H_2D^+ is enhanced – Deuterium is passed down to other species such as DCO, DCN
- If no CO depletion
 - H_2D^+ abundance is limited by CO destruction (+e) – D enrichment of order of 1-10 %
- If CO depletion (and low e)
 - H_2D^+ is further enhanced, which further enhances N_2D^+ , NH_2D , etc.

H^{13}CO^+



N_2D^+

DEC(J2000)



Fundamentals of Interstellar Chemistry

杜福君
DU, FUJUN



References:

- [1] ~~W.W. Duley & D.A. Williams 1984, Interstellar Chemistry~~
- [2] A.G.G.M. Tielens 2005, The physics and Chemistry of the Interstellar Medium

IMPRS Retreat

THE SUNYAEV-ZEL'DOVICH EFFECT

Xun Shi

Felipe Navarrete

Brenda Miranda

Braunfels, Germany

September 16, 2009



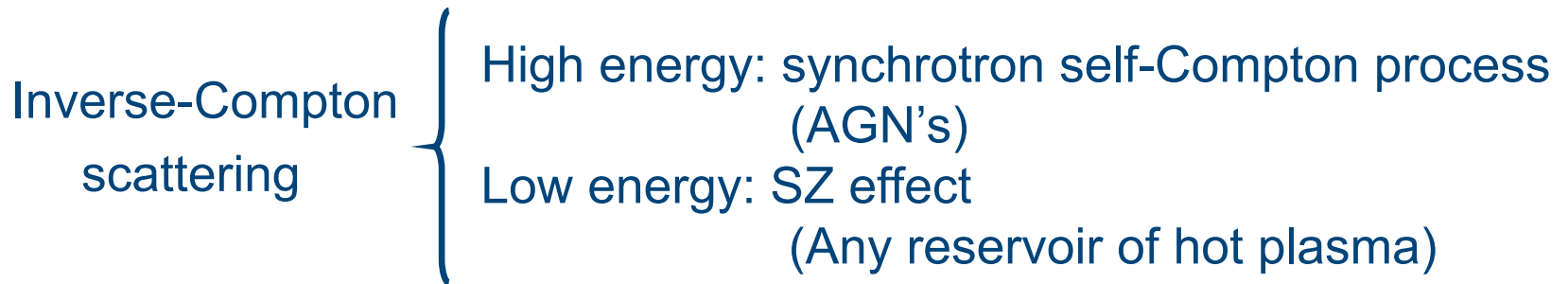
Outline



*All
inclusive!!!*

1. Introduction
2. The physics of the Sunyaev-Zel'dovich effect
3. Measurement techniques
4. Astrophysical applications of SZ effect

1. Introduction: Astrophysical Context



1. Cosmological probe
2. Study the gas properties of galaxy clusters
3. Study the evolution of structure in the Universe
4. Redshift independent

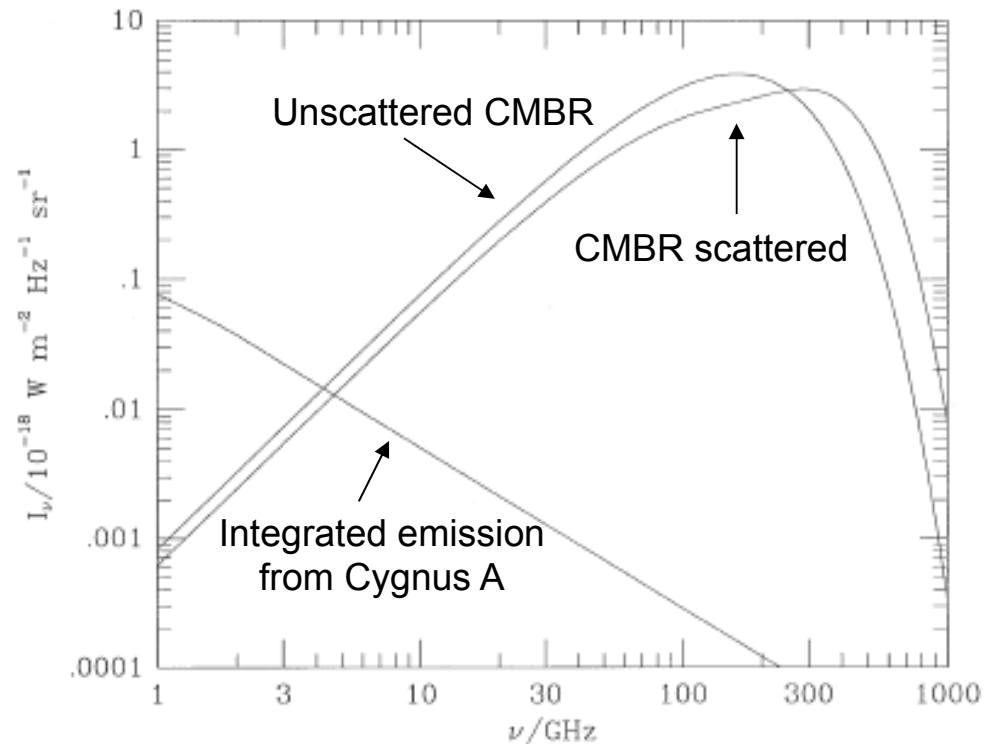
1. Introduction: CMBR

Cosmic Microwave Background Radiation (CMBR)

- Isotropic
- $T_{\text{rad}} \sim 2.725 \text{ K}$
- Specific intensity

$$I_{\nu} = \frac{2h\nu^3}{c^2} (e^{h\nu/k_B T_{\text{rad}}} - 1)^{-1}$$

- $\nu_{\text{max}} \sim 160 \text{ GHz}$
- $\lambda_{\text{max}} \sim 1.9 \text{ mm}$



1. Introduction: CMBR

Origin of the CMB

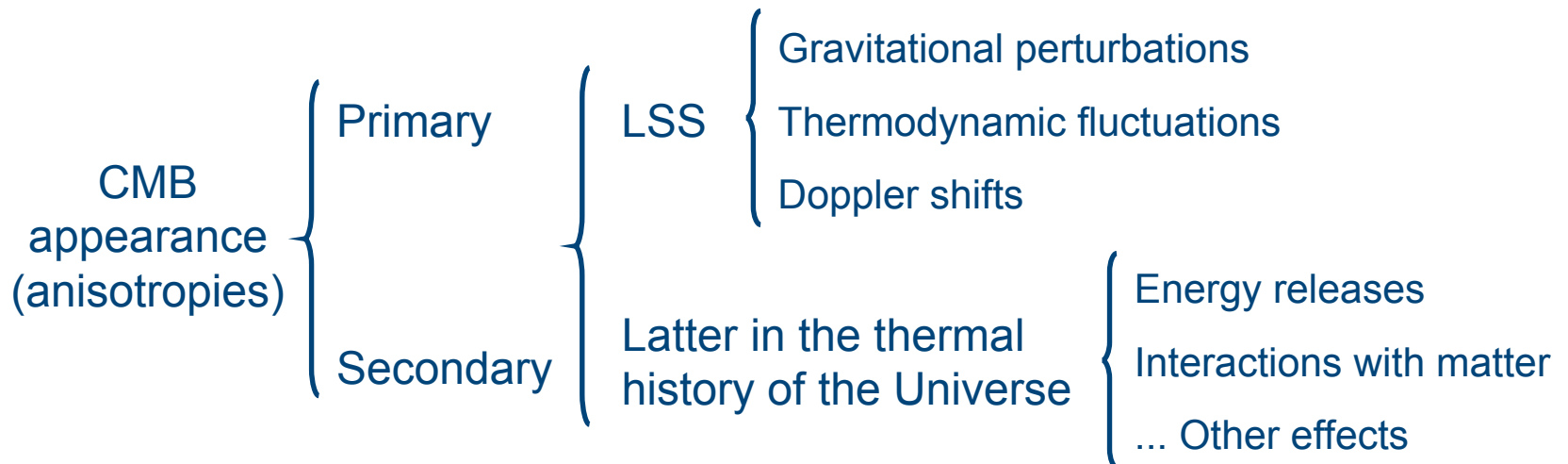
$$1500 < z < 1000$$

Decoupling



Last Scattering Surface

$$(\sim 1.6 \times 10^{-5} (\Omega_0 h_{100}^2))$$



1. Introduction: Galaxy clusters and the CMBR

Basic physic of the Sunyaev-Zel'dovich effect

Cluster of galaxies: $M \sim 3 \times 10^{14} M_{\text{sol}}$, $R_{\text{eff}} \sim \text{Mpc}$. In hydrostatic equilibrium, T_e

$$k_B T_e \approx \frac{GMm_p}{2R_{\text{eff}}} \approx 7 (M/3 \times 10^{14} M_{\odot}) (R_{\text{eff}}/\text{Mpc})^{-1} \text{ keV} .$$

→ X-ray emission

Electrons scatter photons of the CMBR (low energy scattering):

Thomson cross-section σ_T and Optical depth $\tau_e \approx n_e \sigma_T R_{\text{eff}} \sim 10^{-2}$

Mean change of photon energy per scattering: $\Delta \nu / \nu \approx (k_B T_e / m_e c^2) \sim 10^{-2}$

Overall change in brightness of the CMBR $\sim 10^{-4}$

Primordial effects:

*non-localized
not associated with structures
at others wave bands*

*Detectable!! ... but
distinguishable?*

SZ effects:

*localized
seen towards structures visible in
the optical and X-ray band*

2. The physics of the SZ effect: Outline

- Radiation basics
- Inverse-Compton scattering
- Sunyaev-Zel'dovich effect in three flavors:
 - * Thermal SZ effect
 - * Non-thermal SZ effect
 - * Kinematic SZ effect

2. The physics of the SZ effect: Radiation Basics

Radiative transport equation

$$\frac{1}{c} \frac{\partial I_\nu}{\partial t} + \hat{k} \cdot \nabla I_\nu = j_\nu - \alpha_{\nu, \text{abs}} I_\nu - \alpha_{\nu, \text{sca}} I_\nu + \alpha_{\nu, \text{sca}} \int \phi_\nu(\hat{k}, \hat{k}') I_\nu(k') d\Omega' ,$$

Emission
Absorption
Scattering

Description by means:

- Photon distribution function or the occupation number:

$$f_\alpha(r, p, t) = h^{-3} n_\alpha(r, p, t)$$

(Statistical mechanics of photons)

- Specific intensity and Brightness temperature:

$$I_\nu(\hat{k}, r, t) = \sum_{\alpha=1}^2 \left(\frac{h^4 \nu^3}{c^2} \right) f_\alpha(r, p, t) ,$$

$$T_{\text{RJ}}(\nu) = \frac{c^2 I_\nu}{2k_B \nu^2} .$$

(Astrophysical work)

2. The physics of the SZ effect: Inverse-Compton scattering

Inverse-Compton emission step by step:

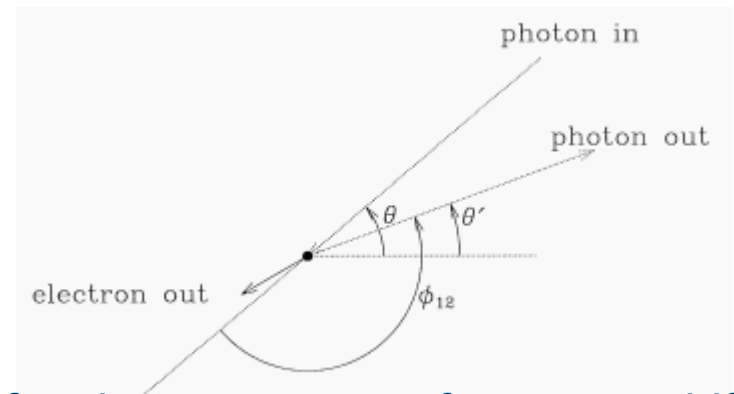
- a. Effect of a single photon-electron scattering
- b. Scattering of photons by an electron population
- c. Effect on radiation spectrum
 - c1. The Kompaneets approximation

2. The physics of the SZ effect: Inverse-Compton scattering

a. Single photon-electron scattering

Compton scattering formula:

$$\varepsilon' = \frac{\varepsilon}{1 + (\varepsilon/m_e c^2)(1 - \cos \phi_{12})},$$



The probability that a single scattering of a photon causes a frequency shift $s = \log(\nu''/\nu')$ from an electron with speed $v_e = \beta c$

$$P(s; \beta) ds = \int p(\mu) d\mu \phi(\mu'; \mu) \left(\frac{d\mu'}{ds} \right) ds.$$

$$p(\theta) d\theta = p(\mu) d\mu = (2\gamma^4(1 - \beta\mu)^3)^{-1} d\mu$$

where: $\phi(\mu'; \mu) d\mu' = \frac{3}{8}(1 + \mu^2\mu'^2 + \frac{1}{2}(1 - \mu^2)(1 - \mu'^2)) d\mu'$

$$\nu'' = \nu (1 + \beta\mu')(1 - \beta\mu)^{-1} \quad \mu' = \cos \theta'.$$

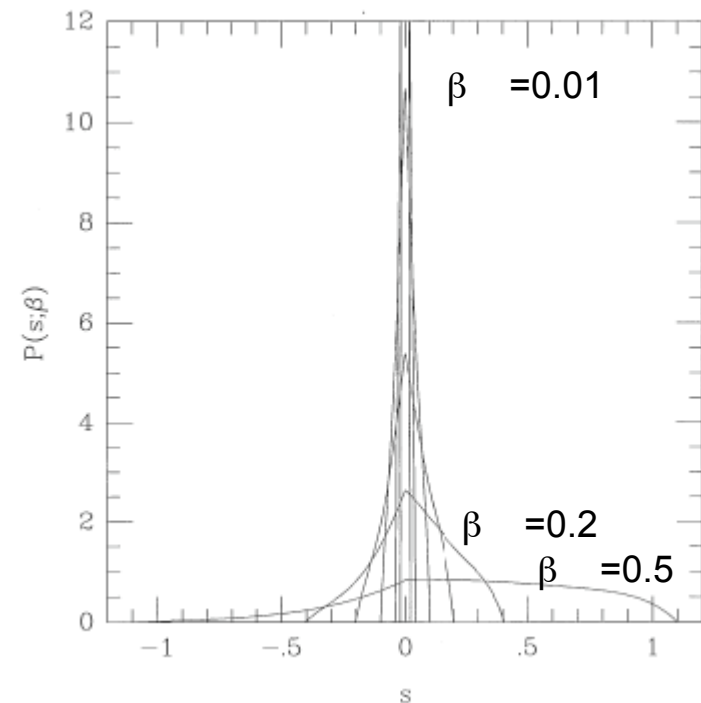
2. The physics of the SZ effect: Inverse-Compton scattering

Then

$$P(s; \beta) = \frac{3}{16\gamma^4\beta} \int_{\mu_1}^{\mu_2} (1 + \beta\mu')(1 + \mu^2\mu'^2 + \frac{1}{2}(1 - \mu^2)(1 - \mu'^2))(1 - \beta\mu)^{-3} d\mu, \quad (1)$$

Integrating ...

as $\beta \uparrow$
 Asymmetry \uparrow
 by relativistic beaming
 Width \uparrow
 because s for a given photon
 angular deflection



2. The physics of the SZ effect: Inverse-Compton scattering

b. Scattering of photons by an electron population

Distribution of photon frequency shifts caused by a population of electrons:

$$P_1(s) = \int_{\beta_{\min}}^1 p_e(\beta) d\beta P(s; \beta) \quad (2)$$

$p_e(\beta)$: electron β distribution $\left\{ \begin{array}{l} \text{Relativistic Maxwellian distribution (thermal)} \\ \text{Power law (non-thermal)} \end{array} \right.$

$P(s; \beta)$: given by eq. (1), probability that a frequency shift s occur from a single scattering from an electron with speed βc

2. The physics of the SZ effect: Inverse-Compton scattering

c. Effect on radiation spectrum

If every photon in the incident spectrum,

$$I_0(\nu) = \frac{2h\nu^3}{c^2} (e^{h\nu/k_B T_{\text{rad}}} - 1)^{-1}$$

Is scattered once, the resulting spectrum is given by

$$I(\nu) = \int_{-\infty}^{\infty} P_1(s) I_0(\nu_0) ds \quad (3)$$

where $P_1(s)$, given by eq. (2), is the scattering kernel.

Then, the change in the radiation spectrum at frequency ν is,

$$\Delta I(\nu) \equiv I(\nu) - I_0(\nu) = \frac{2h}{c^2} \int_{-\infty}^{\infty} P_1(s) ds \left(\frac{\nu_0^3}{e^{h\nu_0/k_B T_{\text{rad}}} - 1} - \frac{\nu^3}{e^{h\nu/k_B T_{\text{rad}}} - 1} \right) \quad (4)$$

2. The physics of the SZ effect: Inverse-Compton scattering

The generalization of equation (3) for an arbitrary optical depth:

$$I(\nu) = \int_{-\infty}^{\infty} P(s) I_0(\nu_0) ds \quad (5)$$

where $P(s)$ is the redistribution function after n scatterings

$$P(s) = e^{-\tau_e} \left(\delta(s) + \tau_e P_1(s) + \frac{1}{2!} \tau_e^2 P_2(s) + \dots \right)$$

For an optically thin medium, with $\tau_e \ll 1$ $P(s) = (1 - \tau_e) \delta(s) + \tau_e P_1(s)$

The resulting intensity change:

$$\Delta I(\nu) = \frac{2h}{c^2} \tau_e \int_{-\infty}^{\infty} P_1(s) ds \left(\frac{\nu_0^3}{e^{h\nu_0/k_B T_{\text{rad}}} - 1} - \frac{\nu^3}{e^{h\nu/k_B T_{\text{rad}}} - 1} \right) \quad (6)$$

2. The physics of the SZ effect: Inverse-Compton scattering

c1. The Kompaneets approximation: non-relativistic limit for a scattering process

$$\frac{\partial n}{\partial y} = \frac{1}{x_e^2} \frac{\partial}{\partial x_e} x_e^4 \left(\frac{\partial n}{\partial x_e} + n + n^2 \right)$$

where $x_e = h\nu / k_B T_e$ and,

$$y = \frac{k_B T_e c t}{m_e c^2 \lambda_e} = \int n_e \sigma_T dl \frac{k_B T_e}{m_e c^2}$$

The resulting spectrum can be written,

$$I(\nu) = \int_{-\infty}^{\infty} P_K(s) I_0(\nu_0) ds \quad \text{where} \quad P_K(s) = \frac{1}{\sqrt{4\pi y}} \exp\left(-\frac{(s + 3y)^2}{4y}\right)$$

The spectral change caused by scattering,

$$\Delta n = x y \frac{e^x}{(e^x - 1)^2} (x \coth(x/2) - 4) \longrightarrow \begin{aligned} \Delta I(x) &= x^3 \Delta n(x) I_0 \\ I_0 &= (2h/c^2)(k_B T_{\text{rad}}/h)^3 \end{aligned}$$

2. The physics of the SZ effect:

Thermal SZ effect

Produce by interaction of the CMB photons with electrons that have high energy due to their temperature. Likely sites to occur:

1. the atmospheres of galaxy clusters,
2. the ionized content of the Universe as a whole, and
3. the ionized gas close to us.

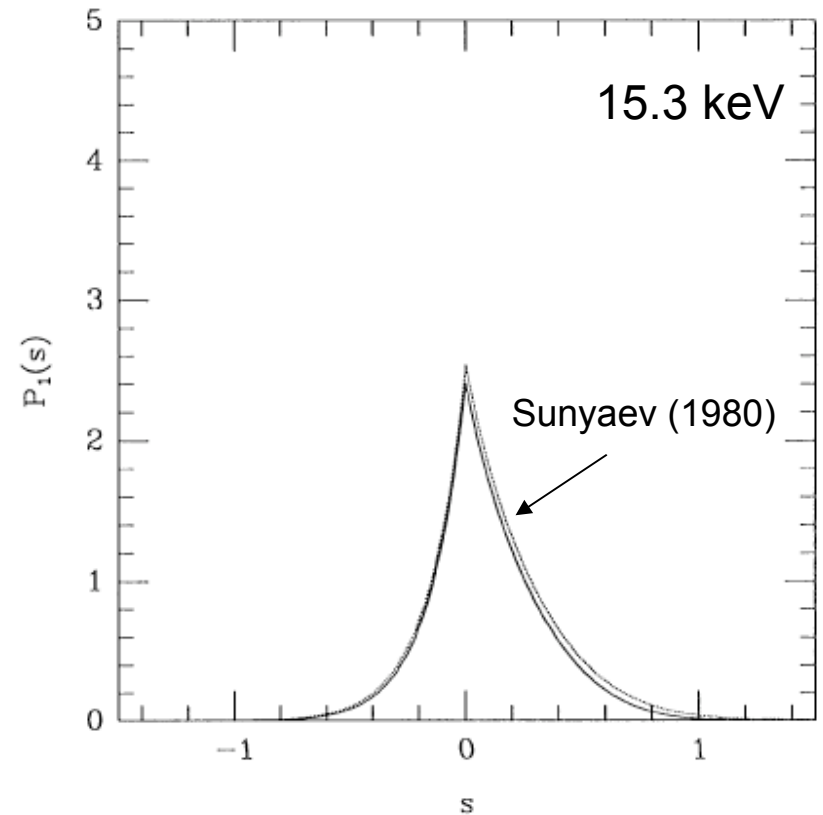
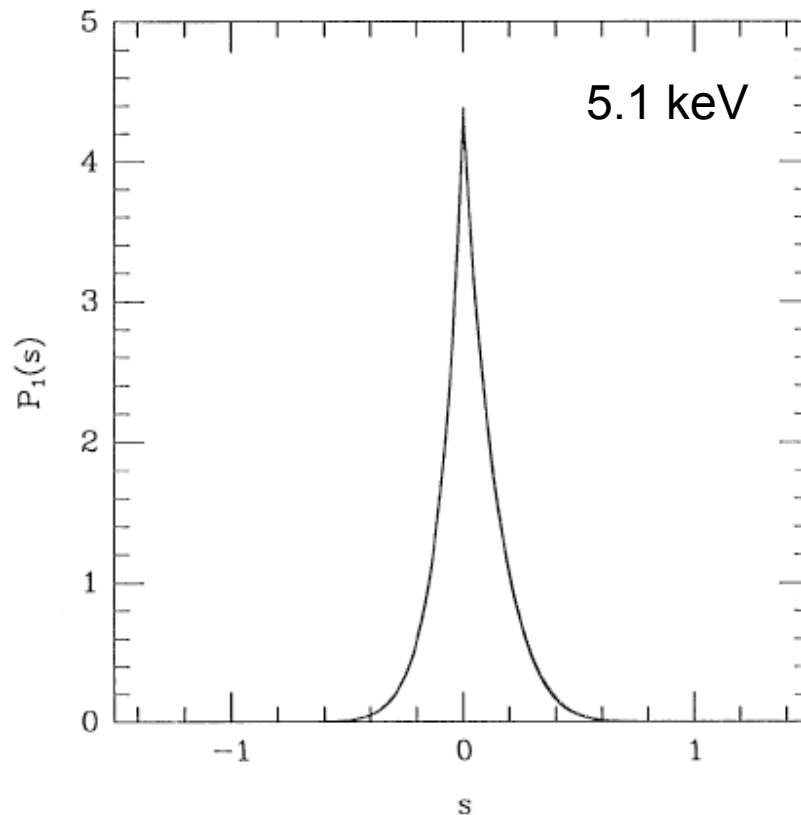
Assuming an electron relativistic Maxwellian distribution,

$$p_e(\beta) d\beta = \frac{\gamma^5 \beta^2 \exp(-\frac{\gamma}{\Theta}) d\beta}{\Theta K_2(\frac{1}{\Theta})}$$

where $\Theta = \left(\frac{k_B T_e}{m_e c^2} \right)$ is the dimensionless electron temperature,

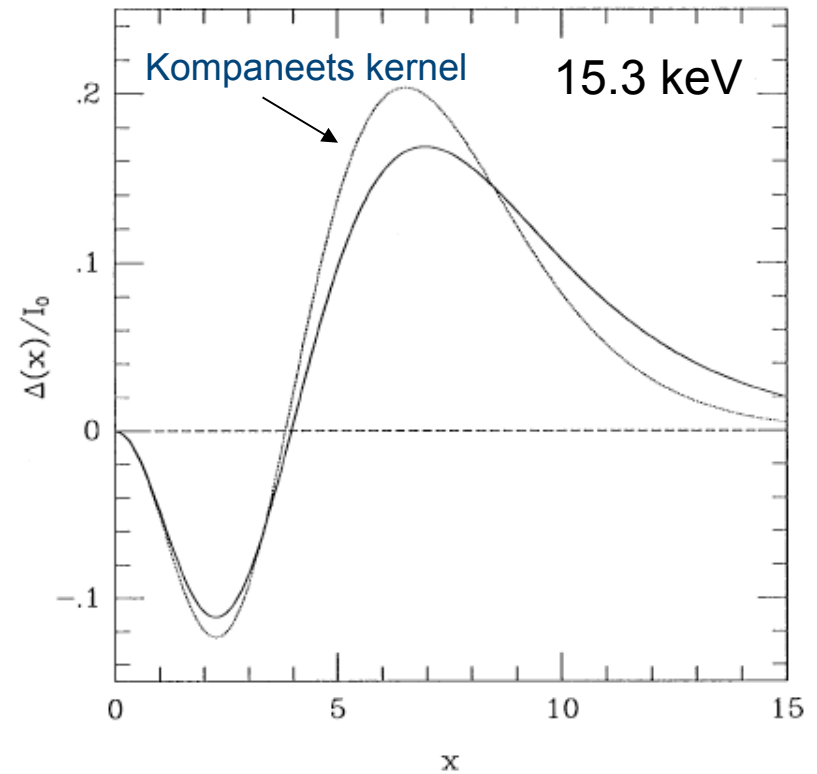
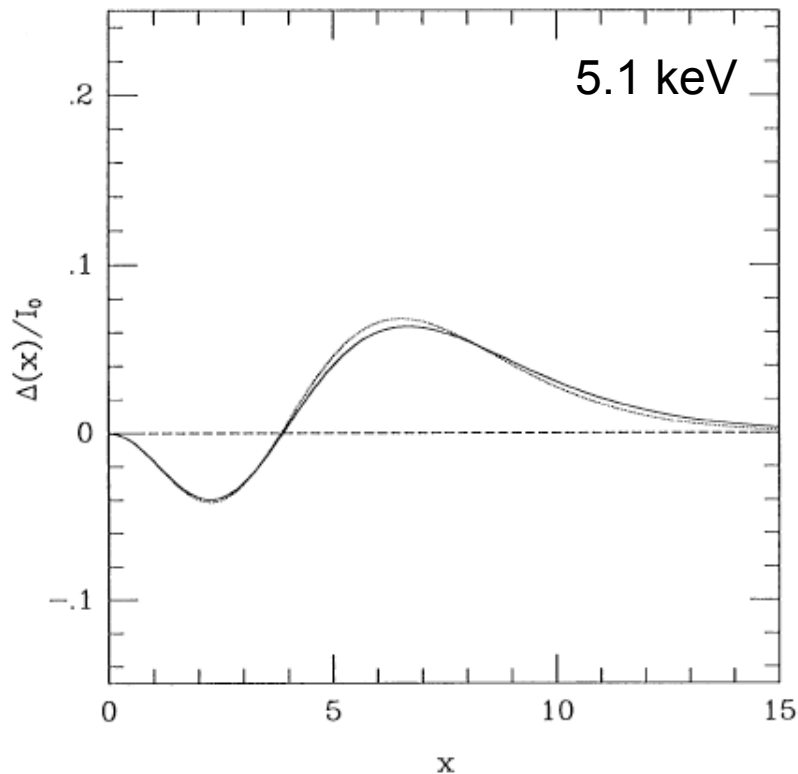
2. The physics of the SZ effect: Thermal SZ effect

The obtained scattering kernel (eq. 2), $P_1(s)$, is shown for two temperatures



2. The physics of the SZ effect: Thermal SZ effect

Integrating eq. 4 using the $P_1(s)$ function shown previously, the change in the radiation spectrum (caused by a single scattering), looks like this:



2. The physics of the SZ effect: Non-thermal SZ effect

Caused by a non-thermal (relativistic) populations of electrons, found in:

1. cluster radio halo sources
2. radio galaxy lobes

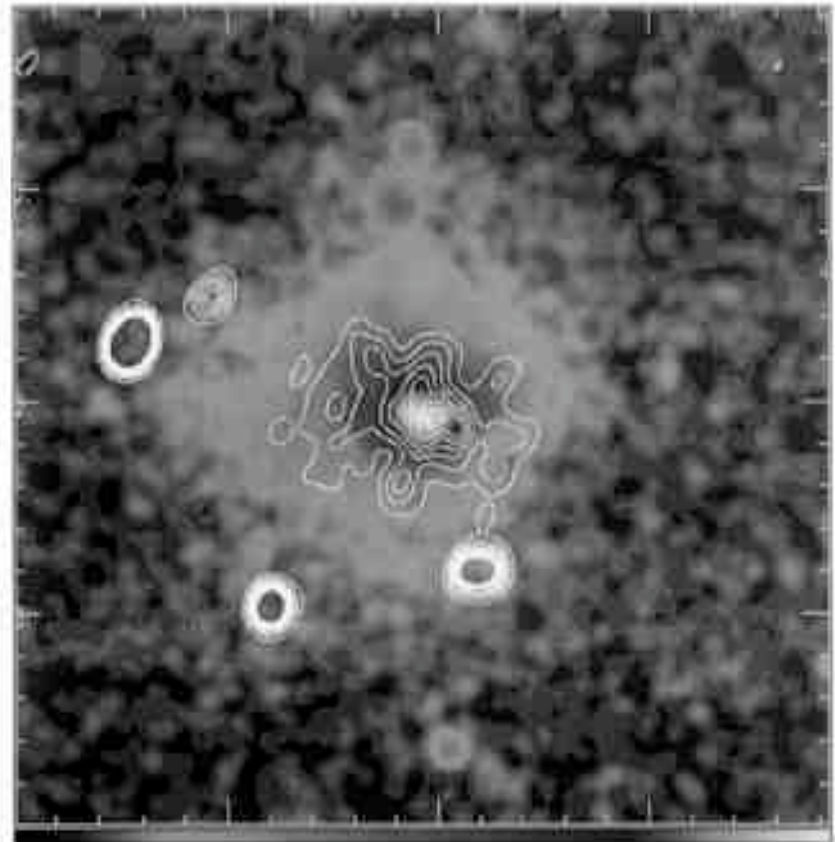
For a power-law distribution of electrons energies:

$$p_e(\gamma) d\gamma = \begin{cases} A \gamma^{-\alpha} d\gamma, & \gamma_1 \leq \gamma \leq \gamma_2 \\ 0, & \text{otherwise} . \end{cases}$$

with a normalizing constant

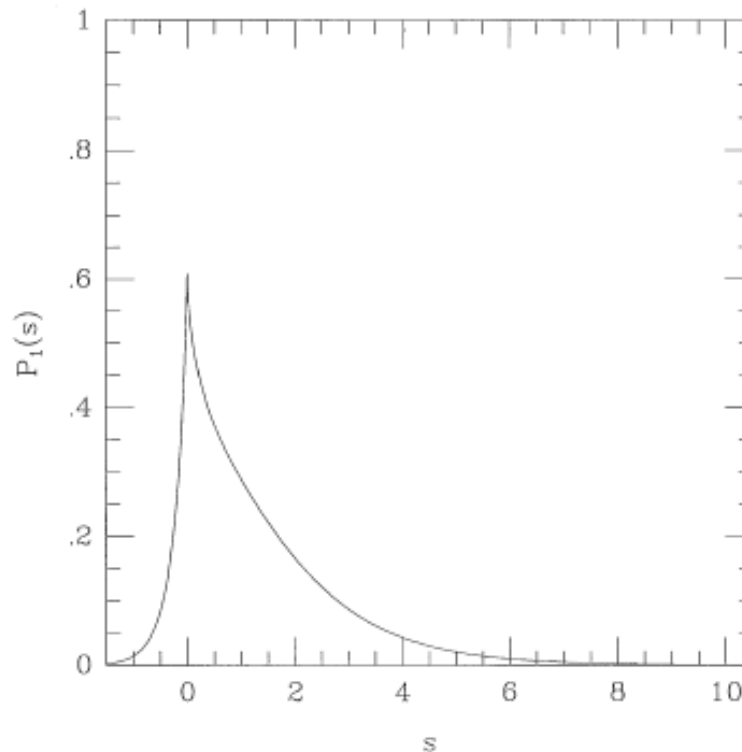
$$A = \begin{cases} \log \gamma_2 - \log \gamma_1, & \alpha = 1 \\ (1 - \alpha)(\gamma_2^{1-\alpha} - \gamma_1^{1-\alpha})^{-1}, & \alpha \neq 1 \end{cases}$$

Abell 2163



2. The physics of the SZ effect: Non-thermal SZ effect

The scattering kernel, $P_1(s)$, for a power-law electron distribution with energy index $\alpha=2.5$.

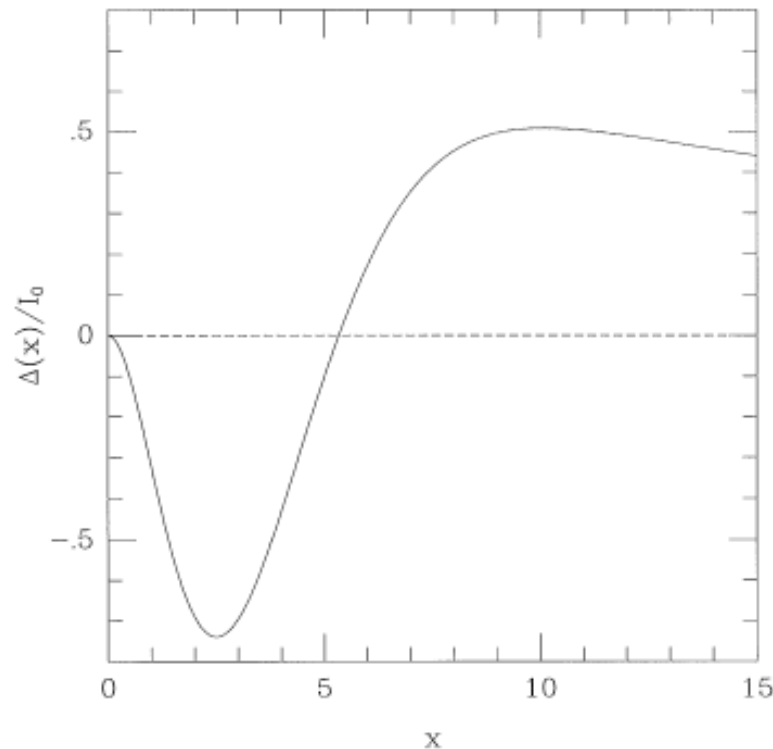


Upscattering tail much more prominent than in thermal case!

More electrons $\gamma \gg 1$ in this distribution

2. The physics of the SZ effect: Non-thermal SZ effect

The fractional spectral deformation caused by a single scattering

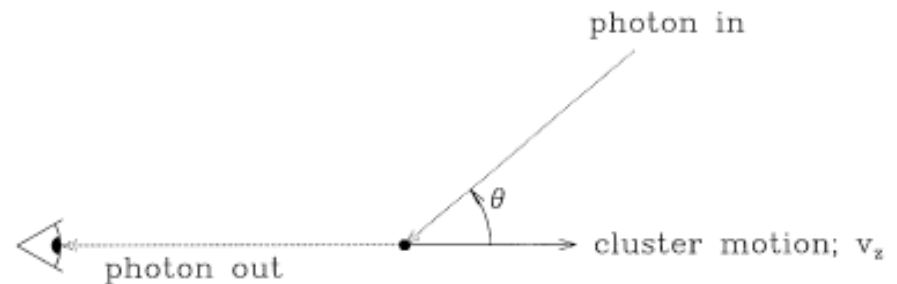


Similar in shape to the thermal case but with a deeper minimum and more extended tail

Thermal SZ effect
dominates
non-thermal SZ effect

2. The physics of the SZ effect: Kinematic SZ effect

The kinematic SZ effect arises if the scattering medium causing the thermal (or non-thermal) SZ effect is moving relative to the Hubble flow.



The change in specific intensity and brightness temperature produced are:

$$\Delta I = -\beta\tau_e I_0 \frac{x^4 e^x}{(e^x - 1)^2}$$

$$\Delta T_{RJ} = -\beta\tau_e T_{rad} \frac{x^2 e^x}{(e^x - 1)^2} \longrightarrow \frac{\Delta T_{rad}}{T_{rad}} \approx -\tau_e \frac{v_z}{c}$$

Comparison with the magnitude thermal SZ effect:

$$\frac{\Delta T_{kinematic}}{\Delta T_{thermal}} = \frac{1}{2} \frac{v_z}{c} \left(\frac{k_B T_e}{m_e c^2} \right)^{-1} = 0.085 (v_z / 1000 \text{ km s}^{-1}) (k_B T_e / 10 \text{ keV})^{-1}$$



Thank you!!

Thank you!!

A black and white portrait of Felipe Navarrete, a man with a full beard and mustache, wearing a suit and tie. The portrait is the background of the slide.

Techniques to observe SZ (Bolometer emphasis)

Felipe Navarrete

IMPRS Retreat
2009

Since 1972 when the Sunyaev-Zeldovich effect was proposed in a theoretical way many efforts have been carried out to detect it.

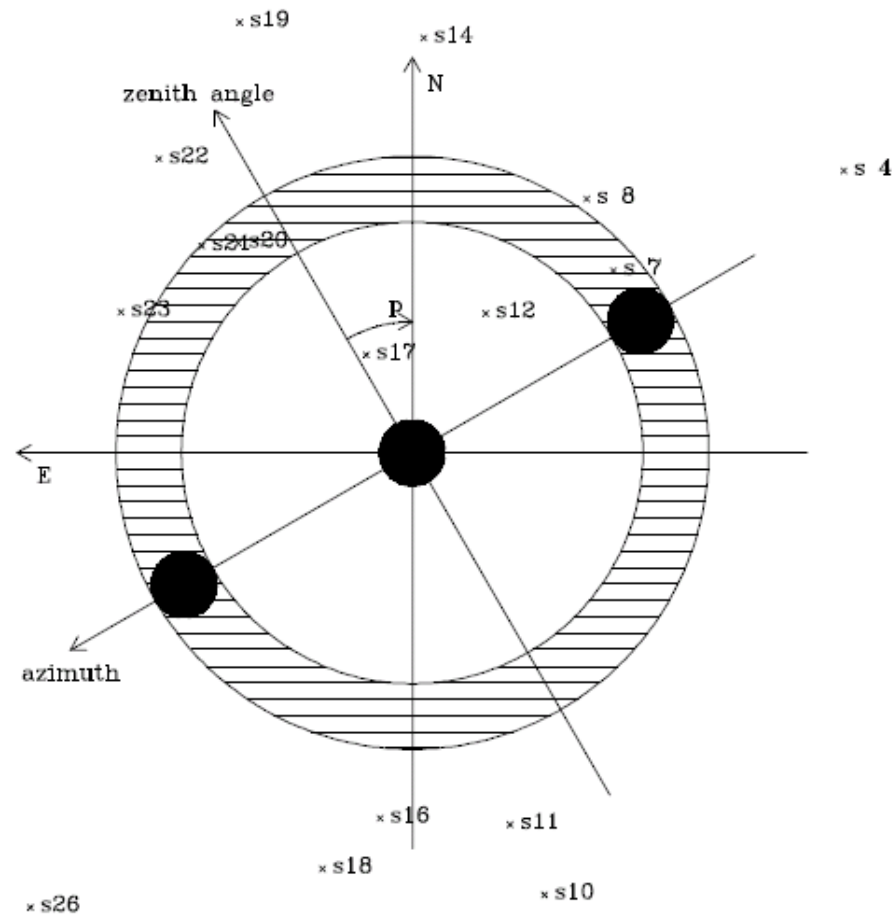
Techniques

- Single Dish
- Interferometers
- Bolometers

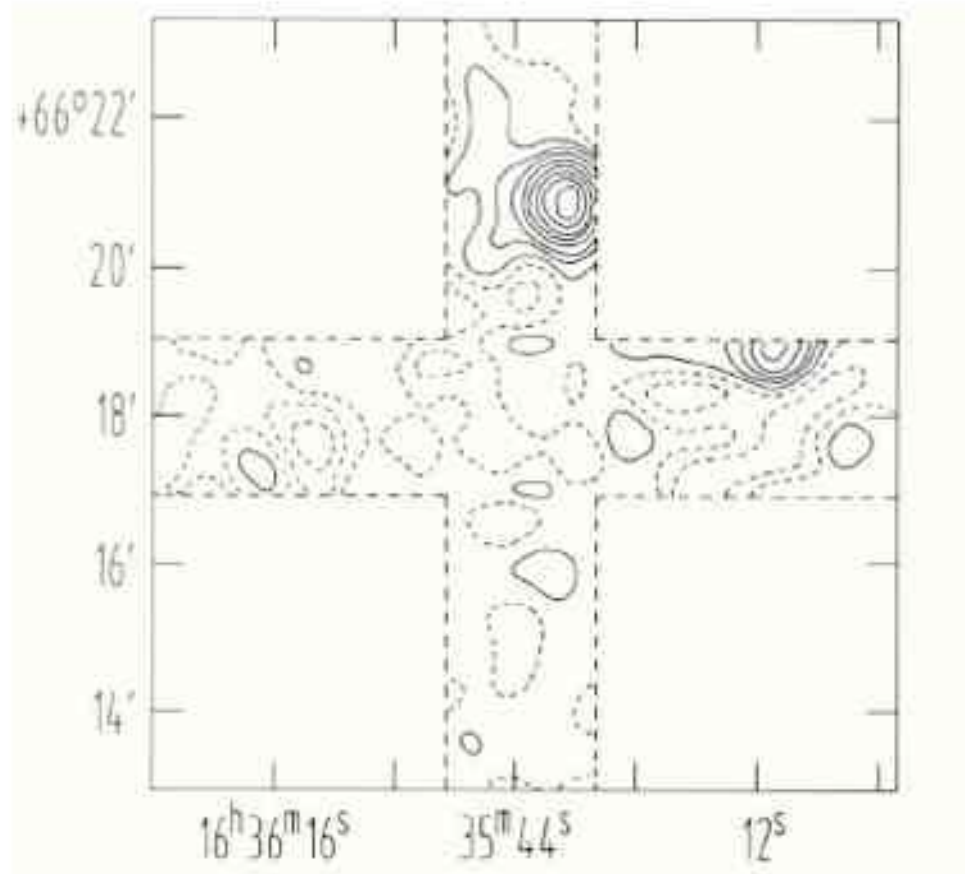
Single dish Radiometers

- Telescopes tend to have beam-sizes of few arcminutes at microwave frequencies. It is similar to the expected dimensions of galaxy clusters.
- Problems:
 - Radio source contamination, calibration and systematic errors introduced by the radiometer or spillover.

Observing



Uyaniker 1997 10.55Ghz

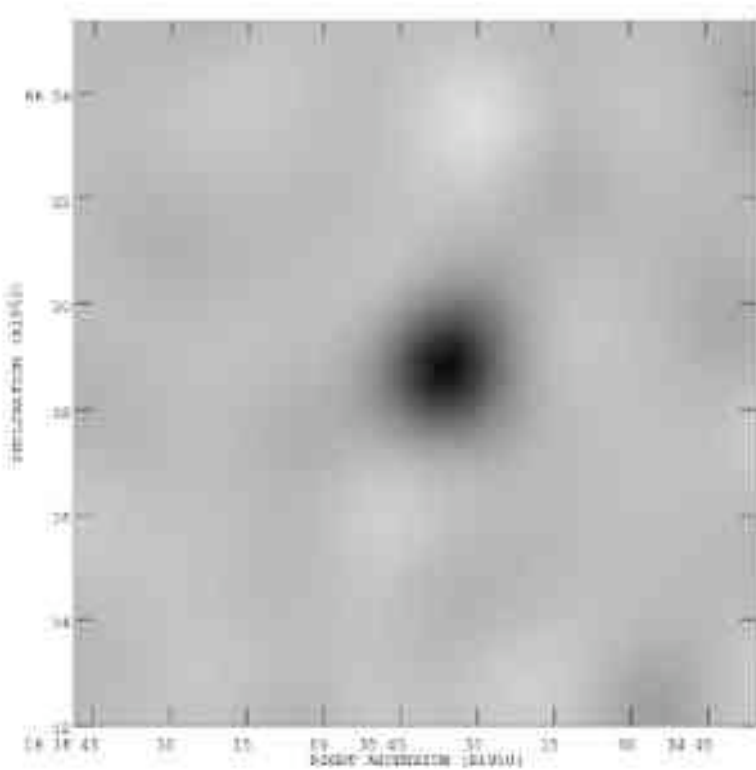


$750 \pm 200 \mu\text{K}$

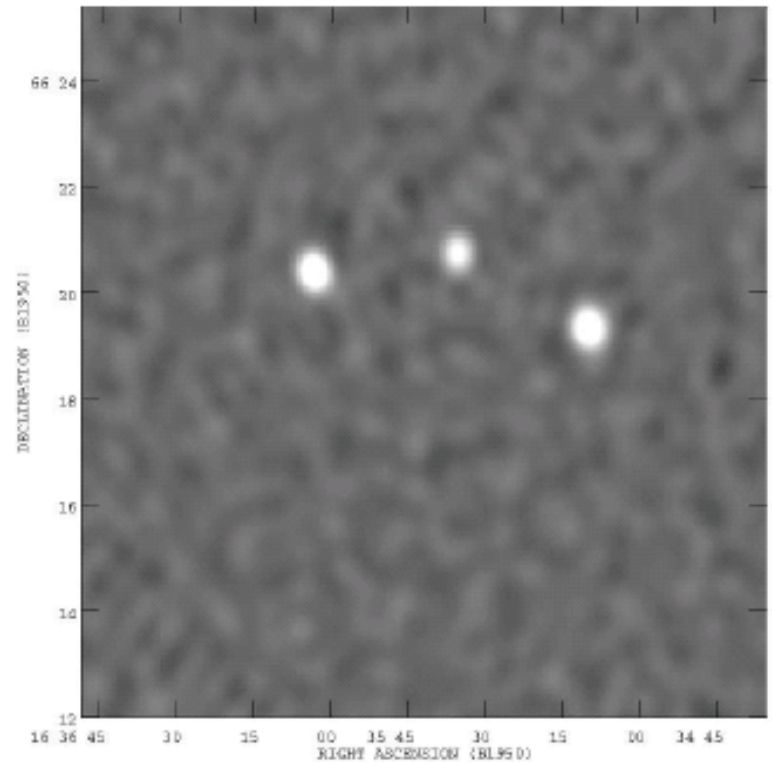
Interferometric

- Combination of long and short baselines.
- Long baselines identify individual sources (high resolution)
- Short baselines mix all the signals.
- Solution:

Jones et al 1993, Abell 2218



—



Short Baselines: 18 m

Long Baselines: 36-108 m

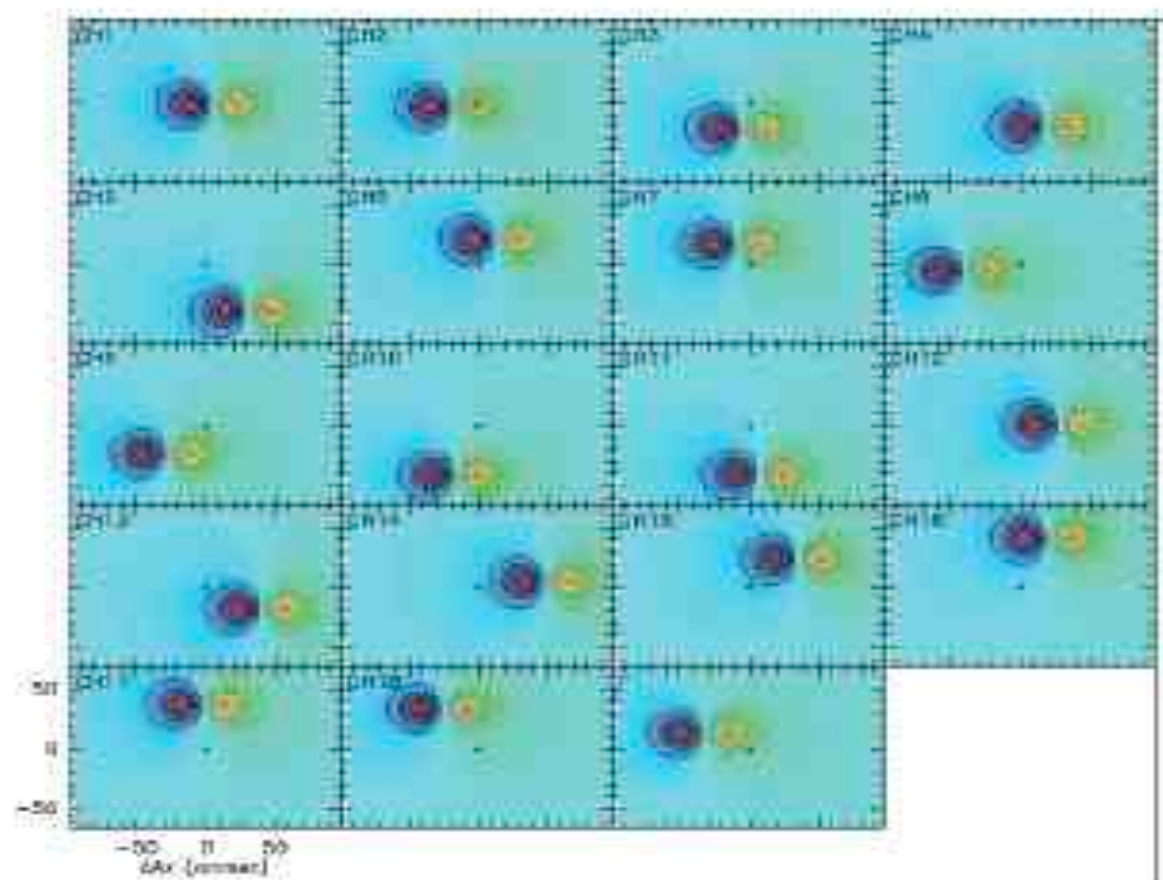
$-580 \pm 110 \mu\text{Jy}$

Bolometric

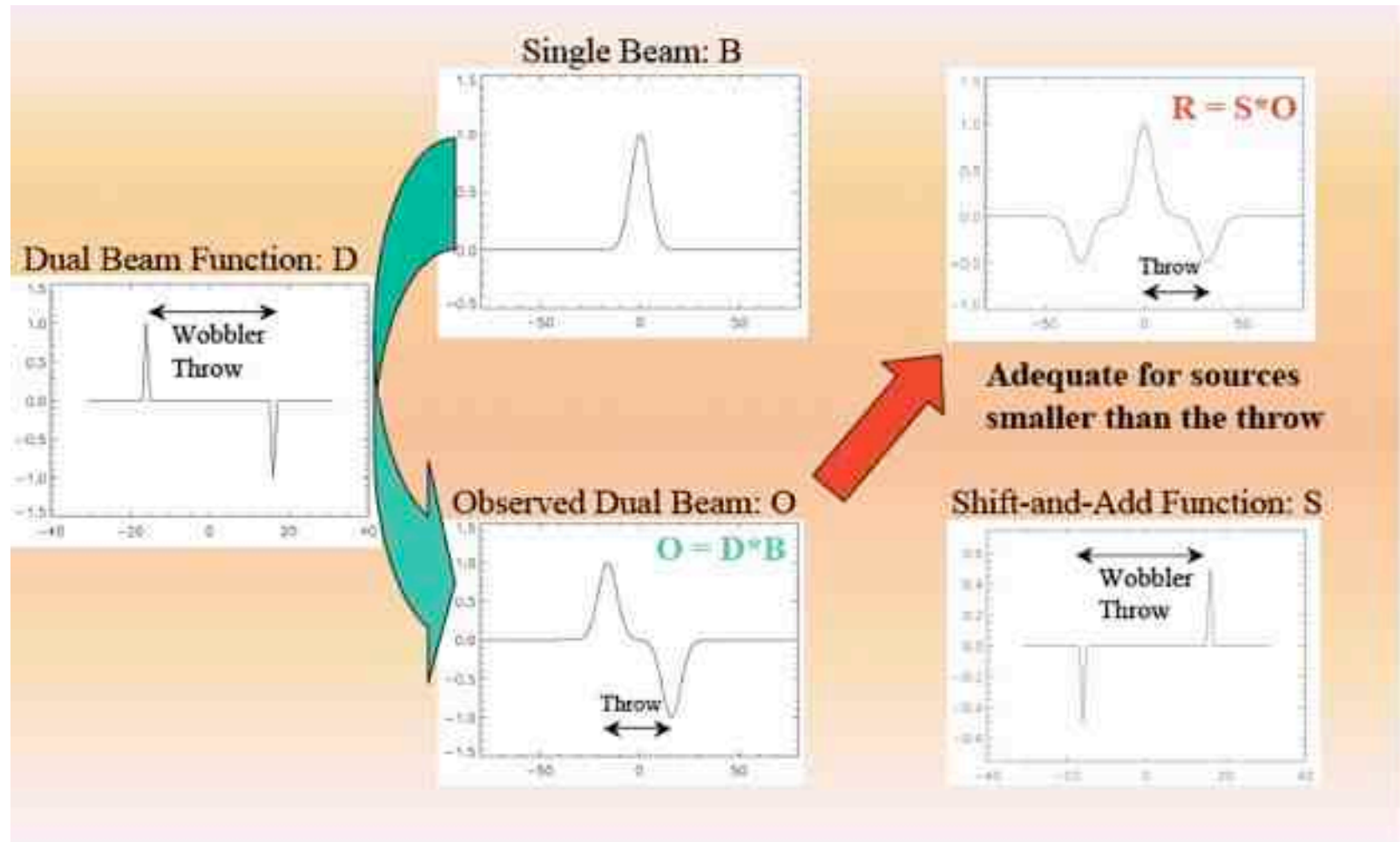
At frequencies higher than 100 GHz, coherent detectors reach their quantum noise limit due to the simultaneous photon position and frequency measurement uncertainty.

Incoherent detectors measure the integrated power of the incident radiation and do not retain any phase information. Due to their superior noise performance above 100 GHz, direct detectors are primarily used for CMB observations at high frequencies.

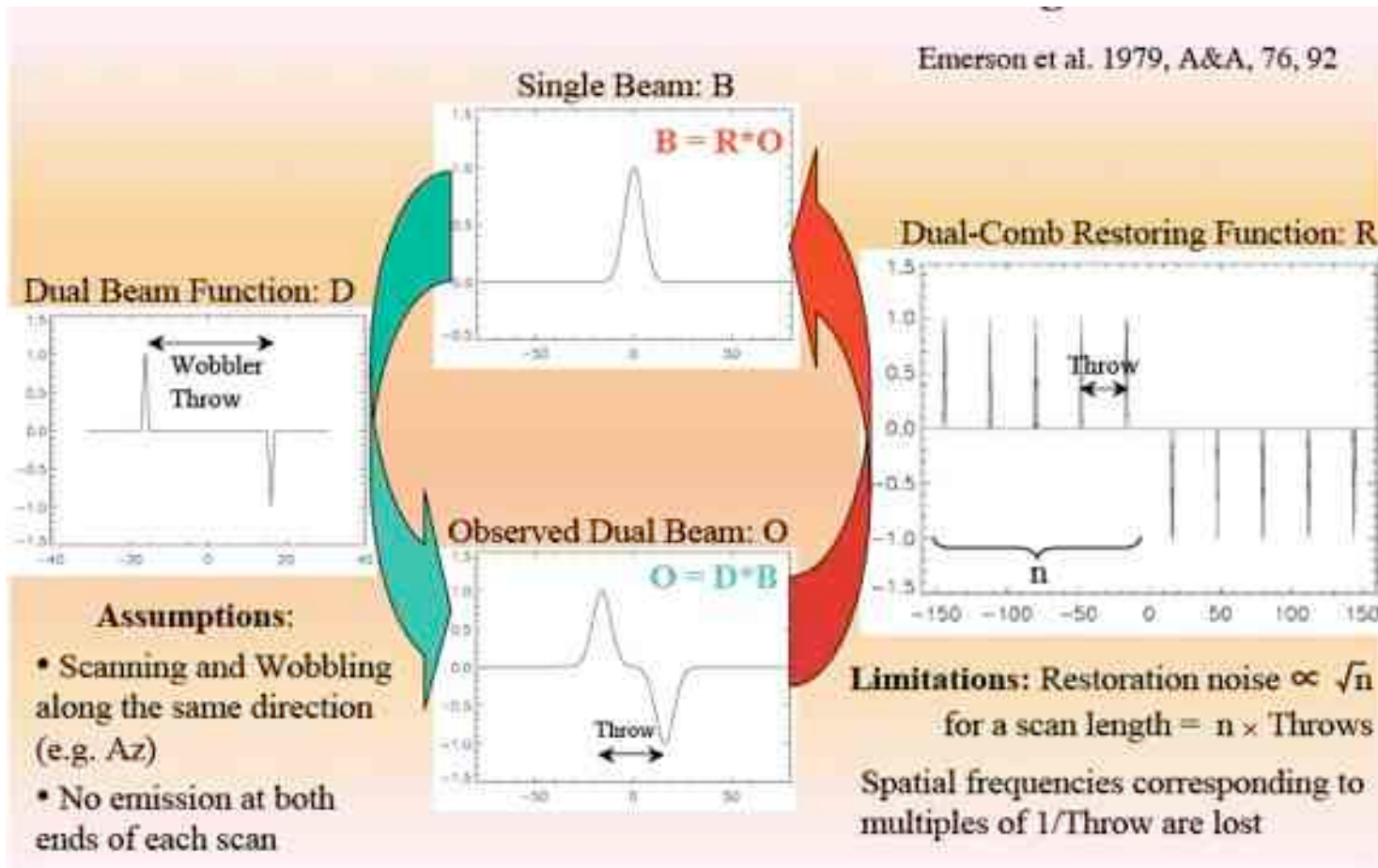
Dual-beam maps



Shift and Add

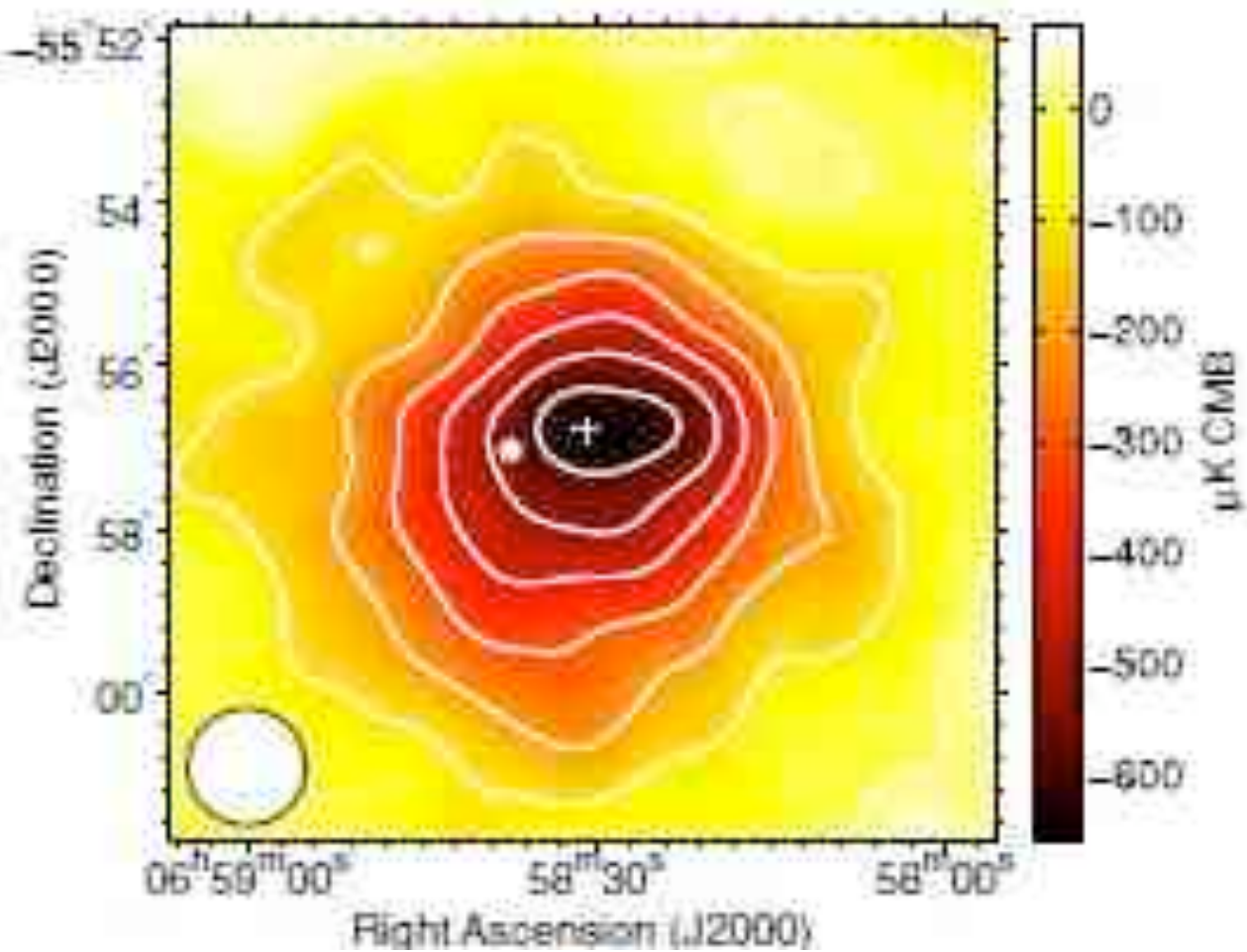


EHK



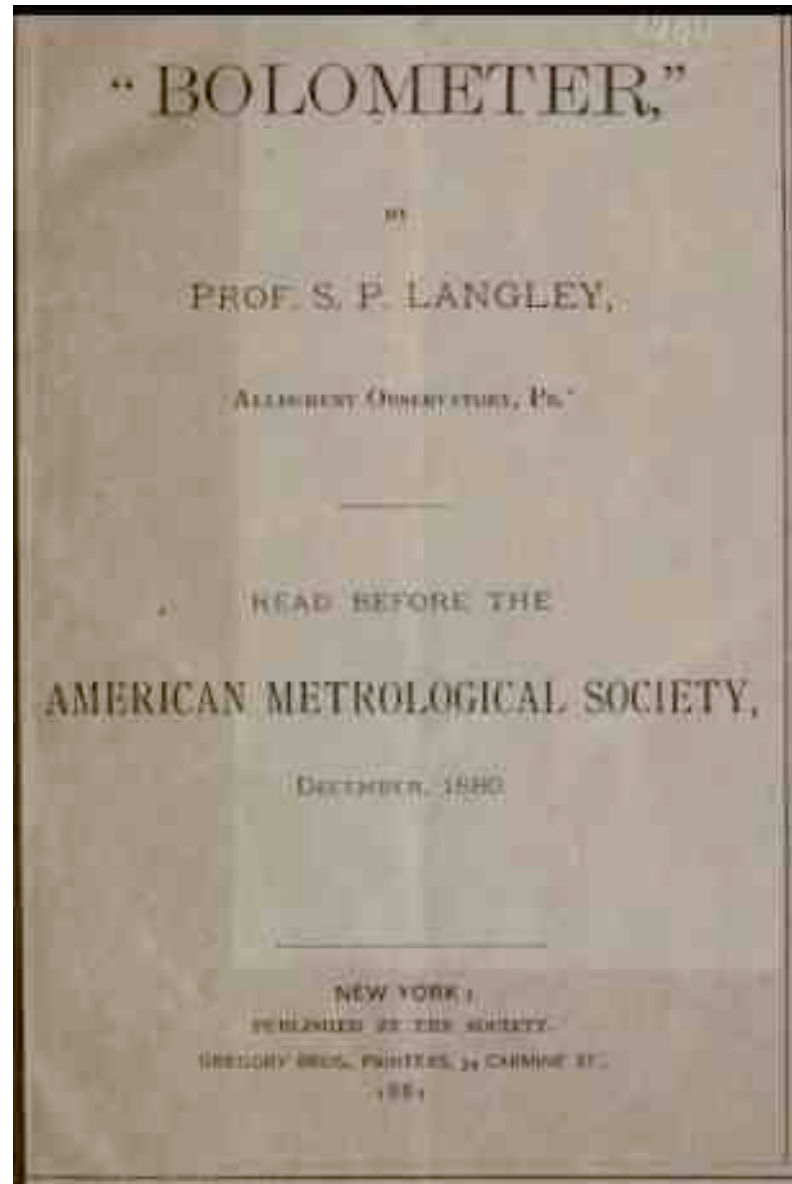
Deconvolve double beam

Convolve with telescope beam



Halverson et al. 2009

The evolution of the bolometer





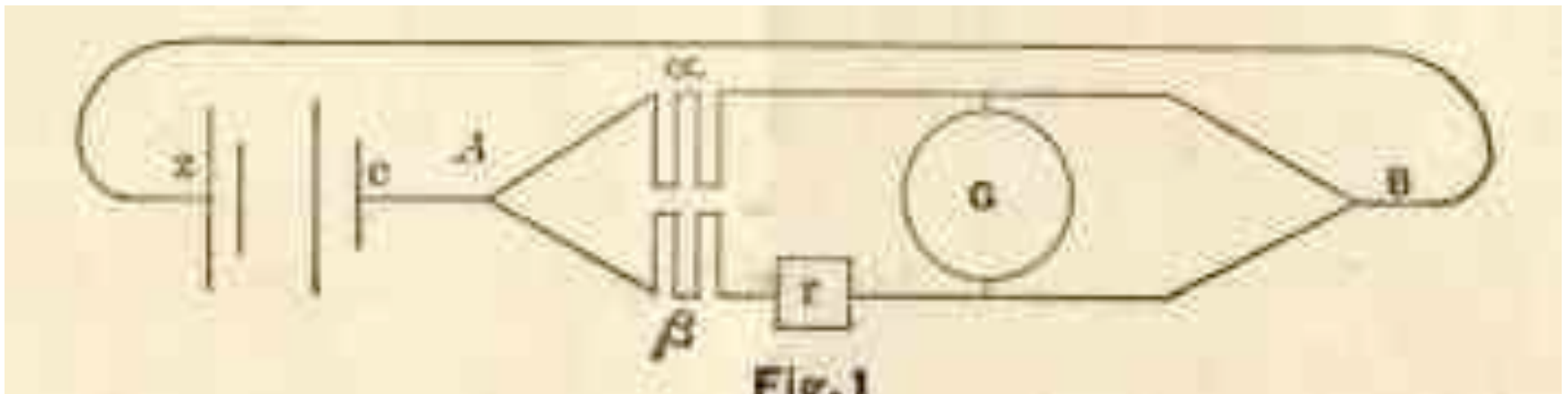
Our Hero



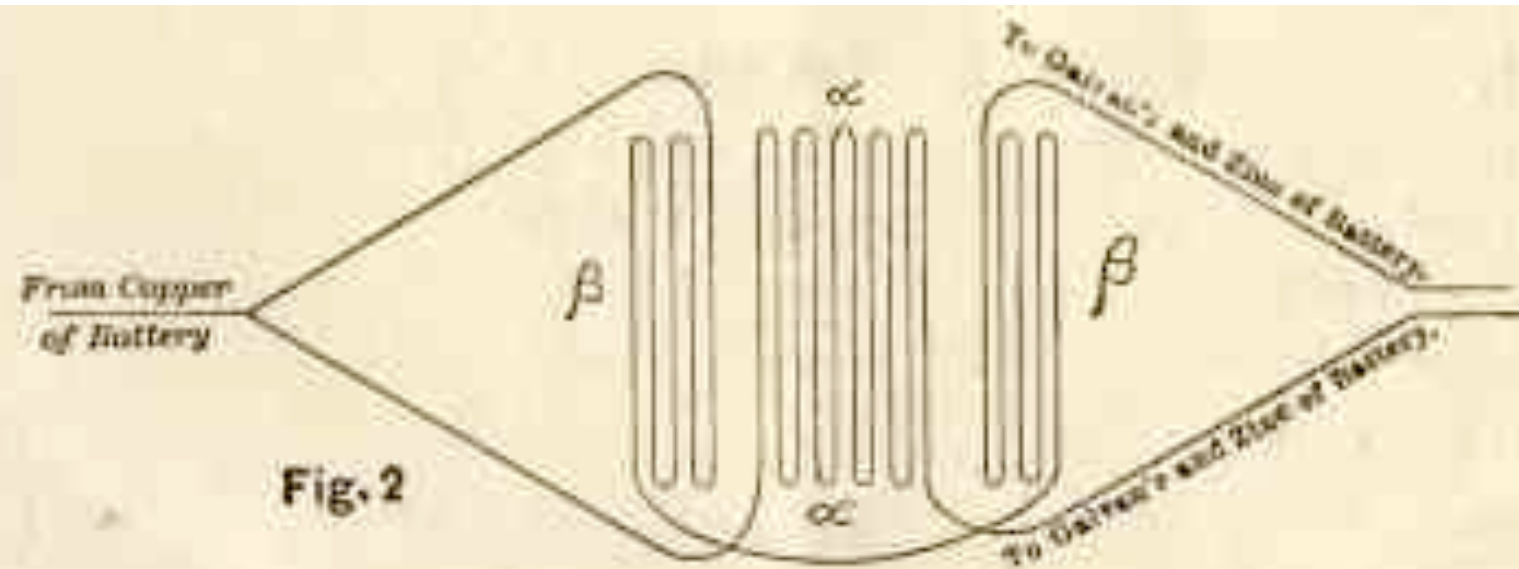
Samuel Langley (1834-1906)



The First Bolometer (1878)



$$\vec{\tau} = \vec{\mu} \times \mathbf{B}$$



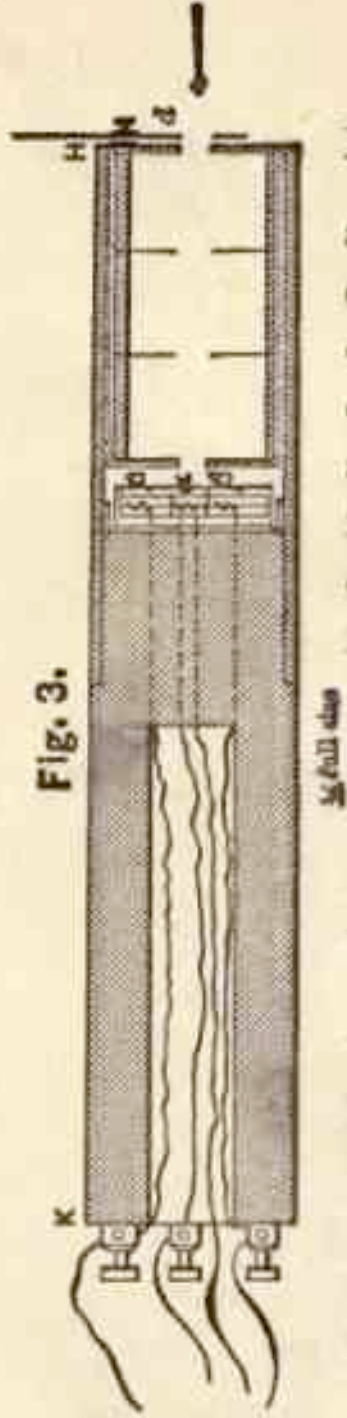


Fig. 3.



Zygmunt Wroblewski

Wroblewski

**Liquid Nitrogen 15th April
1883**



Olszewski

“his investigations on the properties of the matter at low temperatures which lead, inter alia, to the production of liquid helium” Nobel Prize Committee, 1913

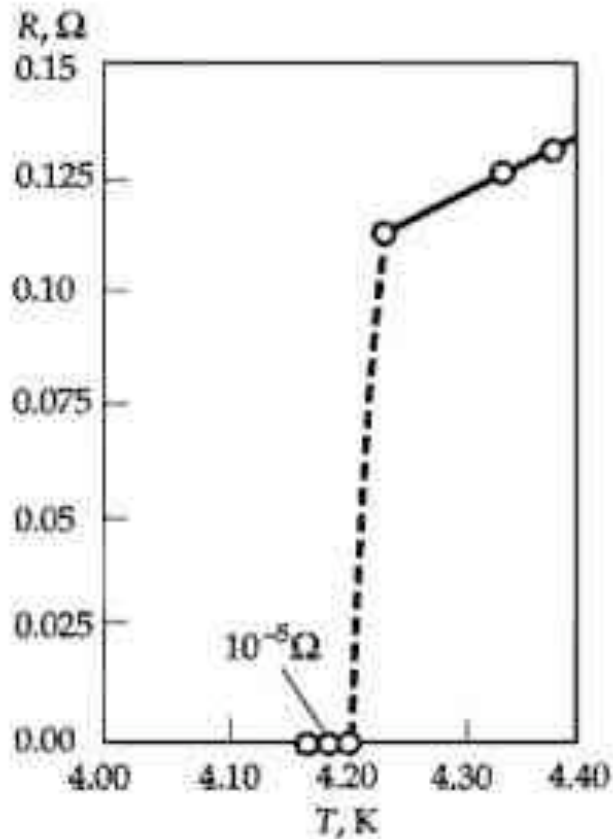


- **Liquid Helium (1908)**
- **Superconductivity (1911)**

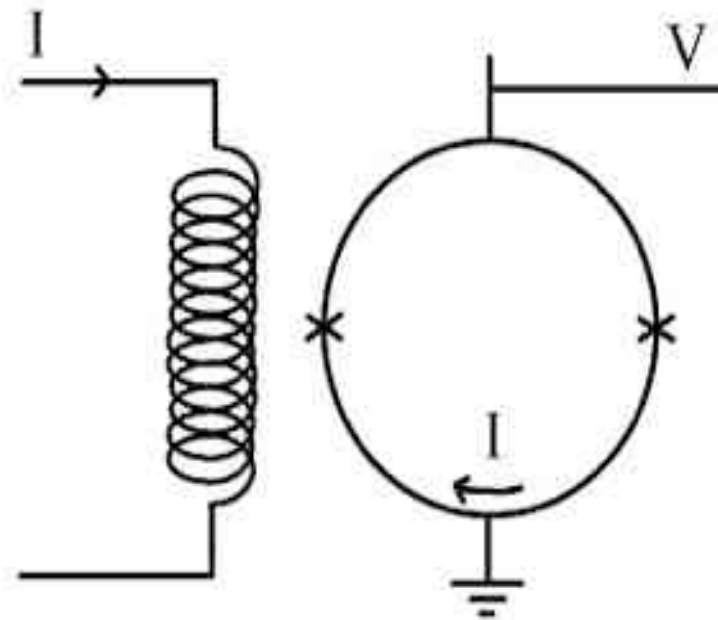
Heike Kamerlingh

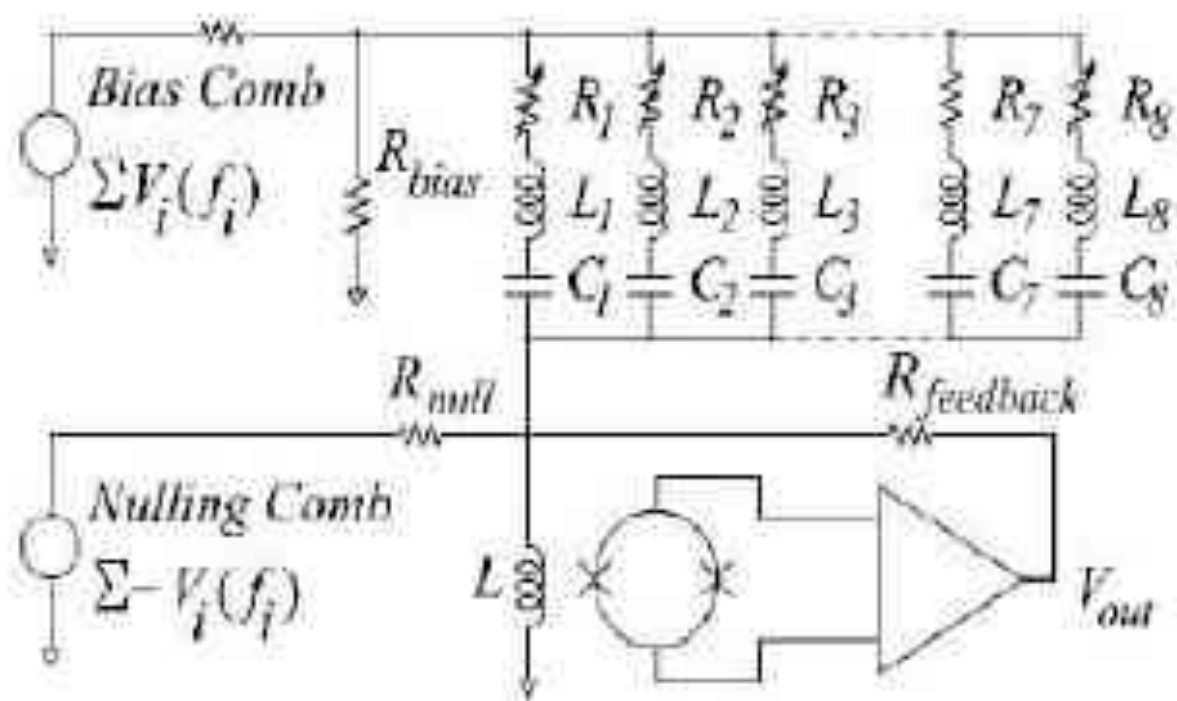
TES (Transition Edge Sensor) Bolometers

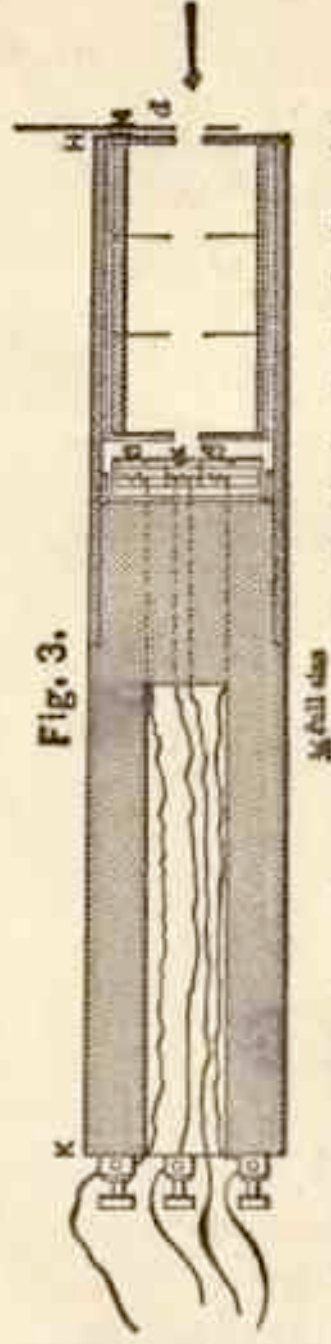
Super Conductor Curve

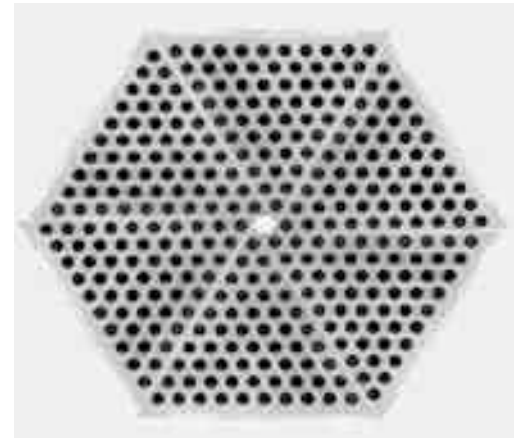


SQUID









THAT'S ALL

